Dynamique des gels physiques en relation avec la synérèse

Said Elmarhoum

THÈSE

Pour obtenir le grade de

DOCTEUR DE L'UNIVERSITÉ GRENOBLE ALPES

École doctorale : I-MEP2 - Ingénierie - Matériaux, Mécanique, Environnement, Energétique, Procédés, Production
Spécialité : MEP : Mécanique des fluides Energétique, Procédés
Unité de recherche : Laboratoire Rhéologie et Procédés

Dynamique des gels physiques en relation avec la synérèse

Physical gels dynamic and syneresis phenomena

Présentée par :

SAID ELMARHOUM

Direction de thèse :

Komla AKO MAITRE DE CONFERENCES, Université Grenoble Alpes	Directeur de thèse
Yahia RHARBI CHARGE DE RECHERCHE HDR, Université Grenoble Alpes	Co-directeur de thèse

Rapporteurs :

Laurent BILLON
PROFESSEUR DES UNIVERSITES, Université de Pau et des Pays de l'Adour
Sylvie TURGEON
PROFESSEUR, Université Laval

Thèse soutenue publiquement le **16 janvier 2023**, devant le jury composé de :

Agnès ROLLAND-SABATE INGENIEUR DOCTEUR, Avignon Université	Examinatrice
Aurélien FORGET DOCTEUR EN SCIENCES, Albert-Ludwigs- Universität Freiburg	Examinateur
Hugues BODIGUEL PROFESSEUR DES UNIVERSITES, Grenoble INP	Président
Laurent BILLON PROFESSEUR DES UNIVERSITES, Université de Pau et des Pays de l'Adour	Rapporteur
Sylvie TURGEON PROFESSEUR, Université Laval	Rapporteure
Komla AKO MAITRE DE CONFERENCES HDR, Université Grenoble Alpes	Directeur de thèse

Invités :

Guéba AGODA-TANDJAWA
INGENIEUR DOCTEUR, CARGILL France
Yahya RHARBI
CHARGE DE RECHERCHE, CNRS, LRP

Remerciements

Cette thèse a été réalisée au Laboratoire Rhéologie et Procédés, soutenue financièrement par Institut National Polytechnique de Grenoble (G-INP) et sous la direction de Monsieur Komla AKO, Maître de conférences à l'Université Grenoble Alpes et Yahya RHARBI, Chargé de recherche au Centre national de la Recherche Scientifique (CNRS).

Les premiers mots de cette thèse sont tout naturellement pour mon directeur de thèse, Monsieur Komla AKO, qui m'a confié ce travail de thèse et qui m'a accepté de me guider et de me superviser tout au long de ces trois années (et deux mois de prolongation) passées au laboratoire. Je tiens à le remercier pour son encadrement, son implication, sa disponibilité, sa confiance, sa sympathie, mais et surtout sa curiosité scientifique pour aller au fond des choses. Je lui dis : « Ce fut un grand plaisir de travailler avec vous ». Je voudrais également remercier grandement mon co-directeur de thèse, Monsieur Yahya RHARBI pour toute son aide, ses conseils et pour toutes les discussions scientifiques que nous avons eues.

J'adresse tous mes remerciements aux membres du jury, Monsieur Laurent BILLON, Madame Sylvie TURGEON, Monsieur Aurélien FORGET, Monsieur Hugues BODIGUEL, Madame Agnès ROLLAND-SABATE et Monsieur Guéba AGODA-TANDJAWA, qui m'ont fait l'honneur de leur présence et d'avoir aimablement accepté de juger mon travail et le temps investi dans l'évaluation de ma thèse. Merci aux rapporteurs de m'avoir fait part de leurs remarques pertinentes lors de la lecture du manuscrit.

Je remercie Nadia El KISSI, ancienne directrice du laboratoire et Frédéric BOSSARD, le directeur actuel, et toute l'équipe administrative et technique du Laboratoire Rhéologie et Procédés pour leur accueil, leur professionnalisme, leur bienveillance et leur gentillesse.

Je veux également remercier tous les chercheurs du laboratoire pour leurs échanges, conseils et discussions scientifique que nous avons eues, sans oublier l'équipe de Polytech de chimie avec laquelle j'ai travaillé comme chargé d'enseignement vacataire dans le cadre des TP. Merci à Youness SOUMANE pour son aide sur la microscopie à fluorescence et la partie MatLab.

Un grand merci à tous les doctorats, les contractuels, les postdoctorats et les stagiaires avec lesquels j'ai travaillé au quotidien : Adja, Alice, Ana, Ayoub, Béatrice, Chaïmaâ, Christian, Clémentine, Dacil, Emelie, Essa, Faisal, Fatou, Hajar, Hanna, Khadija, Lydia, Mai, Mathilde,

Maxime, Mohamad, Mourad, Nishant, Nissrine, Rohan, Samuel, Sarah, Téko, Valentin, Xavier, Youness… et mes collègues de bureau : Diégo, Julie, Houssine, Mehdi, Mohamad, Olivier, Revaz…Et tous ceux que j'ai oubliés, encore merci pour cette formidable expérience scientifique et humaine dont je ressors grandi et que je n'oublierai jamais.

Au cours de cette période passée à Grenoble, j'ai rencontré des belles personnes en dehors du laboratoire : Oualid, Nouâmane, Chafiq, Anas, Yassin, Akram, Mohammed, Brahim (Toulon), Abd ELALI (Paris)… et la famille d'Elmguielle (Mantes-La-Jolie), merci pour tous ces moments inoubliables passés ensemble !

Enfin, je tiens à témoigner toute ma reconnaissance à ma famille au Port de Bouc pour leur soutien inconditionnel tout au long de mes études : Haj Lahoussaine, Hajja Aîcha, Mohamed, Omar, Lala Rkia, Lala Jamila, Abd ELLAH, Fatima, Brahim, Amal, Mustapha, Boubaker… et bien sur ma chère Cousine Keltoum Idbba, pour leurs générosités et leurs aides. Merci à toute ma famille au Maroc.

Je tiens à exprimer ma plus sincère gratitude envers mes parents, ainsi que ma sœur Fadma et mes frères Mohamed, Lahcen, Boubker et Driss, pour leur soutien indéfectible et leurs encouragements tout au long de mon parcours. Je leur suis reconnaissant de tout mon cœur.

Avec tout amour, je dédie ce grade de « Docteur » à ma chère mère « INNA » en vous souhaitant un bon rétablissement, et à l'âme de mon cher père « BABA ». Je vous aime !!

"ⵢⴰⵏ ⵉⵅⵙⴰⵇⵏ ⴰⴷ ⵜⵏⵜ ⵉⵍⴰⵔⵖ, ⵉⵅⵙⴰⵇ ⴰⴷ ⵜⵏⵜ ⵉⴷⵔⵥ" Proverbe Amazigh,

Bref, Celui qui veut réussir trouve un moyen.

Table des matières

Contexte

Contexte

Dans le contexte de l'élaboration de film aux propriétés physicochimiques innovantes, comme des films thermosensibles à mémoire de forme, nous nous sommes intéressés à l'obtention de films par séchage contrôlé d'hydrogel thermosensible. Un hydrogel se présente comme un réseau de filament imbibé d'eau avec un volume pratiquement égal à son volume en eau. L'élimination de l'eau du réseau, laisse un film qui peut redevenir hydrogel lorsqu'il est à nouveau recouvert d'eau. Pour plusieurs raisons d'origine physicochimiques et procédés, qu'on ne maîtrise pas bien, le film gonflé ne donne pas systématiquement la forme initiale de l'hydrogel qui a été séché. On peut donc dire que la transition gel-film n'est pas réversible au regard de la forme et aussi d'autres propriétés du gel qu'on tente de retrouver après le séchage. Grenoble est un pôle d'excellence spécialisé dans l'extraction et la modification de matériaux biosourcés et dans la synthèse de polymères pour des applications à haute valeur technologiques à partir de molécules osidiques. Afin de renforcer les savoirs faires dans ce domaine d'application, dont l'impression 3D de prothèse à base de polysaccharide est un exemple, nous avons choisi comme matériau d'étude dans cette thèse le polysaccharide. On retrouve aussi le polysaccharide dans les objectifs des projets de recherche de l'Institut CarnoPolynat et GlycoAlps auxquels fait parti le Laboratoire Rhéologie et Procédés.

Les hydrogels, sous la forme de film faiblement hydraté, peuvent servir de pansement [1, 2] des plaies sèches. Tandis que les films avec une bonne capacité d'absorption d'eau vont être utilisés comme pansement des plaies exsudatives. Le gonflement d'un film dans un milieu physiologique ou solution dans laquelle des sels et autres types d'ions sont en activité exige une maîtrise des propriétés physicochimiques relatives au gonflement du film, surtout dans le domaine de la santé [3]. Les hydrogels à base de polysaccharide sont couramment rencontrés dans le domaine alimentaire et les films comestibles comme emballage alimentaire, mais les films d'hydrogel déshydraté sont aussi utiles dans le cosmétique [4] et dans le domaine de l'optique. Ces films peuvent servir de revêtement de surface pour les lentilles afin de moduler leurs propriétés optiques comme : la réfringence, l'opacité et la transmission de longueur d'onde spécifique (filtre). Pour toute application des hydrogels, directement ou sous la forme de film, l'étape de la préparation de l'hydrogel est cruciale parce qu'elle détermine par la composition et le procédé des propriétés du produit final. Pour fabriquer des gélules pharmaceutiques, Lafargue et al., (2007) [5] ont utilisé un mélange d'amidon modifié et de kappa-carraghénane, alors que Zhang et al., (2020) [6] ont proposé dans leurs études le mélange pullulane et k-carraghénane

comme substitue à la gélatine animale qui se trouve de plus en plus encadrer et de façon contraignante par la réglementation. Le choix des ingrédients et leur composition ont une influence significative sur l'élasticité, la thermo-moulabilité du film, son gonflement et dissolution. En amont de l'étude des propriétés de l'hydrogel, une attention particulière est accordée à la rhéologie des solutions gélifiées. La dynamique des polysaccharides en solution qui entraine la formation de l'hydrogel et sa propriété filmogène semble jouer un rôle important dans le résultat final. Ce sont tous ces facteurs, ceux liés aux types de polysaccharide, à la composition de la solution jusqu'à la formation de l'hydrogel et aux procédés de séchage qui font que le choix du ou des polysaccharides est crucial. Le fait de disposer de la ressource abondante de polysaccharide est un atout significatif dans cette recherche des polysaccharides adéquats. C'est cet atout qui permet entre autres aux hydrogels biosourcés de pouvoir couvrir de nombreux domaines d'applications comme l'illustre la figure suivante.

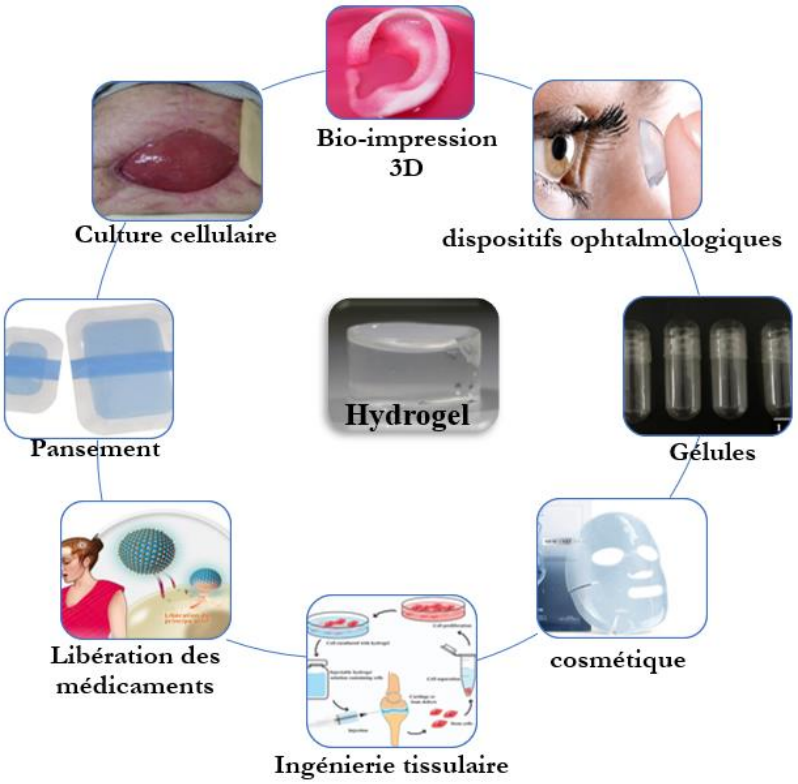

Figure 1: Illustration des différentes applications des hydrogels

Nous avons choisi dans le cadre de cette thèse le kappa-carraghénane pour investiguer la relation entre la structure de l'hydrogel et celle du film obtenu de même que les propriétés du film. Le kappa-carraghénane est un polysaccharide qui est étudié depuis les années 1970. Son utilité dans le domaine de la santé est relativement récente par rapport au domaine agroalimentaire. C'est un polysaccharide qui a été largement étudié en solution, ce qui est un

atout important pour aborder l'étape de la transition gel-film. Ses propriétés en solution sont multifactorielles ; le type de sel, la composition en sel, la concentration en sel et en polysaccharide puis la température sont pour ce système des facteurs déterminant de sa structure, son module viscoélastique en fonction ou non de la fréquence de cisaillement. Ainsi, ce système offre la possibilité de pouvoir jouer sur différents facteurs pour contrôler la structure et la propriété rhéologique de l'hydrogel avant l'étape du séchage. Le fait de pouvoir remettre à l'état liquide l'hydrogel ou de remettre en solution le film et recommencer les tests est très utile pour la répétabilité et la reproductibilité des mesures avec la possibilité de jouer sur les différents facteurs en gardant la même préparation. La figure 2A montre en exemple une préparation d'hydrogel de kappa-carraghénane dont la solution a été étalée puis gélifiée avant le séchage. La même solution dans le récipient est conservée dans les mêmes conditions où on voit du liquide expulsé du gel qui s'est contracté tout en étant au repos (c'est-à-dire, sans contrainte appliquée sur le gel autre que son propre poids).

Figure 2: A) Photo d'une couche de gel pour le séchage, B) Photo du gel restant dans son récipient après 4 jours montrant que le gel s'est contracté en expulsant son solvant (synérèse)

Le phénomène par lequel le liquide est éliminé spontanément du gel s'appelle synérèse. On se doute bien que ce phénomène se produira en même temps que le séchage. Ainsi, suivant la cinétique du séchage par rapport à celle de la synérèse, on peut avoir du liquide expulsé qui s'évapore en laissant de la matière solide notamment les sels se concentrer à la surface du gel. La concomitance de ces deux cinétiques et l'importance que pourrait avoir la synérèse dans le comportement du produit final nous a amené à nous intéresser au phénomène de la synérèse qui s'apparent à une forme d'auto-séchage de l'hydrogel afin d'en comprendre les origines physicochimiques. C'est dans ce contexte que nous avons orienté la bibliographie sur le sujet de la synérèse et son rapport avec la dynamique du système.

Références

[1] S. J. Boateng, K. H. Matthews, H. N. Stevens et G. M. Eccleston, «Wound Healing Dressings and Drug Delivery Systems: A Review,» *Journal of Pharmaceutical Sciences,* vol. 97, pp. 2892-2923 , 2008.

[2] I. Terzic, J. Ivanovic, I. Zizovic et all., «A Novel Chitosan Gels: Supercritical CO2 Drying and Impregnation with Thymol,» *Society of Plastics Engineers,* pp. 2192-2199, 2018.

[3] J. Kopecek, «Hydrogel biomaterials: A smart future?,» *Biomaterials,* p. 5185–5192, 2007.

[4] S. E. Friberg and I. Kayali, "Water Evaporation rates from a model of stratum corneum lipids," *Journal of Pharmaceutical Sciences,* vol. 78, pp. 639-643, 1989.

[5] D. Lafargue, D. Lourdin et J.-L. Doublier, «Film-forming properties of a modified starch/j-carrageenan mixture in relation to its rheological behaviour,» *Carbohydrate Polymers,* vol. 70, pp. 101-111, 2007.

[6] Y. Zhang et all, «Effects of κ-carrageenan on pullulan's rheological and texture properties as well as pullulan hard capsule performances,» *Carbohydrate Polymers,* vol. 238, n° 1116190, 2020.

Bibliographie

Bibliographie

Sommaire

Bibliographie

Cette partie présente sommairement les gels, les différents types de gel en relation avec la synérèse, ainsi qu'une revue des techniques d'évaluation ou de mesure de la synérèse en passant par une brève description des mécanismes d'agrégation et de gélification du kappa-carraghénane.

1 Généralité sur les gels

1.1 Définition

Un gel est un matériau mou, dans un état entre solide et liquide [1], la phase solide selon la définition d'Hermans en 1949 [2] forme un réseau tridimensionnel dans la phase liquide qui constitue généralement le volume ou la masse dominante du gel. Le réseau tridimensionnel occupe entièrement le volume du liquide conférant au gel des propriétés mécaniques semblables à celles d'un solide. Lorsque les liaisons qui caractérisent le réseau sont covalentes, le gel est chimique, dans le cas contraire (liaison non covalente) le gel est physique [3]. Le terme de gel provient du grec « Kolla » qui signifié « colle » [4], mais sa définition scientifique a commencé en 1861 par le chimiste britannique Graham Thomas, qui classe les gels suivant les propriétés communes à l'amidon, la gélatine, les gommes végétales etc. [5].

1.2 Classification des gels

Les gels sont classés selon plusieurs critères :

En fonction de l'origine de la phase solide, on distingue les gels à base de polymères naturels ou biosourcés tel que : les polysaccharides (carraghénanes, alginate, pullulane, Xanthane, acide hyaluronique…), les protéines (gélatines, collagènes, albumines, lactoglobulines, caséines…), ou à base de polymères synthétiques (PEO - oxyde de polyéthylène, PVA - Polyvilylalcool, polyacrylamide, silicone, ...). Des mélanges de ces différents types de matériaux pour former le gel sont étudiés.

En fonction du type de réticulation, on parle des ***gels chimiques*** quand les chaines polymères sont connectées entre elles par des liaisons covalentes (Fig. 1a), ces gels sont stables et irréversibles. L'énergie de liaison est très grande devant kT [4], et les liaisons sont moins sensibles aux facteurs extérieurs à savoir la température, la déformation mécanique, le pH … [6], mais elles peuvent fondre en présence d'un autre solvant et être sensible à l'oxydation. On

parle ***aussi des gels physiques*** (Fig. 1b), totalement ou partiellement réversibles, quand le réseau macromoléculaire est stabilisé par enchevêtrement des chaines, par des nœuds, ponts ou zone de jonction caractérisés par des liaisons ioniques, hydrogène, interactions dipolaires comme celles de Van der Walls [7]. Les interactions hydrophobiques, électrostatiques dans le cas de systèmes chargés et hydrodynamiques sont en compétitions au niveau des zones de jonction (fig. 1), pour définir le niveau de stabilité énergétique de la liaison physique. Les gels physiques peuvent évoluer de l'état sol-gel et gel-sol en modifiant les paramètres physico-chimiques tel que la température, la force ionique, le pH, la contrainte mécanique...).

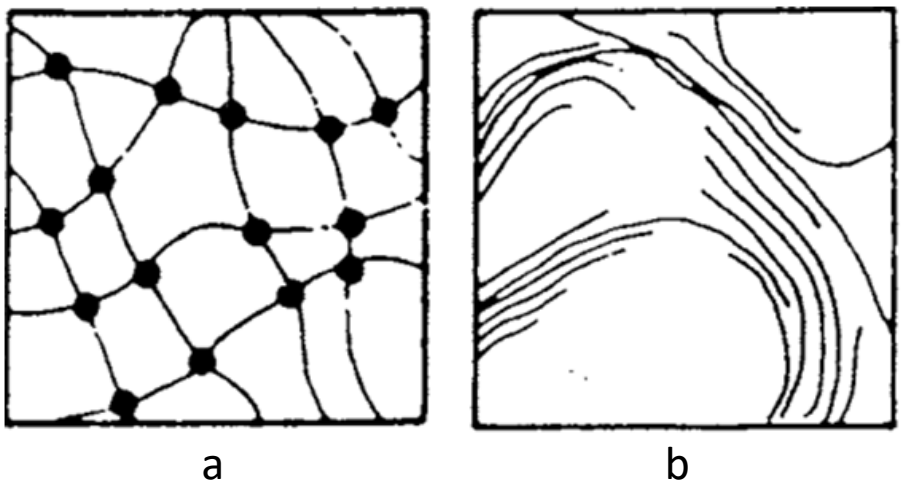

Figure 1: a) Illustration de gel chimique, les points de réticulation sont des liaisons covalentes, b) Illustration de gel physique, les zones de jonctions sont soudées par des interactions physiques.

Si le solvant est l'eau, on parle des hydrogels. Ils peuvent contenir jusqu'à 99.9 % en masse ou volume d'eau dans le réseau [8]. Les autres solvant dans les gels peuvent être organique (alcools, phenyloctane, dioctyl phthalate, toluène, benzène, etc..) qu'on rencontre couramment dans les solutions de polymère synthétiques ou pétrochimique.

Les gels physiques sont souvent présentés comme des états thermodynamiquement instables avec une évolutions plus ou moins lente vers la stabilité thermodynamique [9]. En raison de l'instabilité inhérente à la formation du gel, son évolution dans le temps peut conduire au renforcement du gel qui peut se manifester par l'expulsion de son solvant ayant pour cause la contraction du réseau du gel [10]. C'est ce phénomène qu'on appelle la synérèse que nous allons documenter dans les sections suivantes.

2 La synérèse

Historiquement, le terme synérèse a été énoncé en 1864 par Graham pour désigner la séparation des gels de gélatine, d'agar, d'amidon de leur phase liquide [11]. Dans la littérature, ce terme a été utilisé aussi pour décrire l'expulsion spontanée de liquide de plusieurs produits tels que les sauces, les confitures, les produits à base de viande [7], les peintures à base de latex [12], aussi bien que la contraction de gel avec expulsion de la phase liquide [10] comme la séparation du lactosérum (petit lait) lors de la fabrication du fromage [13].

La synérèse se distingue d'une sédimentation lente par le fait que l'expulsion de la phase liquide se fait par contraction du réseau tridimensionnel sans orientation dans une direction spécifique. La sédimentation et les autres formes de compression osmotique et ou mécanique, pouvant entrainer l'expulsion de liquide du gel sont des causes extérieures au gel. La durée de stockage du gel est un paramètre important dans la manifestation de la synérèse [14, 15]. La température [16], la force ionique [17, 18, 19], la pression [20], le pH [7], la masse moléculaire [7, 21] … sont des paramètres qui influencent la synérèse des gels, mais ceci dépend beaucoup des caractéristiques physicochimiques de la phase solide. Dans tous les cas, la concentration de la phase solide joue un rôle important dans la synérèse [18].

3 Les différents systèmes en rapport avec la synérèse

3.1 Polymère synthétique :

Les hydrogels à base de polymères synthétiques montrent une instabilité au cours du temps, Digiacomo et al., (1983) [22] et Albonico et al., (1993) [23] ont rapporté que les hydrogels synthétiques de Polyacrylamide en présence de Cr^{3+} manifestent la synérèse à la température de 126°C et 120°C respectivement. Le travail de Zhang et al., (2015) [24] explique le mécanisme de synérèse du gel de polyacrylamide partiellement hydrolysé (HPAM) en présence de Cr^{3+}. En effet, la sur-réticulation se produit entre la liaison C-O dans COO- du HPAM et les cations Cr^{3+}, contribue à l'expulsion d'eau. Albonico et al., (1997) [25] ont étudié la synérèse de HPAM en présence de Cr^{3+}, Mg^{2+} et Ca^{2+}, ils ont conclu que les cations Mg^{2+} et Ca^{2+} peuvent réagir avec le carboxylate de HPAM, ce qui augmente la densité de réticulation et cause la synérèse. Ogazawara et al., (1975) [26], Hong et al., (1998) [27] et Takeshita et al., (2001) [28] ont également montré que les gels à base de polymère synthétique Poly(vinylalcohol) (PVA) présentent une tendance à la synérèse.

3.2 Protéine

Les protéines sont des macromolécules constituées d'enchaînements d'acides aminés liés entre eux par des liaisons peptidiques (-CO-NH-), elles peuvent être d'origine végétale, bactérienne ou animale. Les gels à base de protéine de lait [16, 29], la gélatine [11] et la viande [7] sont des protéines susceptibles de manifester la synérèse. Dans l'industrie laitière, la synérèse est considérée comme une étape essentielle du processus de fabrication du fromage au cours duquel le lactosérum, composé d'environ 94% d'eau, est expulsé du gel de lait (caillé) [16]. Cependant, la synérèse peut constituer un défi majeur dans la fabrication du fromage, en perdant une fraction de protéines et de matières grasses par l'expulsion du lactosérum, ceci a un impact sur la saveur, couleur et la qualité du produit final [30, 31, 32]. En outre, la gélatine est la protéine la plus couramment utilisée dans le marché pharmaceutique pour la préparation des capsules [33], il présente aussi une tendance à la synérèse. Il convient de noter que la synérèse est l'un des principaux problèmes de l'industrie de viande car cela affecte considérablement le prix du kilo de viande. En effet, la viande fraîche est une structure protéique complexe avec environ 70% d'eau qui perd une partie de cette eau pendant le stockage [7].

3.3 Polysaccharide

Les polysaccharides, connus encore sous le nom de glycanes ou polyosides, sont des polymères de la famille des glucides, de très hautes masses molaires, constitués par l'enchaînement d'un grand nombre de mono saccharidique liés entre eux par des liaisons osidiques. En raison de leur biocompatibilité, biodégradation et de leur non-toxicité, ils ont attiré beaucoup d'attention dans les secteurs pharmaceutiques, biomédicale, cosmétiques, agroalimentaire et l'industrie papetière [34]. Les polysaccharides sont produits à partir d'une grande variété de ressources naturelles comme les végétaux (amidon, pectine, cellulose), les algues (carraghénanes, alginate, agar-agar, agarose…), les animaux (Chitine…), champignons (pullulane…) ou de sources bactériennes comme xanthane, gellane… [35]. Cependant, il apparaît que la majorité des hydrogels de polysaccharide tels que le pullulane, gellane, carraghénane, alginate, agar, xanthane, amidon et chitosane, expulsent naturellement leur solvant [8, 14, 18, 36, 37, 38, 39].

3.3.1 Carraghénane

Le kappa-carraghénane en présence des contre ions tels que le KCl [18, 40, 41], $CaCl_2$ [41], NaCl [41] présente généralement une synérèse qui augmente au fil du temps, mais en présence d'iodure, un co-ion spécifique, le kappa-carraghénane forme des hélices mais l'agrégation est

inhibée. Iota-carraghénane a peu ou pas de synérèse [41] alors que le lambda-carraghénane ne donne que des solutions visqueuses en présence d'ions mono et divalents [41, 42].

3.3.2 Alginate

Les alginates sont des polysaccharides anioniques obtenus à partir des algues brunes, constitués de deux monomères, linéaire à liaison (1-4) de l'acide α-L-guluronique (G) et l'acide β-D-manuronique (M) [43]. En présence de cations divalents comme Ca^{2+}, les cations forment des zones de jonction entre les séquences de G de l'alginate [44], créant ainsi un réseau tridimensionnel thermostable [45]. Les gels de Ca-alginate montrent une réticulation de zones de jonction donnant lieu à la synérèse [21].

3.3.3 Agar-Agar

L'agar est un polysaccharide linéaire composé de deux saccharides, l'agarose neutre et agaropectine anionique [46]. L'agarose est constituée d'unités alternées de 3,6-anhydro-α-L-galactopyranose et de β-D-galactose liées en (1-3), c'est la fraction gélifiante de l'agar [47]. L'agaropectine est une molécule de la famille des agars mais davantage sulfatée et non gélifiante. L'agar forme des gels physiques thermoréversibles dont l'unité constitutive est une double hélice antisymétrique [48], et présentant une grande hystérésis [37, 49, 50] entre la température de gélification $T_{gel} \approx 40°C$ et de fusion $T_{fus} \approx 80°C$ [49]. Les hydrogels d'agar sont également sujets à la synérèse [37, 49, 51], ce phénomène est expliqué par la contraction du réseau de polymère due à l'agrégation des hélices [52].

3.3.4 Amidon

L'amidon est un glucide complexe constitué de deux homopolymères : l'amylose et l'amylopectine dont les proportions varient avec l'origine botanique de l'amidon (Riz, pomme de terre…), l'amidon contient également un certain nombre de constituants mineurs présents en faible quantité (moins de 1%) [53]. En effet, il est connu que le gel d'amidon présente une synérèse due à l'augmentation de l'association moléculaire entre les chaines d'amidon, en particulier la rétrogradation de l'amylose, formation également de doubles hélices [54] conduisant à une libération d'eau de la structure du gel [53].

3.3.5 Xanthane

Le xanthane est un polysaccharide anionique constitué d'un squelette cellulosique de résidus β-(1-4)-D-glucose, et une chaine de saccharides constituée de β-(1-4)-D-mannose, β-(1,4)-D-glucuronique et un β-(1-2)-mannose attachée en C3 aux résidus alternatifs de glucose de la

chaine principale [55]. En solution, le xanthane est caractérisé par une transition conformationnelle ordre-désordre, à une température de transition T_m, au cours de laquelle les chaines passent d'une conformation ordonnée semi-rigide, à une conformation désordonnée flexible [56]. Les mesures de pouvoir rotatoire de la transition ordre-désordre ont montré que la force ionique croissante rend la conformation ordonnée plus stable (T_m augmente) [56, 57, 58]. Les hydrogels de xanthane libèrent spontanément son solvant par réticulation des chaines du réseau polysaccharidique lors de la conservation [8].

3.3.6 Chitosane

Le chitosane est un polysaccharide cationique d'origine animale, composé d'unités D-glucosamine et de N-acétyle-D-glucosamine reliées par des liaisons β-(1-4) [59], il est produit par désacétylation chimique (en milieu alcalin) ou enzymatique de la chitine [60]. Hirano et al., (1976) [61] et Graham et al., (1980) [39] ont signalé que les gels de chitosane, en milieu acide, sont susceptibles à la synérèse.

D'autre gels de polysaccharide tels que la gomme gellane [14, 51], pullulane [36], pectine [62, 63] sont également susceptibles de manifester la synérèse.

3.4 Émulgels et mélange des polysaccharides

Les émulsions sont des systèmes constitués d'au moins deux liquides non miscibles, l'un étant dispersé sous forme de gouttelettes dans l'autre. Généralement, elles sont obtenues en mélangeant de l'eau avec un composé organique apolaire [64]. Lorsque l'émulsion peut gélifier, on obtient un « émulgels ». Différentes études sur la stabilisation des émulsions, contenant des émulsifiants protéiques, par les polysaccharides ont été réalisées [59, 65, 66, 67]. Laplante et al., (2006) [65] ont montré que l'ajout de chitosane au gel de protéine augmente le module de stockage G' et diminue la synérèse des gels protéiques, la même étude a été faite par Chen et al., (2007) [68] en utilisant les protéines de viande mélangée avec le polysaccharide. Comfort et al., (2003) [69] ont montré que 20% (w/w) de protéines de viande solubles dans le sel (SSMP) forment des gels plus fragiles que les gels produits avec 20% (w/w) de protéines de blé (SWP). Ce dernier étant caractérisé par une faible synérèse. L'ajout de 1% (w/w) de SWP au système SSMP 20% (w/w), triple le module élastique de mélange SSMP/SWP (20 :1), par rapport au gel de SSMP seul et entraine une diminution de 50% de la synérèse. Plusieurs autres études sont faites sur les gels mixtes avec au moins deux hydrocolloïdes pour réduire, ralentir ou arrêter la synérèse des gels ; les exemples incluant les deux polysaccharides sont gellane et agar [51],

kappa et iota-carraghénane [70], kappa-carraghénane avec le xanthane [40], pullulane et kappa-carraghénane [36] et amidon avec le glucomannane de konjac [71] ou encore agarose et iota-carraghénane [47]. Le kappa-carraghénane / agar sont mélangé avec la génipine [72] pour réduire la synérèse.

Tableau 1: Répartition de quelques polymères en relation avec la synérèse

Type de polymère		Origine	Propriété	Condition de la synérèse	Réf
Polysaccharides	Kappa-Carraghénane	Algue	Chargé Thermoréversible	4g/L κ-Carr / 40 mM KCl - 22°C 1à 8 g/L κ-Carr / 40 mM KCl - 9°C 2 et 4 g/L κ-Carr / 10 à 100 mM KCl - 9 °C	[18] [20] [19]
	Alginate	Algue	Chargé Thermosensible	10g/L Alginate / Ca^{+2} ≥15 mM 2% w/w Alginate / 50, 100, 150 et 200 mM Ca^{+2} pH entre 4 et 11	[21] [44]
	Agar	Algue	Thermoréversible	Entre 0.75% et 2% w/w (eau distillée) - 4°C 0,1, 0.2 et 0.3% w/v (eau distillée) - 20°C 1,5% (w/w) - 25°C	[51] [37] [49]
	Amidon	Végétale terrestre	Thermo-irréversible	4 et 8% w/w (eau distillée) - 4°C 9% w/w – 25°C	[73] [38]
	Pectine	Végétale terrestre	---	0,4 et 0.5 % w/w - température ambiante	[62]
	Chitosane	Animale	Non réversible	2.5% chitosane / acide acétique 5% à 25°C	[39]
	Xanthane	Bactérienne	Thermoréversible [56]	4000ppm Xanthane / (50ppm Cr^{3+}+3% KCl)	[8]
	Gellane	Bactérienne	---	1% / entre 2 et 80mM de Ca^{2+} - 4°C Entre 0.25% et 2% (eau distillée) - 4°C	[14] [51]
Protéines	Gel de lait	Animale	---	Gel de lait gélifie par δ-gluconolactone - 5°C et 30°c, pH=4.6	[30]
	Gel de fromage	Animale	---	10 L de fromage - pH=6 et 6.5	[32]
	Gélatine	Animale	---	pH=4.7 à 5°C	[11]
Polymère synthétique	Polyacrylamide	Synthétique	---	Polyacrylamide / Cr^{3+} - 126°C Polyacrylamide / Cr^{3+} - 120°C	[22] [23]
	HPAM/Cr^{3+}	Synthétique	---	HPAM/Cr^{3+} en présence de Na^{+}, Mg^{2+}, Ca^{2+} HPAM/Cr^{3+} en présence de Ca^{2+}, Mg^{2+} -90°C	[24] [25]
	Poly (vinyl alcohol)	Synthétique	Thermoréversible	Poly (vinyl alcohol) / éthylène glycol	[27]
Mélange des hydrocolloïdes	Gellane Agar	Bactérienne Algue	--- Thermoréversible	Gellane / agar (1 :1) de 0.25 à 4% (w/w)	[51]
	Protéine Polysaccharide	Animale végétale	---- Thermoréversible	Protéine 2% / 0 à 2% Gomme de lin - 4°C	[68]
	Protéine Chitosane	Animale Animale	----	Protéine 0-1% / Chitosane 0.075 à 0.3% pH entre 4 et 6 - 20°C	[59]
	Protéine animale Protéine végétale	Animale Végétale	Gel fragile Gel élastique fort	Protéine de viande 20% / Protéine de blé 1%	[69]

4 Mécanisme de la synérèse

Comme mentionné précédemment, la synérèse est définie comme l'expulsion du solvant due à la contraction du gel en l'absence de forces externe (synérèse endogène) ou renforcée par une contrainte externe (synérèse exogène), comme la gravité [19, 74], les forces de surface telles l'adhésion aux parois du récipient [49, 75], ou centrifugation [16, 73, 76]. Dans cette partie, la documentation est limitée à la synérèse endogène. Quel que soit le type de polymère en relation avec la synérèse, le rétrécissement du gel nécessite une force motrice pour qu'il occupe un volume plus faible. La synérèse provient de la transition pelote-hélice et l'agrégation des hélices connue pour de nombreux polysaccharides anioniques, comme le kappa-carraghénane en présence des cations (K+, Na+, Ca^{2+}) et le xanthane en présence de Cr^{3+} [8], ou polysaccharide neutre comme agarose et amidon. Cette transition conformationnelle peut continuer à se produire longtemps après la gélification. Pour l'alginate et en présence de Ca^{2+}, les cations se lient aux unités G d'alginate en formant un réseau de gel tridimensionnel [44]. Au cours de la formation du gel, les groupes carboxylates (-COO-) de l'alginate, chargés négativement, interagissent avec les cations (Ca^{2+}), ce qui entraîne une attraction électrostatique et en conséquence l'expulsion d'eau du gel.

En ce qui concerne les gels de protéines de lait, le rétrécissement du gel est le résultat de la pression endogène formée par les réarrangements des particules des hydrocolloïdes (micelles de caséine) et par les interactions interparticulaires dans le système [7, 16, 31]. Généralement, les auteurs considèrent la sur-réticulation comme étant la raison principale de la synérèse [8, 21, 36, 7, 24, 25, 77, 78, 79, 80].

5 Influence de différents paramètres physico-chimiques sur la synérèse

Au cours du temps, les gels physiques expulsent spontanément le solvant, le taux de la synérèse est influencé par de nombreux facteurs, notamment, les propriétés rhéologiques du gel, la concentration en polymère, la masse moléculaire, la température, le type et la concentration du sel de même que le pH.

5.1 Influence des propriétés rhéologiques du gel sur la synérèse

Plusieurs études montrent la relation entre les propriétés rhéologiques du gel et la synérèse [18, 21, 14, 69]. Ako (2015) [18] a montré que l'élasticité du gel joue un rôle important sur le comportement de la synérèse, en effet, ses résultats montrent une diminution du degré de

synérèse du gel de κ-Car avec l'augmentation de l'élasticité. De même, Mao et al., (2001) [14] et Comfort et al., (2003) [69], ont montré que les gels fragiles de polysaccharides [14] ou de protéines [69] sont plus sensibles à la synérèse que les gels élastiques. On note ici, que la libération du solvant commence lorsque la gélification se produit et si l'élasticité est inférieure à la pression de compression dans le gel [18, 81]. Tous les paramètres pouvant influencer la rhéologie notamment la viscoélasticité du gel aura aussi une influence sur la synérèse. C'est le cas des paramètres suivants.

5.2 Influence de la concentration

L'influence de la concentration sur la synérèse des hydrogels a été examinée sur différents types de polymère à savoir le kappa-carraghénane [18, 20, 82], l'amidon [73], l'agar [49, 51], gellane [51], protéine [16, 68] …. Les résultats montrent que la synérèse diminue avec l'augmentation de la concentration. Pour les polysaccharides, Viebke et al., (1994) [79] expliquent que l'augmentation de la concentration favorise la formation de réticulation physique, et les interactions entre les polysaccharides devraient dominer, ce qui augmente l'élasticité et en conséquence, la diminution de la synérèse. Mizrahi (2010) [7] indique que l'augmentation de la concentration du polymère fait augmenter la pression osmotique et empêche la synérèse.

5.3 Influence de la masse moléculaire Mw

Un autre facteur influençant le taux de la synérèse est le poids moléculaire, Draget et Al., (2001) [21] ont montré que pour le gel de Ca-alginate, la synérèse a été réduite en diminuant la Mw [17]. En effet, les longues chaines moléculaires présentent une flexibilité importante, ce qui augmente le nombre de réticulation et donc le taux de la synérèse. Souza et al., ont trouvé que les échantillons de carraghénane présentant la plus grande masse moléculaire Mw, forment des gels moins élastiques [83], ce qui augmente le degré de synérèse [18].

5.4 Influence de type et de concentration de sel

Plusieurs auteurs ont proposé une dépendance de la synérèse avec le sel, type et concentration. Gales et al., (1994) [8] ont étudié la stabilité du gel de xanthane en présence de Cr^{3+}, ils ont montré que l'augmentation du Cr^{3+} conduisait à une augmentation de la synérèse. Albonico et al., (1997) [24, 25] et Zhang et al., (2015) [25] ont trouvé le même résultat pour les gels de HPAM/Cr^{3+} sous l'effet du Ca^{2+} et de Mg^{+2} respectivement. Ce résultat a été expliqué par le

fait que le sel augmente la densité de réticulation, qui contribue au rétrécissement du gel. Ramdhan et al., (2019) [44] ont étudié l'effet de $CaCl_2$ sur le degré de la synérèse de gel d'alginate, ils ont rapporté que l'augmentation de la concentration de $CaCl_2$ entraînait une accélération du temps de gélification, une augmentation de la force du gel et un degré plus élevé de synérèse. En effet, les groupes carboxylates de l'alginate (-COO-), chargé négativement, interagissent avec le Ca^{2+}, cette attraction électrostatique entraîne un rétrécissement macroscopique du gel en expulsant l'eau de son réseau. Le taux de synérèse sature en présence d'un excès de $CaCl_2$ [44].

Contrairement à ces résultats, la synérèse de κ-Car provient de la transition pelote-hélice, agrégation de double hélice selon le modèle de Rees 1969 [84] et de Morris (1980) [85], ou de simple hélice selon Smidsrod (1984) [86] pour former du gel tridimensionnel continu. Au fur et à mesure que la concentration de KCl augmente la température de gélification, le gel devient de plus en plus fort conduisant à une diminution de la synérèse [18, 82]. Notons ici, que le type de sel joue sur l'élasticité et en conséquence sur la synérèse du gel [80, 87].

5.5 Influence de la température

Ako (2015) [18] a montré que la synérèse du gel de κ-Car ne change pas significativement pour les températures loin de la température de gélification où les gels étaient forts. Cette température de changement de conformation dépend principalement du type et de la concentration de sel [41, 85, 88].

5.6 Influence de pH

Le pH est un facteur susceptible de modifier les propriétés des gels, telles que la rigidité, la perméabilité et donc le comportement de synérèse [10]. En effet, pour le gel d'alginate en présence de CaCl2, l'augmentation du pH entraîne une diminution du degré de synérèse [44, 89], même résultat a été trouvé pour le gel de lait [16, 32, 90]. Ceci est expliqué par l'augmentation de groupes chargés avec le pH, ce qui affecte la pression osmotique d'alginate [7] et la répulsion électrostatique entre les micelles de caséine [32].

6 Gélification et synérèse du kappa Carraghénane

6.1 Transition conformationnelle et sélectivité ionique

Par des mesures de polarimétrie, Rees et al., (1969) [91] ont observé une augmentation du pouvoir rotatoire au moment de la gélification caractérisant un changement de conformation (désordonnée à ordonnée). Cette transition a été mise en évidence par différentes techniques à savoir, la diffusion de la lumière [92, 93], la RMN [94], la calorimétrie [95], la diffraction des rayon X [96], et la rhéométrie [18]. D'un point de vue général, en solution aqueuse, les chaines de kappa et iota carraghénane sont dans un état désordonné sous la forme dite pelote à chaud, et en état ordonné sous forme d'hélice à froid. Rinaudo et al., (1979) [97] ont montré que la température de transition pelote-hélice dépend du type et de la concentration des contre ions cationiques présents dans la solution. En effet, le potassium réduit fortement la charge nette et par conséquence la solubilité du polysaccharide.

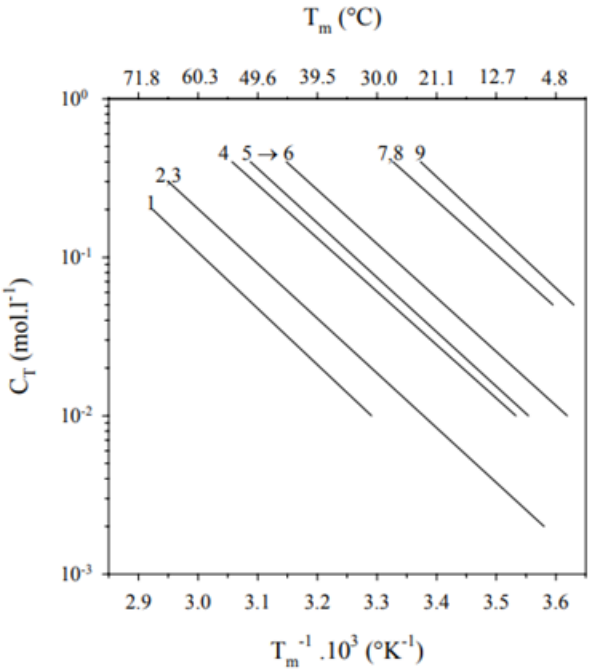

Figure 2: Température de transition pelote-hélix T_{ph} en fonction de la concentration totale C_T de sel pour différents types de contre ions, 1→ 4: Rb^+, K^+, Cs^+, $NH4^+$. 5 → 6: Ba^{2+}, Ca^{2+}, Sr^{2+}, Mg^{2+}, Zn^{2+}, Co^{2+}. 7 → 9: Na^+, $N(CH3)_4^+$, Li^+ [98]

En solution et sous la forme pelote, l'ajout du potassium conduit à une transition de conformation pelote-hélice et à la formation du gel. En utilisant la polarimétrie, Rochas et al., (1980) [98] ont déterminé la dépendance de la température de transition pelote-hélice T_{ph}, avec

la concentration et la nature de différents sels. Cette étude permet, d'établir une classification de la capacité des ions à stabiliser la conformation hélicoïdale. Elle montre aussi la relation entre la température de transition et la concentration ionique (Fig. 2). Les travaux de Rochas [98] montrent la classification suivante de l'effet des sels sur la transition pelote-hélix :

Dans le cas des ions monovalents : $Rb^+ > Cs^+ > K^+ > NH4^+ > N(CH3)4^+ > Na^+ > Li^+$.

Dans le cas des ions bivalents : $Ba^{2+} > Ca^{2+} > Sr^{2+} > Mg^{2+} > Zn^{2+} > Co^{2+}$.

En présence des contres ions spécifiques, Hermansson et al., (1989) [99] et Morris et al., (1997) [100] ont observé par microscope électronique que le κ-Car forme des agrégats rigides assimilés à des bâtonnets rigides lors du refroidissement de la solution en dessous de T_{ph}. D'autre part, les co-ions n'avaient pas d'influence sur la stabilité de la conformation, sauf l'iodure en tant que co-ion participe avec le contre ion au changement conformationnel [93, 101]. Par exemple, les solutions de κ-Car en présence d'iodure de sodium ne gélifient pas, alors qu'elles gélifient en présence de chlorure de sodium.

Pour expliquer ce phénomène, Grasdalen et al., (1981) [101] ont montré par des mesures RMN ^{127}I, que l'existence des liaisons spécifiques entre le carraghénane et l'iodure donne lieu à une stabilisation des hélices. Cette hypothèse a été renforcée par les études faites par Nerdal et al., (1993) [102], et Zhang et al., (1992) (1993) [103, 104].

6.2 Mécanisme de gélification des carraghénanes

Le mécanisme de gélification du kappa et iota carraghénane est un sujet de discussion entre les différents auteurs dont les modèles s'opposent sur l'idée de simple ou mono-hélix et double hélix. Cependant, les auteurs sont d'accord sur le mécanisme en deux étapes : 1) La transition pelote-hélice, et 2) agrégation des hélices. En effet, la présence des contre ions permet de neutraliser ou d'écranter les charges des groupements sulfates et conduit à l'agrégation et à la formation d'un réseau tridimensionnel [85].

Le premier modèle présenté par Rees [84] suppose la formation de double hélice. Les zones de jonctions du gel sont formées par l'agrégation de ces doubles hélices et par la suite la formation du réseau tridimensionnel par l'existence d'irrégularités « kinks » de la structure primaire (Fig. 3).

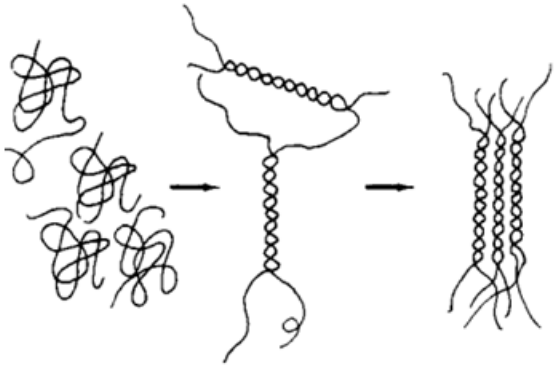

Figure 3: Modèle de transition sol-gel selon Rees [84]

Par la suite, Morris et al., (1980) [85] montrent que les carraghénanes à l'état ordonné ont une conformation de doubles hélices. En présence des cations, ces doubles hélices s'associent entre elles pour former des jonctions ioniques (Fig. 4).

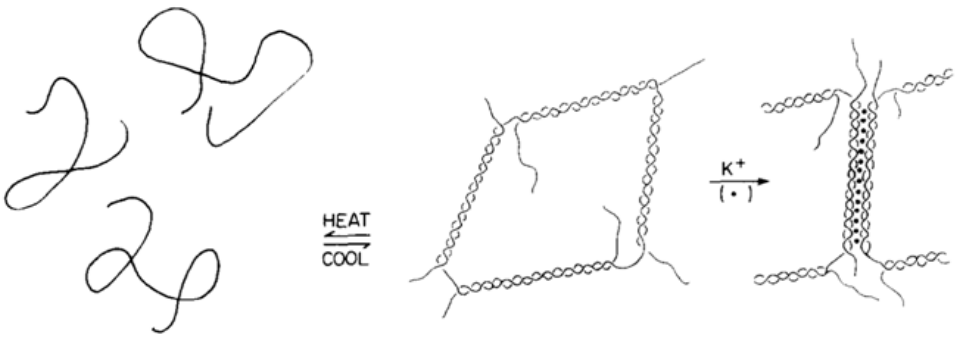

Figure 4: Modèle de transition sol-gel selon Morris [85]

Le second modèle proposé par Smidsrod et al., [105] implique la transition en structure ordonnée mais en simple hélice et les jonctions spécifiques entre les mono-chaines (simple hélix) se font par pont potassium.

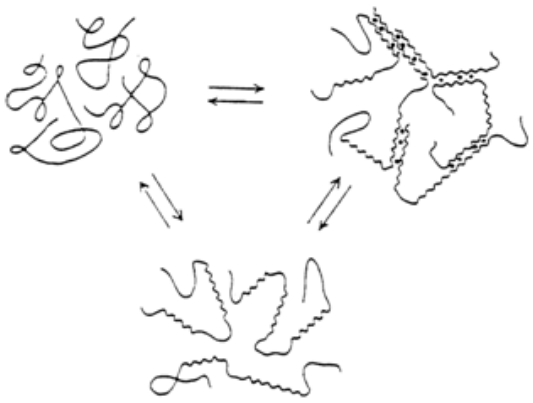

Figure 5: Modèle de transition sol-gel selon Smidsrod [105]

Rochas a établi un diagramme de phases (Fig. 6) qui met en évidence l'existence de plusieurs domaines en se basant sur la détermination des températures de transition pelote-hélice par polarimétrie. Cette méthode permet de caractériser les différentes conformations adoptées par le κ-Car.

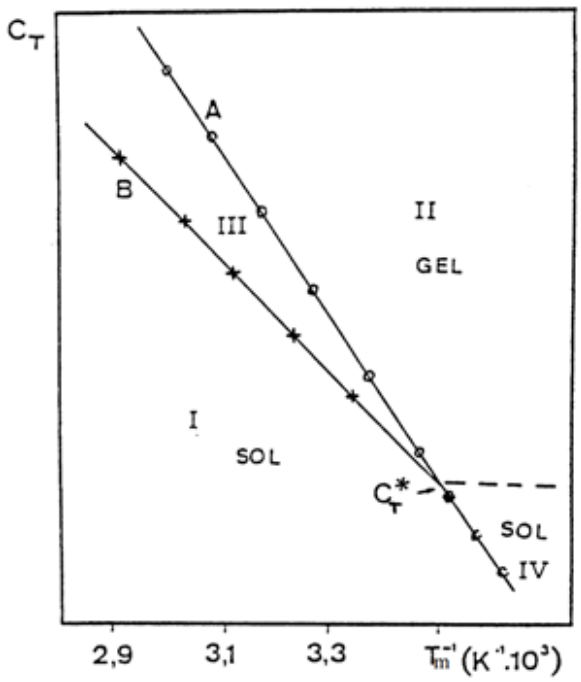

Figure 6: Variation de l'inverse de T_{ph} ou T_m en fonction de C^T en ion K+ lors du refroidissement (cercle) et du chauffage (croix) [98]

✓ Région I : le κ-carraghénane a une conformation non ordonnée (pelotes macromoléculaires en solution).

✓ Région II : la température inférieure à T_{ph} et $C_T > C_T^*$, le κ-carraghénane adopte une conformation ordonnée (hélice dans l'état gel). Ces hélices sont agrégées et la transition conformationnelle présente un cycle d'hystérèse.

✓ Région III : elle correspond à l'écart entre les températures de transition au chauffage et au refroidissement (Cycle d'hystérèse). L'état hélix ou pelote dépend de la rampe de température.

✓ Région VI : le κ-carraghénane a une conformation ordonnée sous forme de dimères d'hélices non agrégés (sol), ici la transition conformationnelle se fait sans hystérésis.

La question de la structure des carraghénanes dans sa conformation ordonnée a une longue histoire et n'est toujours pas résolue [106]. Viebke et al., (1995) [107] et Ueda et al., (1998) [108] ont déterminé la masse molaire de κ-Car en état pelote et en conformation hélicoïdale

induite par l'ajout d'iodure, co-ion spécifique, qui empêche l'agrégation, les résultats de la chromatographie d'exclusion stérique couplée à des mesures de diffusion de la lumière montrent un doublement de la masse molaire au cours de la transition pelote-hélice. Les auteurs, par ces résultats, confirment la formation de doubles hélices. Les travaux menés par Slootmaekers et al., (1998) [93] vont dans le sens de la formation de simples hélices, en accord avec les résultats de Bongaerts et al., (1999) [109] et Meunier et al., (2001) [106]. La structure locale, simple ou double, de κ-carraghénane sous forme hélicoïdale est importante pour comprendre les mécanismes impliqués dans l'agrégation et la gélification ultérieures [106]. Comme la transition pelote-hélice est thermoréversible, la gélification de κ-Car peut être inversée par chauffage, mais la température de transition gel-sol (fusion) est souvent plus élevée que la température de transition sol-gel (gélification). Ce phénomène a été observé par les mesures, en continu en utilisant la rampe de montrée et de descente de la température du pouvoir rotatoire [85, 108, 110], du module élastique [41], de l'intensité de transmission des photons [111], de l'intensité de fluorescence [112]. Le comportement d'hystérèse a été interprété par la stabilisation de la conformation hélicoïdale (ordonnée) par l'agrégation [85, 108, 110]. Les mesures du pouvoir rotatoire [4] montrent qu'en présence de forte concentration en ions K^+, le κ-carraghénane passe rapidement d'un état sol désordonné à l'état gel ordonné. Meunier et al., (1999) [113], ont montré que la gélification est très lente près de T_{ph}, mais le taux de gélification du κ-Car en présence de KCl augmente avec la diminution de la température et avec l'augmentation de la concentration en polymère dans la gamme de 0.2 à 2 g/L de κ-Car.

L'effet de la concentration en sel sur l'agrégation et la gélification de κ-Car a été étudié en détail dans les travaux de Meunier portant sur le polysaccharide. En effet, l'augmentation de la force ionique, augmente la température de transition et le taux d'hélices, ce qui contribue à accélérer considérablement la cinétique d'agrégation des hélices et la gélification [4].

7 Différentes méthodes d'évaluation et de quantification de la synérèse

La synérèse des hydrogels peut être facilement détectée par observation si elle est importante, cette méthode est simple mais qualitative. Les mesures quantitatives de la synérèse consistent simplement à peser la perte de solvant pour les gels ou à mesurer les changements de masse des solides restants. Boral et al., (2010) [37] ont déterminé la cinétique de la synérèse des hydrogels d'agar en retirant périodiquement l'eau accumulée sur la surface du gel, et sa masse a été mesurée à l'aide d'une microbalance. Ako (2017) [20] a utilisé cette méthode en plaçant le gel de κ-Car en présence de KCl dans une seringue perforée graduée pour suivre le volume du gel.

Charoenrein et al., (2008) [38] ont utilisé une méthode pas trop loin de celle-ci, en mettant le gel d'amidon sur un papier filtre permettant à l'eau de s'écouler par gravité. Le taux de la synérèse a été exprimé en déterminant la variation relative de masse [37, 38] ou du volume de gel [20]. Une autre méthode utilisée par Boral et al., (2010) [37] et Ako (2017) [20] consiste à retirer l'eau de synérèse à l'aide d'une micropipette et à la remettre en place après avoir mesuré la masse du gel. Laplante et al., (2005) [59] ont déterminé le taux de la synérèse d'émulgel composé d'un mélange de chitosane, protéine et d'huile colorée, en plaçant l'émulsion dans un tube en verre afin de suivre l'évolution de l'épaisseur de couche de la phase inférieure quotidiennement. La phase inférieure étant l'émulgel coloré et la phase supérieure étant le solvant d'apparence transparente, ou semi-transparente. Chen et al., (2007) [68] ont mesuré le pourcentage de liquide surnageant l'émulgel de protéine/gomme de lin après centrifugation pendant 20 min à 4 °C afin d'accélérer le processus. Cette méthode est utilisée par plusieurs auteurs [7, 16, 38, 51, 73, 76]. La masse ou le volume du liquide perdu par la synérèse est directement mesuré par le changement de la masse ou du volume de gel restant. D'autres méthodes en ligne permettant de surveiller et de mesurer la synérèse, comme les techniques de vision par ordinateur, d'analyse d'image [114], l'analyse de la couleur [32], ou d'analyse des spectres obtenus à partir de capteur de lumière en ligne visible étendue au proche infrarouge (NIR - Near Infra Red) [115]. La mesure de la synérèse par macro-indentation a été utilisée par Mao et al., (2017) [116] pour étudier le vieillissement et les propriétés mécaniques des gels d'agar. Nous avons accordé une attention particulière à cette méthode de mesure de la synérèse dans cette thèse vu que les résultats de cette méthode sont directement comparables aux résultats obtenus par la méthode de la seringue perforée qui avait été utilisée au laboratoire. La variation relative de la hauteur du gel mesurée par la méthode de la seringue perforée ou celle de la macro-indentation se traduit en taux de synérèse.

8 Références

[1] K. Almdal, J. Dyre, S. Hvidt et O. Kramer, «Towards a Phenomenological Definition of the term "Gel",» Polymer Gels and Networks, vol. 1, pp. 5-17, 1993.

[2] P. Herman, 11, ed, H. R. Kruyt, Elsevier publ. Co. Inc., 1949:, Colloid Science.

[3] L. Rogovina, V. G. Vasil'ev et E. Braudo, «Definition of the Concept of Polymer Gel,» Polymer Science, vol. 50, pp. 85-92 , 2008.

[4] V. Meunier, Etude de l'agrégation et de la gelification du kappa-carraghenane, Le Mans: Thèse de l'université du Mans, 1999.

[5] T. Graham, X. Liquid Diffusion applied to Analysis, transactions of the Royal Society of London, 1861.

[6] M. Madau, Hydrogels adaptatifs stimuli-sensibles (temperature et lumière) à base d'acide hyaluronique (HA), Rouen: thèse de l'Université de Rouen Normandie, 2021.

[7] S. Mizrahi, «Syneresis in food gels and its implications for food quality,» Chemical Deterioration and Physical Instability of Food and Beverages, Vols.1 pp. 2324-348, 2010.

[8] J. Gales, T. Young, G. Willhite et D. Green, «Equilibrium Swelling and Syneresis Properties of Xanthan Gum/Cr(III) Gels,» SPE Advanced Technology, vol. 2(2), pp. 190-198, 1994.

[9] V. Gopalakrishnan, K. Schweizer et C. Zukoski, «Linking single particle rearrangements to delayed collapse times in transient depletion gels,» Journal of Physics: Condensed Matter, vol. 18, pp. 11531-11550, 2006.

[10] G. Scherer, «Mechanics of syneresis,» Journal of Non-Crystalline Solids, vol. 108, pp. 18-27, 1989.

[11] M. Kunitz, «Syneresis and swelling of gelatin,» The Journal of General Physiology, pp. 289-312, 1928.

[12] F. Anwari, B. Carlozzo et K. Chokshi, «Clear Liquid Separation in Latex Paints containing cellulosic/associative thickener systems,» Journal of Coatings technolgy, vol. 65(825), pp. 123-134 , 1993.

[13] P. Gelebart, Modulation de la texture de gels acides laitiers par addition d'agrégats de protéines laitières, Nantes : Thèse de l'Université ed nantes, 2019.

[14] R. Mao, J. Tang et B. Swanson, «Water holding capacity and microstructure of gellan gels,» Carbohydrate Polymers, vol. 46, pp. 365-371, 2001.

[15] G. Toncheva, D. Hadjikinov et I. Panchev, «Investigation of syneresis of agar jellies,» Food Chemistry, vol. 49, pp. 29-31 , 1994.

[16] M. Pearse et A. Mackinlay, «Biochemical Aspects of Syneresis: A Review,» Journal of Dairy Science, vol. 72, pp. 1401-1407, 1989.

[17] K. Draget, K. Ostgaard et O. Smidsrod, «Homogeneous Alginate Gels: A Technical Approach,» Carbohydrate Polymers, vol. 14, pp. 159-178, 1991.

[18] K. Ako, «Influence of elasticity on the syneresis properties of k-carrageenan gels,» Carbohydrate Polymers, vol. 115, pp. 408-414, 2015.

[19] K. Ako, «Influence of osmotic and weight pressure on water release from polysaccharide ionic gels,» Carbohydrate Polymers, vol. 169, pp. 376-384, 2017.

[20] K. Ako, «Yield study with the release property of polysaccharide-based physical hydrogels,» International Journal of Biological Macromolecules, vol. 101, pp. 660-667, 2017.

[21] K. Draget et a. all, «Effects of molecular weight and elastic segment flexibility on syneresis in Ca-alginate gels,» Food Hydrocolloids, vol. 15, pp. 485-490 , 2001.

[22] P. M. Digiacomo et C. M. Schramm, «Mechanism of Polyacrylamide Gel Syneresis Determined by C-13 NMR,» Society of Petroleum Engineers of AIME, vol. SPE11787, pp. 165-172, 1983.

[23] P. Albonico et T. P. Lockhart, «Divalent Ion-Resistant Polymer Gels for High-Temperature Applications: Syneresis In hibiting Additives,» Society of Petroleum Engineers, vol. SPE 25220, pp. 651-665, 1993.

[24] G. Zhang, L. Chen, J. Ge, P. Jiang et X. Zhu, «Experimental research of syneresis mechanism of HPAM/Cr3+ gel,» Colloids and Surfaces A: Physicochemical and Engineering Aspects, vol. 483, pp. 96-103, 2015.

[25] P. Albonico et T. P. Lockhart, «Stabilization of polymer gels against divalent ion-induced Syneresis,» Journal of Petroleum Science and Engineering, vol. 18, pp. 61-71, 1997.

[26] K. Ogasawara, T. Nakajima, K. Yamaura et S. Matsuzawa, «Effect of syndiotacticity on the aqueous poly (vinyl alcohol) gel,» Progress Colloid & Polymer Science, vol. 58, pp. 145-151 , 1975.

[27] P. D. Hong, J. H. Chen et H. L. Wu, «Solvent Effect on Structural Change of Poly(vinyl alcohol) Physical Gels,» Journal of Applied Polymer Science, vol. 69, pp. 2477-2486, 1998.

[28] H. Takeshita, T. Kanaya, K. Nishida et K. Kaji, «Spinodal Decomposition and Syneresis of PVA Gel,» Macromolecules, vol. 34, pp. 7894-7898, 2001.

[29] N. Amalfitano, C.-G. Cipolat-Gotet, A. Cecchinato, M. Malacarne, A. Summer et G. Bittante, «Milk protein fractions strongly affect the patterns of coagulation, curd firming, and syneresis,» Journal of Dairy Science, vol. 102(4), pp. 2903-2917, 2019.

[30] J. Lucey et H. Singh, «Formation and physical properties of acid milk gels: a review,» Food Research Iniernational, vol. 30, n° 17, pp. 529-542, 1998.

[31] M. Castillo, J. A. Lucey, T. Wang et F. A. Payne, «Effect of temperature and inoculum concentration on gel microstructure, permeability and syneresis kinetics. Cottage cheese-type gels,» International Dairy Journal, vol. 16, p. 153–163, 2006.

[32] C. Everard, D. O'Callaghan, C. Fagan, C. O'Donnell, M. Castillo et F. Payne, «Computer Vision and Color Measurement Techniques for Inline Monitoring of Cheese Curd Syneresis,» Journal of Dairy Science, vol. 90(7), pp. 3162-3170, 2007.

[33] J. Barbosa, M. M. Al-Kauraishi, A. M. Smith, B. R. Conway et H. A. Merchant, «Achieving gastroresistance without coating: Formulation of capsule shells from enteric polymers,» European Journal of Pharmaceutics and Biopharmaceutics, vol. 144, pp. 174-179, 2019.

[34] J. Liu, S. Willfor et C. Xu, «A review of bioactive plant polysaccharides: Biological activities, functionalization, and biomedical applications,» Bioactive Carbohydrates and Dietary Fibre, vol. 5, pp. 31-61 , 2015.

[35] R. Walter, Polysaccharide dispersions: Chemistry and technology in food, vol. 236, San Diego, California, USA: Academic Press, 1997.

[36] Y. Zhang et all, «Effects of κ-carrageenan on pullulan's rheological and texture properties as well as pullulan hard capsule performances,» Carbohydrate Polymers, vol. 238, n° 1116190, 2020.

[37] S. Boral, A. Sexena et H. Bohidar, «Syneresis in agar hydrogels,» International Journal of Biological Macromolecules, vol. 46, pp. 232-236, 2010.

[38] S. Charoenrein, O. Tatirat et J. Muadklay, «Use of centrifugation–filtration for determination of syneresis in freeze–thaw starch gels,» Carbohydrate Polymers, vol. 73, pp. 143-147, 2008.

[39] K. M. Graham et G. A. F. Roberts, «Chitosan gels: 1. Study of reaction variables,» International Journal of Biological Macromolecules , vol. 2, pp. 73-77, 1980.

[40] S. Hotchkiss, M. Brooks et R. Campbell, The use of carrageenan in food, Leonel Pereira-Nova Science Publishers, Inc, 2016.

[41] V. Lai, P. Wong et C. Lii, «Effects of Cation Properties on Sol-gel Transition and Gel Properties of k-carrageenan,» Food Engineering and Physical Properties, vol. 62(8), pp. 1332-1337, 2000.

[42] C. A. Running, R. Falshaw et S. Janaswamy, «Trivalent iron induced gelation in lambda-carrageenan,» Carbohydrate Polymers, vol. 87, p. 2735–2739, 2012.

[43] H. Ertesvåg, S. Valla et G. Skjåk-Bræk, Enzymatic Alginate Modification. In B.H.A. Rehm (ed.), Alginates: Biology and Applications, Springer-Verlag Berlin Heidelberg, 2009.

[44] T. Ramdhan, S. H. Ching, S. Prakash et B. Bhandaria, «Time dependent gelling properties of cuboid alginate gels made by external gelation method: Effects of alginate-CaCl2 solution ratios and pH,» Food Hydrocolloids, vol. 90, p. 232–240, 2019.

[45] P. Agulhon, M. Robitzer, L. David et F. Quignard, «Structural Regime Identification in Ionotropic Alginate Gels: Influence of the Cation Nature and Alginate Structure,» Biomacromolecules, vol. 13, pp. 215-220, 2011.

[46] M. Duckworth et W. Yaphe, «The structure of agar, Part I. Fractionation of a complex mixture of polysaccharides,» Carbohydrate research, vol. 16, pp. 189-197, 1971.

[47] F. B. A. Descallar, A. Wang et S. Matsukawa, «The influence of iota carrageenan on water mobility and aging of agarose gels,» Food Hydrocolloids , vol. 123 (106930), 2022.

[48] E. Pines et W. Prins, «Structure-Property Relations of Thermoreversible: Macromolecular Hydrogels,» Macromolecules, vol. 6(6), pp. 888-895, 1973.

[49] T. Divoux, B. Ma et P. Snabre, «Syneresis and delayed detachment in agar plates,» Soft Matter, vol. 11, pp. 3677-3685, 2015.

[50] Z. H. Mohammed, M. W. N. Hember, R. K. Richardson et E. R. Morris, «Kinetic and equilibrium processes in the formation and melting of agarose gels,» Carbohydrate Polymers, vol. 36, pp. 15-26, 1998.

[51] S. Banerjee et S. Bhattacharya, «Compressive textural attributes, opacity and syneresis of gels prepared from gellan, agar and their mixtures,» Journal of Food Engineering, vol. 102, pp. 287-292, 2011.

[52] C. Lain et D. Rees, «Affinity Interactions Between Agarose and B-1,4-Giycans: a Model for Polysaccharide Associations in Algal Cell Walls,» Carbohydrate Polymers, vol. 7, pp. 183-224, 1987.

[53] C. Lafarge, Impact du glucomannane de konjac sur les interactions composés volatils - amidon de pomme de terre dans un gel hydraté, Dijon: Thèse de l'Université de Bourgogne, 8 décembre 2016.

[54] V. Morris, «Starch gelation and retrogradation,» Trends in Food Science & Technology, vol. 1, pp. 2-6, 1990.

[55] E. Pelletier, C. Viebke, J. Meadowq et P. Williams, «A rheological study of the order–disorder conformational transition of xanthan gum,» Biopolymers, vol. 59, pp. 339-346, 2001.

[56] E. Morris, D. Rees, G. Young, M. Walkinshaw et A. Darke, «Order-disorder transition for a bacterial polysaccharide in solution. A role for polysaccharide conformation in recognition between Xanthomonas pathogen and its plant host,» Journal of Molecular Biology, vol. 110, pp. 1-16, 1977.

[57] I. T. Norton, D. M. Goodal, S. A. Frangou, E. R. Morris et D. A. Rees, «Mechanism and dynamics of conformational ordering in xanthan polysaccharide,» Journal of Molecular Biology, vol. 175(3), pp. 371-394, 1984.

[58] C. Viebke, Order-disorder conformational transition of xanthan gum., Polysaccharides: Structural diversity and functional versatility,2, 2005.

[59] S. Laplante, S. L. Turgeon et P. Paquin, «Effect of pH, ionic strength, and composition on emulsion stabilising properties of chitosan in a model system containing whey protein isolate,» Food Hydrocolloids, vol. 19, pp. 721-729, 2005.

[60] «https://fr.wikipedia.org/wiki/Chitosane,» Wikipédia, 19 Avril 2022. [En ligne].

[61] S. Hirano et R. Yamaguchi, «N-Acetylchitosan Gel: A Polyhydrate of Chitin,» Biopolymers, vol. 15, pp. 1685-1691, 1976.

[62] L. Figueroa et D. Genovese, «Pectin Gels Enriched with Dietary Fibre for the Development of Healthy Confectionery Jams,» Food Technology and Biotechnology, vol. 56, n° 13, pp. 441-453, 2018.

[63] U. Einhorn-Stoll, «Pectin-water interactions in foods e From powder to gel,» Food Hydrocolloids, vol. 78, pp. 109-119, 2018.

[64] T. Merland, «Nanocomposite hydrogels from the self-assembly of an amphiphilic polymer and fullerene,» Thèse de Le Mans Université, Le Mans, 15 décembre 2021.

[65] S. Laplante, S. L. Turgeon et P. Paquin, «Emulsion-stabilizing properties of chitosan in the presence of whey protein isolate: Effect of the mixture ratio, ionic strength and pH,» Carbohydrate Polymers, vol. 65, pp. 479-487, 2006.

[66] E. Dickinson et V. B. Galazka, «Emulsion stabilization by ionic and covalent complexes of -lactoglobulin with polysaccharides,» Food Hydrocolloids, vol. 5, n° 13, pp. 281-296, 1991.

[67] A. Benichou, A. Aserin et N. Galti, «Protein-Polysaccharide Interactions for Stabilization of Food Emulsions,» Journal of Dispersion Science and Technology, vol. 23, pp. 93-123, 2002.

[68] H.-H. Chen, S.-Y. Xu et Z. Wang, «Interaction between flaxseed gum and meat protein,» Journal of Food Engineering, vol. 80, pp. 1051-1059, 2007.

[69] S. Comfort et N. Howell, «Gelation properties of salt soluble meat protein and soluble wheat protein mixtures,» Food Hydrocolloids, vol. 17, pp. 149-159, 2003.

[70] DANISCO CULTOR, «Introduction to GRINDSTED™ Carrageenan,» [En ligne]. Available: https://aditiva-concepts.ch/download/Carrageenan.pdf .

[71] S. Ma, P. Zhu, M. Wang, F. Wang et N. Wang, «Effect of konjac glucomannan with different molecular weights on physicochemical properties of corn starch,» Food Hydrocolloids, vol. 96, pp. 663-670, 2019.

[72] R. Meena, K. Prasad et A. Siddhanta, «Development of a stable hydrogel network based on agar– kappa-carrageenan blend cross-linked with genipin,» Food Hydrocolloids, vol. 23, pp. 497-509, 2009.

[73] L. C. Gonzalez, M. A. Loubes, M. M. Bertotto, R. I. Baeza et M. P. Tolaba, «Flow behavior and syneresis of ball milled rice starch and their correlations with starch

structure,» Carbohydrate Polymer Technologies and Applications , vol. 2, n° 1100168, 2021.

[74] S. Manley, J. M. Skotheim, L. Mahadevan et D. A. Weitz, «Gravitational Collapse of Colloidal Gels,» Physical Revieux Letters, vol. 94 (218302), 2005.

[75] Q. Wu, J. van der Gucht et T. E. Kodger, «Syneresis of Colloidal Gels: Endogenous Stress and Interfacial Mobility Drive Compaction,» Physical Review Letters, vol. 125 (208004), 2020.

[76] D. Verbeken, K. Bael, O. Thas et K. Dewettinck, «Interactions between k-carrageenan, milk proteins and modified starch in sterilized dairy desserts,» International Dairy Journal, vol. 16, pp. 482-488, 2006.

[77] J. Zhang, W. Ji, T. Liu et C. Feng, «Tuning syneresis properties of Kappa-Carrageenan hydrogel by C2-symmetric benzene-based supramolecular gelators,» Macromolecular Chemistry and Physics, vol. 217, pp. 1197-1204, 2016.

[78] T. Van Vliet, H. J. M. Van Dijkl, P. Zoon et P. Walstra, «Relation between syneresis and rheological properties of particle gels,» Colloid & Polymer Science, vol. 269, pp. 620-627, 1991.

[79] C. Viebke, L. Piculell et S. Nilsson, «On the Mechanism of Gelation of Helix-Forming Biopolymers,» Macromolecules, vol. 27(15), pp. 4160-4166, 1994.

[80] L. Piculell, I. S. Borgström, I. S. Chronakis, P. O. Quist et C. Viebke, «Organisation and association of k-carrageenan helices under different salt conditions,» International Journal of Biological Macromolecules, vol. 21, pp. 141-153, 1997.

[81] K. Ako, «HDR,» Université Grenoble Alpes, Grenoble.

[82] D. E. Dunstan, R. Salvatore, M. Jonsson et M.-L. Liao, «Syneresis of k-carrageenan gels at different KCl and LBG concentrations,» Gum and Stabilisers for the Food Industry 10, pp. 137-147, 2000.

[83] H. K. S. Souza, L. Hillioua, M. Bastos et M. P. Gonçalves, «Effect of molecular weight and chemical structure on thermal and rheological properties of gelling k/i hybrid carrageenan solutions,» Carbohydrate Polymers, vol. 85, pp. 429-438, 2011.

[84] D. A. Rees, «Structure, Conformation, and Mechanism in the Formation of Polysaccharide Gels and Networks,» Advances in Carbohydrate Chemistry and Biochemistry, vol. 24, pp. 267-332, 1969.

[85] E. Morris, D. Rees et G. Robinson, «Cation-specific Aggregation of Carrageenan Hekes : Domain Model of Polymer Gel Structure,» Journal of Molecular Biology, vol. 138, pp. 349-362, 1980.

[86] O. Smidsrod et H. Grasdalen, «Conformations of K-carrageenan in solution,» Hydrobiogia, vol. 116/117, pp. 178-186, 1984.

[87] A. M. Hermansson, E. Eriksson et E. Jordansson, «Effects of potassium, sodium and calcium on the microstructure and rheological behaviour of kappa-carrageenan gels,» Carbohydrate Polymers, vol. 16 (3), pp. 297-320, 1991.

[88] M. Ciancia, M. Milas et M. Rinaudo, «On the specific role of coions and counterions on K-carrageenan conformation,» International Journal of Biological Macromolecules, vol. 20, pp. 35-41, 1997.

[89] B. Doumèche, M. Küppers, S. Stapf, B. Blümich, W. Hartmeier et M. B. Ansorge-Schumacher, «New approaches to the visualization, quantification and explanation of acid-induced water loss from Ca-alginate hydrogel beads,» Journal of Microencapsulation, vol. 21(5), pp. 565-573, 2004.

[90] C. Daviau, A. Pierre, M. H. Famelart, H. Goudedranche, D. Jacob, M. Garnier et J. L. Maubois, «Characterisation of whey drainage kinetics during soft cheese manufacture in relation with the physicochemical and technological factors, pH at renneting, casein concentration and ionic strength of milk,» Lait 80, pp. 417-432, 2000.

[91] D. Rees, I. W. Steele et W. F. B., «Conformational Analysis of Polysaccharides. III. The Relation between Stereochemistry and Properties of Some Natural Polysaccharide Sulfates,» Journal of Polymer Science,, vol. 28, pp. 261-276, 1969.

[92] I. T. Norton et D. M. Goodall, «Role of Cations in the Conformation of Iota and Kappa Carrageenan,» Journal of the Chemical Society, vol. 79, pp. 2475-2488, 1983.

[93] D. Slootmaekers, C. De Jonghe, H. Reynaers, F. A. Varkevisser et C. J. Bloys van Treslong, «Static light scattering from k-carrageenan solutions,» International Journal of Biological Macromolecule, vol. 10, pp. 160-168, 1988.

[94] C. Rochas et M. Rinaudo, «Structural and conformational investigation of Carrageenans,» Biopolymers, vol. 19, pp. 2165-2175, 1980.

[95] C. Rochas et J. Mazet, «The conformational transition of κ-carrageenan using microcalorimetry,» Biopolymers, vol. 23, pp. 2825-2833, 1984.

[96] R. P. Millane, R. Chandrasekaran et S. Arnott, «The molecular structure of kappa-carrageenan and comparison with iota-carrageenan,» Carbohydrate Research, vol. 182, pp. 1-17, 1988.

[97] M. Rinaudo, A. Karimian et M. Milas, «Polyelectrolyte Behaviour of Carrageenans in Aqueous Solutions,» Biopolymers, vol. 18, pp. 1673-1683, 1979.

[98] C. Rochas et M. Rinaudo, «Activity Coefficients of Counterions and Conformation in Kappa-Carrageenans Systems,» Biopolymers, vol. 19, pp. 1675-1687, 1980.

[99] A.-M. Hermansson, «Rheological and microstrructural evidence for transient states during gelation of Kappa-carrageenan in the presence of potassium,» Carbohydrate Polymer, vol. 10, pp. 163-181, 1989.

[100] V. J. Morris, A. P. Gunning, A. R. Kirby, A. Round, K. Waldron et A. Ng, «Atomic force microscopy of plant cell walls, plant cell wall polysaccharides and gels,» International Journal of Biological Macromolecules, vol. 21, pp. 61-66, 1997.

[101] H. Grasdalen et O. Smidsröd, «Iodide-specific formation of κ-carrageenan single helices. 127I NMR spectroscopic evidence for selective site binding of iodide anions in the ordered conformation,» Macromolecules, vol. 14, pp. 1842-1845, 1981.

[102] W. Nerdal, F. Haugen, S. Knutsen et H. Grasdalen, «Evidence for double helical kappa-carrageenan in aqueous LiI-solution and model for iodide binding,» Journal of Biomolecular Structure & Dynamics, vol. 10(5), pp. 785-791, 1993.

[103] W. Zhang, L. Piculell et S. Nilsson, «Effects of specific anion binding on the helix-coil transition of lower charged carrageenans. NMR data and conformational equilibrium analysed within the Poisson-Boltzmann cell model,» Macromolecules, vol. 25, pp. 6165-6172, 1992.

[104] W. Zhang et I. Furo, «127I NMR studies of anion binding to κ-carrageenan,» Biopolymers, vol. 11, pp. 1709-1714, 1993.

[105] O. Smidsrod, I.-l. Andresen, H. Grasdalen, B. Larsen et T. Painter, «Evidence for a salt-promoted “freeze-out” of linkage conformations in carrageenans as a prerequisite for gel-formation,» Carbohydrate Research, vol. 80(1), pp. C11-C16, 1980.

[106] V. Meunier, T. Nicolai et D. Durand, «Structure of aggregating kappa-carrageenan fractions studied by light scattering,» International Journal of Biological Macromolecules, vol. 28, pp. 157-165, 2001.

[107] C. Viebke, J. Borgström et L. Piculell, «Characterisation of kappa- and iota-carrageenan coils and helices by MALLS/GPC,» Curbohjdrarr Polymers, vol. 27, pp. 145-154, 1995.

[108] K. Ueda, M. Itoh, Y. Matsuzaki, H. Ochiai et A. Imamura, «Observation of the Molecular Weight Change during the Helix-Coil Transition of k-Carrageenan Measured by the SEC-LALLS Method,» Macromolecules, vol. 31, pp. 675-680, 1998.

[109] K. Bongaerts, H. Reynaers, F. Zanetti et S. Paoletti, «On the Molar Mass of κ-Carrageenan in the Course of Conformational Transition from the Disordered to the Fundamental Ordered Form,» Macromolecules, vol. 32, pp. 675-682, 1999.

[110] C. Rochas et M. Rinaudo, «Mechanism of Gel Formation in k-Carrageenan,» Biopolymers, vol. 23, pp. 735-745, 1984.

[111] S. Kara, «Hysteresis During Sol–Gel and Gel–Sol Phase Transitions of k-Carrageenan: A Photon Transmission Study,» Journal of Bioactive and Compatible Polymers, vol. 18(1), pp. 33-44, 2003.

[112] Ö. Tari, S. Kara et Ö. Pekcan, «Critical exponents of kappa carrageenan in the coil-helix and helix-coil hysteresis loops,» Journal of Macromolecular Science, Part B: Physics, vol. 48, pp. 812-822, 2009.

[113] V. Meunier, T. Nicolai et D. Durand, «Light Scattering and Viscoelasticity of Aggregating and Gelling kappa-Carrageenan,» Macromolecules, vol. 32, pp. 2610-2616, 1999.

[114] C. C. Fagan, C.-J. Du, C. P. O'Donnell, M. Castillo, C. D. Everard, D. J. O'Callaghan et F. A. Payne, «Application of Image Texture Analysis for Online Determination of Curd Moisture and Whey Solids in a Laboratory-Scale Stirred Cheese Vat,» Food Engineering and Physical Properties, vol. 73 (6), pp. E250-E258, 2008.

[115] M. J. Mateo, D. J. O'Callaghan, C. D. Everard, M. Castillo, F. A. Payne et C. P. O'Donnell, «Evaluation of on-line optical sensing techniques for monitoring curd moisture content and solids in whey during syneresis,» Food Research International, vol. 43, p. 177–182, 2010.

[116] B. Mao, A. Bentaleb, F. Louerat, T. Divoux et P. Snabre, «Heat-induced aging of agar solutions: Impact on the structural and mechanical properties of agar gels,» Food Hydrocolloids, vol. 64, pp. 59-69, 2017.

Chapitre 1

Introduction générale

Chapitre 1 : Introduction générale

1 Généralité sur les gels de polymères et la configuration des polymères en solution

Un gel est un assemblage d'unité microscopique sous forme macromoléculaire, colloïdale ou polymère en unité macroscopique généralement de densité bien plus faible que celle des unités dont il est constitué. L'assemblage des unités microscopiques en unité macroscopique peut passer par des unités intermédiaires (mésoscopiques) qui sont des amas d'unités microscopiques ou agrégats, de densité intermédiaire, qui s'associent ensuite pour former le gel. La dynamique d'un tel système est complexe car elle peut être caractérisée par la dynamique des unités microscopiques en corrélation avec leur disposition et des liaisons entre elles dans le gel. Le mouvement d'une unité est donc lié au mouvement de l'autre et ainsi de suite jusqu'au mouvement de l'ensemble que représente le gel dans un état pseudo-statique. L'évaluation de l'équilibre du gel devient un problème de temps. Le temps relatif à l'observation ou à la mesure et au mouvement du gel dépend fortement des moyens humains et techniques déployés pour comprendre l'équilibre du gel [1]. Dans sa revue sur la contrainte seuil, Howard A. Barnes [2] formule l'idée selon laquelle "tout coule" en soulignant nos difficultés techniques et expérimentales à pouvoir mesurer les déformations extrêmement faibles des matériaux solides qualifié d'ultra durs et soumis à des forces de contrainte constante mais sur des durées très longues. Cette difficulté de temps d'observation et de mesure de très faibles déformations s'applique aussi au gel qui sont des matériaux mous et qui sont soumis à des forces de contraintes bien plus faible que les solides. Dans tous les cas, l'énoncé de Barnes vient en opposition ou du moins attire notre attention sur la loi de Hook qui formule l'idée selon laquelle la déformation des matériaux élastiques dont les gels évoluerait linéairement avec la force appliquée, c'est-à-dire, une force une déformation. Il devient difficile de traiter le sujet de la dynamique du gel sans tenir compte de la relation qui oppose la déformation perpétuelle et l'équilibre lorsque le gel est soumis à une force. En effet, la synérèse ou contraction spontanée avec expulsion de liquide du gel est une démonstration de l'existence de force en activité à l'intérieur du gel. Cette force endogène met en mouvement les unités microscopiques ou mésoscopique dans l'unité macroscopique représentée par le gel qui manifeste visiblement la synérèse qu'on veut étudier. Il va de soi qu'on s'intéresse à la dynamique des unités microscopiques et mésoscopiques du gel pour comprendre l'origine de son mouvement global, c'est-à-dire, la synérèse.

Nous avons choisi comme unité microscopique pour la formation des gels dans cette étude, le polysaccharide suivant les raisons évoquées dans le contexte. Nous avons utilisé des polysaccharides qui sont des assemblages linéaires de monosaccharides dont le nombre dans la chaine peut être très élevé dépassant facilement 1000 monosaccharides, ce qui présente le polysaccharide comme une chaine plus ou moins flexible dans une configuration plus ou moins aléatoire. En suivant la chaine des monosaccharides d'un bout à l'autre, il n'est pas sûr qu'on s'écarte de son point de départ lorsque la chaine est dans la configuration aléatoire et lorsqu'on s'en écarte franchement, la chaine est plutôt dans une configuration ordonnée. La configuration d'une chaine qu'elle que soit son origine (naturelle ou synthétique) n'est jamais à 100 % aléatoire ou ordonnée à cause d'une part de la longueur de persistance qui caractérise les chaines et du caractère entropique qui résulte de la dynamique de la chaine dans son milieu. La longueur de persistance est la longueur en dessous de laquelle la chaine est rigide, la flexibilité de la chaine commence à s'exprimer seulement à partir d'une longueur de chaine plus grande. Le caractère entropique de la configuration de la chaine résulte du fait que la chaine et le volume qu'elle occupe forme un système qui obéit au principe de l'énergie minimale. Selon l'environnement de la chaine, si l'état ordonné coûte trop d'énergie, alors la chaine restera dans un état plutôt aléatoire.

La probabilité que la chaine soit dans une configuration plutôt aléatoire ou ordonnée dépend de l'énergie et des caractéristiques physiques et chimiques de la chaine en relation avec celles de son environnement. Les travaux de Michael Rubinstein et de nombreux auteurs dont Ralph H. Colby sont très explicites sur l'importance de la qualité du solvant pour la configuration et la dynamique des polymères en solution [3, 4]. Ces travaux montrent l'évolution de la taille des polymères dans une configuration aléatoire, que les travaux de De Gennes [5] avaient prédit suivant le concept de loi d'échelle et selon laquelle les solvants seraient classés en trois grandes classes par rapport à leurs affinités avec le polymère : bon, mauvais et solvant-θ. En effet, dans un bon solvant, le caractère entropique est favorable à l'expansion du polymère, et lorsque les conditions physicochimiques du système changent la qualité du solvant en mauvais solvant, la perte d'affinité du polymère avec le solvant fait que l'entropie est moins favorable à l'expansion par conséquence la chaine de polymère se contracte tout en gardant une configuration aléatoire. La figure suivante montre ces différentes configurations en lien avec la qualité du solvant.

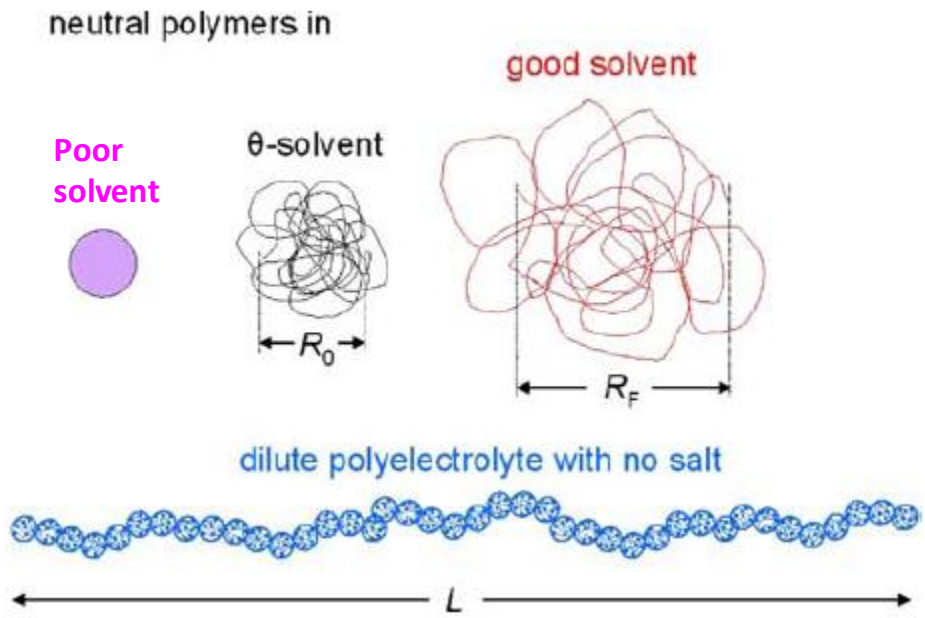

Figure 1: Configuration des polymères neutres en solution diluée. Le polymère neutre dans un mauvais solvant est comme une bille dense de petite taille comparée au même polymère mais dans un solvant-thêta. Le même polymère dans un bon solvant voit sa taille augmentée par rapport à sa taille dans le solvant-thêta. Les polymères chargés électroniquement adopte la configuration la plus expansée dans l'eau déminéralisée en raison des répulsions électrostatiques en plus du fait que le polymère est dans un bon solvant. $R_0 \approx N^{0.5}$ *et* $R_F \approx N^{0.59}$ *avec N une unité de taille du polymère assimilable à la longueur de persistance* [4].

2 Cas particulier du kappa-carraghénane par rapport au polymère standard

La littérature est explicite sur la particularité du comportement en solution du kappa-carraghénane avant la formation du gel, lorsqu'on le compare au polymère standard qu'il soit neutre ou chargé électroniquement. Le kappa-carraghénane en tant que polymère polyélectrolyte possède les propriétés d'un polymère standard. On peut souligner la disposition aléatoire de la chaine de monomères dans l'espace qu'on désigne par la configuration pelote et le fait aussi qu'il existe pour le kappa-carraghénane une température critique de solution. Il existe pour les polymères en solution deux types de températures critiques de solution, supérieure (UCST pour Upper Critical Solution Temperature) [6, 7] et inférieure (LCST pour Lower Critical Solution Temperature) [6, 7, 8]. Le mélange polymère-solvant est une solution lorsque la température est inférieure au LCST ou lorsque la température est supérieure au UCST. Pour le kappa-carraghénane et les polysaccharides de la même famille, il s'agit plutôt

d'un UCST, le système est sous forme de solution lorsque la température est supérieure à une valeur critique [9, 10, 11, 12]. En solution, le comportement du kappa-carraghénane suit plus ou moins les concepts en physicochimie des polymères qui sont fondés sur la loi d'échelle et le comportement des polymères chargés en présence de sel. En plus des caractéristiques observables chez les polymères standards, le kappa-carraghénane adopte une conformation hélicoïdale en solution, lorsque la température baisse en dessous de l'UCST qu'on qualifie de température de transition pelote - hélix. Cette transition n'est pas exclusive au kappa-carraghénane [13], l'agarose [14, 15], la gélatine [16] et bien d'autres systèmes adopte ce changement de conformation avant la gélification. Une particularité remarquable du kappa-carraghénane qui le distingue des polymères polyélectrolytes standard est sa sélectivité ionique [17, 18]. Le fait que le kappa-carraghénane soit plus sensible aux ions potassium qu'aux ions divalents distingue ce type de système des polyélectrolytes standard, défiant notre compréhension de la dynamique des polyélectrolytes en présence de sel. Ainsi, on ne peut pas strictement parlant déduire de ce qu'on connait du comportement des polymères polyélectrolytes en solution celui de kappa-carraghénane en présence de sel. La sélectivité ionique et le rôle qu'elle joue dans la synérèse va être scrutée dans cette thèse car elle met en évidence des caractéristiques physicochimiques essentielles pour comprendre la dynamique du polysaccharide selon qu'il est en présence du sel sélectionné ou du sel de faible affinité.

3 De la solution au gel de kappa-carraghénane

La préparation des solutions de kappa-carraghénane sont stables dans la gamme de pH 6 et 7. En plus d'être un système dont on dispose suffisamment de donner dans la littérature qui sont utiles pour l'étude de la synérèse, la stabilité au pH des solutions est un atout de plus par rapport aux systèmes protéiques pour lesquels on a besoin d'ajuster le pH. La température de dissolution du kappa-carraghénane dans l'eau déminéralisée est généralement bien au-dessus de 70 °C et ce fait sous agitation pendant des heures jusqu'à l'obtention d'une solution [9, 19]. La température est un paramètre clé dans le changement conformationnel du polysaccharide qui précède la formation du gel. Cependant, le lien entre ce paramètre clé et la synérèse du gel qui résulte du refroidissement de la solution n'a pas été étudié. La température étant intrinsèquement liée à la dynamique des unités microscopique et mésoscopique desquelles résultent la formation et les propriétés du gel, il va de soit que nous étudions l’influence de la température sur la synérèse du gel formé. De plus, l'unité microscopique que représente le polysaccharide par rapport au gel a la propriété d'augmenter ou de contracter le volume de l'espace qu'elle occupe

dans le gel, c'est-à-dire, qu'elle n'est pas une sphère dure. Pour cette raison, nous allons particulièrement orienter la recherche de l'origine de la synérèse sur le rôle de la température dans l'expansion et la contraction des chaines de polysaccharide, de même que l'influence du sel dans la relation température - volume du polysaccharide. Cette première partie sera suivie de l'étude sur la sélectivité ionique afin de mettre en évidence en fonction du résultat de l'étude le rôle de la structure chimique du polysaccharide dans la gélification et par conséquence la synérèse.

4 Références

[1] B. Mao, A. Bentaleb, F. Louerat, T. Divoux et P. Snabre, «Heat-induced aging of agar solutions: Impact on the structural and mechanical properties of agar gels,» Food Hydrocolloids, vol. 64, pp. 59-69, 2017.

[2] H. A. Barnes, «Thixotropy - a review,» Journal of Non-Newtonian Fluid Mechanics, vol. 70, pp. 1-33, 1997.

[3] T. Ge, S. Panyukov et M. Rubinstein, «Self-Similar Conformations and Dynamics in Entangled Melts and Solutions of Nonconcatenated Ring Polymers,» Macromolecules, vol. 49, pp. 708-722, 2016.

[4] R. H. Colby, «Structure and linear viscoelasticity of flexible polymer solutions: comparison of polyelectrolyte and neutral polymer solutions,» Rheol Acta, Vols. 1 sur 2425-442, p. 49, 2010.

[5] P. D. Gennes, «Dynamics of Entangled Polymer Solutions. I. The Rouse Model,» Macromolecules, vol. 9(4), pp. 587-593, 1975.

[6] S. Saeki, N. Kuwahara, M. Nakata et M. Kaneko, «Upper and lower critical solution temperatures in poly (ethylene glycol) solutions,» Polymer, vol. 17, pp. 685-689, 1976.

[7] M. T. Cook, P. Haddow, S. B. Kirton et W. J. McAuley, «Polymers Exhibiting Lower Critical Solution Temperatures as a Route to Thermoreversible Gelators for Healthcare,» Advanced Functional Materials, vol. 31(2008123), pp. 1-25, 2021.

[8] A. Tager, A. Safronov, E. Berezyuk et I. Galaev, «Lower critical solution temperature and hydrophobic hydration in aqueous polymer solutions,» Colloid and Polymer Science, vol. 272, pp. 1234-1239, 1994.

[9] K. Ako, «Influence of elasticity on the syneresis properties of k-carrageenan gels,» Carbohydrate Polymers, vol. 115, pp. 408-414, 2015.

[10] E. Morris, D. Rees et G. Robinson, «Cation-specific Aggregation of Carrageenan Hekes : Domain Model of Polymer Gel Structure,» Journal of Molecular Biology, vol. 138, pp. 349-362, 1980.

[11] V. Lai, P. Wong et C. Lii, «Effects of Cation Properties on Sol-gel Transition and Gel Properties of k-carrageenan,» Food Engineering and Physical Properties, vol. 62(8), pp. 1332-1337, 2000.

[12] M. Ciancia, M. Milas et M. Rinaudo, «On the specific role of coions and counterions on K-carrageenan conformation,» International Journal of Biological Macromolecules, vol. 20, pp. 35-41, 1997.

[13] C. Rochas et M. Rinaudo, «Mechanism of Gel Formation in k-Carrageenan,» Biopolymers, vol. 23, pp. 735-745, 1984.

[14] Z. H. Mohammed, M. W. N. Hember, R. K. Richardson et E. R. Morris, «Kinetic and equilibrium processes in the formation and melting of agarose gels,» Carbohydrate Polymers, vol. 36, pp. 15-26, 1998.

[15] S. Boral, A. Sexena et H. Bohidar, «Syneresis in agar hydrogels,» International Journal of Biological Macromolecules, vol. 46, pp. 232-236, 2010.

[16] D. Prystupa et A. Donald, «Infrared study of gelatin conformations in the gel and sol states,» Polymer Gels and Networks, vol. 4, pp. 87-110, 1996.

[17] M. Rinaudo, A. Karimian et M. Milas, «Polyelectrolyte Behaviour of Carrageenans in Aqueous Solutions,» Biopolymers, vol. 18, pp. 1673-1683, 1979.

[18] C. Rochas et M. Rinaudo, «Activity Coefficients of Counterions and Conformation in Kappa-Carrageenans Systems,» Biopolymers, vol. 19, pp. 1675-1687, 1980.

[19] K. Ako, «Yield study with the release property of polysaccharide-based physical hydrogels,» International Journal of Biological Macromolecules, vol. 101, pp. 660-667, 2017.

Chapitre 2

Mesure et analyse quantitative de la synérèse

Chapitre 2

Mesure et analyse quantitative de la synérèse

Sommaire

Chapitre 2

Mesure et analyse quantitative de la synérèse

Authors and affiliations:

Said ELMARHOUM, Komla AKO, Yahya RHARBI

Univ. Grenoble Alpes, CNRS, Grenoble INP, LRP, 38000 Grenoble, France

Résumé

Les gels de polysaccharides ont montré une forte sensibilité à leurs conditions de préparation et de conservation ou manipulation. Ils ont la facilité de se contracter en expulsant spontanément le liquide qu'ils renferment, ce qui limite leurs usages dans de nombreuses applications dans l'agroalimentaire, en cosmétique ou dans le domaine de l'impression 3D. Pour ces applications, l'exigence d'avoir des gels relativement peu concentrés et stables est forte. La mesure de la synérèse est une étape essentielle dans l'étude et la compréhension de l'évolution de ce phénomène pendant la conservation des gels. Différentes méthodes de mesure ont été explorées dans cette partie, notamment : la microscopie à fluorescence, la macro-indentation et le cisaillement des solutions à l'état gel ou liquide. Les deux premières méthodes citées ne permettent pas d'obtenir des mesures reproductibles. La mauvaise étanchéité des échantillons, l'ajout de particules marquées de rhodamine et le temps d'acquisition des mesures sont des facteurs majeurs qui affectent la fiabilité des mesures. Nous avons introduit l'étude de la viscosité des solutions en fonction de la concentration en polysaccharide et température, car ces mesures sont stables et permettent d'étudier la dynamique des unités microscopiques qui forment les gels et qui pourraient être à l'origine de leur synérèse. Cependant, les méthodes de cisaillement donnent des résultats qui ne sont pas des mesures directes de variations macroscopiques de volume des gels.

Mots clés : Microscopie à fluorescence, macro-indentation, synérèse, mesures

1 Introduction

La synérèse des hydrogels peut être facilement détectée par observation, mais cette méthode est qualitative. Les mesures quantitatives de la synérèse consistent simplement à peser la perte de solvant par les gels ou par les changements de masse des gels. Boral et al., (2010) [1] ont déterminé la cinétique de la synérèse des hydrogels d'agar en retirant périodiquement l'eau accumulée sur la surface du gel. La masse d'eau a été mesurée à l'aide d'une microbalance. Ako (2017) [2] a utilisé le principe de cette méthode en mettant le gel de κ-carraghénane (κ-Car) dans une seringue perforée graduée pour suivre le volume du gel pendant qu'il expulse l'eau dans le tube qui recouvre la seringue perforée en la maintenant au-dessus de l'eau expulsée. Charoenrein et al., (2008) [3] ont utilisé une méthode différente consistant à placer le gel d'amidon sur un papier filtre permettant à l'eau de s'écouler par gravité. Le taux de la synérèse est obtenu en déterminant la variation de masse [1, 3] ou du volume de gel [2] par rapport à la masse ou volume initial du gel, respectivement. Laplante et Al., (2005) [4] ont déterminé le taux de la synérèse d'émulgel composé de chitosane, protéine et d'huile colorée. L'émulsion d'huile colorée est placée dans un tube en verre et l'évolution de l'épaisseur de l'émulsion (phase colorée) ou de l'eau (phase claire) est suivie quotidiennement.

Chen et al., (2007) [5] ont mesuré le pourcentage de liquide surnageant un émulgel à base de protéine/gomme de lin après centrifugation pendant 20 min à 4 °C afin d'accélérer le processus de synérèse. Cette méthode est couramment utilisée par plusieurs auteurs [3, 6, 7, 8, 9, 10]. La masse ou le volume du liquide perdu par la synérèse est directement mesuré par le changement de la masse ou du volume de gel restant. Il existe d'autres méthodes permettant de surveiller et de mesurer la synérèse en direct, comme les techniques microscopiques, telles que l'analyse de la texture des images [11], l'analyse de la couleur [12], ou l'analyse des spectres obtenus à partir de capteur de lumière en ligne visible étendue au NIR (Near Infra Red) [13].

2 Mesure de la synérèse par microscopique à fluorescence

Les techniques expérimentales de caractérisation de la synérèse s'établissent sur différentes échelles : industrielle comme c'est le cas dans la production des produits laitiers [10, 12], dans la recherche, avec des échantillons allant de quelques grammes [2, 14] à une centaine de grammes [13, 15, 16, 17]. Nous allons nous intéresser à la mesure de la synérèse des gels de carraghénane à l'aide de la microscopie à fluorescence. Les gels sont disposés dans un milieu confiné (1 cm x 1 cm x 250 µm) où on injecte une masse de 250 µg.

2.1 Principe de fonctionnement

La fluorescence est une émission lumineuse se produisant suite à l'excitation par absorption de photons par une molécule dite fluorescente. La microscopie de fluorescence repose sur la formation d'une image par la détection des photons émis qui se produisent lors des transitions électroniques d'une molécule à partir d'un état excité de haute énergie vers l'état fondamental. La facilité d'observation de la fluorescence dépend de la différence d'énergie entre les deux états : plus celle-ci est grande, plus la fluorescence est facilement observable [18]. Un microscope à fluorescence est un outil optique qui utilise des échantillons fluorescents. Il est équipé d'un filtre d'excitation, d'un miroir dichroïque et d'un filtre d'excitation.

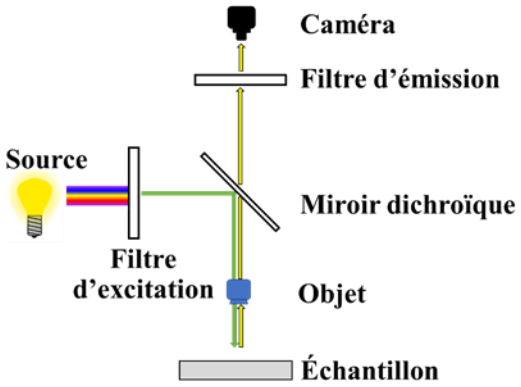

Figure 1: Schéma illustrant le mode de fonctionnement d'un microscope à fluorescence

La figure 1, illustre le cheminement des faisceaux lumineux depuis la source jusqu'au détecteur.

✓ Filtre d'excitation : Le premier filtre sélectionne une longueur d'onde de la source blanche à partir de spectre d'absorption de l'échantillon.

✓ Miroir dichroïque : réfléchit le faisceau émis par la source vers l'échantillon, avant de traverser l'objectif qui le focalise sur l'échantillon. Après l'excitation des molécules fluorescentes, la lumière émise est collectée à travers l'objectif, puis transmise par le miroir dichroïque vers le détecteur.

✓ Filtre d'émission : sert à sélectionner les longueurs d'ondes que nous souhaitons analyser par le détecteur. Ce filtre est choisi à partir de spectre d'émission de la molécule sondée.

Dans notre étude, nous avons utilisé la rhodamine-B qui absorbe les radiations vertes à 541 nm et émet dans le rouge à 572 nm [19].

2.2 Dispositif expérimental

Les gels sont formés entre une lame et une lamelle, puis examinés sous un microscope à fluorescence OLYMPUS de modèle CKX53 équipé d'une caméra rapide (Hamamatsu ORCA-Flash4.0 V3), d'un objectif apochromatique (plan) de grossissement × 1.25 et d'un adaptateur optique (monture C- 0.5X U-TV0.5XC-3-8) de grossissement de × 0.5. Les lames et lamelles sont scellées hermétiquement avec du Gene Frame, formant une cellule de 1 cm × 1 cm × 250 µm et d'un volume de 25 µL.

2.3 Préparation de l'échantillon

L'usage des particules fluorescentes industrielles est très courant dans la recherche scientifique, mais leur coût est élevé [19], pour cette raison, nous avons ajouté à l'échantillon, la rhodamine-B et des particules de PMMA (poly méthacrylate deméthyle) de 20 µm de diamètre (Spheromers CA 20 fourni par Microbeads). Le mélange se fait à 60°C, supérieure à la température de gélification, pendant 20 min pour homogénéiser le mélange, puis, nous mettons l'échantillon à l'état liquide entre lame et lamelle. Une fois terminé, nous commençons l'observation au microscope. Le principe de cette méthode consiste à piéger les particules de PMMA dans le gel pendant la synérèse, et la différence de couleurs observée permet de distinguer le gel du solvant en cas de synérèse. La figure 2 présente l'image réelle (a) et l'image prise au microscope à fluorescence (b). Les images seront traitées ultérieurement à l'aide de logiciel MatLab et Image-J afin d'analyser le phénomène de la synérèse.

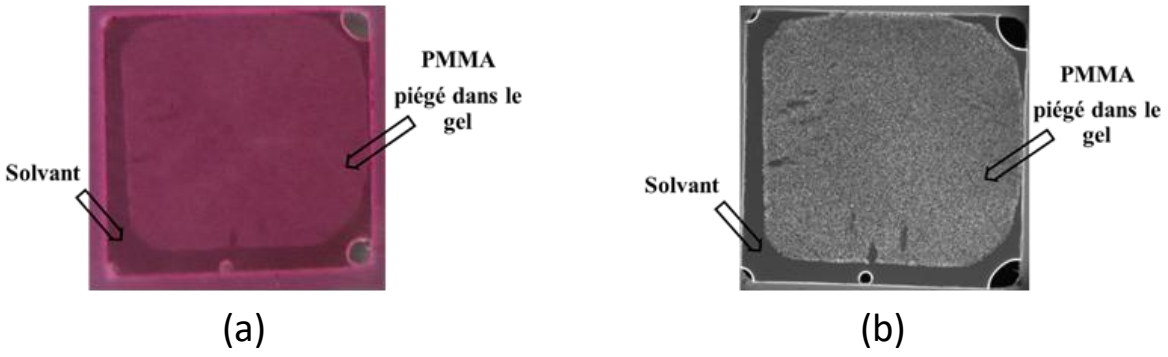

Figure 2: (a) Image réelle de gel confiné dans "Gene frame" de dimension 1cm × 1cm × 250 µm. *(b) Image microscope montrant les particules de PMMA de Ø=20 µm piégées dans le gel pendant la synérèse*

2.4 Résultats des testes

La figure 3 révèle une séquence d'images qui montre le rétrécissement du gel au fil du temps. Au cours des premiers instants, les images sont prises toutes les 10 secondes (120 images) car la cinétique de la synérèse est très rapide. Après 1200s (20min), la cinétique ralentit et les images sont prises toutes les 60 secondes pendant 40 minutes (40 images). Ensuite, la synérèse devient très lente et les images sont prises toutes les 15 minutes.

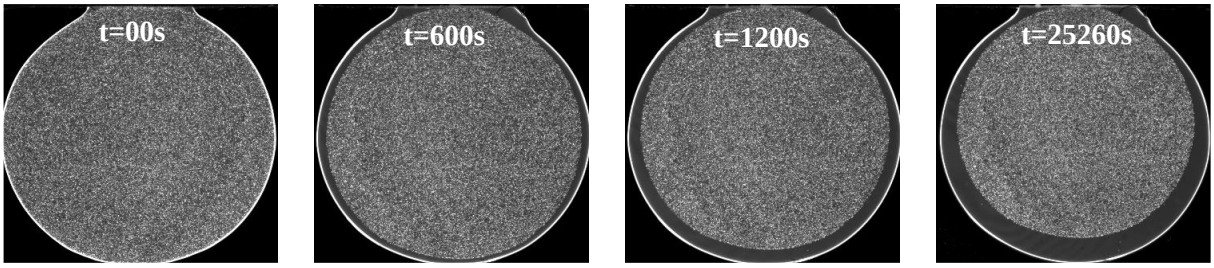

Figure 3: Sélection d'images enregistrées aux différents instants du gel 3g/L de κ-Carr – 40 mM KCl lors de la synérèse observée par microscope à fluorescence

La phase de traitement d'images sur Matlab implique de trouver un seuil d'intensité pour distinguer la phase de gel, plus lumineuse et contenant les particules de PMMA piégées, de la phase solvant moins lumineuse. La figure 4 ci-dessous présente la courbe de l'augmentation temporelle de la surface (nombre de pixels) du solvant par rapport à la surface initiale du gel, cette fraction représente le taux de la synérèse.

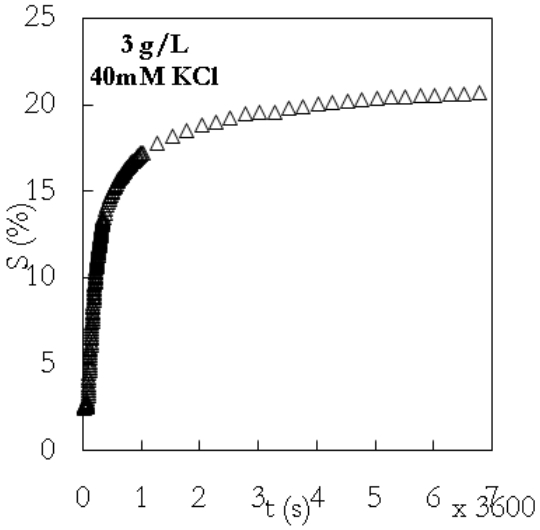

Figure 4: La cinétique de la synérèse dans un milieu confiné de dimension 1cm x 1cm x250µm du gel de κ-Carr 3g/l-40mM KCl

La figure 4 montre la courbe de la cinétique de synérèse obtenue pour un gel de k-Carr en présence de 40 mM de KCl. On constate que les résultats de la figure 5 ne sont pas cohérents avec les données de la littérature, qui montrent que la synérèse baisse lorsque la concentration du gel augmente. Ces observations peuvent-être expliquées par l'effet de force de surface exercée sur le gel, plusieurs auteurs ont déjà mis en évidence l'influence de forces de surface telles que l'adhésion aux parois du récipient sur la synérèse des gels colloïdaux [20, 21]. Certains tests montrent des gels piégés sans aucune contraction au cours du temps, ceci est dû à une force d'adhésion importante par rapport aux forces endogènes qui se développent à l'intérieur du gel et qui entraînent normalement la contraction (synérèse) [20].

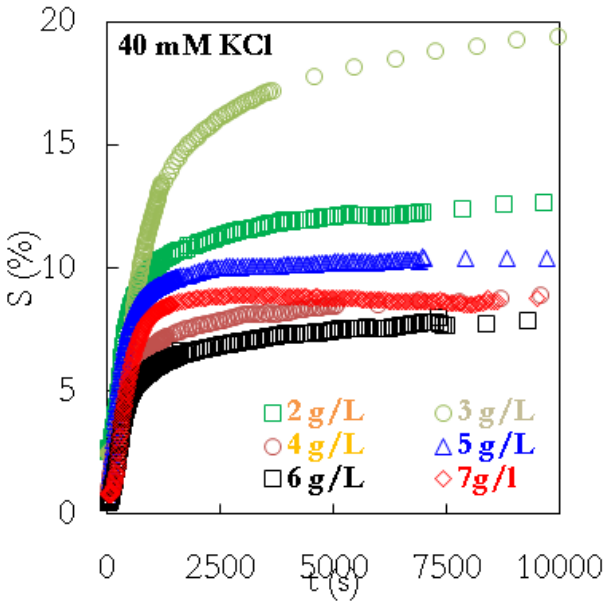

*Figure 5: Variation temporelle de S (%) pour les gels de K-Carr de concentration entre 2 g/L et 7 g/L en présence de 40 mM de KCl dans un milieu confiné de dimension 1 cm * 1cm * 250 µm*

2.5 Conclusion

Au terme de cette étude qui avait pour objectif de mettre en évidence une technique de mesure de la synérèse à courte durée, c'est-à-dire, la mesure du régime permanent après quelques heures (2.5h max). Les résultats montrent la possibilité de mesurer la cinétique de rétrécissement du gel avec une grande précision par ladite méthode. De nombreux autres travaux devraient être consacrés à l'amélioration de la fiabilité (robustesse), élimination des artéfacts de cette méthode. Le but est d'éviter les problèmes pour mesurer d'une manière fiable et reproductible la cinétique de la synérèse.

3 Mesure de la synérèse par macro-indentation

3.1 Principe de fonctionnement

La macro-indentation est une technique utilisée pour détecter et suivre la surface des gels pendant la synérèse. Elle consiste à appliquer une faible force sur la surface du gel pour la détecter. L'indentateur ou la sonde de détection a une géométrie plane et est intégré au rhéomètre ARES-G2. La force normale appliquée pour détecter la surface ne doit pas déformer le gel au point d'influencer la synérèse du gel.

3.2 Dispositif expérimental

Nous avons utilisé un rhéomètre à déformation imposée ARES-G2 (TA Instruments) équipé d'une géométrie plan-plan de Ø = 10 mm et d'un dispositif Peltier qui permet le contrôle de la température par un thermorégulateur à circulation d'eau (Lauda Microcool MC600).

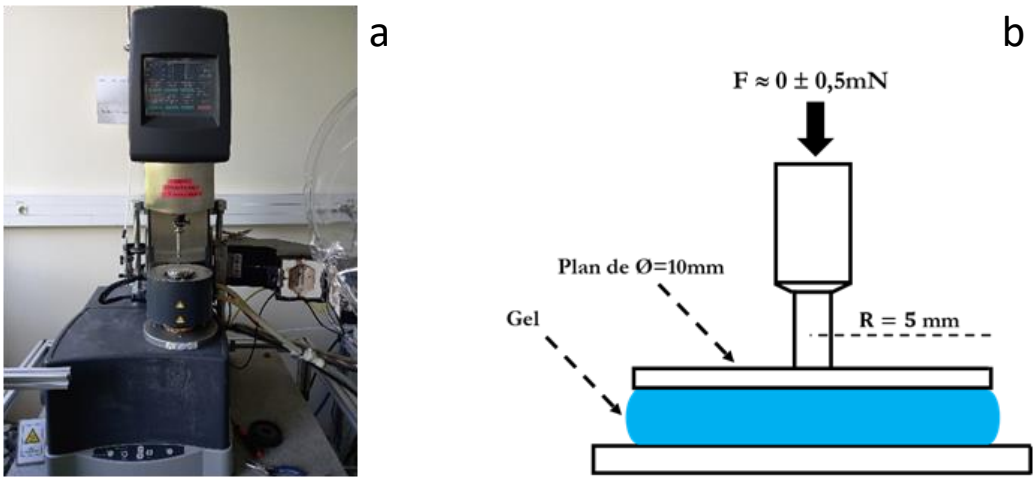

Figure 6: Photo du rhéomètre ARES-G2 (a) et schéma de la géométrie utilisée (b)

En pratique, les critères de sélection pour choisir un rhéomètre à déformation contrôlée tel que l'ARES-G2 pour l'essai sont les suivants :

- ✓ La sensibilité de l'appareil en force : l'Ares-G2 est capable de faire des mesures à une force axiale nulle avec une sensibilité de l'ordre de 50 µN.
- ✓ La sensibilité spatiale : Les mesures durent 10 heures avec un changement de gap entre 3 mm (Gap initial) et le gap final presque égal à 2 mm et le déplacement minimum de l'instrument est de 0.5 µm, ce qui convient parfaitement aux mesures souhaitées.

3.3 Préparation des échantillons

L'échantillon de κ-Car a été préparé par dilution dans l'eau déminéralisée contenant 200 ppm de NaN_3 et du sel à la concentration appropriée. Après l'agitation à 60°C, une masse de 0.3 g de solution (à l'état liquide) a été versée dans un moule de Ø =10 mm placée sur la plaque inférieure de la géométrie. Une fois la gélification terminée, on enlève le moule et on place le gel dans l'appareil de mesure pour de commencer les mesures.

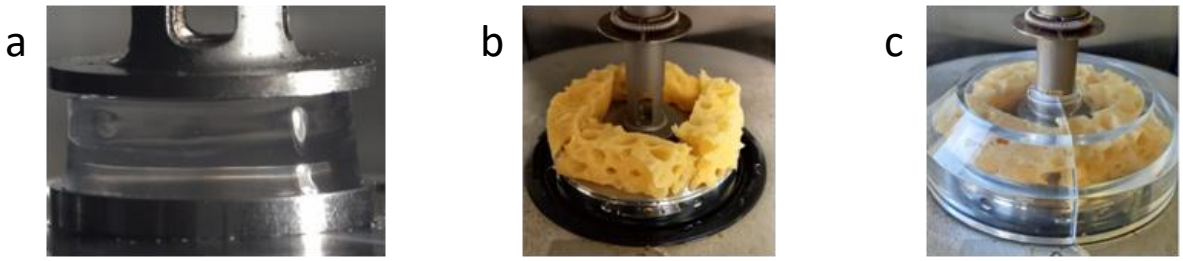

Figure 7: (a) Photo de la géométrie utilisée, (b) l'éponge enrichie d'eau et (c) le couvercle anti-évaporation

Afin de minimiser l'évaporation pendant les mesures, l'environnement autour de l'échantillon est saturé avec de l'eau en utilisant une éponge comme montré dans la figure 7b. Pour mesurer la cinétique de la synérèse, nous avons utilisé un programme qui consiste dans un premier temps à trouver la surface du gel (gap initial) en descendant le plan supérieur, initialement à 10 mm, vers la surface du gel avec une vitesse de 0.05 mm/s jusqu'à la détection d'une force supérieure ou égale à 0.8 mN. Une fois le gap initial détecté, la géométrie suit la surface du gel en maintenant une force axiale nulle. La figure 8 montre la variation au cours du temps du gap et de la force axiale exercée par la géométrie sur le gel. La courbe de la force montre que la force axiale exercée par la géométrie sur l'échantillon varie entre 0.5 mN et -0.5 mN, ce qui est très faible par rapport à la force nécessaire pour comprimer le gel. Ainsi, cette méthode permet de mesurer la variation du gap et donc de la synérèse sans appliquer de force extérieure significative.

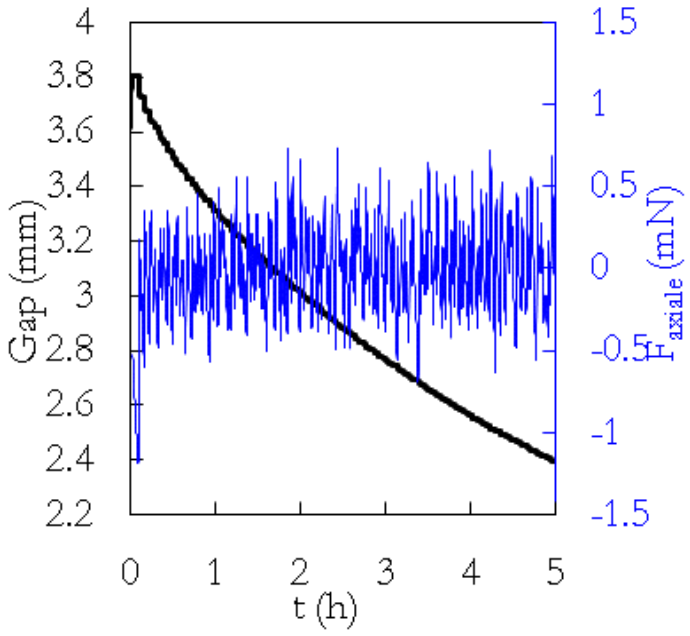

Figure 8: Variation temporelle du gap et de force axiale pour le gel de κ-Car 4g/l à 40mM KCl de Ø=10mm

Par la suite, tous les tests sont faits à la température ambiante (20°C) et la cinétique de la synérèse est mesurée en utilisant la formule suivante (Éq. 1).

$$S_t(\%) = \frac{h_0 - h_t}{h_0} \qquad 1$$

Le problème inhérent de cette méthode est l'évaporation. Nous avons donc réalisé des tests préliminaires pour contrôler ce phénomène, en travaillant dans un environnement humide.

3.4 Résultats des testes

Influence de l'évaporation pendant les mesures

Comme indiqué dans la section de préparation des échantillons, nous avons utilisé une éponge riche d'eau pour limiter l'évaporation. Pour mettre en évidence l'évolution du gap due à l'évaporation, nous avons réalisé des mesures sur le carbopol à de concentration 0,2% w/w. Le carbopol donne un gel stable [22]. La figure 9 montre la variation du gap (%) pour le gel de carbopol utilisé comme référence.

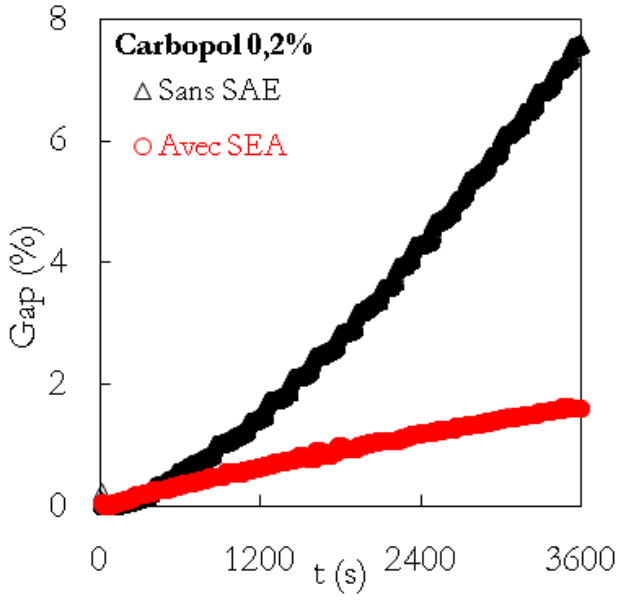

Figure 9: Variation temporelle du gap en % pour le gel de carbopol de concentration de 0.2%.

On constate que le gap (%) évolue dans le temps à cause de l'évaporation. L'utilisation du dispositif anti-évaporation (SAE) a permis de réduire la cinétique d'évaporation de 6% en une heure, passant de 7,5% sans SAE à 1,5% avec SAE.

Pour améliorer la fiabilité des résultats en minimisant l'évaporation, de nombreuses tentatives ont été effectuées pour mesurer la synérèse en faisant à chaque fois des modifications pour améliorer le dispositif anti-évaporation comme illustré dans la figure 10.

Figure 10: Système anti-évaporation (SAE) développé. Le bassin d'eau n'est pas en contact avec le gel (a), Éponge enrichie d'eau (b), La géométrie n'est pas en contact avec le plexiglass (c), Toit en éponge gonflée d'eau, La géométrie n'est pas en contact avec le couvercle.

L'environnement de mesure est finalement enrichi en eau à l'aide d'un bassin d'éponge imbibée d'eau. Les photos de la figure 10 montrent le protocole expérimental adopté dans la suite de l'étude.

Influence du temps d'acquisition

La figure 11b montre le zoom sur la période 1600 s et 2600 de la courbe de la figure 11a. Nous observons des chutes périodiques du gap lors des mesures, suggérant que la diminution du gap est plus rapide suite à l'écrasement du gel (figure 11c) plutôt qu'à la synérèse (figure 11d).

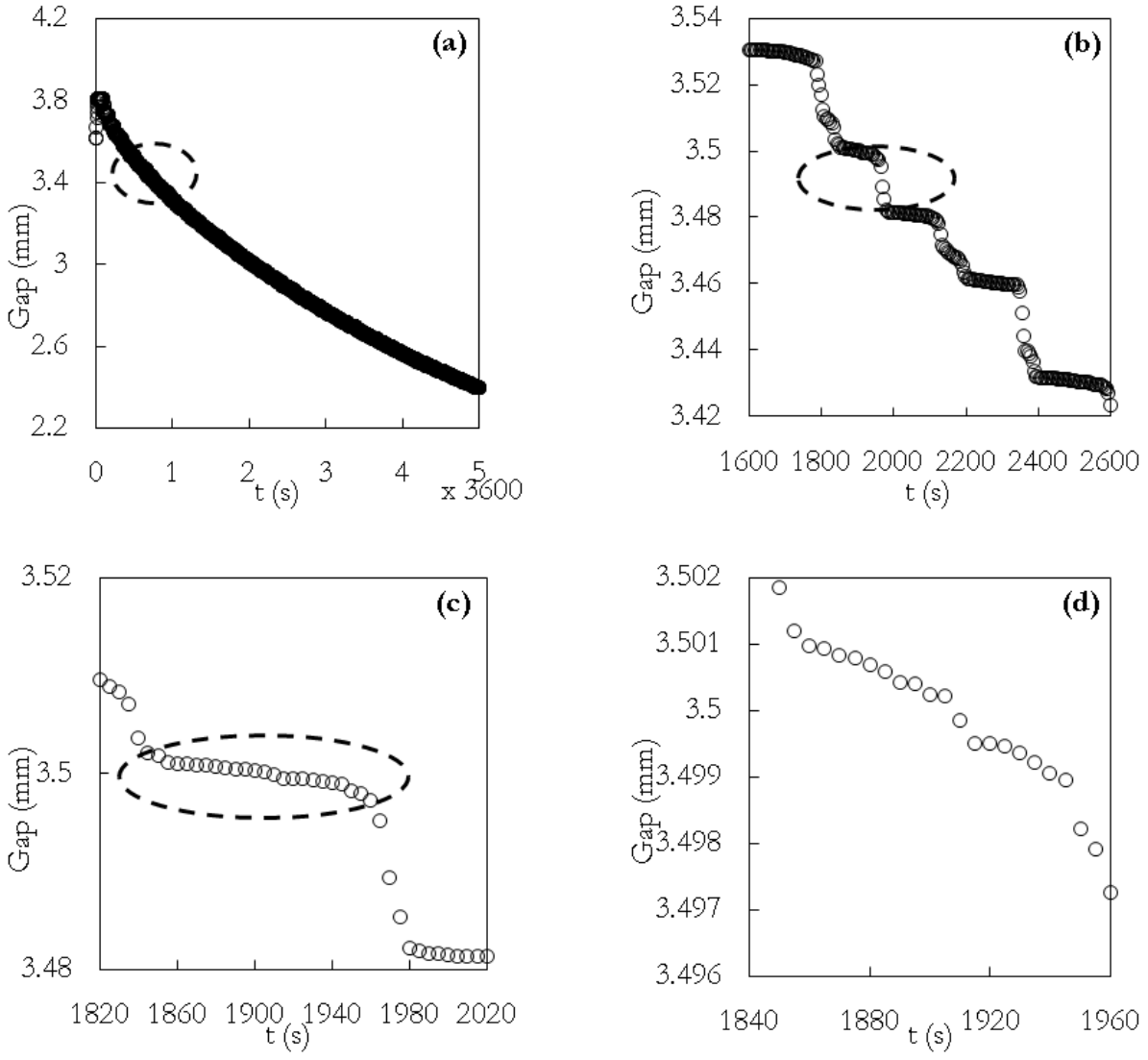

Figure 11: (a) Coupe de la courbe 6 entre la période 1600 et 2600s. La figure (b) montre un zoom sur la courbe (a) pour illustrer les pas d'écrasement du gel. (c) montre la cinétique de la synérèse entre les instants 1840 s et 1960 s

Ces deux chutes rapides et lentes, apparaissent systématiquement dans toutes les mesures effectuées à une fréquence d'acquisition d'un point toutes les 5 secondes. L'écrasement conduit à une surestimation du taux de synérèse.

Les courbes présentées dans la figure 12 montrent une forte dépendance de la cinétique de la synérèse S(%) en fonction du temps d'acquisition, ce qui peut être attribué à la combinaison de la cinétique propre à la synérèse des gels, l'expulsion d'eau liée à l'écrasement des gels et à l'évaporation. La figure 12b indique que le S_{max} (%) est très dépendant de la fréquence d'acquisition (inverse du temps d'acquisition). Pour des temps d'acquisition inférieurs à 600 s/pts, S_{max}(%) diminue avec le temps d'acquisition, car la géométrie déforme le gel. Pour les temps d'acquisition supérieurs à 600 s/pts, S_{max} (t) augmente avec le temps d'acquisition, ce qui peut être expliqué par le fait que la géométrie se détache de l'échantillon après chaque point de mesure, laissant la surface supérieure du gel en contact avec l'air ambiant pendant la période d'attente avant la prochaine détection de la surface du gel. Plus cette période d'attente est longue, plus grande sera l'évaporation, ce qui contribue à la cinétique de croissance de la synérèse.

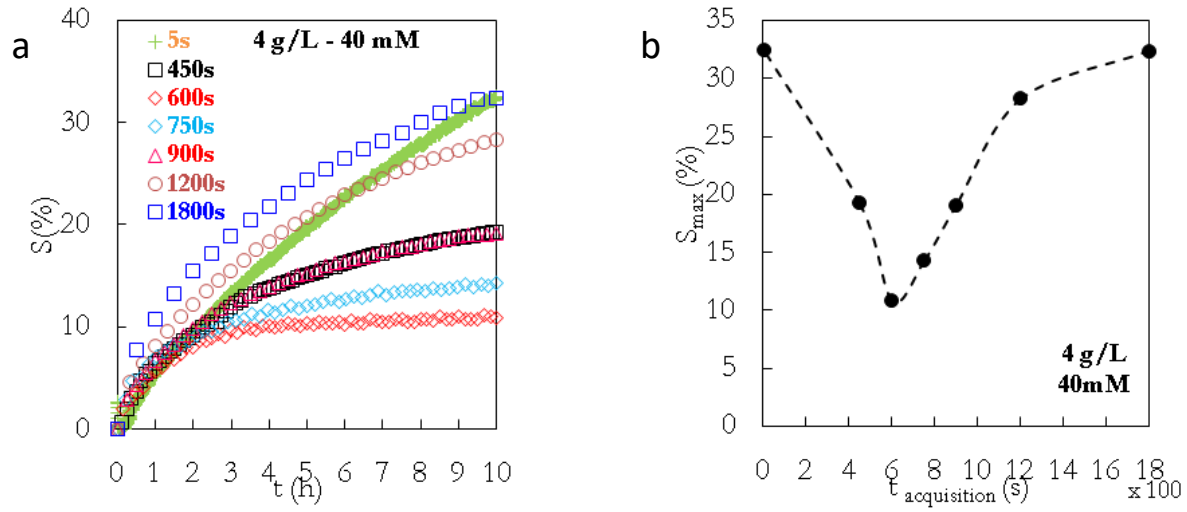

Figure 12: La cinétique de la synérèse de K-Carr/KCl (4g.L-1/40mM) pour différents temps d'acquisitions des données (450s/pts à 1800s/pts). Ø=10mm, 20°C.

Après plusieurs essais visant à surmonter les problèmes d'écrasement du gel pour les temps d'acquisition courts (grande fréquence) et d'évaporation pour les temps d'acquisition longs (faible fréquence), le compromis optimal est un temps d'acquisition de 600 s/point. C'est à ce point que l'influence des problèmes susmentionnés sur le taux de synérèse est minimale, comme le montre la figure 12b.

Influence de la concentration

Afin de vérifier la fiabilité du protocole expérimental, il est nécessaire de faire une étude sur la cinétique de la synérèse en fonction de la concentration en polysaccharide, et de comparer les résultats avec ceux rapportés dans la littérature, Dunstan et al., (2000) [23], Ako (2015) et (2017) [24, 2] montrent que la synérèse augmente avec la diminution de la concentration. Pour cela, une série de concentrations de κ-Car de 4, 6 et 8 g/L ont été testées en présence de 40 mM de KCl. Les résultats obtenus ont été comparés avec ceux obtenus à l'aide d'une seringue perforée, présentés dans la figure 13b. Les courbes montrent une diminution de S_{max}(%) avec l'augmentation de la concentration de κ-Carr pour les deux méthodes.

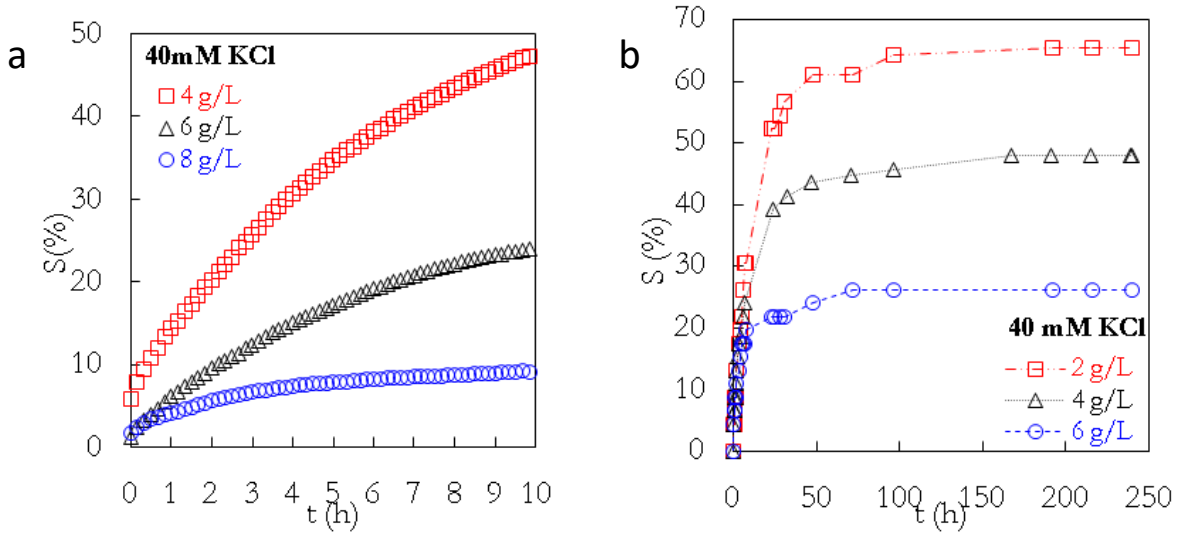

Figure 13: La cinétiques de la synérèse de κ-Carr à 40 mM KCl (a) à l'aide d'ARES-G 2 de Ø =10 mm avec une fréquence d'acquisition égal à 1pts / 600 s et (b) dans un tube perforé

La technique macro-indentation montre une synérèse plus importante que les mesures effectuées à l'aide d'une seringue perforée. Les difficultés soulignées dans la méthode macro-indentation ne favorise pas une comparaison fiable entre les deux méthodes sans mesures additionnelles pour isoler les effets dus à la masse du gel testé, qui pourrait jouer un rôle dans les deux méthodes.

Teste de reproductibilité

Nous avons évalué la reproductibilité des mesures par la méthode de macro-indentation sur des gels de 4g/L de κ-Car contenant 40mM de KCl. Nous avons suivi le même protocole de préparation des échantillons en prélevant une masse d'environ 0.3 g de solution, laissée à gélifier pendant 5 min à température ambiante avant de commencer les mesures de cinétique de

la synérèse. Ces mesures ont été réalisées sur 9 échantillons de la même préparation en prenant un point toutes les 600s. La figure 14 présente l'évolution du taux de la synérèse au cours du temps. Cependant, les courbes de neuf tests montrent une faible reproductibilité des résultats.

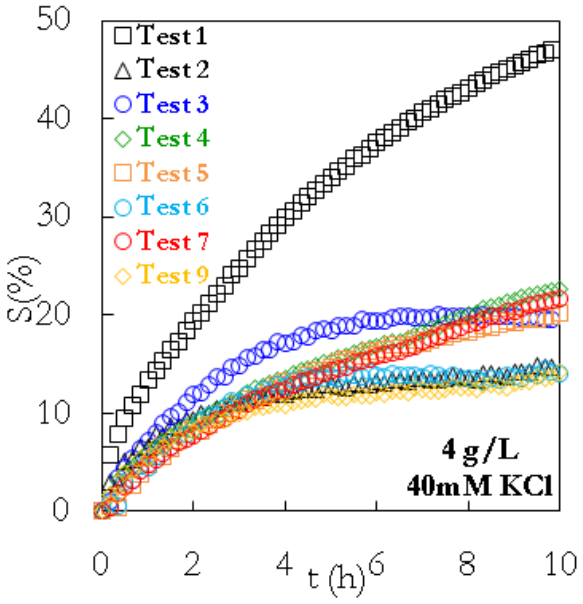

Figure 14: Cinétique de synérèse en pourcentage S(%) de 9 échantillons de la même solution de κ-Carr 4 g/L - 40 mM KCl pendant 10 heures, 600 s/pts à l'aide d'ARES-G2

3.5 Conclusion

L'étude de l'utilisation de la macro-indentation comme méthode de mesure de la synérèse des gels présente quelques points forts et des points faibles. C'est une méthode très intéressante parce qu'elle permet d'effectuer des mesures sur de faible volume de gel et de suivre des variations axiales millimétriques du volume des gels, mais avec l'application d'une force supposément négligeable sur la surface des gels. Ces points forts sont atténués par les nombreuses difficultés à pouvoir contrôler l'évaporation de l'échantillon entre deux mesures de la hauteur des gels, lorsque le temps qui sépare ces deux temps de mesures est grand, c'est-à-dire, > 600 s. Cependant, si on réduit ce temps de mesure pour éviter le problème lié à l'évaporation, les résultats des mesures montrent que la force supposément faible qu'on applique est relativement grand par rapport à la dureté du gel. Les multiples petites déformations que subissent les gels macro-indentés accroissent artificiellement la synérèse naturelle du gel qu'on cherche à quantifier. La non-reproductibilité des mesures montre que ces artéfacts ne sont pas maîtrisés, ce qui nécessite un temps d'investigation considérable pour tenter de séparer la synérèse induite de la naturelle. C'est seulement après l'obtention de résultats reproductibles

qu'on pourra mettre en évidence, s'il en existe une, l'influence de la masse initiale du gel sur les mesures de la synérèse. Ces derniers résultats vont permettre des comparaisons effectives des mesures de la synérèse entre différentes méthodes.

4 Mesure et étude de la synérèse par la rhéologie

4.1 Principe de la mesure

Contraction du gel

L'idée de mesurer la synérèse par la méthode de cisaillement est le résultat de la corrélation entre la synérèse des gels et le module viscoélastique affiché. Cette corrélation est apparue pour la première fois dans les mesures d'Hermansson (1989) [25] (Figure 15a) et elle a été mise en évidence clairement par Richardson et Goycoolea (1994) [26] (Figure 15b). Ces derniers ont montré que le pic dans la mesure du G' (Pa) du gel de κ-Car en fonction du temps ou de la température est causé par la synérèse des gels et par effet de glissement ou de perte d'adhésion entre la surface des gels cisaillés et la surface de la géométrie. En effet, selon les récentes mesures d'Ako (2015), plus l'expulsion de liquide par le gel est importante, plus l'amplitude du pic est grande, de sorte que le module élastique du gel peut tomber plus bas que la sensibilité de l'appareil. Afin d'améliorer le contact entre le gel et la géométrie, les mesures du module viscoélastique sont généralement réalisées avec une géométrie rugueuse, ceci évite les problèmes de glissement.

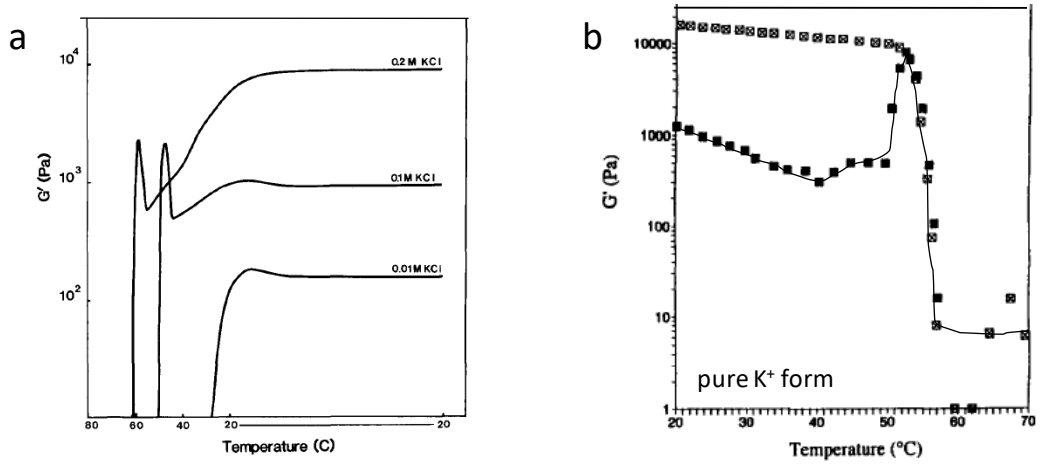

Hermansson et al., 1989 *Richardson et al., 1994*

Figure 15: Evolution du module viscoélastique en fonction de la température. Le pic dans les figures caractérise la synérèse du gel de kappa-carraghénane en présence du KCl.

La corrélation entre la chute du module élastique et la synérèse nous a amené à penser que la décroissance du G' en fonction du temps, comme on peut le voir sur la figure 16a, peut être traduite en évolution de la synérèse en fonction du temps (figure 16b) selon l'expression suivante :

$$S(\%) = \frac{G'_{max} - G'_t}{G'_{max}} \qquad 2$$

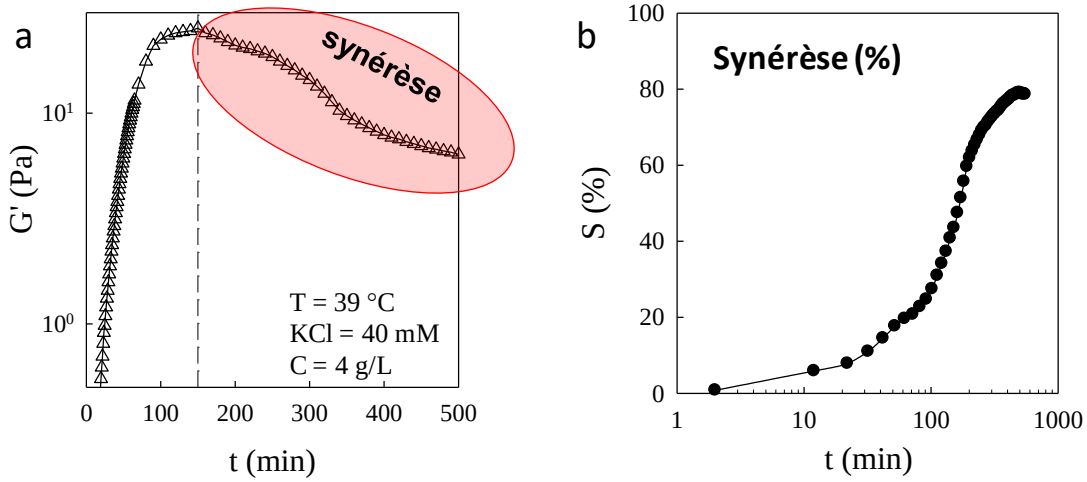

Figure 16: a) Evolution du module élastique en fonction du temps et b) traduction de la décroissance du module élastique en évolution de la synérèse en fonction du temps à température constante (39 °C) pour le gel de kappa-carraghénane à 4 g/L, 40 mM KCl.

Contraction des chaines de polysaccharide (en solution)

Le phénomène de synérèse est un mécanisme de contraction de volume à une échelle qui affecte macroscopiquement le volume du gel. La contraction peut se manifester à l'échelle des chaines de polysaccharide (échelle ou unité microscopique), d'agrégats de polysaccharide (échelle ou unité mésoscopique) et ou du gel (échelle ou unité macroscopique). Lorsque le rétrécissement du volume du gel ne concerne que l'échelle macroscopique du gel, c'est-à-dire, n'est pas le résultat de contraction des agrégats de polysaccharide, c'est que ces derniers sont suffisamment rigides ou dense de sorte que leurs tailles ne peuvent plus se contracter. En revanche, le volume interstitiel se rétrécit et le liquide dans ce volume est expulsé entrainant la contraction du gel. Lorsque le rétrécissement du gel est causé par la contraction des chaines de polysaccharides, ce mécanisme peut être mise en évidence par le comportement en solution des chaines de polysaccharide en étudiant la viscosité des solutions de polysaccharide. Lorsque le volume de la chaine de polysaccharide en solution baisse, ceci contribue généralement à faire baisser la

viscosité de la solution. Ainsi, pour mettre en évidence la synérèse ou étudier son origine, nous avons étudié la viscosité des solutions de polysaccharide dans une cellule Couette dans différentes conditions expérimentales.

4.2 Dispositif expérimental

Les mesures du module viscoélastique ont été réalisées à l'aide de DHR3 (TA Instruments) avec une géométrie cône/plan rugueuse de référence (Ø50 mm, 2.0°, TADC2°InR500) et d'entrefer de 110,0 µm. L'appareil est équipé d'un dispositif à effet Peltier qui permet le contrôle de la température (Figure 17). Une portion de la solution à analyser est chargée à chaud sur le Peltier du rhéomètre réglé initialement à une température supérieure à celle de gélification de l'échantillon. Après avoir chargé l'échantillon, la surface est recouverte d'une fine couche d'huile minérale pour éviter l'évaporation. Ensuite, le programme de mesure a été lancé. Les conditions de chaque mesure seront précisées dans le texte du manuscrit. Le balayage de température a été exécuté pour déterminer la température de gélification (T_{gel}) qui est définie comme la température à laquelle G' commence à augmenter rapidement.

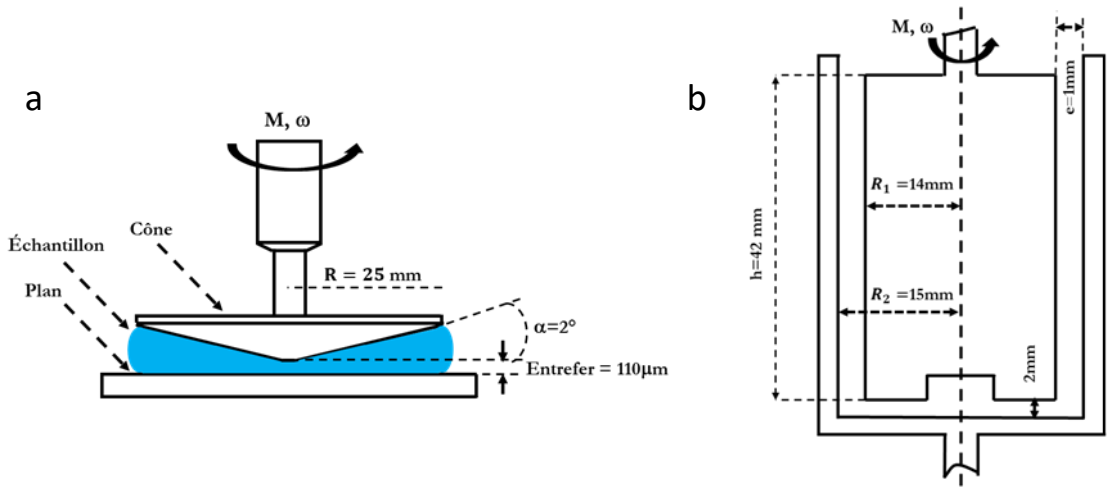

Figure 17: (a) Schéma d'une géométrie cône-plan utilisée pour les mesures de module viscoélastique, (b) Schéma de la géométrie Couette utilisée pour les mesures de viscosité

Les mesures de la viscosité ont été réalisées en géométrie Couette à l'aide d'un rhéomètre rotatif à contrainte imposée DHR3 (marque TA Instruments). La géométrie Couette est formée de deux cylindres coaxiaux, un cylindre intérieur en rotation (appelé rotor) et un cylindre extérieur creux immobile (appelé stator) avec un rayon R1 de 14 mm et R2 de 15 mm, définissant un espace horizontal (R2 - R1) de 1 mm et un rayon moyen R de 14,5 mm (R1 + R2)/2. La hauteur du « Stator » était de 42 mm, et son écart vertical avec la coupelle était fixé à 2 mm (Figure

17b). Les couples minimum et maximum de l'instrument étaient respectivement 5 µNm et 5×10^3 Nm.

Le dispositif expérimental utilisé permet d'effectuer les mesures de la viscosité à des taux de cisaillement variés, allant de 0.001 à 100 /s. Le rhéomètre est équipé d'un dispositif à effet Peltier qui permet le contrôle de la température avec une précision de ± 0.5°C grâce à un thermorégulateur à circulation d'eau (Microcool LAUDA MC600). Les conditions de chaque mesure sont précisées dans le manuscrit.

4.3 Préparation des échantillons

Nous avons utilisé différents volumes d'échantillons dans le Couette avec différents volumes d'huile minérale (Sigma Aldrich, $\eta^{20°C}$ = 0.35 Pa.s) pour couvrir la surface des échantillons afin de négliger l'effet d'évaporation de l'eau. La viscosité n'a pas été affectée ni par l'huile ni par l'évaporation lorsque 8 mL des échantillons ont été introduits dans le Couette et recouverts de 1mL d'huile minérale. Le domaine d'écoulement Newtonien des solutions a été défini en mesurant la viscosité des échantillons et de l'eau en fonction du taux de cisaillement pour différentes températures dans l'intervalle comprise entre 5°C et 60 °C. L'évolution de la viscosité des échantillons et de l'eau a également été mesurée à un taux de cisaillement constant à 15 /s, en balayant les températures avec une vitesse de 2°C/min et de 0.5 °C/min pour les rampes de montée et de descente respectivement. Enfin, la variation temporelle de la viscosité (cinétique) a été mesurée à un taux de cisaillement constant de 15 /s et à température constante.

4.4 Conclusion

Nous avons observé que les mesures en cisaillement sont plus stables et reproductibles car moins impactées par les difficultés d'évaporation. Cependant, les mesures en cisaillement traduites en mesure de taux de synérèse par la variation relative du module élastique G' des gels ne sont pas des données directement utilisables comme des données de variation de dimension métrique. Pour cette raison, les données en G' et G" doivent être analysées afin de trouver la relation qui les relie aux variations des dimensions du gel. Les masses de gel analysées sont aussi très faibles par rapport à celles utilisées dans les méthodes courantes pour quantifier le taux de synérèse. Si on veut comprendre la contribution du poids des gels dans leur dynamique macroscopique au repos et les conséquences de cette dynamique dans la synérèse des gels, il est nécessaire de pouvoir convertir la décroissance des G' et G" en variation de masse ou de volume des gels. La viscosité des solutions de polysaccharide offre la possibilité de déterminer

une concentration critique (C*) à une température donnée. Le C* (g/L) étant relatif à la masse et au volume qu'occupe les polysaccharides en solution, il se présente comme une quantité physique intéressante pour la suite de notre étude.

5 Références

[1] S. Boral, A. Sexena et H. Bohidar, «Syneresis in agar hydrogels,» International Journal of Biological Macromolecules, vol. 46, pp. 232-236, 2010.

[2] K. Ako, «Yield study with the release property of polysaccharide-based physical hydrogels,» International Journal of Biological Macromolecules, vol. 101, pp. 660-667, 2017.

[3] S. Charoenrein, O. Tatirat et J. Muadklay, «Use of centrifugation–filtration for determination of syneresis in freeze–thaw starch gels,» Carbohydrate Polymers, vol. 73, pp. 143-147, 2008.

[4] S. Laplante, S. L. Turgeon et P. Paquin, «Effect of pH, ionic strength, and composition on emulsion stabilising properties of chitosan in a model system containing whey protein isolate,» Food Hydrocolloids, vol. 19, pp. 721-729, 2005.

[5] H.-H. Chen, S.-Y. Xu et Z. Wang, «Interaction between flaxseed gum and meat protein,» Journal of Food Engineering, vol. 80, pp. 1051-1059, 2007.

[6] S. Mizrahi, «Syneresis in food gels and its implications for food quality,» Chemical Deterioration and Physical Instability of Food and Beverages, Vols.1, pp. 2324-348, 2010.

[7] M. Pearse et A. Mackinlay, «Biochemical Aspects of Syneresis: A Review,» Journal of Dairy Science, vol. 72, pp. 1401-1407, 1989.

[8] S. Banerjee et S. Bhattacharya, «Compressive textural attributes, opacity and syneresis of gels prepared from gellan, agar and their mixtures,» Journal of Food Engineering, vol. 102, pp. 287-292, 2011.

[9] L. C. Gonzalez, M. A. Loubes, M. M. Bertotto, R. I. Baeza et M. P. Tolaba, «Flow behavior and syneresis of ball milled rice starch and their correlations with starch

structure,» Carbohydrate Polymer Technologies and Applications, vol. 2, n° 1100168, 2021.

[10] D. Verbeken, K. Bael, O. Thas et K. Dewettinck, «Interactions between k-carrageenan, milk proteins and modified starch in sterilized dairy desserts,» International Dairy Journal, vol. 16, pp. 482-488, 2006.

[11] C. C. Fagan, C.-J. Du, C. P. O'Donnell, M. Castillo, C. D. Everard, D. J. O'Callaghan et F. A. Payne, «Application of Image Texture Analysis for Online Determination of Curd Moisture and Whey Solids in a Laboratory-Scale Stirred Cheese Vat,» Food Engineering and Physical Properties, vol. 73 (6), pp. E250-E258, 2008.

[12] C. Everard, D. O'Callaghan, C. Fagan, C. O'Donnell, M. Castillo et F. Payne, «Computer Vision and Color Measurement Techniques for Inline Monitoring of Cheese Curd Syneresis,» Journal of Dairy Science, vol. 90(7), pp. 3162-3170, 2007.

[13] M. J. Mateo, D. J. O'Callaghan, C. D. Everard, M. Castillo, F. A. Payne et C. P. O'Donnell, «Evaluation of on-line optical sensing techniques for monitoring curd moisture content and solids in whey during syneresis,» Food Research International, vol. 43, p. 177–182, 2010.

[14] K. Ako, «Influence of osmotic and weight pressure on water release from polysaccharide ionic gels,» Carbohydrate Polymers, vol. 169, pp. 376-384, 2017.

[15] G. Scherer, «Mechanics of syneresis,» Journal of Non-Crystalline Solids, vol. 108, pp. 18-27, 1989.

[16] M. Castillo, J. A. Lucey, T. Wang et F. A. Payne, «Effect of temperature and inoculum concentration on gel microstructure, permeability and syneresis kinetics. Cottage cheese-type gels,» International Dairy Journal, vol. 16, p. 153–163, 2006.

[17] T. Van Vliet, H. J. M. Van Dijkl, P. Zoon et P. Walstra, «Relation between syneresis and rheological properties of particle gels,» Colloid & Polymer Science, vol. 269, pp. 620-627, 1991.

[18] «owlapps,» owlapps, 25 09 2022. [En ligne]. Available: Microscopie à fluorescence | owlapps.

[19] Y. Soumane, «Étude microfluidique du colmatage d'un milieu poreux modèle par un écoulement de suspension,» Thèse de l'Université Grenoble Alpes, Grenoble, 2021.

[20] Q. Wu, J. van der Gucht et T. E. Kodger, «Syneresis of Colloidal Gels: Endogenous Stress and Interfacial Mobility Drive Compaction,» Physical Review Letters, vol. 125 (208004), 2020.

[21] L. Cipelletti, S. Manley, R. C. Ball et D. A. Weitz, «Universal Aging Features in the Restructuring of Fractal Colloidal Gels,» Physical Review Letters, vol. 84(10), pp. 2275-2278, 2000.

[22] B. Das, A. K. Nayak et U. Nanda, «Topical gels of lidocaine HCl using cashew gum and Carbopol 940: Preparation and in vitro skin permeation,» International Journal of Biological Macromolecules, vol. 62, pp. 514-517, 2013.

[23] D. E. Dunstan, R. Salvatore, M. Jonsson et M.-L. Liao, «Syneresis of k-carrageenan gels at different KCl and LBG concentrations,» Gum and Stabilisers for the Food Industry 10, pp. 137-147, 2000.

[24] K. Ako, «Influence of elasticity on the syneresis properties of k-carrageenan gels,» Carbohydrate Polymers, vol. 115, pp. 408-414, 2015.

[25] A.-M. Hermansson, «Rheological and Microstructural Evidence for Transient States During Gelation of Kappa-Carrageenan in the Presence of Potassium,» Carbohydrate Polymers, vol. 10, pp. 163-181, 1989.

[26] R. K. Richardson et F. M. Goycoolea, «Rheological measurement of c-carrageenan during gelation,» Carbohydrate Polymers, vol. 24, pp. 223-225, 1994.

Chapitre 3

Origine thermodynamique de la synérèse : Partie A

Chapitre 3

Origine thermodynamique de la synérèse : Partie A

Sommaire

Chapitre 3

Origine thermodynamique de la synérèse : Partie A,

Concentration critique, viscosité intrinsèque et synérèse

Résumé de l'article

Les travaux dans cet article présentent l'évolution de la concentration critique (C* en g/L) et de la viscosité intrinsèque ([η] en L/g) des solutions de kappa-carraghénane (kC) en fonction de la température. La solution à C* est présentée comme un empilement compact de sphères de même concentration que la solution, le volume de la sphère étant occupé par une chaine de polymère. L'expression rhéologique de C* est largement décrite dans la littérature. La [η] suivant nos études mesure la part d'eau qui est fixée dans la sphère. L'évolution de C* et [η] des solutions de kC en fonction de la température montre un minimum à ≈ 0.44 g/L et un maximum à ≈ 1.23 L/g respectivement. Les deux températures, au minimum de C* et au maximum de [η], sont respectivement ≈ 30 °C et ≈ 20 °C. Le gonflement de la chaine de kC est optimal à la température de ≈ 30 °C (plus basse C*) qu'on note LCCT pour "Lower Critical Concentration Temperature". Mais la quantité d'eau fixée ou transportée par le kC dans sa dynamique est optimale à ≈ 20 °C. Ainsi, la quantité C*×[η] définit le coefficient de d'imperméabilité hydrodynamique qui caractérise la résistance au flux d'eau à travers le gel, si ce dernier se forme à C* par exemple. Plus [η] est grande, le gel à C* est moins perméable. L'imperméabilité hydrodynamique décroît faiblement avec un coefficient de 2.6×10^{-3} /°C lorsque la solution est chauffée entre 0 °C et 45 °C puis fortement avec un coefficient de 22.5×10^{-3} /°C entre 60 °C et 100 °C. Si une solution de kC gélifie à la température LCCT ou les chaines sont gonflées au maximum et si le gel est conservé à une température plus basse que LCCT, le gel va se contracter au même rythme que le dégonflement des chaines, c'est la synérèse. Mais ce dégonflement sera freiné ou bloqué par l'augmentation du coefficient d'imperméabilité hydrodynamique et du module viscoélastique du gel.

Mots clés : Rhéologie, polymère gonflé, volume hydrodynamique, capacité de rétention d'eau.

https://doi.org/10.1016/j.foodhyd.2021.107346 ; Food Hydrocolloids 124 (2022) 107346

Highlights

* For kappa-Carrageenan suspensions, it exists a lower critical concentration temperature (LCCT)

* The gelation temperature (T_{gel}) of the systems was found below their LCCT

* Cooling the kappa- Carrageenan suspensions from the LCCT to T_{gel} causes syneresis reaction at the gel point

Graphical abstract

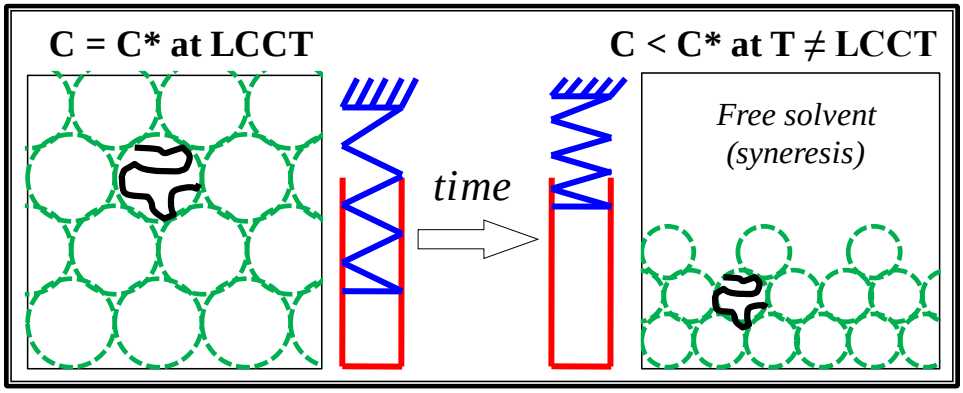

The determination of the lower critical concentration temperature and intrinsic viscosity: the syneresis reaction of polymeric gels

Authors and affiliations:

Komla AKO [a], Said ELMARHOUM [a], Claire D. MUNIALO [b]

a) Univ. Grenoble Alpes, CNRS, Grenoble INP, LRP, 38000 Grenoble, France

b) School of Life Sciences, Coventry University, Priory Street, Coventry, CV1 5FB, UK

*__Corresponding author__: komla.ako@univ-grenoble-alpes.fr; akokomla@hotmail.com

Abstract

This work studies (by rheological method) the temperature dependence of coil-to-coil contact critical concentration (C* in g/L) and the intrinsic viscosity ([η] in L/g) as the capacity of a single-coil to bind the solvent molecules and increase the solution viscosity accordingly. The C* and [η] were measured and fitted by a model to characterize the thermodynamic stability of the kappa-carrageenan (kC) polysaccharide in solution. The weakest C* and greatest [η] of the kC was found to be ≈ 0.44 g/L and ≈ 1.23 L/g, respectively. The temperature where the C* was weakest was found at ≈ 30 °C and is referred to as the lower critical concentration temperature (LCCT). The expansion of the polysaccharide was greater at the LCCT, but its capacity to bind the solvent molecules was found greater at ≈ 20 °C according to the model. The hydrodynamic permeability resistance was defined as C*[η] and was shown to decrease smoothly by a slope of 2.6×10^{-3} /°C with the increase in temperature from 0 °C to 45 °C, then strongly by a slope of 22.5×10^{-3} /°C after 60 °C. Therefore, if a polymer solution at LCCT is gelled at lower or higher temperature, the polymer sizes will decrease (syneresis reaction), but the [η] and gel elasticity will interfere with the kinetics of the reaction to determine thereafter the serum holding capacity of the gels.

Keywords: Rheology, polymers expansion, hydrodynamic volume, water-holding capacity

1. Introduction

Kappa-Carrageenan (kC) is a polysaccharide that is extracted from marine algae, which forms gels in the appropriate conditions such as polysaccharide concentration, ionic strength, type of ions, and temperature (Ciancia, Milas & Rinaudo, 1997; Morris & Chilvers, 1983). However, the gels that are formed by kC in the presence of K^+ and Ca^{2+} ions have been characterized by the spontaneous release of water (syneresis) (Lai, Wong & Lii, 2000). The elasticity is reported to explain the syneresis of these gels (Ako, 2015; Mao, Tang & Swanson, 2001). Other polysaccharide gels such as starch, alginate, agar and pectin have also been reported to be susceptible to syneresis (Divoux, Mao & Snabre, 2015; Draget et al., 2001; Einhorn-Stoll, 2018; Lee, Baek, Cha, Park & Lim, 2002).

As a natural resource, polysaccharides form the major component of the human diet and are therefore used by the food industries to process food with particular specifications (Kaur, Singh & Sodhi, 2002; Lee, Baek, Cha, Park & Lim, 2002; Teko, Osseyi, Munialo & Ako, 2021). For instance, polysaccharides are used as thickeners and viscosity controlling agents of many suspensions and beverages for managing swallowing disorders for dysphagic patients and the elderly (Munialo, Kontogiorgos, Euston & Nyambayo, 2020; Yousefi & Ako, 2020). In most cases, foods that are made with thickeners and viscosity controlling agents are usually stored until consumption, which in some cases may be more than 3 months. However, a prolonged storage of polysaccharide suspensions which are susceptible to syneresis promotes the exhibition of the syneresis (Mao, Tang & Swanson, 2001). The duration that it takes for these systems to exhibit syneresis is not yet well understood even though the chemical nature and associative mechanism of the constituents have been reported (Boral, Saxena & Bohidar, 2010; Scherer, 1989). This time depends on the chemical or mechanical kinetics of the ageing or phase separation which induces the syneresis process (Scherer, 1989; Takeshita, Kanaya, Nishida & Kaji, 2001; Vliet, Dijk, Zoon & Walstra, 1991), and the technique or method used for the detection of the polysaccharide susceptibility to syneresis (Ako, 2015; Einhorn-Stoll, 2018; Richardson & Goycoolea, 1994). When syneresis is discovered accidentally after several weeks of storage, it may cause considerable waste of time, matter, energy and money for the companies. Kappa-carrageenan and those polysaccharides that are susceptible to syneresis have many applications in pharmaceutical and biomedical industries, including cosmetic surgery, surface coating for drug and protein carriers, making them ubiquitous in our daily life (Berger, Reist, Mayer, Felt & Gurny, 2004; Field & Kerstein, 1994; Hoffman, 2012; Klouda & Mikos,

2008; Liu, Subhash & Moore, 2011). Their capacity to form strong gels and biocompatibility extends the application areas to designing 3D structures as scaffolds or cell culture substrates for tissues engineering (Drury & Mooney, 2003). Therefore, the inadvertent occurrence of syneresis may be lethal for biomedical and pharmaceutical applications. The growth of cells in agar gels for the detection of diseases for instance is damaged by the syneresis phenomena as the solvent is released with the cell nutrients. Mechanical contact problems also arise from the instabilities of gel dimensions (Divoux, Mao & Snabre, 2015). Chemical and mechanical aspect of the syneresis converge to i) chemical modification (Campo, Kawano, da Silva Jr & Carvalho, 2009), ii) the use of super gelling agents, and iii) an increase of material concentration (Zhang, Ji, Liu & Feng, 2016) to stop the occurrence of syneresis. However, it is not yet clear whether these methods actually stop the syneresis or they simply delay the time it takes to exhibit syneresis.

Kappa-Carrageenan (kC) and in general polysaccharides are processed in solution at temperatures between 60 °C and 90 °C then the solutions or gels are cooled and stored at ambient or lower temperatures before applications (Ako, 2015; Mao, Tang & Swanson, 2001). Given the temperature changes that occur from the sample preparation to their applications, the thermodynamic stability of the kC polysaccharide in solution at various temperatures were investigated in this study. In general, gels can reach the thermodynamic equilibrium very fast if their constituent units can move freely, i.e. no additional energy is required for the motions such as contraction, stretching, rotation or diffusion. Ideally, free contraction motion of the kC chains should take place conceptually at concentration below or equal to the critical concentration (Morris, Cutler, Ross-Murphy, Rees & Price, 1981) without energy of liaison at the contact points. The critical concentration C* is reciprocal to the volume of the smallest mass moving freely which is the blob stand by the polysaccharide chain. At C*, the concentration of the solution is equal to the concentration defined by a polymer chain volume in the solvent. The intrinsic viscosity [η] which is the capacity of the polysaccharide to increase the viscosity of the system has been determined by a linear Huggins and Kraemer analysis and used to characterize the interaction between the polymers and the solvent molecules (Brunchi, Morariu & Bercea, 2014; Chronakis, Doublier & Piculell, 2000). In this study, we define the [η] parameter as the capacity of a polymer chain to bind the solvent molecules and show that both physical quantities, C* and [η], are time-independent. The sensitivity of both quantities to the temperature is demonstrated to show the susceptibility of the polysaccharide to syneresis at the macromolecular scale. Supposing for instance that change of the temperature leads to

remarkable change of the [η] and C*, then the system must evolve toward a new equilibrium state with a time evolution function that would depend on the stresses in competition in the systems.

In this work, the evolution of the C* as a function of the temperature was investigated using a model that allows the determination of the C* in the temperature interval from 0°C to near 100°C.

2. Materials and methods

2.1 Sample characteristics

The kappa-carrageenan (kC) polysaccharide was kindly provided by Rhodia Food (Switzerland), product name and reference: MEYPRO-GEL 01/2001 WG95-37 K-Car. The kC is made of a sequence of alternating disaccharides, α-(1-3)-D-Galactose-4-Sulfate and β-(1-4)-3,6-anhydrous-D-Galactose. The dialyzed product may contain a weak amount of glucose and was found in the pure potassium kC form of total potassium no more than 4.2 % (w/w), the other salts are considered to be only trace amounts. The molecular weight of the kC was M_w = 3.3×10^5 g/mol and the indices of polydispersity (Ip) = 2.02. It is worth mentioning that the kC is a polyelectrolyte and thermoreversible polymer. The kC in solution can turn from liquid to solid state by cooling and from the solid to liquid state by heating. This behaviour makes kC a perfect material for temperature ramp measurements to be repeated at different conditions on the same sample. During the cooling ramp, kC changes from random coil to helix conformation. The temperature where the coil-helix transition takes place is dependent on the ionic strength and the type of salt. The helix-coil transition takes place during heating ramp at temperature above the coil-helix transition temperature. The coil-helix transition changes the flow properties of the solution.

2.2 Sample preparation

Twenty g/L of kC solution was prepared by dissolving the powder in demineralized water in the presence of 200-ppm sodium azide (NaN_3) as a bacteriostatic agent. The mixture was then heated at 90°C under stirring for 10h. The solution was then dialyzed in 4 L of ultrapure water in the presence of 200-ppm NaN_3 for 3 days using a dialysis membrane of 6-8 kDa molecular weight cut off. The dialysis water was exchanged thrice the first day and twice the second and third day respectively. The dialyzed solution was then filtered with Anotop syringe filter with

0.45 μm pore size to constitute the stock solution. The final concentration of the stock solution was adjusted by the dilution factor after the dialysis step. All samples that were analyzed were prepared by diluting the stock solution to give the desired final kC concentration and mixed under heating in a water bath at 60 °C for approximately 15 min to give homogeneous solutions prior the viscosity measurements. The system is comparable to a polyelectrolyte polymer solution with no additional salt except the presence of 200-ppm NaN_3, which was added to prevent spoilage of the samples.

2.3 Viscosity measurements

The viscosity measurements were performed in Couette geometry using a DHR3 Rheometer (TA Instrument).The Couette geometry consisted of a concentric cylinder geometry of an inner rotor cylinder (bob) and outer stator cylinder (cup) of respectively a radius R_1 of 14 mm and R_2 of 15 mm defining a horizontal gap (R_2 - R_1) of 1 mm and an average radius R of 14.5 mm as (R_1 + R_2)/2. The height of the bob was 42 mm and the vertical gap between the bob and cup was set at 2 mm. The minimum and maximum torque of the instrument were 5 μNm and 5×10^3 Nm respectively. Both the torque (M) and the angular velocity (Ω) of the bob were measured by the rheometer. The Ω is related to the shear rate by the expression:

$$\dot{\gamma} = \frac{R}{R_2 - R_1} \cdot \Omega \tag{1}$$

and the shear stress is related to the torque by the expression:

$$\sigma = \frac{1}{2\pi hR^2} \cdot \mathrm{M} \tag{2}$$

Shear viscosity is defined as the shear stress divided by the shear rate, which is proportional to M/Ω, by the constant:

$$K_G = \frac{R_2 - R_1}{2\pi hR^3} \tag{3}$$

which is considered as the geometry constant applied by the DHR3 software (TA Instruments V9.49) to convert M/Ω into a viscosity data. The expression of the bob wall velocity is deduced as:

$$v_0 = \frac{R_1 \cdot (R_2 - R_1)}{R} \dot{\gamma} \quad (4)$$

When Eq.4 is compared with the velocity of plate-plate geometry wall of radius R_1 having the same Ω on a gap = R_2 - R_1, the comparison yields the following relationship of the shear rate between the plate-plate geometry and Couette geometry:

$$\dot{\gamma}_p = \frac{2R_1}{R_2 + R_1} \dot{\gamma} \approx 0.96\dot{\gamma} \quad (5)$$

This gives the factor between the viscosity from plate-plate geometry and Couette geometry. The results obtained by the use of a Couette geometry were comparable. However, it is worth to note that theoretically the Couette shear rate is higher than the plate shear rate by 4 %.

The temperature of the samples was controlled with a precision of ± 0.5 °C by a water circulation thermoregulator (Microcool LAUDA MC600). Prior to this study, the viscosity of the stock solution and a series of diluted samples were tested. The viscosity was determined as a function of the shear rate from 0.3 s^{-1} to 30 s^{-1} to define the Newtonian flow domain at a constant temperature in the range between 5 °C and 60 °C. The viscosity was also measured at a constant shear rate of 15 s^{-1} while cooling or heating at 2 °C min^{-1} or a lower rate 0.5 °C min^{-1}. The viscosity was neither affected by the oil nor by the evaporation when 8 mL of the samples were introduced in the Couette and covered with 1 mL of mineral oil. Seven g/L stock solution was kept at 5 °C and the viscosity was measured over 2 months using the reported shear rate intervals. The viscosity of the stock solution was constant over the interval of shear rate and storage time. For all the samples tested in this study, the viscosity of a given concentration was shown to exclusively depend on the temperature and not on the shear rate except in cases where there was an experimental error. Therefore, all the samples of the study behave like Newtonian fluids, and their viscosity can be assimilated to the zero shear viscosity. The measurement of the viscosity including the viscosity of the solvent was done at 15 s^{-1} shear rate to yield a sensitive torque value.

2.4. Temperature dependence of the viscosity analysis

The viscosity of the solvent was measured as the solvent contributes to the viscosity of the sample. The viscosity of the solutions as a function of the concentration must cross the viscosity axis at the solvent viscosity. Although the viscosity of water is reported in literature, its value by the instrument used in this study is unknown because it may depend on the constant of the

geometry (Eq.5) used to perform the measurement. Moreover, the viscosity of the solvent gives an insight on the precision of the instrument while measuring the viscosity of the sample at concentrations approaching zero. The raw data of the temperature dependence of the viscosity of the solvent (demineralized water with 200-ppm NaN_3) is shown in **Figure 1**. The values of the viscosity of water by DHR3 rheometer using Couette geometry and the value reported by Korson et al 1969 (Korson, Drost-Hansen & Millero, 1969) for water using Cannon-Ubbelohde viscometer are in good agreement by a constant factor. Therefore, the viscosity data analyses should not depend on this factor. The Couette geometry viscosity was greater than the Cannon-Ubbelohde viscosity by 10 %, which could be attributed to the geometry effects.

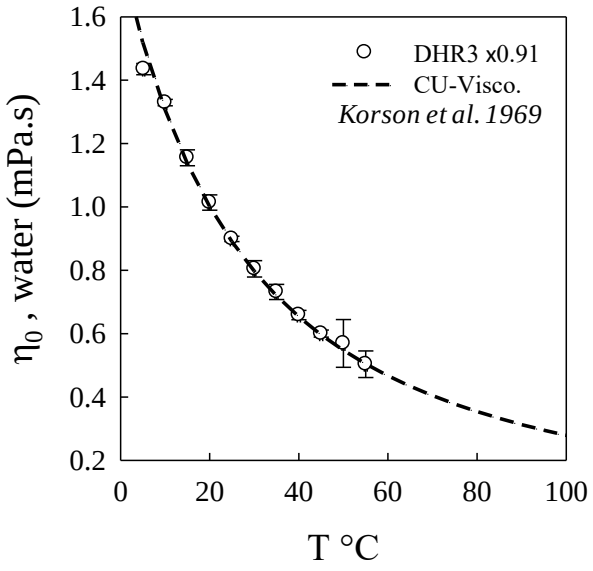

Figure 1*: Temperature dependence of the viscosity of demineralized water in presence of 200-ppm of NaN_3. The viscosity by the DHR3 instrument using the Couette geometry and the viscosity reported by Korson et al. 1969 using Cannon-Ubbelohde viscometer (CU-Visco) are shown in Figure 1. The viscosity data by the DHR3 were multiplied by a factor of 0.91 to yield the same viscosity with the standard. The temperature values should be considered with ± 0.5 °C. The vertical viscosity error bars are ± the standard deviation of the viscosity from the corresponding temperature interval.*

The standard deviation of the viscosity increases with the temperature. This fact impedes the calculation of accurate specific viscosity $\eta_{sp} = (\eta - \eta_0)/\eta_0$. When the sample viscosity is close to the solvent viscosity, for temperatures > 50 °C and concentrations < 0.01 % (w/w) the fluctuation may yield negative η_{sp}.

The viscosity can be understood by the association of a perfect elastic (spring) and gas systems. Thus, we propose the following modelling of the temperature dependence of Newtonian fluid viscosity. The model is a concept based on the definition of the Newton's law of dynamic viscosity, i.e. the rate of transfer of momentum across a unit area as the measurement of the resistance of a fluid to deformation at a given rate. The experimental viscosity is equivalent to mass per unit of length and time, and this mass can be represented by a force if it is just scaled with the gravitational constant g ($F = m_{eq} \times g$). Given that the mass is the equivalence of the resistance of the fluid to deformation, this mass reflects the resistance to displacement of any single particle of the fluid. This mass is noted here as m_{eq} and is the expression of the sum of a "static" and "dynamic" mass. The static mass, m, is the mass of the fluid flowing without any interactions between the particles in motion. This mass is the conventional (real) mass, and it does not depend on the temperature, it is constant for a given system. The dynamic mass, m_D, is given here to represent the interaction forces between all the fluid constituents, which could also be referred to as the virial mass of the system. The dynamic mass is null, if the fluid is treated as a perfect gas. Given that the interaction forces between the solvent molecules depend on temperature, the m_{eq} as the viscosity depends on the temperature too.

$$m_{eq}^{T} = m_{D}^{T} + m \tag{6}$$

Hence, for a given system, the m_{eq} per unit of length and time evolves with the temperature following the temperature dependence of the m_D, which is related to the force at work in the system. At a given temperature, the model to give the m_{eq} uses the property of perfect spring and considers that the m_{eq} deforms a perfect spring on undetermined length (z) for a given time Δt or on a given length (z) but for an undetermined time. If the force is scaled with the restoring force constant k_o ($F = k_o \times z$), it results in the relation:

$$m_{eq}^{T} \cdot g = k_o \cdot z^{T} \tag{7}$$

which equalizes the resistance of the fluid and the resistance of the spring (restoring force), with both resistances being dependent on temperature. The temperature dependence of z characterizes the influence of temperature on the interaction forces between the fluid constituents as m_D and the constituents' momentum as m velocity. The flow could be pictured as the stretching of a perfect spring with constant sectional dimension *S*. Hence, taking a constant time unit Δt of the deformation of the spring on length z, the viscosity scaled with z as:

$$\eta^T \equiv k_o \cdot \frac{\Delta t}{S} \cdot z^T \tag{8}$$

The Eq.8 establishes a relation between the property of a perfect spring and the flow property of a fluid, but the properties of many fluids namely, the osmotic pressure and elasticity, are reported as the properties of perfect gases ($R \times T$, where R is the gas constant) with a correcting function or parameters which take into account the potential of interactions at work in the fluids (Fernandez-Nieves, Fernandez-Barbero, Vincent & de las Nieves, 2000; Horkay, Tasaki & Basser, 2000). Therefore, the relative variation of the volume at constant external pressure P, (∂V/V), of fluids could be scaled with the relative variation of the volume of a perfect gas by a factor f at a given temperature T. For a perfect gas, the relative variation of the volume is reported to be equal to the relative variation of the temperature (∂T/T). Hence, when the temperature varies, the volume of the fluid varies relatively as a factor of (∂T/T). Given that the fluid is modelled by a cylindrical spring with constant sectional area, the relative variation of its volume scaled with the relative variation of the temperature as:

$$\left(\frac{\partial z}{z}\right)_P = f^T \cdot \frac{\partial T}{T} \tag{9}$$

where in Eq.9 the factor $f = 1$ if the fluid was treated as a perfect gas. From Eqs.8 and 9 the relative variation of the viscosity ($\partial\eta/\eta$), which is the derivation of the logarithm of the viscosity, Ln(η), scaled with (∂T/T) as (∂z/z). We define the derivation of the function $F(T)$ as $\partial F(T) = \partial\eta/\eta$, which gives the Eq.10

$$\frac{\partial F(T)}{\partial T} = f^T \cdot \frac{1}{T} \tag{10}$$

as the derivation of the logarithm of the temperature dependence of the viscosity η^T and that could be obtained experimentally. If the temperature is increased from T_o arbitrary initial condition of T, the viscosity η^T scaled as a factor of $Exp[F(T)-F(T_o)]$, which results from the integral of the derivation of Ln(η) with the function $F(T)$. The viscosity η^T could be scaled as $K_o \times Exp[F(T)]$ defining K_o (Eq.11) as the viscosity at an arbitrary original conditions.

$$K_o = k_o \cdot z_o \cdot \frac{\Delta t}{S} \cdot e^{-F(T_o)} \tag{11}$$

However, the factor K_o is simplified by considering the viscosity at any reference temperatures T_1.

If the fluid is presented as a mass of particles or molecules without interactions between them, it is well described theoretically that the fluids viscosity increases with the temperature as the momentum of the particles. The water in the liquid state is a mass of water molecules interacting with each other. The evolution of the viscosity with the temperature of colloidal suspensions where the colloids interact is not easily predictable. This means that the temperature dependence of the interaction forces, which we refer to as dynamic, or virial mass is unknown. However, the viscosity of the suspension of free colloids increases with temperature. Therefore, the viscosity of the water should increase with the temperature when its molecules are able to move freely. This means that the interactions between the molecules are substantially weakened. We hypothesise that the evolution of the viscosity of practically all liquid with the temperature on a large temperature interval may show where the contribution of the interactions between the liquid molecules are reduced. This should be evidenced if the viscosity is measured using a force to measure the deformation for a given frequency. This means that, the pressure being constant, it should be possible to observe a decrease in the viscosity of the water but to a minimum with increasing the temperature to the critical temperature T_c where the water molecules mostly become free. Therefore, a viscosity value of a given fluid exists at two temperatures i) T_1 in the state of the fluid below T_c and ii) T_2 in the state of the fluid above T_c. T_1 and T_2 are paired to the same viscosity value. However, the model herein does not show precisely how the viscosity increases above the critical temperature T_c. The theory of the viscosity of the perfect gas systems predicts that the viscosity of the systems as the average velocity of its particles is proportional to $\sqrt{T}$, which suggests that the thermal energy is exclusively converted to kinetic energy (Sutherland, 1893). We propose that the conditions $\eta(T_1) = \eta(T_2)$ are verified if $F(T_2) = F(T_1)$,therefore a second polynomial regression function is used for F(T) and expressed as:

$$F(T) - F(T_1) = B_2 \cdot (T - T_1) \cdot (T - T_2) \quad (12)$$

The minimum of Eq.12 may coincide with the minimum of the viscosity at the critical temperature T_c. B_2 reflects the thermal resistance of the fluid as a monophasic system. As such, B_2 is weak when it costs more energy to reach the viscosity of T_2. Therefore, B_2 somehow reflects the cost of energy reciprocally from expansion to evaporation of the liquid. The critical temperature which is $(T_1 + T_2)/2$ evolves as T_2. Thus, this model could use only one adjusting parameter, i.e. B_2 if T_c was known or determined using other techniques. The viscosity of all the examined samples have been fitted using the viscosity model:

$$\eta^{T} = \eta^{T_1} \cdot Exp\ \left[B_2 \cdot (T - T_1) \cdot (T - T_2)\right] \quad (13)$$

For the present study, the reference T_1 = 20 °C and T_2 is determined by the fit function as well as B_2. The values of B_2 and T_c were examined as function of the polysaccharide concentration to show the influence of the polysaccharide on the solution resistance to thermal flow.

The experimental data of the concentration dependence of the viscosity for various temperatures were analysed using Huggins and Kraemer function to obtain the C* and the intrinsic viscosity [η] (Chronakis, Doublier & Piculell, 2000). The C* and [η] were evaluated as function of the temperature and the results used to discuss the thermal stability of the polysaccharide in solution.

3. Results and Discussion

3.1 Temperature dependence of the viscosity

The temperature dependence of the solvent viscosity (demineralized water with 200-ppm NaN_3) and kappa-carrageenan (kC) solutions from 0.12 g/L to 7.0 g/L were measured in the temperature intervals from 5 °C to 60 °C. The fit to Eq.13 data of demineralized water are shown in **Table 1** for the current viscosity data and the data of Korson et al. 1969 (Korson, Drost-Hansen & Millero, 1969). As aforementioned, it is imperative to note that the objective of determining the viscosity of demineralized water was not to report on the true value of the viscosity of water for the various temperatures but to use the appropriate viscosity of the solvent displayed by the instrument in our experimental conditions for the study.

The fit function is assumed to provide the appropriate solvent viscosity for the temperature given that beyond 50 °C, it was not possible to measure the viscosities of either the solvent or the samples at lower concentrations accurately. The concept on which the fit function is based on leads to the comparison of the critical temperature T_c with the water evaporation temperature. As we found a similar value, the coincidence is interesting for the acceptability of the model for calculating the viscosity for various temperatures from 0 °C to T_c. The coincidence could be fortuitous, because taking T_c from the viscosity data reported by Korson et al., 1969 (Korson, Drost-Hansen & Millero, 1969), one cannot tell exactly how the experimental set up influenced the accuracy of T_c.

***Table 1**: The parameters of the fit to Eq.13 used to fit the temperature dependence of the water viscosity from the DHR3-Couette geometry and of the water viscosity data reported by Korson et al. 1969 (Korson, Drost-Hansen & Millero, 1969)*

Type of solvent (water)	Water + 200-ppm NaN_3	From the literature Korson et al. 1969
Instrument	DHR3 Rheometer with Couette geometry	Cannon-Ubbelohde Viscometer
η_0 (20 °C) reference	1.114 ± 0.030 mPa.s	1.002 mPa.s
T_1 (Liq.)	20.4 ± 0.5 °C	20.8 °C
T_2 (Gas)	180.0 ± 3.9 °C	256 °C
T_c	100.2 ± 1.7 °C	138.6 °C
B_2	1.57×10^{-4} °C^{-2}	1.01×10^{-4} °C^{-2}
R^2	0.995	0.999

Figure 2a shows the temperature ramp of the viscosity for the solvent and for various kC concentrations with the fit function, Eq.13, through the data. The mean square regression coefficient (R^2) for all of the samples and solvent examined lies between 0.988 and 1, the average of R^2 is 0.997 ± 0.003. The results show a strong correlation of the viscosity with the temperature, which characterizes the temperature dependence of the dynamic mass (m_D) of the system. Given that the static mass (m) per unit of volume, which is explicitly the concentration, is constant, it is, therefore, the decrease of the m_D that causes the decrease of the viscosity when the temperature increases (**Figure 2a**). Thus, the increase of the temperature leads the system constituents to behave more and more like an individual. The resistance of the constituents to behave like an individual characterizes somehow the affinity between the polymers and the polymers with the solvent molecules with which they form a monophasic system. This affinity within the solution is reflected by the fit parameters, namely the coefficient B_2 and T_c shown in **Figure 2b**.

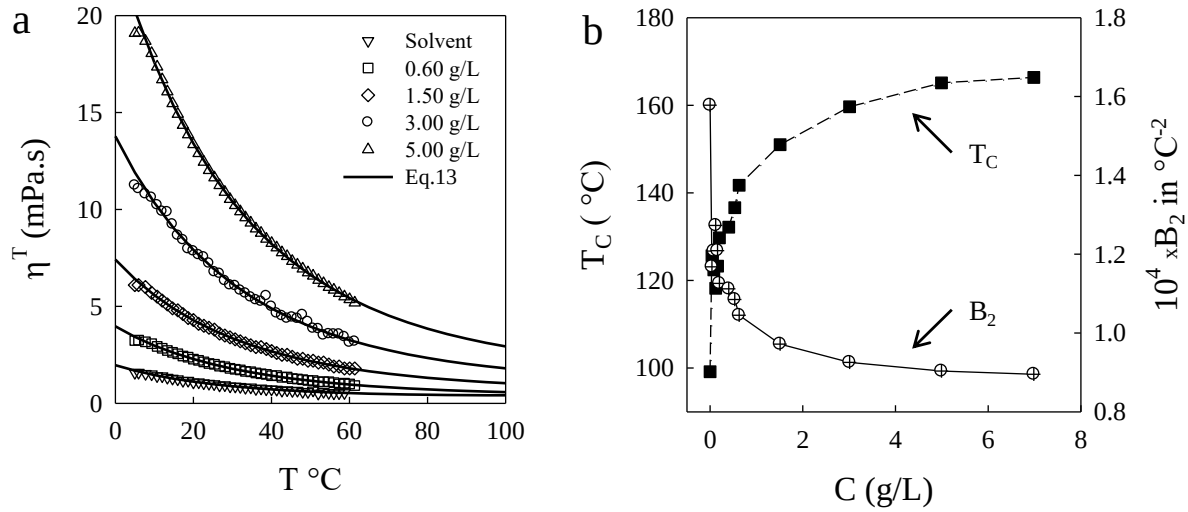

Figure 2: *a) Temperature dependence of the viscosity for various concentrations of kC solution. The full lines through the data are the fit function to Eq. 13. b) the fit parameters for B_2 and critical temperature, T_c, which is the temperature corresponding to the predicted minimum of the viscosity of the fluid where according to the model the interactions in the systems are weak.*

The increase of the critical temperature or the diminution of the coefficient B_2 shows that the polysaccharide likes to dwell in the solvent (resistance to evaporation). As we look at the quantity $T_c \times B_2$, we found $1.5\times10^{-2} \pm 3.7\times10^{-4}$ /°C, the same value as that reported for the kC solution in presence of KCl salt by Elmarhoum and Ako 2021 (Elmarhoum & Ako, 2021). This value is almost constant on the interval of the concentrations studied in the present work, except for the solvent for which the value is 1.6×10^{-2} /°C. Thus, the quantity $T_c \times B_2$ depends on the presence of the polymer rather than the concentration. Therefore, the critical temperature controls the temperature dependence of the viscosity by factor $T_c \times B_2$, which depends mainly on the system composition. Thus, the temperature dependence of the viscosity data could be fitted with the viscosity model using only one fit parameter because if T_c is known by other techniques, then B_2 remains the parameter to fit the temperature dependence of the viscosity data. The derivation of the polynomial function of Eq.10 could be expressed as:

$$\frac{1}{T} f^T = 2T_c B_2 \cdot \left(\frac{T}{T_c} - 1 \right) \tag{14}$$

with T between 0 °C and T_c (°C). The Eq.14 gives the quantity $T_c \times B_2$ as the absolute value of the limit of $(\partial\eta/\eta)$ when $T \rightarrow 0$ °C. The negative value of the limit could be the result of the inter and intramolecular forces acting in the system to oppose its thermal deformation.

3.2 Concentration dependence of the viscosity

The viscosity values of the samples (η) were recorded at 20 °C, which is the temperature at which the viscosity of the reference was measured experimentally. The data are plotted versus the concentrations in log-log scale (**Figure 3**) for determining the relationship of the function between the viscosity and the concentration for this temperature as denoted in Eq.15

$$\eta - \eta_0 = \eta_0 \cdot a \cdot C^b \tag{15}$$

where η_0 is the solvent viscosity, a is an adjusting parameter and b is the scaling power. Eq.15 fairly fits well the viscosity data from the lower to the higher concentration (**Figure 3**, solid line). This shows that the specific viscosity $\eta_{sp} = (\eta - \eta_0)/\eta_0$, scales as a power law function of the concentration $\eta_{sp} \approx C^b$ as shown by the straight dash line in **Figure 3** which is in agreement with the scaling law theory for polymers in solution.

The polymer in solution theory predicts a power law function of b ≈1.3 for a flexible polymer in a good solvent and ≈ 0.5 for polyelectrolyte in solution with no-salt for the concentrations in semi-dilute unentangled regime which concentration domain is identified here as dilute and semi-dilute regime (Colby, 2010). In the case of the present study, the value of b ≈ 1.15 is comparable to that of flexible polymer in good solvent weakly expanded by intramolecular repulsive forces.

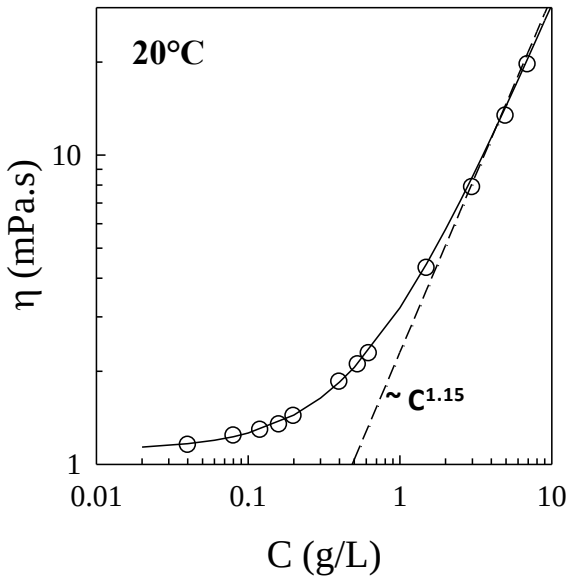

***Figure 3**: Concentration dependence of the viscosity of kC solution for 20 °C. The solid and dash line represent the scaling law of the viscosity from the solvent viscosity and the viscosity*

increment with the concentration respectively. The dash line is comparable to the theoretical prediction of the viscosity for neutral flexible polymer in a good solvent ~$C^{1.3}$ at C < C, i.e. the semi-dilute unentangled regime. The overlapping regime of the hydrodynamic volume for the kC is like unentangled regime for the neutral flexible polymer in good solvent because of likely repulsive interactions between the kC.*

The scaling power remains constant in the concentration intervals explored which means that the double logarithm plot of the η_{sp} versus concentration is not appropriate to determine the C*. This seemingly is not what reflect the results reported by Croguennoc et al. 2000 and co-workers on the C* value using light scattering and rheometer methods (Croguennoc, Meunier, Durand & Nicolai, 2000). The authors determined the z-average radius of the coil, R_{gz} by light scattering measurement then used the Eq.16

$$C^* = \frac{3M_w}{4\pi N_A R_{gz}^3} \tag{16}$$

to obtain the C*, which gives C* = 0.45 g/L for the kC in 0.1 M NaCl solution. The C* from the viscosity measurement was estimated by using Huggins Eq.17 to derive the intrinsic viscosity $[\eta]_H$ by extrapolation to infinite dilution as the inverse of $[\eta]_H$, ($C^* \approx 1/[\eta]_H$).

$$\frac{\eta_{sp}}{C} = [\eta]_H + k_H [\eta]_H^2 C \qquad \text{Huggins} \tag{17}$$

which gives C* = 1.1 g/L for an intrinsic viscosity of 0.94 L/g for 4.3×10^5 g/mol in 0.1 M NaCl solution at 20 °C. Chronakis et al. 2000(Chronakis, Doublier & Piculell, 2000) combined both Huggins Eq.17 and Kraemer Eq.18 to derive C* value by extrapolation to infinite dilution

$$\frac{Ln(\eta/\eta_0)}{C} = [\eta]_K + k_K [\eta]_K^2 C \qquad \text{Kraemer} \tag{18}$$

but the C* was not derived directly as the inverse of the intrinsic viscosity. It was determined as the transition point between two concentration regimes characterized by isolated coil kC in the dilute regime to coil overlap entangled semi-dilute regime as a change of the scaling power b. The authors found $C^* \approx 0.9$ g/L with an intrinsic viscosity of 2.34 L/g for 7×10^5 g/mol in 0.2 M NaI at 25 °C. The critical concentration determination from the viscosity measurement in log-log representation is very sensitive to the change of slope of the specific viscosity when turning the concentration from one regime to another. The difficulty of detecting the C* may

be due to the weakness of the degree of the hindrance of the polymer motion due the presence of others polymers when their hydrodynamic volume or the electrostatic potential shell length start overlapping. The repulsive interaction and the affinity of the polymer to the solvent may contribute to weakening of the hindrance effects around the C*. Therefore, changing the affinity between the solvent and the polysaccharide could result in better detection of the point at which the concentration regime changes. The concentration dependence of the viscosity of various temperatures including for 0 °C and 90 °C which were obtained from the fit (Eq.13), i.e. the temperature dependence of the viscosity for various concentrations are shown in **Figure 4**.

The specific viscosity is plotted as function of the concentration for various temperatures to identify the transition from dilute and semi-dilute regime for determining the C*. For a large range of temperature, from 0 °C to roughly 45 °C, the concentration where the slope changes was not clearly identified. Nevertheless, the slope changes more or less remarkably from temperature above 45 °C using the fit.

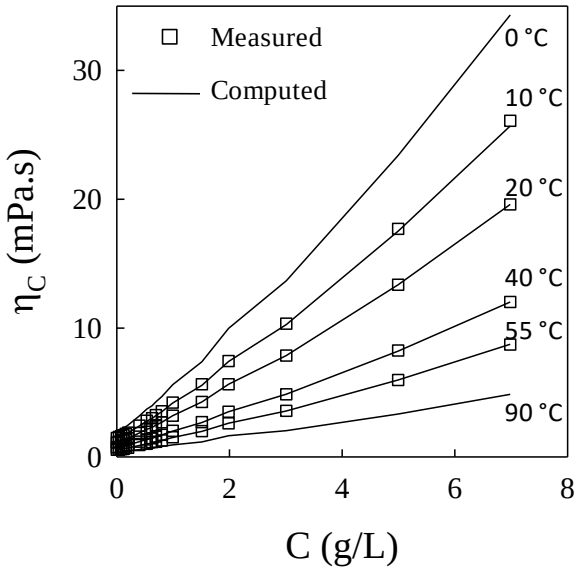

***Figure 4**: Concentration dependence of the viscosity for various temperatures. The symbols are the measured data and the solid lines are the data obtained with Eq. 13.*

The specific viscosity versus the concentration in double logarithm plot for 20 °C and 70 °C are shown in **Figure 5a** to illustrate the difficulty of identifying the C*. For 20 °C, no change of slope was observed. With the fit a change of the slope at 70 °C was seen. The viscosity of the samples versus the concentration for 70 °C show a clear change of the scaling power slope from 1.1 to 1.6 characterizing the shift from semi-dilute to dilute regime respectively which is

observed at a critical concentration of 0.54 g/L. Thus, the lower concentrations for determining the intrinsic viscosity are defined as concentration < 0.5 g/L. The intrinsic viscosities were determined by combined Huggins Eq.17, and Kraemer Eq.18, extrapolation to infinite dilution. The Huggins plot (H-plot) and Kraemer plot (K-plot) theoretically cross at [η] when C → 0. However, because of experimental imprecision the cross point does not occur exactly at the 0 axis of the concentration. Thus, we denote $[\eta]_H$ and $[\eta]_K$ the intrinsic viscosity from the H-plot and K-plot respectively. An illustration of the H-plot and K-plot for 20 °C and 40 °C are provided in **Figure 5b**. The plots are acceptably linear which give $[\eta]_H$ and $[\eta]_K$ respectively 1.23 L/g and 1.25 L/g for 20 °C, 1.10 L/g and 1.13 L/g for 40 °C. The intrinsic viscosity from both plots are similar. The concentration where the two plots cross is 0.02 g/L for 20 °C and 0.04 g/L for 40 °C. When the intrinsic viscosity ranges between 0.1 L/g and 2 L/g this characterizes an extended chain or very flexible chain rather than a compact coil as reported by Chronakis et al. 2000 (Chronakis, Doublier & Piculell, 2000).

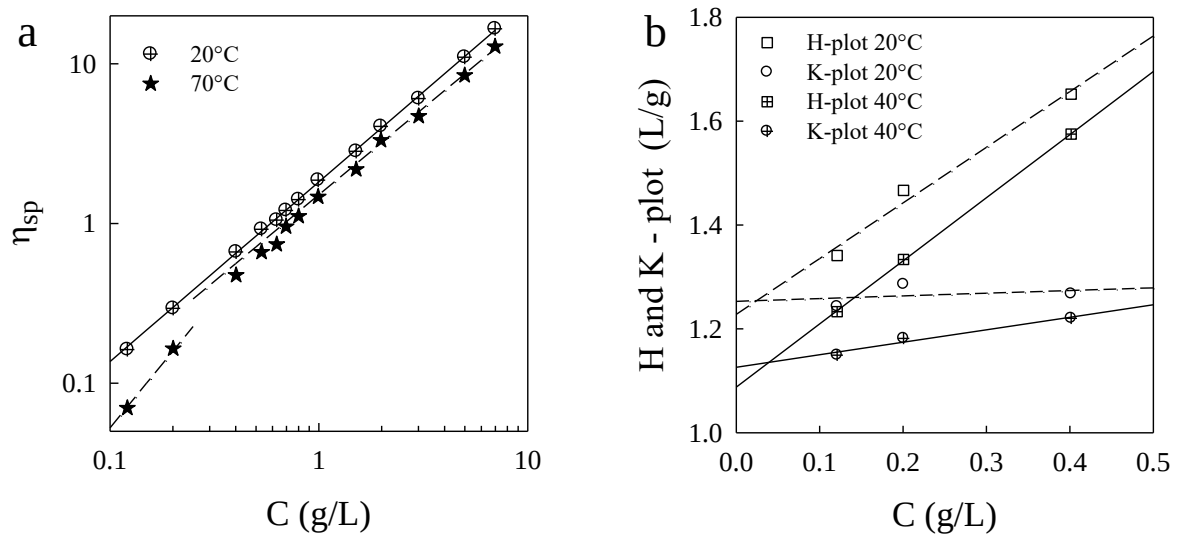

Figure 5: *a) Concentration dependence of the specific viscosity for 20 °C and 70 °C in double logarithmic plot. The data of 70 °C were predicted using Eq. 13. The solid and dash line represent the scaling law of the viscosity with the concentration as ~C^b where power-b is the slope of the lines. b) Is the Huggins Eq.17 and Kramer Eq.18 plots for the concentration lower than 0.5 g/L.*

Comparatively, the intrinsic viscosity of the current study is greater than what was reported by Croguennoc et al. 2000 for the same temperature but in the presence of 0.1 M NaCl

(Croguennoc, Meunier, Durand & Nicolai, 2000). It is not surprising that we found a greater intrinsic viscosity because Slootmaker et al. 1988 have reported an increasing tendency of the intrinsic viscosity with decreasing the NaCl ionic strength for 3.3×10^5 g/mol kC (Slootmaekers, De Jonghe, Reynaers, Varkevisser & van Treslong, 1988). The intrinsic viscosity of kC was found to increase almost linearly as a function of the inverse root of the NaCl concentration (Slootmaekers, De Jonghe, Reynaers, Varkevisser & van Treslong, 1988). This gives roughly a corresponding presence of 10 mM NaCl for $[\eta] \approx 1.23$ L/g at 25 °C. Thus, there is a probability that traces of salt could still be in the kC solution after the dialysis step in the present study.

We found that when the Kraemer function (Eq.18) is plotted as function of Log(C) the plots clearly show the frontier between the concentration regimes for all the temperatures examined. We denoted this type of representation Kraemer-LogC or K-LogC. Therefore, we did the same with the Huggins function (Eq.17), Huggins-LogC or H-LogC. The H-LogC and K-LogC are shown in **Figure 6a** for 20 °C and in **Figure 6b** for 70 °C. For 20 °C the H-LogC does not show the existence of C* as it is clearly defined for the K-LogC. The K-LogC shows a C* for 20 °C at 0.45 g/L. In comparison with the result reported by Croguennoc et al. 2000, the C* is similar with the value that the authors found by light scattering technique, which corresponds to $R_{gz} \approx$ 66 nm using Eq.16 (Croguennoc, Meunier, Durand & Nicolai, 2000). However, for 70 °C both H-LogC and K-LogC showed the same position of C* at 0.55 g/L (**Figure 6b**).

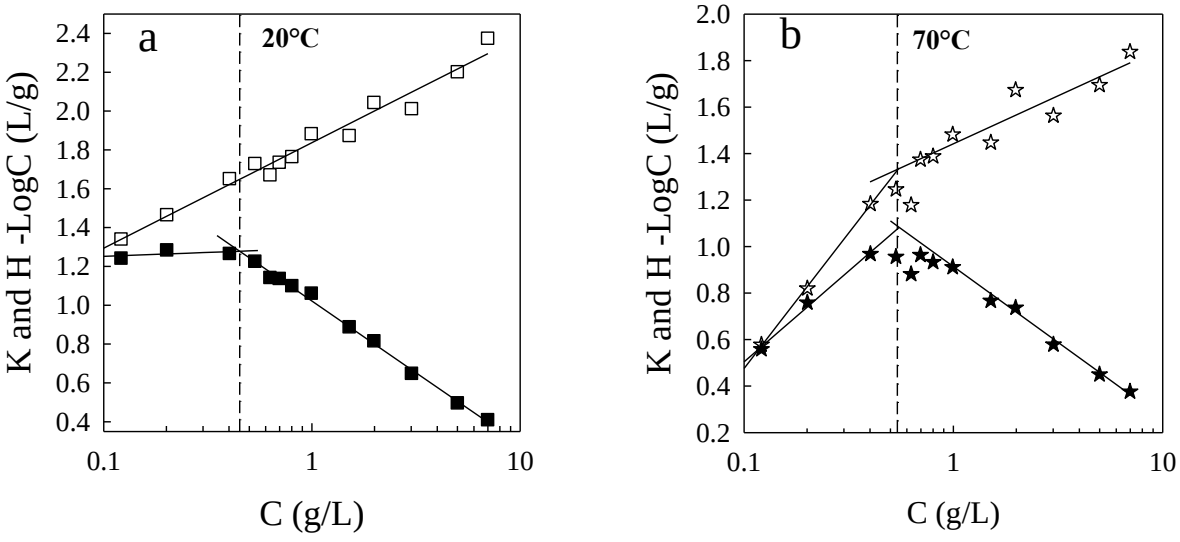

***Figure 6**: Concentration dependence of η_{sp}/C (Eq.17) open symbols and $Ln(\eta_r)/C$ (Eq. 18) full symbols in Lin-Log plot for a) 20 °C and b) 70 °C. The dash line indicates the C*.*

It results from the comparison of both methods for determining C* that Kraemer representation in Log(C) allows an accurate determination of C* of all the temperatures examined in this study. The following equations are therefore proposed for determining the C* but only Eq. 20 was used thereafter.

$$\frac{\eta_{sp}}{C} = A_H^* + A_H \cdot Ln(C) \tag{19}$$

$$\frac{Ln(\eta_C / \eta_0)}{C} = A_K^* + A_K \cdot Ln(C) \tag{20}$$

The coefficients of the Eqs.19 and 20 depend on the regime of concentration, but at C* both semi-dilute and dilute regime yield the same value.

The temperature dependence of the intrinsic viscosity, Huggins $[\eta]_H$ and Kraemer $[\eta]_K$, are shown in **Figure 7a**. Due to the considerable fluctuation of the measured viscosity of the solvent for T > 45 °C the intrinsic viscosity was not determined for the higher temperature. The model was used to extrapolate data to these temperatures (solid line). The intrinsic viscosity is maximum $[\eta] \approx 1.24$ L/g around 20 °C.

The decrease of the intrinsic viscosity characterizes the diminution of the capacity for the polymer to increase the viscosity when its presence is increased in the solution. In the semi-dilute regime, this diminution of the thickening capacity result directly from the loss of affinity with the solvent. The fact that the affinity of the polysaccharide increases then decreases thereafter interrogates the complex relation between solvent-solvent molecular interactions and solvent-polysaccharide interactions.

We hypothesize that when the temperature decreases below 20 °C the solvent-solvent molecular interactions prevail over the solvent-polysaccharide interactions. Above 20 °C, the heat weakens the physical bonds between the solvent molecules and the polysaccharide. Subsequent increase of heat increases the degree of liberty of the molecules to free motion. We propose that the thermal properties of the solvent are very crucial in understanding the intrinsic viscosity of the solutions.

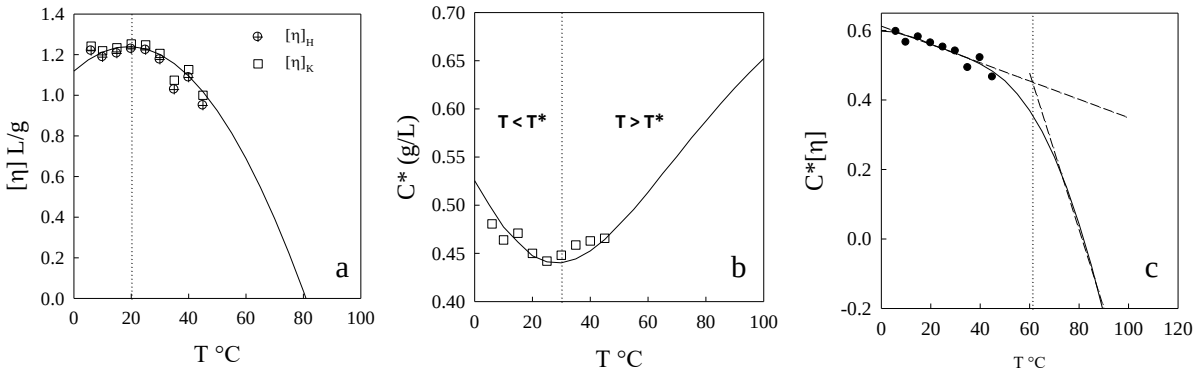

Figure 7*: Temperature dependence of a) the intrinsic viscosity from both Huggins and Kraemer functions. The solid line represents the average results from the fit to Eq. 13 of the Huggins and Kraemer function, b) the critical concentration where the solid line represents the result from the fit to Eq.13 and T* is the temperature where the C* is lower. c) the dimensionless quantity C*[η] which could characterize the evolution of the amount of solvent molecules carried at C* by the polymer.*

When the temperature approaches the solvent liquid-gas or liquid-solid transition, the dynamic of the molecules, which characterize the m_D of the molecular interaction forces, increases or decreases respectively. The thermal property of water may interfere with the polysaccharide capacity to carry the water molecules and to affect the intrinsic viscosity of the system when the temperature varies. For a system of a given quantity or mass of polysaccharides, the m_D increases with the amount of solvent carried. The viscosity of the system increases accordingly. The temperature dependence of the critical concentration is shown in **Figure 7b**. At the critical concentration, the concentration of the global system is considered equal to the concentration of the volume occupied by a single polysaccharide blob. The solid line is data from the model. The lower C* corresponds to a higher blobs volume (Eq.16). We have denoted T* the lower critical concentration temperature (LCCT) of C*. The C* ≈ 0.44 g/L is lower at T* ≈ 30 °C which corresponds to the maximum average of the blobs volume (**Figure 7b**). This means that the increase or decrease of the temperature from T* ≈ 30 °C leads to the shrinking of the polymer sizes. The intrinsic viscosity data shown in **Figure 7a**, suggest that the temperature where the polymer expansion is higher is not necessarily equal to the temperature where the polysaccharides chains may bind the greatest amount of solvent molecules. However, the amplitude of variation of the C* with the temperature was weak to clearly show the minimum in the temperature range [10 °C - 45 °C] where the measurements were done. The lower value of C* became evident after application of the model as the model gives the C* values for a

larger range of temperature [0 °C - 100 °C]. For this polysaccharide system, the results from the model suggest that the capacity of the polysaccharide to increase the viscosity of the solution by its presence is higher at ≈ 20 °C, whereas the polymer expansion is higher at T* ≈ 30 °C which is a gap of 10 °C that could not be neglected. There is a possibility of the coincidence of both temperatures being fortuitous.

Slootmaekers et al., have reported the hydrodynamic volume as a characteristic parameter of hydrodynamic permeability of polymers (Slootmaekers, De Jonghe, Reynaers, Varkevisser & van Treslong, 1988).The hydrodynamic permeability of a polymer in solution could be understood as the permeability of a gel of this polymer at the critical concentration C* of the same hydrodynamic volume. The permeability of a gel characterizes the capacity of the gel to transmit fluid. Therefore, the higher the hydrodynamic volume which corresponds to lower C* of the polymer, the higher the permeability of the gel if the solvent in the blobs is free. Given that a fraction of solvent in the blob is linked to the polymers, the hydrodynamic permeability of the polymers would result from the intrinsic viscosity coefficient [η] too. Hence, the higher the amount of solvent that the polymer blobs could bind, the lower the amount of free solvent that could flow through them. Therefore, the polysaccharide's capacity to transmit fluid decreases with increasing both C* and [η]. The temperature dependence of the C* and [η] shows that when the systems' temperature decreases (cooling from ≈ 100 °C) the hydrodynamic volume and the intrinsic viscosity increase. From T* ≈ 30 °C, the hydrodynamic volume decreases but the intrinsic viscosity still increases until T ≈ 20 °C where the intrinsic viscosity decreases. The two quantities are therefore independent. The intrinsic elastic property of the polysaccharide chains would be at work interfering with the dynamic induced by the solvent molecules adsorption to the expansion of the polymers (Draget et al., 2001). The enthalpy of adsorption and the elastic potential energy may control the hydrodynamic permeability of the system, which may evolve as a factor of the hydrodynamic volume per the intrinsic viscosity. For the system at C* the hydrodynamic volume per intrinsic viscosity gives an expression which is proportional to 1/C*[η]. Hence, the dimensionless quantity C*[η] gives the capacity of the polymer to resist the flow of the solvent at a given temperature. Therefore, when the quantity C*[η] increases the hydrodynamic permeability decreases (**Figure 7c**) which is characterized by the increase of the viscosity for the polymer in solution. C*[η] is connected with the Flory-Fox relationship Eq.21 (Morris, Cutler, Ross-Murphy, Rees & Price, 1981; Slootmaekers, De Jonghe, Reynaers, Varkevisser & van Treslong, 1988).

$$\Phi^* = \frac{4\pi}{3} N_A C^* [\eta] \quad (21)$$

For the present study, C*[η] increases linearly when the temperature decreases (cooling), which is indicated by the linear least squares fit (dash line) in **Figure 7c**. The slope of the linear correlation between C*[η] and T changes at the adsorption and desorption critical temperature $T_{ad} \approx 60$ °C from 2.6×10^{-3} /°C for T < 60 °C to 22.5×10^{-3} /°C for T > 60 °C. The fact that the hydrodynamic permeability of the polysaccharide increases sharply from $T_{ad} \approx 60$ °C when the temperature increases may energetically result from the dynamic of the adsorption and desorption reaction of the polysaccharide with the solvent molecule at this temperature. We propose this to be Gibbs energy of the reaction:

$$[kC] + x[H_2O] \Leftrightarrow [kC][H_2O]_x \quad \text{R1}$$

$$\Delta G^o = -RT_{eq} Ln(K_{eq}) \quad (22)$$

with K_{eq} the constant of the reaction equilibrium, may provide an explanation of the determination of the temperature T_{ad} from which the hydrodynamic permeability of the polysaccharide increases sharply. It was assumed that the polysaccharide hydration reaction equilibrium characterized by T_{eq} could determine the temperature T_{ad}, but this needs to be well documented.

The temperature dependence of the hydrodynamic permeability of the system is therefore determinant for understanding the water holding capacity of the polymers and syneresis property of the gels or bulk. Actually, the concentration of the gels or bulk is set constant while the hydrodynamic volume of the system constituents changes with the temperature. The change of constituent's hydrodynamic volume may lead to space vacancy (contraction) or overlapping hydrodynamic volume (swelling). If the initial concentration of the sample coincides with the minimum C* and if we assume that the sample gels at the LCCT, i.e. T* then this study demonstrates that for highly thermosensitive constituents at $T \neq T^*$, the bulk may evolve toward space vacancy which is characterized by solvent release (syneresis). Therefore, the concentration has to be increased to keep the solvent inside the gel as depicted in **Figure 8**. However, if the viscosity of the solvent at the temperature at which the sample is kept is predominant, i.e. for instance, when the temperature of the water approaches 0 °C, the solvent is capable of staying inside the gel because of low motion of the molecules.

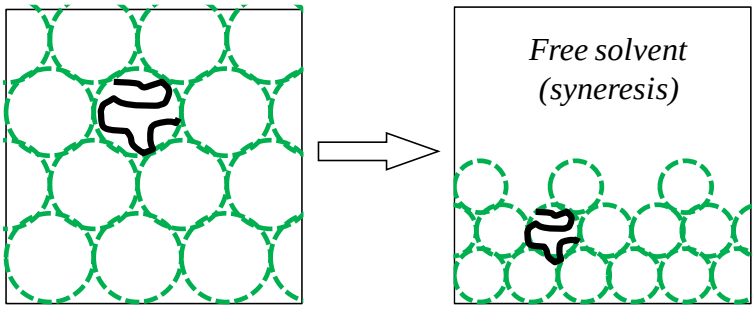

***Figure 8**: Illustration of the syneresis reaction of blobs from the situation where the gel is formed at C* and T*. The T* is the temperature where the C* of the system is lower. The solution of the polymer at C* is pictured as a blobs of radius R_g in contact with each other to fill the space. The reduction of the size of the blobs due to conservation of the system at $T \neq T^*$ leads to contraction of the blobs (Syneresis).*

4. Conclusion

The kC solution in the absence of additional salts shows a Newtonian flow behavior for the concentrations examined and a large temperature dependence of the critical concentration C* as the weight per volume of the blobs and of the intrinsic viscosity [η] as the volume of solvent carried by the blobs per their weight. The stability of these parameters characterise the thermodynamic stability of the polysaccharide in solution. The viscosity model applied in this study fits well the temperature dependence of the viscosity of the solvent and all the kC solutions with a $R^2 = 0.997 \pm 0.003$. According to this viscosity model the solution exhibits a minimum C* ≈ 0.44 g/L at a temperature called lower critical concentration temperature (LCCT) denoted T* which was found for the kC to be ≈ 30 °C and a maximum [η] ≈ 1.23 L/g or change of slope of the [η] at ≈ 20 °C. The dimensionless quantity C*[η] was shown in this work to be the capacity of the polysaccharide to retain the solvent in solution. The C*[η] constantly decreases with the temperature from 0 °C to 45 °C following a slope of 2.6×10^{-3} /°C. The decrease became stronger from T ≈ 60 °C with a slope of 22.5×10^{-3} /°C. Cooling the kC solution from higher temperature (≈ 100 °C) to the LCCT, the kC blobs expanded and carried more solvent molecules accordingly. From the LCCT to 20 °C, the kC blobs volume decreases but the blobs still carried more solvent molecules, leading to the assumption that the temperature dependence of the solvent density could be at work in the [η] value. From 20 °C to lower temperature (0 °C), the kC blobs constantly decrease and the amount of solvent molecules

carried remained almost constant with a decreasing tendency. We hypothesise that pair interactions of solvent molecules may affect both the solvent density and the polymer-solvent interactions, and this plays a significant role in determining the intrinsic viscosity of hydrocolloid in solution. The water holding capacity as the hydrodynamic permeability of the polysaccharide is therefore determined fundamentally by both the pair interaction of solvent molecules with the polymers and the C* before gelation of the solution interferes with this.

5. Conflict of interest

The authors declare no conflicts of interest.

6. Acknowledgement

We thank Vincent VERDOOT for his technical assistance on the Rheometer Instruments. The authors thank Pr. Marguerite Rinaudo for providing us with the kappa-Carrageenan product. We thank Laurine Buon and Eric Bayma from Cermav for their kind assistance on the product composition. This work was financially supported by I-MEP2 PhD graduate school. The Laboratoire Rhéologie et Procédés (LRP) is part of the LabEx Tec 21 (Investissements d'Avenir - grant agreement n°ANR-11-LABX-0030) and of the PolyNat Carnot Institut Investissements d'Avenir - grant agreement n°ANR-11-CARN-030-01).

7. References

Ako, K. (2015). Influence of elasticity on the syneresis properties of kappa-carrageenan gels. *Carbohydrate Polymers, 115*, 408-414.

Berger, J., Reist, M., Mayer, J. M., Felt, O., & Gurny, R. (2004). Structure and interactions in chitosan hydrogels formed by complexation or aggregation for biomedical applications. *European Journal of Pharmaceutics and Biopharmaceutics, 57*, 35-52.

Boral, S., Saxena, A., & Bohidar, H. B. (2010). Syneresis in agar hydrogels. *International Journal of Biological Macromolecules, 46*, 232-236.

Brunchi, C.-E., Morariu, S., & Bercea, M. (2014). Intrinsic viscosity and conformational parameters of xanthan inaqueous solutions: Salt addition effect. *Colloids and Surfaces B, 122*, 512-519.

Campo, V. L., Kawano, D. F., da Silva Jr, D. B., & Carvalho, I. (2009). Carrageenans: Biological properties, chemical modifications and structural analysis - A review. *Carbohydrate Polymers, 77*, 167-180.

Chronakis, I. S., Doublier, J.-L., & Piculell, L. (2000). Viscoelastic properties for kappa- and iota-carrageenan in aqueous NaI from the liquid-like to the solid-like behaviour. *International Journal of Biological Macromolecules, 28*, 1-14.

Ciancia, M., Milas, M., & Rinaudo, M. (1997). On the specific role of coions and counterions on kappa-carrageenan conformation. *International Journal of Biological Macromolecules, 20*, 35-41.

Colby, R. H. (2010). Structure and linear viscoelasticity of flexible polymer solutions: comparison of polyelectrolyte and neutral polymer solutions. *Rheologica Acta, 49*, 425-442.

Croguennoc, P., Meunier, V., Durand, D., & Nicolai, T. (2000). Characterization of Semidilute k-Carrageenan Solutions. *Macromolecules, 33*, 7471-7474.

Divoux, T., Mao, B., & Snabre, P. (2015). Syneresis and delayed detachment in agar plates. *Soft Matter, 11*, 3677-3685.

Draget, K. I., Gaserod, O., Aune, I., Andersen, P. O., Storbakken, B., Stokke, B. T., & Smidsrod, O. (2001). Effects of molecular weight and elastic segment flexibility on syneresis in Ca-alginate gels. *Food Hydrocolloids, 15*, 485-490.

Drury, J. L., & Mooney, D. J. (2003). Hydrogels for tissue engineering: scaffold design variables and applications. *Biomaterials, 24*.

Einhorn-Stoll, U. (2018). Pectin-water interactions in foods - From powder to gel. *Food Hydrocolloids, 78*, 109-119.

Elmarhoum, S., & Ako, K. (2021). Lower critical concentration temperature as thermodynamic origin of syneresis: Case of kappa-carrageenan solution. *Carbohydrate Polymers, 267*.

Fernandez-Nieves, A., Fernandez-Barbero, A., Vincent, B., & de las Nieves, F. J. (2000). Charge Controlled Swelling of Microgel Particles. *Macromolecules, 33*, 2114-2118.

Field, C. K., & Kerstein, M. D. (1994). Overview of Wound Healing in a Moist Environment. *The American Journal of Surgery, 167*.

Hoffman, A. S. (2012). Hydrogels for biomedical applications. *Advanced Drug Delivery Reviews, 64*, 18-23.

Horkay, F., Tasaki, I., & Basser, P. J. (2000). Osmotic Swelling of Polyacrylate Hydrogels in Physiological Salt Solution. *Biomacromolecules, 1*, 84-90.

Kaur, L., Singh, N., & Sodhi, N. S. (2002). Some properties of potatoes and their starches II. Morphological, thermal and rheological properties of starches. *Food Chemistry, 79*, 183-192.

Klouda, L., & Mikos, A. G. (2008). Thermoresponsive hydrogels in biomedical applications. *European Journal of Pharmaceutics and Biopharmaceutics, 68*, 34-45.

Korson, L., Drost-Hansen, W., & Millero, F. J. (1969). Viscosity of Water at Various Temperatures. *The Journal of Physical Chemistry, 78*, 34-39.

Lai, V. M. F., Wong, P. A.-L., & Lii, C.-Y. (2000). Effects of Cation Properties on Sol-gel Transition and Gel Properties of k-carrageenan. *Journal of Food Science, 65*(8), 1332-1337.

Lee, M. H., Baek, M. H., Cha, D. S., Park, H. J., & Lim, S. T. (2002). Freeze-thaw stabilization of sweet potato starch gel by polysaccharide gums. *Food Hydrocolloids, 16*, 345-352.

Liu, Q., Subhash, G., & Moore, D. F. (2011). Loading velocity dependent permeability in agarose gel under compression. *Journal of the Mechanical Behavior of Biomedical Materials, 4*, 974-982.

Mao, R., Tang, J., & Swanson, B. G. (2001). Water holding capacity and microstructure of gellan gels. *Carbohydrate Polymers, 46*, 365-371.

Morris, E. R., Cutler, A. N., Ross-Murphy, S. B., Rees, D. A., & Price, J. (1981). Concentration and shear rate dependence of viscosity in random coil polysaccharide solutions. *Carbohydrate Polymers, 1*, 5-21.

Morris, V. J., & Chilvers, G. R. (1983). Rheological Studies of Specific Cation Forms of Kappa Carrageenan Gels *Carbohydrate Polymers, 3*, 129-141.

Munialo, C. D., Kontogiorgos, V., Euston, S. R., & Nyambayo, I. (2020). Rheological, tribological and sensory attributes of texture-modified foods for dysphagia patients and the elderly: A review. *International Journal of Food Science and Technology, 55*, 1862-1871.

Richardson, R. K., & Goycoolea, F. M. (1994). Rheological measurement of kappa-carrageenan during gelation. *Carbohydrate Polymers, 24*, 223-225.

Scherer, G. W. (1989). Mechanics of syneresis I. *Journal of Non-Crystalline Solids, 108*, 18-27.

Slootmaekers, D., De Jonghe, C., Reynaers, H., Varkevisser, F. A., & van Treslong, C. J. (1988). Static light scattering from κ-carrageenan solutions. *International Journal of Biological Macromolecules, 10*, 160-168.

Sutherland, W. (1893). The viscosity of gases and molecular force. *Philosophical Magazine Series 5, 36*, 507-531.

Takeshita, H., Kanaya, T., Nishida, K., & Kaji, K. (2001). Spinodal Decomposition and Syneresis of PVA Gel. *Macromolecules, 34*, 7894-7898.

Teko, E., Osseyi, E., Munialo, C. D., & Ako, K. (2021). The transitioning feature between uncooked and cooked cowpea seeds studied by the mechanical compression test. *Journal of Food Engineering, 292*, 110368-110376.

Vliet, T. v., Dijk, H. J. M. v., Zoon, P., & Walstra, P. (1991). Relation between syneresis and rheological properties of particle gels. *Colloid Polymer Science, 269*, 620-627.

Yousefi, A. R., & Ako, K. (2020). Controlling the rheological properties of wheat starch gels using Lepidium perfoliatum seed gum in steady and dynamic shear. *International Journal of Biological Macromolecules, 143*, 928-936.

Zhang, J., Ji, W., Liu, T., & Feng, C. (2016). Tuning Syneresis Properties of Kappa-Carrageenan Hydrogel by C2-Symmetric Benzene-Based Supramolecular Gelators. *Macromol. Chem. Phys., 217*, 1197-1204.

Chapitre 4

Origine thermodynamique de la synérèse : Partie B

Chapitre 4

Origine thermodynamique de la synérèse : Partie B

Sommaire

Chapitre 4

Origine thermodynamique de la synérèse : Partie B,

Effet du KCl sur la concentration critique minimale des solutions de kappa-carraghénane

Résumé de l'article

La présence de sel dans les solutions de kappa-carraghénane (kC) favorise la formation de gel, mais lorsque les contres ions du polysaccharide qui assurent la neutralité de la solution dialysée ne sont pas assez important, les solutions ne gélifient pas sans ajout de sel dans l'intervalle de 5 °C à 60 °C des températures (T) couramment explorées. Dans cet article, l'évolution de la concentration critique des solutions en fonction de la température est présentée pour les concentrations de KCl de 5, 10 et 15 mM. Pour ces trois concentrations, les températures auxquelles les chaines de kC sont présentées dans une configuration aléatoire et comme des sphères, se trouvent respectivement au-dessus de 15 ± 2 °C, 27 ± 3 °C et 38 ± 1 °C. Les résultats de nos études donnent pour les trois concentrations de sel des LCCT plus grandes que les températures de conservation des solutions. Ainsi, lorsque la solution de 5 g/L de kC en présence de 15 mM de KCl est par exemple conservée à 20 °C, sachant que les chaines de kC sont gonflées à leur maximum à T où LCCT > 60 °C, on peut s'attendre à une contraction du volume des chaines à 20 °C. Si entre temps la solution gélifie, mais lentement à partir de 24 °C, le gel va continuer de se rétracter en expulsant sa phase liquide. C'est ce que montre la figure suivante après des jours de conservation de la solution à 20 °C entre l'état (A) et (B).

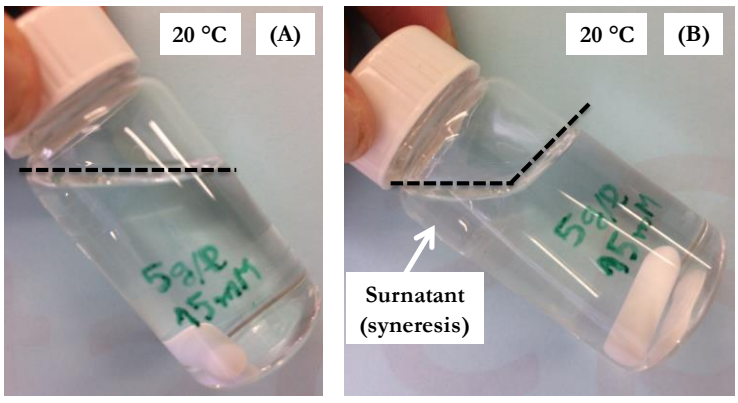

Mots clés: Polysaccharide, Rhéologie, perméabilité hydrodynamique, Synérèse, Thermodynamique

https://doi.org/10.1016/j.carbpol.2021.118191 ; Carbohydrate Polymers 267 (2021) 118191

Highlights

* It exists a lower critical concentration temperature (LCCT) for kappa-carrageenan (kC) suspensions
* The gelation temperature (T_g) of the solutions was found below their LCCT
* The T_g and LCCT increase with the potassium concentration
* Cooling the kC suspensions from the LCCT to T_g causes syneresis

Graphical abstract

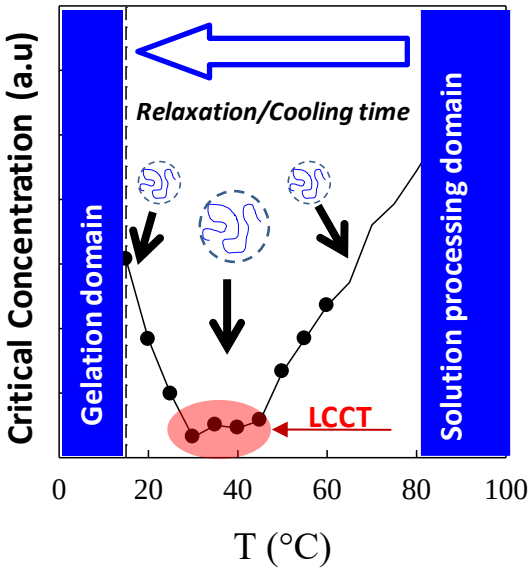

Lower critical concentration temperature as thermodynamic origin of syneresis: Case of kappa-carrageenan solution

Authors and affiliations:

Said ELMARHOUM [a, b], Komla AKO * [a, b],

a) Univ. Grenoble Alpes, LRP, F-38000 Grenoble, France

b) CNRS, LRP, F-38000 Grenoble, France

***Corresponding author**: komla.ako@univ-grenoble-alpes.fr; akokomla@hotmail.com

Abstract

Polysaccharide ubiquity is trimmed for applications of low syneresis impact. This syneresis may be crucial for specific applications that are very sensitive to gel dimension stability, namely, 3D scaffolds for cell culture for disease diagnosis and tissue engineering. We hypothesized that the syneresis origin results from the kappa-carrageenan (kC) polysaccharide thermodynamic instability, and we demonstrated this by measuring the critical (coil-to-coil contact) concentration as a function of temperature. The impact of 5 mM, 10 mM and 15 mM KCl salt on the critical concentration of the solution and the lower critical concentration temperature (LCCT) were particularly investigated. For the kC polysaccharide, the gelation temperature (T_g) falls at temperatures below the LCCT, which explains the shrinking or syneresis reaction of the polysaccharide gels. The gap between T_g and LCCT would be the thermomotive force of the syneresis of many colloidal gels.

Keywords: Polysaccharide, Rheology, Hydrodynamic permeability, Syneresis, Thermodynamic

1. Introduction

Kappa-carrageenan (kC) is a marine algae polyelectrolyte polysaccharide that in solution forms a gel at the appropriate temperature, ionic strength and kC concentration via a mechanism of random coils to helices, conformational transformation and aggregation of the helices (Chronakis, Doublier & Piculell, 2000; Morris, Rees & Robinson, 1980; Rochas, Rinaudo & Vincendon, 1980). However, the gel spontaneously releases its serum by contraction of the polysaccharide network during its conservation. This behaviour is termed syneresis and was reported to depend on the solution composition, ionic strength and kC concentration but also on the temperature at which the gel was conserved. When the kC concentration increases, the syneresis amplitude decreases for various constant KCl salt concentrations and temperatures, as reported by Ako 2015 & 2017 (Ako, 2015, 2017a). The influence of ionic strength and temperature on the syneresis property in the case of kC has shown an interdependent relationship, according to work reported by Ako 2015 (Ako, 2015). This interdependence was characterized by (1) the ionic strength dependence of the gelation temperature (T_g) of the kC solution, (2) the thermoreversible property of the gelation and the viscoelastic modulus, and (3) the ionic strength dependence of the gel mechanical properties. Therefore, the syneresis of kC gels would reflect the interdependence relationship between the temperature and ionic strength. The syneresis measurements were usually conducted on gel samples; for kC systems, this restricted the experimentation temperature to $T \leq T_g$. However, in the gel state, the dynamics of blob contraction are likely to slow down by gel elasticity, which may lead to a substantial time delay of the syneresis exhibition.

The syneresis characterizes many polysaccharides (Mao, Tang & Swanson, 2001) as well as many other gel systems (Labudzinska & Ziabicki, 1971; Lucey, van Vliet, Grolle, Geurts & Walstra, 1997; Scherer, 1988). When syneresis occurs inadvertently after a long storage time of the products, it may cause important financial losses and severe damage in medical areas given the applications of those systems in medical and biopharmaceutical areas (Bittante, Contiero & Cecchinato, 2013; Cheng, Wu, Guan & Zhang, 2012). Mechanical contact problems also arise from the instabilities of the gel dimensions (Divoux, Mao & Snabre, 2015). The chemical and mechanical aspects of the syneresis phenomena converge to i) chemical modification of the hydrocolloids (Campo, Kawano, da Silva Jr & Carvalho, 2009), ii) the use of supergelling agents (Zhang, Ji, Liu & Feng, 2016), and iii) an increase in material concentration (Ako, 2015, 2017b) to stop the occurrence of the syneresis. However, it is not yet

clear whether these methods actually stop syneresis or whether they simply delay the time it takes to exhibit syneresis.

To thermodynamically characterize the occurrence of syneresis in kC gels, we propose to study the contraction of the kC chains (coils) in the aqueous phase rather than the contraction of the bulk (gel) by measuring the temperature dependence of the critical concentration of the systems using rheological methods. The systems are defined by the type of solvent, salt and salt concentrations because those parameters affect the thermal properties of the kC polysaccharides. For a given kC polysaccharide system defined by the composition of the aqueous phase, how the hydrocolloid volume of the polysaccharide changes from the temperature it is dissolved to the temperature of conservation of the solution? By keeping in mind that gelation of the solution could take place, in this study, each coil is treated as a rigid porous sphere of volume equal to the hydrodynamic volume of the coils (Chronakis, Doublier & Piculell, 2000; Morris, Cutler, Ross-Murphy, Rees & Price, 1981).

2. Materials and methods

2.1. Samples characteristics

The kappa-carrageenan (kC) polysaccharide is a gift from Rhodia Food Switzerland, product name and reference: MEYPRO-GEL 01/2001 WG95-37 K-Car. It is made of a sequence of alternating disaccharides, α-(1-3)-D-galactose-4-sulfate and β-(1-4)-3,6-anhydrose-D-galactose. The dialyzed product may contain a weak amount of glucose and was found in the pure potassium kC form of total potassium at no more than 4.2 % (w/w); the other salts were considered to be only trace amounts. The molecular weight of the polysaccharide was determined by GPC-MALLS. The polysaccharide was dissolved in water to form a transparent solution of 2 g/L after 6 h of stirring. The solution was filtered through a 0.2 µm pore size before it was injected into two Shodex OHpak SB 806 M HQ colons set at 30 °C. The colon exclusion limit using pullulan polysaccharide as a reference was 20 000 kDa. The eluant is a solution of sodium nitrate 0.1 M with 300 ppm sodium azide with a flow rate of 0.5 mL/min. One hundred microlitres of the sample solution was injected for each measurement, and the retention time was 70 min. Detection was performed using a Wyatt refractometer and a Shimadzu UV-visible spectrophotometer at 280 nm and Wyatt light scattering at three angles. The dn/dC was 0.155 mL/g. The measurement was done in triplicate. The average molecular weight of the polysaccharide was $M_w = 3.3\times10^5$ g/mol, with an average polydispersity index of Ip = 2.02.

2.2. Samples preparations

A 20 g/L solution of the polysaccharides was prepared by dissolving the powder in demineralized water with 200 ppm sodium azide as the bacteriostatic agent. The mixture was heated at 90 °C under stirring for 10 h. Then, the solution was dialyzed in 4 L of ultrapure water with 200 ppm sodium azide for 3 days to remove the residual salts using a dialysis bag with a 6-8 kDa molecular weight cut off. The dialysis water was renewed three times on the first day and two times on the second and third days. The dialyzed solution was filtered with a 0.45 µm anotop syringe filter to constitute the stock solution. The concentration of the stock solution was adjusted by the dilution factor after dialysis to ≈ 9 g/L kC. All samples examined were prepared by diluting the stock solution at room temperature with the appropriate amount of demineralized water containing KCl salt with 200 ppm sodium azide to give the desired final concentration of polysaccharide and KCl salt concentration. The kC concentration ranges from 0.1 g/L to 7 g/L, and the salt concentration ranges from 0 mM to 15 mM KCl. The samples were mixed under heating in a water bath at 60 °C for approximately 15 min to give a homogeneous solution for the viscosity measurement. The kC solution is thermoreversible, and the sample can turn from liquid to solid-state by cooling and from the solid-state to liquid by heating the same sample, making this system a perfect material for repeating different temperature ramps and measurement conditions on the same sample.

2.3. Viscosity measurements

The viscosity measurements were performed in Couette geometry using a DHR3 Rheometer TA Instrument. The Couette geometry consists of a concentric cylinder geometry of an inner rotor cylinder (bob) and outer stator cylinder (cup) with a radius R_1 of 14 mm and R_2 of 15 mm, defining a horizontal gap (R_2 - R_1) of 1 mm and an average radius R of 14.5 mm as (R_1 + R_2)/2. The height of the bob was 42 mm, and the vertical gap between the bob and cup was set at 2 mm. The minimum and maximum torques of the instrument were 5 µNm and 5×10^3 Nm, respectively. The rheometer measures both the torque M and the angular velocity Ω of the bob. The shear rate is related to the angular velocity by the relation

$$\dot{\gamma} = \frac{R}{R_2 - R_1} \cdot \Omega \qquad 1$$

and the shear stress to the torque by the relation

$$\sigma = \frac{1}{2\pi hR^2} \cdot \mathrm{M} \qquad 2$$

Shear viscosity is defined as the ratio of the shear stress to the shear rate, which is proportional to the ratio M/Ω by the constant

$$K_G = \frac{R_2 - R_1}{2\pi hR^3} \qquad 3$$

which is considered the geometry constant applied by the DHR3 software to convert M/Ω into viscosity data.

The expression of the bob wall velocity is deduced as

$$v_0 = \frac{R_1 \cdot (R_2 - R_1)}{R} \dot{\gamma} \qquad 4$$

When Eq.4 is compared with the velocity of the plate-plate geometry wall of radius R_1 having the same angular velocity Ω on a gap = R_2 - R_1, the comparison yields the following relationships of the shear rate between the plate-plate geometry and Couette geometry:

$$\dot{\gamma}_p = \frac{2R_1}{R_2 + R_1} \dot{\gamma} \approx 0.96\dot{\gamma} \qquad 5$$

which gives the factor between the viscosity from plate-plate geometry and Couette geometry. The results are comparable; however, it is worth noting that theoretically, the Couette shear rate is slightly greater than the plate shear viscosity by 4 %.

The sample's temperature was controlled with a precision of ± 0.5 °C by a water circulation thermoregulator. Before the beginning of the study, the viscosity of the stock solution and a sample of lower concentration were tested as a function of the shear rate from 0.5/s to 30/s to define the Newtonian flow domain in the temperature interval [5 °C, 60 °C] for both the cooling and heating ramps by 0.5 °C/min and 2 °C/min, respectively. We used different volumes of the samples in Couette with different volumes of mineral oil (Sigma Aldrich, $\eta^{20°C}$ = 0.35 Pa.s) to cover the surface of the samples to neglect the water evaporation effect. The viscosity was affected neither by the oil nor by the evaporation when 8 mL of the samples were introduced in the Couette and covered with 1mL of mineral oil. The stock solution (9 g/L) was kept at 5 °C, and its viscosity was measured over two months in the indicated shear rate interval. The

viscosity of the stock solution was constant over the interval of shear rate and stock time. For all the samples tested in this study, the viscosity does not depend on the shear rate except experimental errors. Therefore, all the samples of the study behave like Newtonian fluids, and their viscosity can be assimilated to zero shear viscosity. The measurement of the sample's viscosity and the solvent was performed at 15 s^{-1} when the temperature was varied to yield a torque value in agreement with the instrument's sensitivity.

3. Results and discussion

The critical concentrations, namely, the concentration of the transition between the dilute to semidilute regime or the transition from the semidilute to entanglement regime, are obtained from the concentration dependence of the viscosity of suspensions for a given temperature. Given that kC polysaccharides are put in solution at higher temperatures, most of the time above 60 °C, and the suspensions are stoked at lower temperatures, the hydrodynamic volume of the polysaccharide chains may change with the temperature. Flexible polymers, in general, are characterized by their capacity to adopt different conformations in solution as a function of temperature. The viscosity of the solution changes accordingly as a function of temperature η^T at a constant concentration. However, the viscosity of the solvent also changes. The temperature dependence of the critical concentrations is obtained by treating the η^T data at constant C with the concentration dependence data of the viscosity η_C at constant T in the absence of KCl salt and for the three KCl salt concentrations (5 mM, 10 mM and 15 mM).

3.1. Temperature dependence of the viscosity

Figure 1a shows the temperature dependence of the solvent's viscosity (demineralized water with 200 ppm) and the solution of kC polysaccharide of 0.12 g/L without additional salt. However we did the measurements for various kC concentrations. We display the measurements of 0.12 g/L to show the difficulties of having a clear gap between the viscosity of the solvent and solution of lower concentrations. The viscosity of the solvent and the solution decreases with increasing temperature.

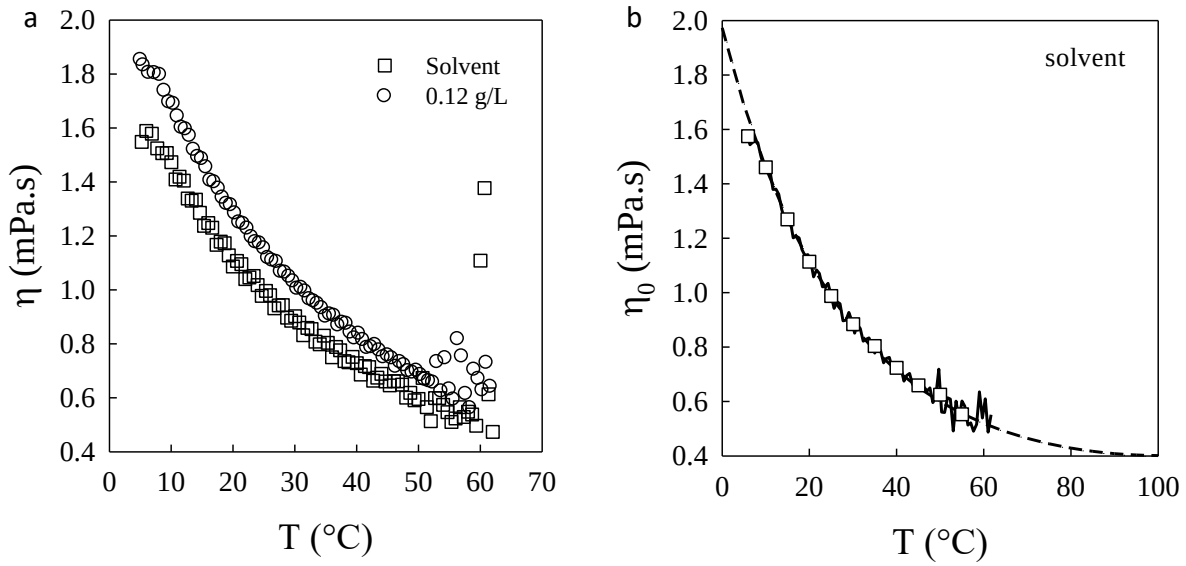

Figure 1: a) Temperature dependence of the viscosity for the solvent and kC solution of 0.12 g/L, b) temperature dependence of the viscosity of the solvent (water + 200-ppm sodium azide). The solid line is the raw data from Figure 1a. The square symbol is the viscosity data averaged on T ± 0.5 °C and displayed by step of 5 °C. The dashed line is the fit to Eq. 6 using $T_1 \approx 20$ °C, $T_c \approx 100$ °C and $B_2 \approx 1.6\times10^{-4}$ /°C^2, the correlation coefficient $R^2 \approx 0.995$.

The fluctuations of the viscosity values increase with the temperature for the solvent. They are pronounced for both the solvent and the solutions of lower concentrations when the temperature approaches 60 °C, which may lead falsely to the viscosity of the solvent being greater than the viscosity of the solutions. These errors could result from slipping effects and the technique sensitivity. To address the fluctuation impact on the data analysis, we fit the viscosity data with a 2nd-order polynomial function F(T) expressed as:

$$Ln\left(\frac{\eta^{T}}{\eta^{T_1}}\right) = B_2 \cdot (T - T_1) \cdot (T - T_2) \qquad 6$$

where T_1 is a reference temperature, and B_2 with T_2 are the fit parameters. The concept supporting a 2nd polynomial function to fit the viscosity data is presented in detail in another paper that is out of the present study's scope. Briefly, the argument is based on the fact that, in general, the liquid transition to gas is characterized by the transition of viscosity decrease for the liquid to viscosity increase for the gas state, which may occur at a critical temperature (T_c) when the temperature increases (Sutherland, 1893). Therefore, B_2 and T_c could be taken as the

fit parameters of the temperature function of the viscosity. For water, $T_c \approx 100$ °C fits the data of Figure 1b well with a correlation coefficient R^2 of 0.995; therefore, the fit parameters may be reduced to only one parameter, B_2, when the T_c of the system is measured using another technique.

For temperatures approaching T_c, the viscosity values were calculated using Eq. 6. However, the viscosity for the reference temperature (T_1) is always measured because it cannot be obtained by the model. For this study, the choice of the reference temperature is discussed based on the results of Figure 2a. The goal of this study restricts us to time-independent viscosity. Rochas et al. 1984 demonstrated that the temperature where the viscosity rises sharply is concomitant with the coil-helix transition (Rochas & Rinaudo, 1984). The transition is an activated energy process characterized by the temperature dependence of the rate of the transition. Because of interference of the coil-helix transition with the viscosity, the time to the stability of the viscosity depends on the temperature and all factors affecting the kinetics of the transition, namely, the type of salt and salt concentration. Salt increases the temperature where the transition occurs, as shown in Figure 2a, but in the presence of KCl salt, the temperature's value depends on the temperature ramp slope (cooling or heating). When the solutions are heated, the transition (helices to coils) occurs at temperatures higher than the temperature of the coils to helices transition when the solution is cooled. It is characterized by a loop (hysteresis) in the temperature dependence of the viscosity data or, more generally, in the properties of these systems in the presence of salt when the temperature is varied (heating or cooling) (Ciancia, Milas & Rinaudo, 1997; Ikeda & Nishinari, 2001; Morris, Rees & Robinson, 1980). Many authors explain the causes of the syneresis by the delay of the mechanism preceding gelation (Bittante, Contiero & Cecchinato, 2013; Chen, Liao & Dunstan, 2002; Cheng, Wu, Guan & Zhang, 2012; Scherer, 1988), which implies for kC and many other types of biopolymer systems a delay of the coil-helices transition and the helices association kinetics (Ciancia, Milas & Rinaudo, 1997; Djabourov, Leblond & Papon, 1988; Higgs & Ball, 1989; Ikeda & Nishinari, 2001; Morris, Rees & Robinson, 1980; Norton & Goodall, 1983; Rochas & Rinaudo, 1984). The current study is restricted to the temperature domain, where both cooling and heating ramps yield the same viscosity values for the various KCl salt concentrations, which was observed in the case of kC for temperatures above the helices-to-coils transition temperature. For the helices-to-coils transition temperature, we found 15 ± 2 °C, 27 ± 3 °C and 38 ± 1 °C for 5, 10 and 15 mM KCl salt concentrations, respectively, which led to restriction of the viscosity measurements within the temperature ranges of [15 °C, 60 °C], [27 °C, 60 °C] and [38 °C, 60

°C] for 5, 10, and 15 mM KCl salt concentrations, respectively. We can see that increasing the salt concentrations leads to shrinkage of the temperature domain, which can be explored within the framework of this study. The samples with no additional KCl salt did not show the helix-coil transition temperature for T ≥ 5 °C. Those samples were kept at 5 °C, including the stock solution (≈ 9 g/L), over 2 months, but their viscosities did not change during this period, which means that the residual salts were considerably removed by dialysis to neglect their influence on the helix/coil transition temperature in this work (Ciancia, Milas & Rinaudo, 1997). Therefore, this temperature domain [5 °C, 60 °C] was explored for the 0 mM KCl salt samples in which the gelation temperature (T_g) was not determined. Within those temperature domains, the samples are in the coil state and behave like a Newtonian fluid, which is the main concern of the present work. Hence, the temperature dependence of the viscosity of the systems studied in those temperature domains was time-independent (thermodynamically stable at the various temperatures), and they may be fitted with Eq.6.

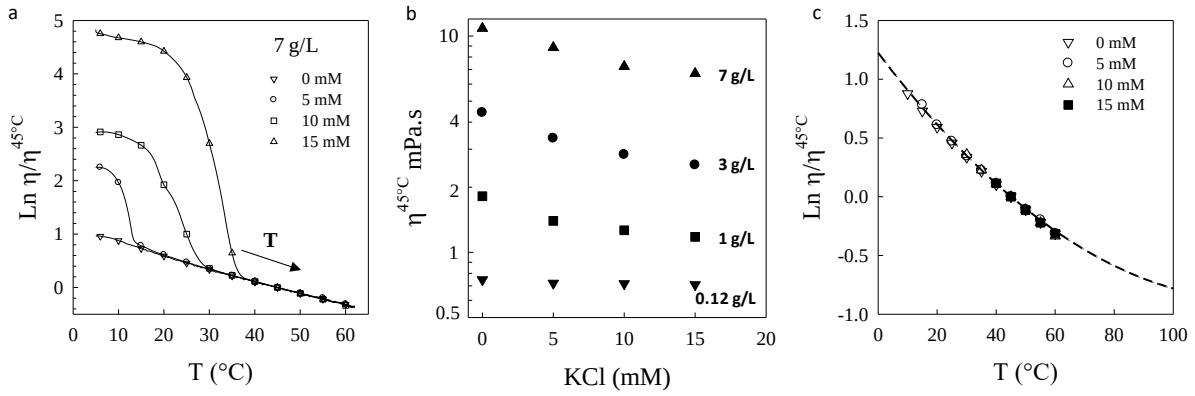

Figure 2: a) Temperature dependence of the logarithm of the viscosity for different KCl salt concentrations for rising temperature for 7 g/L, b) KCl salt concentration dependence of the viscosity of the sample in the coil regime for 45 °C used to normalize the temperature dependence of the viscosity for the different kC concentrations explored, c) Temperature dependence of the logarithm of normalized viscosity value for the kC polysaccharide solution of 7 g/L in the coil regime for the different KCl salts indicated in the figure. The dashed line represents the fit to Eq.6 (R2 = 0.997 ± 0.003).

To apply the fit function of Eq.6, we use the viscosity of the samples at 45 °C as a reference ($\eta^{45°C}$) to keep the same reference temperature for all the samples. The viscosity values of the samples at T_1 = 45 °C are displayed in Figure 2b. We can see that the viscosity of the solutions

in the coil regime decreases when KCl salt is added but increases with the concentration of kC. When the temperature dependence of the viscosity for the various constant salt systems is normalized by $\eta^{45°C}$, the curves superimpose on the same master curves within the temperature domain of interest (Figure 2a, c shows the results for 7 g/L). The fit through the data in Figure 2c represents the global tendency of the viscosity of kC polysaccharide solutions in the coil state with the temperature. However, it is a demonstration of the prevailing feature of the temperature dependence of the solvent viscosity. This implies the weakness of the interactions between the macromolecular components. We understand those interactions by the obstacle to the motion of the polysaccharide chains. The nearly free motion of the macromolecules is in agreement with the Newtonian flow behaviour of the solution, at least in the coil regime, i.e., in the absence of KCl salt or for temperatures above the helix-coil transition temperature. However, for a given kC concentration, the values of the fit parameters of the various sample viscosities show weak differences, namely, the factors B_2 and the critical temperature T_c. Eq.6 fits the viscosity data with a correlation coefficient R^2 that varies between 0.988 and 1 for all the samples tested. The average of R^2 was 0.997 ± 0.003. When the reference temperature T_1 approaches the liquid-gas transition, the error in the calculation of T_c increases. For the lower kC concentration and the higher KCl concentration, we have been limited by the consideration of the temperature interval where fluctuation of the viscosity is less. 45 °C is a compromised temperature for T_1; although the reference temperature is arbitrary, it is strained by the prevailing conditions. Fundamentally, the choice of T_1 should not affect the T_c, but the precision of determining T_c could be affected by error on the viscosity value at T_1, therefore we should not focalize the discussion on the absolute values of the fit parameters but on their relationship with the kC / KCl salt concentrations.

We did not observe a clear relationship of the fit parameters with the salt concentrations, probably because of a lack of data points. We have to include more salt concentration points to conclude on the impact that KCl salt has on the relationship between the viscosity and temperature in the coil regime. However, the kC polysaccharide concentration dependence of the fit parameters was clearly observed. T_c increases while B_2 decreases with increasing polysaccharide concentration, leading to a strikingly constant result of the product $T_c \times B_2$. For the overall samples explored in this study, approximately 70 samples in the absence and presence of salt, the result of $T_c \times B_2$ yields $1.50 \times 10^{-2} \pm 5.0 \times 10^{-4}$/°C. This value is independent of the salt and polysaccharide concentration explored. The incertitude on the product $T_c \times B_2$ is 100 times lower than the average, which may lead to considering the value of $T_c \times B_2$ as constant.

Thus, the fit parameters are relatively reduced to one parameter, $T_{c,}$ for kC polysaccharide solutions. We think that the constant is characteristic of the presence of the polysaccharide in the solvent with which it forms a homogenous phase and Newtonian fluid systems. For comparison with another fluid system, when the same method was applied to mineral oil at temperature intervals from 10 °C to 150 °C, we found 2.3×10^{-2} /°C for the constant ($T_c\times B_2$) and 169 °C for T_c. The values of the fit parameters were independent of T_1. We can conclude that the same T_c systems may not yield the same constant $T_c\times B_2$ and assume that the value of $T_c\times B_2$ is characteristic of the resistance to thermal deformation of the solvent in interaction with the thermoelasticity of the individual macromolecules in solution. The thermoelasticity of the polysaccharide chain was suggested by Ako, 2015 to partly explain the contraction of the bulk at lower temperatures (Ako, 2015), but the relaxation time of the chain and its implication in the bulk contraction are still not resolved. A full understanding of the fundamental causes of the syneresis would help to resolve the part played by the thermoelastic property of the individual polysaccharide chains and their interaction with the solvent molecules.

3.2. Concentration dependence of the viscosity in kC coil regime

The way the viscosity of the solutions ranges with the kC concentration is investigated to determine the critical concentrations for different temperatures because the viscosity ranges with concentration are characteristic of the interactions prevailing in the solution (Colby, 2010; Wyatt & Liberatore, 2009). Figure 3a presents the concentration dependence of the viscosity for different temperatures of the samples in the presence of 5 mM KCl. The data in the figure are those collected from the experimental measurements (symbols) with those obtained from the fit function (solid lines). In the presence of 5 mM, we found a helix-coil transition of ≈ 15 °C; therefore, the experimental data start here from 20 °C for the coil regime. The experimental data are limited to 60 °C because of viscosity weakness/apparatus sensitivity, particularly for the solvent and lower concentration solution. However, the fit function gives viscosity data for temperatures higher than 60 °C and lower than 15 °C. By assuming the coil regime was below 15 °C, the viscosity data could be computed for the temperatures over the coil temperature regime explored (full line in Figure 3a).

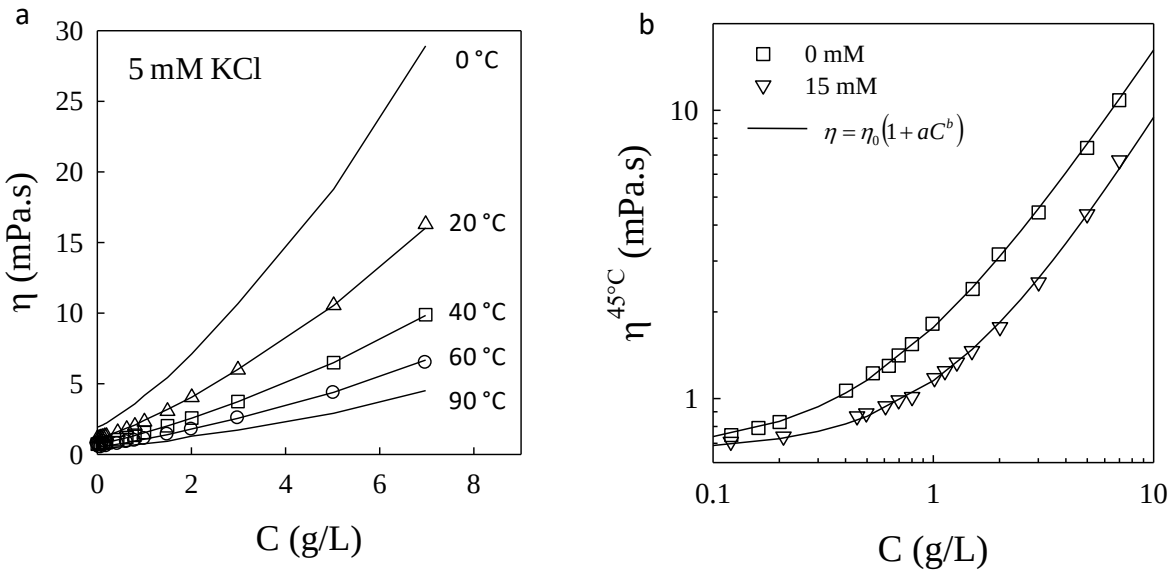

Figure 3: a) kC polysaccharide concentration dependence of the viscosity in the coil regime for 5 mM and for different temperatures indicated in the figure. The experimental data in the coil regime start above the helix-coil transition, which is 15 °C for 5 mM. The solid line is the data obtained by the fit function and extrapolated to 0 °C and 90 °C assuming the coil regime over the coil temperature regime. b) kC polysaccharide concentration dependence of the viscosity at 45 °C for the samples without additional salt and the samples in the presence of 15 mM KCl. The solid line through the experimental data is the fit function shown in the figure, where b is the scaling law power, η0 is the solvent viscosity, and a is an adjusting parameter. b for 0 mM and 15 mM is 1.15 and 1.25, respectively.

The experimental viscosity data at 45 °C, $\eta^{45°C}$, are shown in Figure 3b on a double logarithmic scale with the solid line through the data, which represent the scaling function of the viscosity with the concentration expressed as:

$$\eta - \eta_0 = \eta_0 \cdot a \cdot C^b \qquad 7$$

where η_0 is the solvent viscosity at the corresponding temperature, and a and b are the adjusting parameter and scaling power, respectively. The plots did not display the critical concentrations, namely, the overlap concentration commonly noted as C* and the entangled concentration C_e, which situate the concentration regimes, namely, the dilute ($C < C^*$), semidilute ($C^* < C < C_e$) and entangled ($C > C_e$) regimes. The identification of those critical concentrations is crucial to demonstrate the expansion/contraction dynamics of the polymer chain as an isolated coil to thermodynamically determine the syneresis origin.

The viscosity data displayed in Figure 3b were fitted with Eq.7 using a scaling power b of 1.15 for the sample without additional salt and 1.25 for the samples with 15 mM KCl. the results suggest that the scaling law of the specific viscosity

$$\eta_{sp} = \frac{\eta}{\eta_0} - 1 \qquad 8$$

with the concentration $\propto C^b$ in this study is monotonic for the different salt concentrations, objectively impeding the situation of the overlap concentration in the range of the polysaccharide concentration explored. However, this seemingly is not in agreement with the reports of other authors; for example, a critical concentration below 2 g/L was reported for the kC polysaccharide in a solution of 100 mM NaCl salt (Croguennoc, Meunier, Durand & Nicolai, 2000). The viscosity scaling power, characteristic of the conformation of flexible polymers in the different concentration regimes, is proven (Colby, 2010). For neutral polymers in θ-solvent and good solvent, the scaling law theory of viscosity is well established and used as a reference to explain the behaviour of many other complex systems, such as polyelectrolyte systems. For neutral polymers in a good solvent, the theory predicts a power of 1.3 with concentrations ranging in the semidilute and unentangled regimes. A decrease in the scaling power is correlated with the expansion of the polymer chain. For example, polyelectrolytes with no salt stand for the condition of the greatest expansion that neutral polymer systems could have imaging electrostatic repulsion as an expansion force at work inside neutral polymers to expand it. For these polyelectrolytes systems, the viscosity is predicted to scale with the concentration in the unentangled semidilute regime to a power of 0.5. Therefore, the scaling power of 1.15 and 1.25 is between 0.5 and 1.3 and suggests that the kC polysaccharide behaves like a neutral polymer in good solvent with relatively weak electrostatic repulsion activity between monomers of the same chain. The increase in the scaling power from 1.15 to 1.25 due to the addition of KCl suggests a decrease in polysaccharide expansion, which may be understood as a decrease in the degree of the repulsion forces at work inside the polymer when salt is added to the solution, which is in agreement with the screening effect of salt. The scaling power of 1.15 in the absence of additional salt may reflect the counterion activity and probably the presence of residual salt not totally removed by dialysis. Thus, the addition of salt to the solution shrinks the hydrodynamic volume of the polysaccharide in the coil state, in agreement with the claim of Slootmaker et al. 1988 (Slootmaekers, De Jonghe, Reynaers, Varkevisser & van Treslong, 1988). However, the fact that the viscosity drops with salt addition is another characteristic of the system to find the concentration regime in which this behaviour is possible.

Evidence of the concentration regimes for polyelectrolytes in solutions where long-range, electrostatic, interaction are at work is seemingly a challenging task regarding the method and technique used by experimentalists. Croguenoc et al., 2000 reported 0.45 g/L and 1.1 g/L kC polysaccharides in the coil regime using light scattering and rheological techniques, respectively (Croguennoc, Meunier, Durand & Nicolai, 2000). The concentration regime, particularly the existence of an unentangled semidilute regime for the polyelectrolyte, could be uncertain or fortuitous based exclusively on the viscosity scaling agreement with the theory (Chronakis, Doublier & Piculell, 2000; Croguennoc, Meunier, Durand & Nicolai, 2000; Wyatt, Gunther & Liberatore, 2011). The interpenetration concentration regime identification is puzzled because the definition of entangle versus overlap regimes would not be clear, sometimes leading to confusion between Ce and C*, except if experimentally the gap between C* and Ce recalls the tangibility of the difference between the two critical concentrations (Colby, 2010). The results of the salt dependence of the viscosity in Figures 3b and 2b show a decrease in the viscosity but with a stronger viscosity-concentration scaling law for the solution in the presence of salt. Given that the scaling power of the screened polysaccharide is greater, the viscosity in the presence of KCl monovalent salt should exceed the salt-free solution at some higher concentration, which is relatively the outset of a new concentration regime. For xanthan gum polysaccharides, the viscosity after the addition of 50 mM NaCl salt compared with the free salt solution was reported to be lower in the unentangled semidilute regime but higher in the entangled regime (Wyatt, Gunther & Liberatore, 2011). By analogy, the results in Figures 3b and 2b suggest that the concentration of kC explored was below the entanglement concentration. The concentration dependence of the viscosity should situate the C* below the Ce. The difficulty of evidencing the C* suggests a weak difference of the physical interactions, namely, exclude volume interactions, hydrodynamic interactions and electrostatic interactions, activity on the viscosity-concentration scaling power between the dilute ($C < C^*$) and unentangled semidilute ($C < Ce$) regime. Unlike the statement that those physical interactions are screened when $C > C^*$ (Colby, 2010), we think that the electrostatic repulsion forces would still be at work, giving way to the continuation of both excluded volume interactions with hydrodynamic interactions to a certain degree.

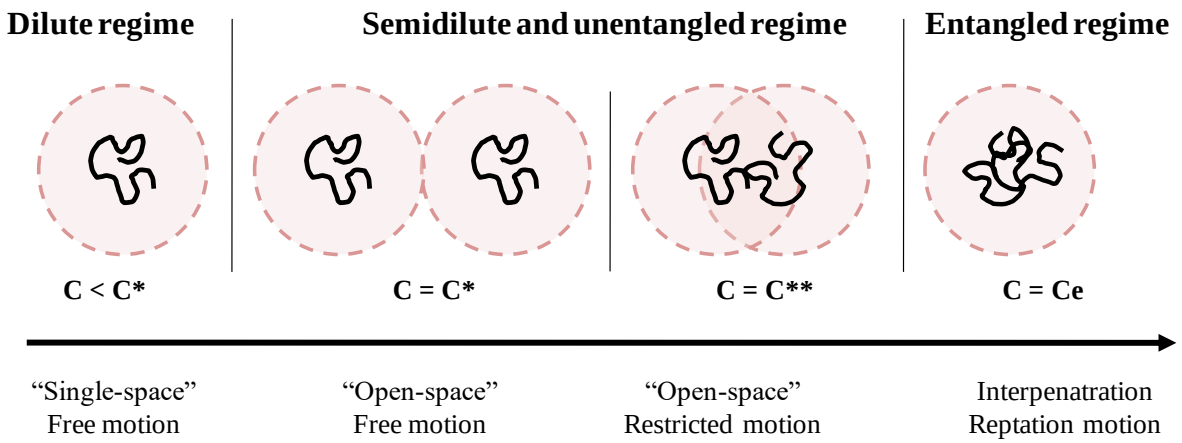

Figure 4: Sketch of the concentration regimes for a polyelectrolyte in solution showing the first overlap concentration C as a result of electrostatic potential contact to gradually a second overlap concentration C** characterizing the polymer chain-to-chain contact. For C above the entanglement concentration Ce, the polyelectrolyte behaves like a neutral polymer.*

Thus, the concentration regime for C < Ce could be characterized by two overlapping concentrations (Figure 4): (i) overlap concentration C = C* due to overlap of electrostatic potential and solvation shell around the isolated polyelectrolyte coil. C < C* pictures the isolated coil as being in "single-space", (ii) overlap concentration C = C** due to overlap of the gyration volume of the polymer chain. C* < C < C** picture the isolated coil as being in "open-space". The isolated coils can still move without remarkable difficulty, but the presence of the other polymers may lead to optimization of their space occupancy regarding the pressure prevailing in the media around them, namely, osmotic and electrostatic pressure, as well as their degree of flexibility. In C** < C < Ce, the polymers are strained to lose their freedom; that is, their capacity of motion is drastically restricted to almost their exclude volume as neutral polymer. Above Ce, the motion of the chain should be one dimensional by reptation, as has reported de Genne (De Gennes, 1976). To demonstrate the critical concentrations in the C < Ce region, we tried different representations by using the Huggin and Kraemer equation (Chronakis, Doublier & Piculell, 2000). When the concentration dependence of the viscosity was plotted as $Ln(\eta/\eta_0)/C$ vs. Ln(C), striking evidence of those critical concentrations was clarified. Figure 5 shows the plots for 0 mM, 5 mM, and 15 mM.

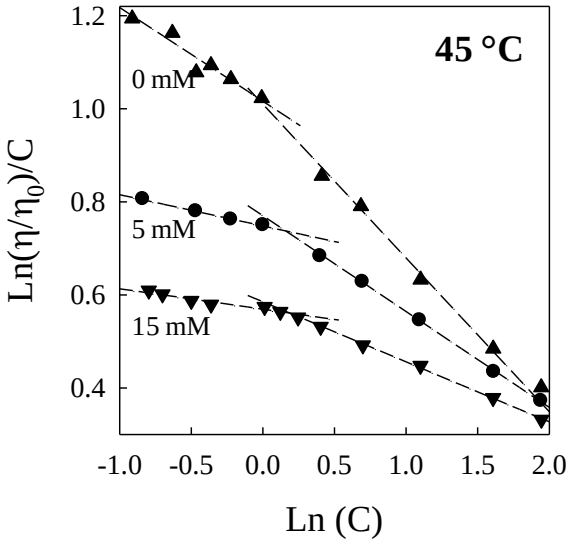

*Figure 5: Logarithm of kC polysaccharide concentration, C, dependence of the logarithm of the relative viscosity per C for different KCl salt concentrations indicated in the figure for 45 °C. The dashed line shows the linear least regression through the data for the two different concentration regimes identified. The intersection point is assigned to C**.*

The plots evolve linearly in the different concentration regimes, with the slopes characterizing the regime. The intersection point between the dashed lines is assigned to C** for each salt concentration. Actually, C* appears below C** (results not shown). Given that the viscosity is lowered by KCl salt, the quality of the measurement was low for those systems. Therefore, the precision of the regression function was less pertinent for the C* of the greater salt concentration and temperature compared to that of 0 mM and 5 mM KCl salt concentrations.

3.3. Temperature dependence of the critical concentration

Temperature action on the dynamics of the systems and quality of the solvent may lead to conformational changes in the polymer systems and size according for particularly flexible polymers. The kC polysaccharide remarkably exhibits temperature dependence of its conformation, so its hydrodynamic size may be impacted accordingly. In the unentangled regime, the critical concentrations, C* and C**, reflect the average hydrodynamic size of the polysaccharide in solution in the coil regime. Its dependence on the temperature is crucial for determining the thermodynamic origin of syneresis. Figure 6 shows for 0 mM (a), 5 mM (b), 10 mM (c), and 15 mM (d), the temperature dependence of C** on their corresponding

temperature ranges defined by the coil regimes. We remind that the temperature window is trimmed to the helix-coil transition temperature, whose limit is represented by dashed lines. For the various salt concentrations, the solid lines display the C** over the explored temperature range using the fit function Eq.6.

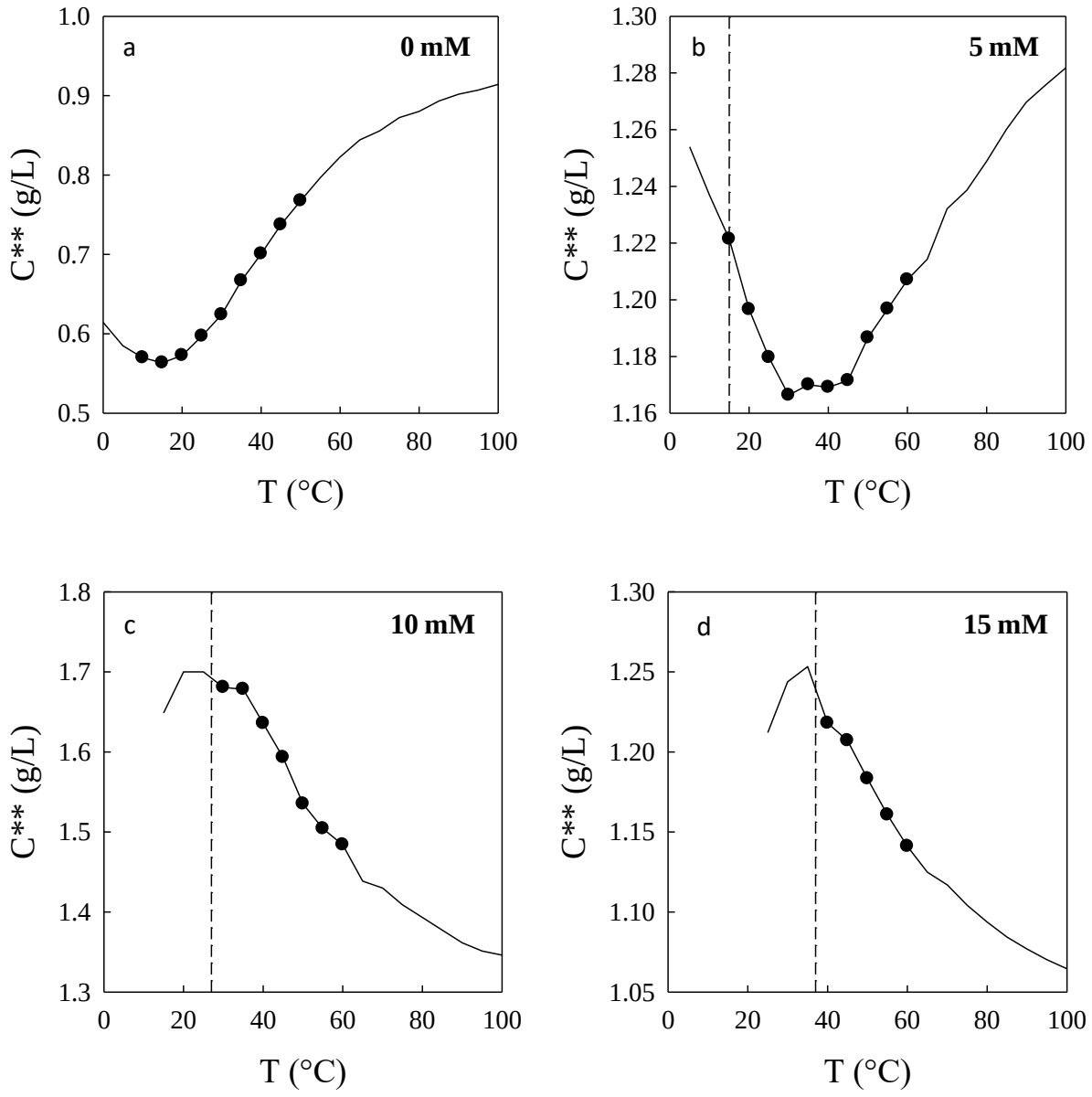

*Figure 6: Temperature dependence of the critical concentration C** for a) 0 mM, b) 5 mM, c) 10 mM, and d) 15 mM KCl salt solutions. The dots show the temperature range for measured data in the coil regime, and the solid line used the viscosity-temperature fit function in the coil regime. The dashed vertical line situates the helices-to-coils transition temperature.*

The lower limit of the temperature for the model is trimmed to 0 °C and the helix-coil transition temperature (dashed line) for the free salt solution and the solution in the presence of salt,

respectively. The upper limit of the temperature is trimmed to the critical temperature $T_c \approx 100$ °C of the solvent (water). The temperature dependence of the critical concentration yields a minimum critical concentration. The temperature of the lower C**, which we called the lower critical concentration temperature (LCCT) and denoted T**, shifts downward when the salt concentration is lowered. Both T** and C**, as well as by analogy T* and C*, characterize the conditions of the stability of the polyelectrolyte conformation sizes. For all particles and particularly for flexible polymers, we postulate a temperature at which their conformation sizes are optimal regardless of the polymer's chemical characteristics and the quality of the solvent surrounding the polymers. For the different salt concentrations explored, the LCCT is the temperature where the average size of the polymer is larger. When the temperature deviates from the LCCT, the polymer size shrinks to the corresponding size at the rate determined by the thermodynamic physical quantity. For the kC polysaccharide, gelation of the systems takes place at a temperature T_g below the LCCT. It is well documented that the T_g of kC solution in the presence of salt is below the coil-helix transition temperature (cooling) (Ako, 2015; Ciancia, Milas & Rinaudo, 1997; Piculell, Borgström, Chronakis, Quist & Viebke, 1997). Hence, the T_g values for solutions of 5, 10 and 15 mM KCl salt concentrations were clearly below 15 °C, 27 °C and 38 °C, respectively. In Figure 7, we show, for example, the samples with 15 mM KCl gel at ambient temperature ≈ 20 °C, but the time required for the samples to gel increases when the kC concentration decreases. The pictures of Figure 7 (B) show a serum on the top of the gel of 5 g/L kC in the presence of 15 mM KCl, which is a demonstration of the syneresis property for this system. The T_g of the system, i.e., where G' rises sharply was found at ≈ 24 °C. The solution was prepared at 60 °C and then kept at 20 °C. For this system, Figure 6d shows that the critical concentration at 60 °C is lower than the critical concentration at 20 °C by extrapolation, which means that the polysaccharide chains shrink to fit their appropriate size corresponding to 20 °C when the system is cooled to 20 °C, which is the cause of the syneresis. From the gelation time, the mechanisms for adoption of the new size could be slowed down by the viscoelasticity of the bulk (gel).

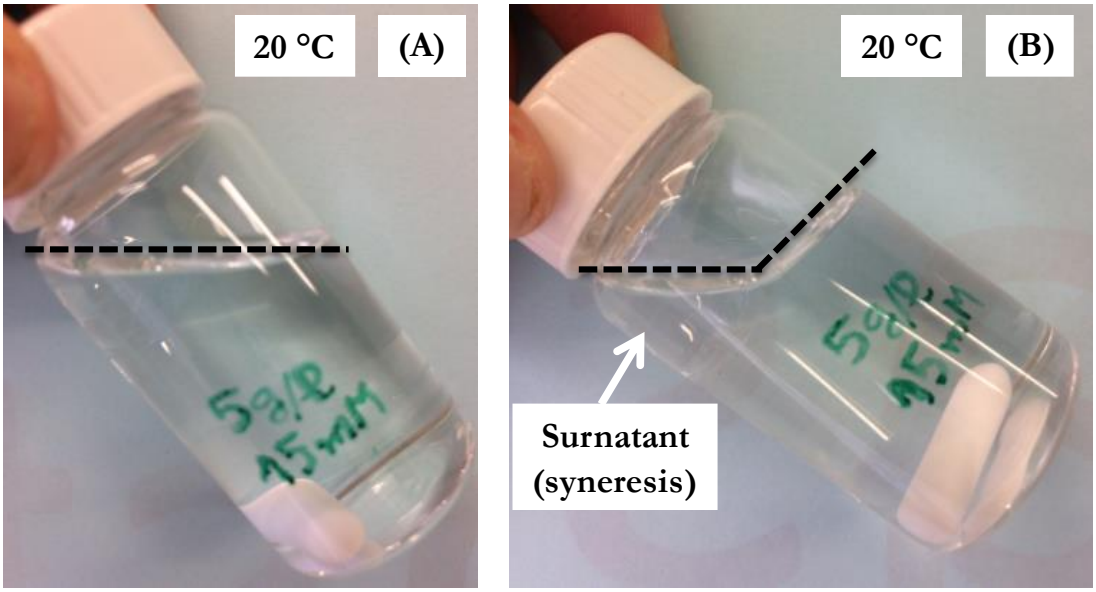

Figure 7: Pictures of 5 g/L kC in solution with 15 mM KCl (Tg ≈ 24 °C) at ambient temperature ≈ 20 °C before gelation (A) and after gelation (B.) The serum on the top of the gel is caused by the contraction of the polysaccharide network (syneresis).

In general, when the gelation of polysaccharides takes place at a temperature T_g not equal to the LCCT, we claim that the polysaccharide size shrinks to a new size corresponding to the T_g. We think that for gelling systems in which $T_g \neq$ LCCT, the gap between the rate of the network formation kinetics and the shrinking kinetics of the particles defines the two kinetics in competition to determine the stability and structure of the gels. This gap is a crucial parameter for understanding the thermodynamic stability of the gel. Two main cases explain the gel thermodynamic stability. For the sake of simplicity, gelation is set out at the chain-to-chain contact concentration and at temperature T_g: (i) For $T_g \neq$ LCCT, if link reactions are faster than the particles shrinking, then gelation takes place, but the gel is forced to collapse due to shrinking stress (negative internal pressure) in the gel; inversely, gelation cannot take place because the shrinkage of the particle size breaks the contact between them. (ii) For T_g = LCCT, link formation gives a thermodynamically stable gel with no shrinking or expansion stress (the internal pressure is null). In case gelation occurs at T_g, but the gel is stocked at T close to the LCCT, the polymer chain expands to reach its greatest size in the prevailing condition, leading to positive internal pressure (inverse of syneresis).

For systems of the first case, $T_g \neq$ LCCT, the shrinking rate should decrease when the concentration increases above the critical concentrations. In the concentration regime above C_e, that is, reptation governs the chain motion, the shrinking rate could drop drastically. If the low

motion of the chains in the entangled regime is combined with strong links between chains, the gel could give the impression of being thermodynamically stable. Therefore, the syneresis for those pseudoequilibrium gels may be exposed after a very long storage time. The time can span several decades.

4. Conclusions

The present work addresses the causes of the syneresis of kappa-carrageenan (kC) polysaccharide gels. The study was restricted to the solution of the polysaccharide in the coil regime where the solution was Newtonian and reached faster equilibrium when the temperature changed at a rate lower than ± 2 °C/min. The concentration dependence of the viscosity exhibits a critical concentration C**, which varies as a function of temperature for the different KCl salt concentrations explored from 0 mM to 15 mM. The plots of C** versus temperature show a lower C** at the lower critical concentration temperature (LCCT) denoted T** in reference to C**. Thus, the conformation sizes of the kC polysaccharide coil chains in solution are greater at T**. For the kC systems explored, the gelation temperatures T_g of the systems are lower than the LCCT; therefore, for this system, the thermodynamic origin of the synersis as well as for those systems in which $T_g \neq$ LCCT is resolved.

Conflict of interest

The authors declare no conflicts of interest.

5. Acknowledgements

We thank Vincent VERDOOT for his technical assistance with the rheometer instruments. The authors thank Pr. Marguerite Rinaudo for providing us with the kappa-carrageenan product. We thank Laurine Buon and Eric Bayma from Cermav for their kind assistance with the product composition. We thank the IUT-Chimie Grenoble for their kind assistance with the mineral composition of the product. This work was financially supported by I-MEP2 PhD graduate school. The Laboratoire Rhéologie et Procédés (LRP) is part of the LabEx Tec 21 (Investissements d'Avenir - grant agreement n°ANR-11-LABX-0030) and of the PolyNat Carnot Institut Investissements d'Avenir - grant agreement n°ANR-11-CARN-030-01).

6. References

Ako, K. (2015). Influence of elasticity on the syneresis properties of kappa-carrageenan gels. *Carbohydrate Polymers, 115*, 408-414.

Ako, K. (2017a). Influence of osmotic and weight pressure on water release from polysaccharide ionic gels. *Carbohydrate Polymers, 169*, 376-384.

Ako, K. (2017b). Yield study with the release property of polysaccharide-based physical hydrogels. *International Journal of Biological Macromolecules, 101*, 660-667.

Bittante, G., Contiero, B., & Cecchinato, A. (2013). Prolonged observation and modelling of milk coagulation, curd firming, and syneresis. *International Dairy Journal, 29*, 115-123.

Campo, V. L., Kawano, D. F., da Silva Jr, D. B., & Carvalho, I. (2009). Carrageenans: Biological properties, chemical modifications and structural analysis - A review. *Carbohydrate Polymers, 77*, 167-180.

Chen, Y., Liao, M.-L., & Dunstan, D. E. (2002). The rheology of K^+-kappa-carrageenan as a weak gel. *Carbohydrate Polymers, 50*, 109-116.

Cheng, D., Wu, Y., Guan, Y., & Zhang, Y. (2012). Tuning properties of injectable hydrogel scaffold by PEG blending. *Polymer, 53*, 5124-5131.

Chronakis, I. S., Doublier, J.-L., & Piculell, L. (2000). Viscoelastic properties for kappa- and iota-carrageenan in aqueous NaI from the liquid-like to the solid-like behaviour. *International Journal of Biological Macromolecules, 28*, 1-14.

Ciancia, M., Milas, M., & Rinaudo, M. (1997). On the specific role of coions and counterions on kappa-carrageenan conformation. *International Journal of Biological Macromolecules, 20*, 35-41.

Colby, R. H. (2010). Structure and linear viscoelasticity of flexible polymer solutions: comparison of polyelectrolyte and neutral polymer solutions. *Rheologica Acta, 49*, 425-442.

Croguennoc, P., Meunier, V., Durand, D., & Nicolai, T. (2000). Characterization of Semidilute k-Carrageenan Solutions. *Macromolecules, 33*, 7471-7474.

De Gennes, P. G. (1976). Dynamics of Entangled Polymer Solutions. I. The Rouse Model. *Macromolecules, 9*(4), 587-593.

Divoux, T., Mao, B., & Snabre, P. (2015). Syneresis and delayed detachment in agar plates. *Soft Matter, 11*, 3677-3685.

Djabourov, M., Leblond, J., & Papon, P. (1988). Gelation of aqueous gelatin solutions. I. Structural investigation. *J. Phys. France, 49*, 319-332.

Higgs, P. G., & Ball, R. C. (1989). Formation of gels and complexes by pairwise interacting polymers. *J. Phys. France, 50*, 3285-3308.

Ikeda, S., & Nishinari, K. (2001). "Weak-Gel"-Type Rheological Properties of Aqueous Dispersions of Nonaggregated K-Carrageenan Helices. *Journal of Agricultural and Food Chemistry, 49*, 4436-4441.

Labudzinska, A., & Ziabicki, A. (1971). Effect of composition and gelation conditions on structural changes accompanying the gelation of PAN, PVA and gelatin solutions. *Kolloid-Z. u. Z. Polymere, 243*, 21-27.

Lucey, J. A., van Vliet, T., Grolle, K., Geurts, T., & Walstra, P. (1997). Properties of acid casein gels made by acidification with GDL. 2. syneresis, permeability and microstructural properties. *International Dairy Journal, 7*, 389-397.

Mao, R., Tang, J., & Swanson, B. G. (2001). Water holding capacity and microstructure of gellan gels. *Carbohydrate Polymers, 46*, 365-371.

Morris, E. R., Cutler, A. N., Ross-Murphy, S. B., Rees, D. A., & Price, J. (1981). Concentration and shear rate dependence of viscosity in random coil polysaccharide solutions. *Carbohydrate Polymers, 1*, 5-21.

Morris, E. R., Rees, D. A., & Robinson, G. (1980). Cation-specific Aggregation of Carrageenan Helices : Domain Model of Polymer Gel Structure. *Journal of Molecular Biology, 138*, 349-362.

Norton, I. T., & Goodall, D. M. (1983). Role of Cations in the Conformation of Iota and Kappa Carrageenan. *Journal of the Chemical Society, Faraday Transactions 1, 79*, 2475-2488.

Piculell, L., Borgström, J., Chronakis, I. S., Quist, P.-O., & Viebke, C. (1997). Organisation and association of k-carrageenan helices under different salt conditions. *International Journal of Biological Macromolecules, 21*, 141-153.

Rochas, C., & Rinaudo, M. (1984). Mechanism of gel formation in κ-Carrageenan. *Biopolymers, 23*(4), 735-745.

Rochas, C., Rinaudo, M., & Vincendon, M. (1980). Structural and conformational investigation of carrageenans. *Biopolymers, 19*(12), 2165-2175.

Scherer, G. W. (1988). Aging and drying of gels. *Journal of Non-Crystalline Solids, 100*, 77-92.

Slootmaekers, D., De Jonghe, C., Reynaers, H., Varkevisser, F. A., & van Treslong, C. J. (1988). Static light scattering from κ-carrageenan solutions. *International Journal of Biological Macromolecules, 10*, 160-168.

Sutherland, W. (1893). The viscosity of gases and molecular force. *Philosophical Magazine Series 5, 36*, 507-531.

Wyatt, N. B., Gunther, C. M., & Liberatore, M. W. (2011). Increasing viscosity in entangled polyelectrolyte solutions by the addition of salt. *Polymer, 52*, 2437-2444.

Wyatt, N. B., & Liberatore, M. W. (2009). Rheology and Viscosity Scaling of the Polyelectrolyte Xanthan Gum. *Journal of Applied Polymer Science, 114*, 4076-4084.

Zhang, J., Ji, W., Liu, T., & Feng, C. (2016). Tuning Syneresis Properties of Kappa-Carrageenan Hydrogel by C2-Symmetric Benzene-Based Supramolecular Gelators. *Macromol. Chem. Phys., 217*, 1197-1204.

Chapitre 5

Origine chimique de la synérèse : Partie A

Chapitre 5

Origine chimique de la synérèse : Partie A

Sommaire

Chapitre 5

Origine chimique de la synérèse : Partie A,

Nombre et position du groupement sulfate dans la sensibilité au sel du carraghénane

Résumé de l'article

Le comportement en solution des polysaccharides ioniques de la famille des carraghénanes, identifiés par les monosaccharides 3,6-anhydro-D-galactose (DA) et D-galactose (G), a montré une forte relation avec le type de contre ions utilisés. A concentration égale à 10 mM, le KCl induit la gélification des solutions de kappa-carraghénane (κ-Car) à une température bien plus grande que le $CaCl_2$, mais ce dernier fourni plus de charge positive à la solution que le KCl. En revanche, l'iota-carraghénane (ι-Car) réagit en présence de 10 mM de $CaCl_2$ plus qu'en présence de 20 mM de KCl. La sensibilité au nombre de charge positive des contre ions a longtemps été attribuée au nombre de charge négative sur le carrabiose. L'étude du comportement de l'α-carraghénane (α-Car) a montré une meilleure sensibilité au Ca^{2+} par rapport au K^+, alors qu'il porte un sulfate mais sur le monosaccharide (DA). Cependant, la sensibilité au Ca^{2+} de l' α-Car est plus faible que celle de l'ι-Car qui est doublement plus chargé que α-Car. Pour cela, nous avons étudié aussi l'influence sur la gélification et la synérèse de la proportion des α-carrabioses par rapport aux ι-carrabioses dans une même chaine (hybride α- / ι-Car) et séparément (α-Car et ι-Car). L'évolution du module élastique de ces différentes solutions dans 20 mM de $CaCl_2$ a été mesurée. Pour l'hybride à 67 % α-Car, on trouve deux températures de transition, l'une correspondant à l' α-Car et l'autre à ι-Car. Un résultat qui rappelle celui obtenu par d'autres auteurs mais avec des mélanges (κ-Car et ι-Car). L'analyse de ces observations montre que, sous forme d'hybride ou non, les changements de conformation en présence des sels résultent de comportent individuel des chaines de carraghénane en solution avec une sensibilité ionique qui dépend du nombre et de la position des sulfates par rapport à la fonction anhydro dans la chaine.

Mots clés: Alpha-carraghénane; Position des sulfates; Fonction anhydro; Viscosité; Sensibilité ionique; Synérèse

https://doi.org/10.1016/j.carbpol.2022.120166 ; Carbohydrate Polymers 299 (2023) 120166

Highlights

* The sulfate groups position is tuned to change carrageenan sensitivity to salt.
* The sulfate group of 3,6-anhydro-D-galactose is rather sensitive to divalent salt.
* The sulfate groups of D-galactose is rather sensitive to monovalent salt.
* The α-carrageenan gels are more stable than κ-carrageenan gels against syneresis.

Graphical abstract

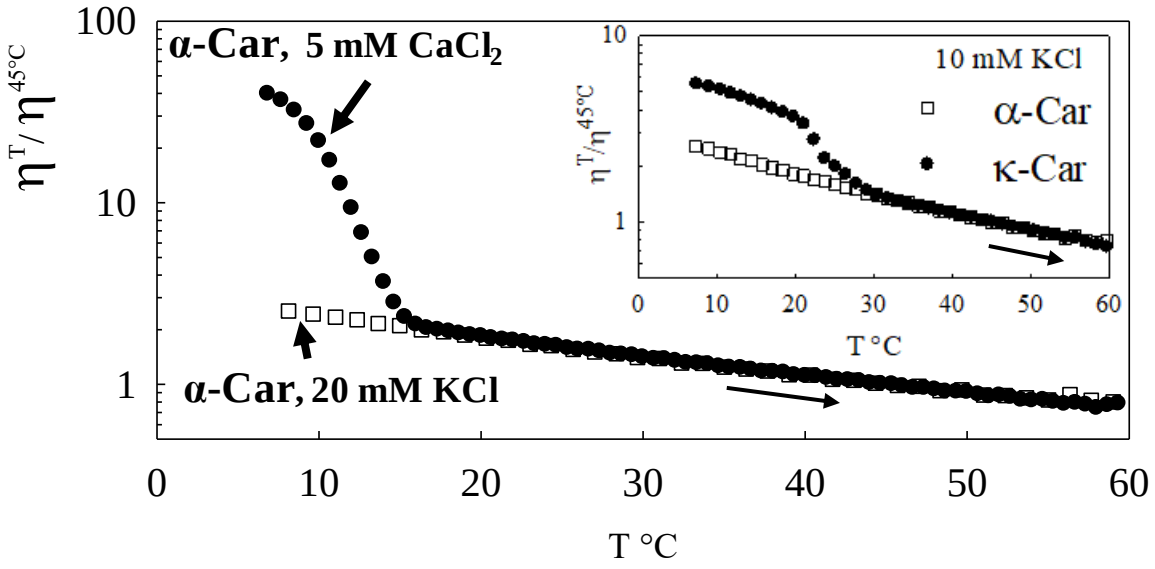

Sulfate groups position determines the ionic selectivity and syneresis properties of carrageenan systems

Authors and affiliations:

Said ELMARHOUM [a], Sophie MATHIEU [b], Komla AKO * [a], William HELBERT [b]

a) Univ. Grenoble Alpes, CNRS, Grenoble INP, LRP, 38000 Grenoble, France

b) Univ. Grenoble Alpes, CNRS, CERMAV, F-38000 Grenoble, France

*__Corresponding author__: komla.ako@univ-grenoble-alpes.fr; akokomla@hotmail.com

Abstract

The salt sensitivity and selectivity feature of α-carrageenan (α-Car) were investigated and compared with κ-carrageenan (κ-Car) and iota-carrageenan (ι-Car). These carrageenans are identified by one sulfate group on the 3,6-anhydro-D-galactose (DA) for α-Car, D-galactose (G) for κ-Car and on both carrabiose moieties (G and DA) for ι-Car. The viscosity and temperature, where order-disorder transition have been observed, were greater in presence of $CaCl_2$ for α-Car and ι-Car compared with KCl and NaCl. Conversely, the reactivity of κ-Car systems were greater in presence of KCl than $CaCl_2$. Unlike κ-Car systems, the gelation of α-Car in presence of KCl was observed without syneresis. Thus, the position of sulfate group on the carrabiose determines the importance of counterion valency too. The α-Car could be a good alternative to κ-Car to reduce the syneresis effects.

Keywords: Alpha-carrageenan; Sulfate group position; Anhydro-ring; Viscosity; Salt sensitivity; Syneresis

1 Introduction

Numerous applications of natural polymers are limited by the ability of the polymers to give a gel with exudation (syneresis) (Chen, Xu & Wang, 2007; Gonzalez, Loubes, Bertotto, Baeza & Tolaba, 2021; Laplante, Turgeon & Paquin, 2006). Some of the applications are relevant for human health management like cell cultures in hydrogels for disease diagnostics and tissue engineering (Divoux, Mao & Snabre, 2015; Hoffman, 2012; Jafari, Farahani, Sedighi, Rabiee & Savoji, 2022; Peppas, Bures, Leobandung & Ichikawa, 2000; Zhang et al., 2020). To understand the physicochemical causes of syneresis of natural polymers hydrogels, kappa-carrageenan polysaccharide is used as the material of this investigation, because this material exhibits severe syneresis in relatively short experimental time with a dependence to many physicochemical factors (Ako, 2015; Elmarhoum & Ako, 2021). In this study, the target is the sulfate, $-SO_3^-$, ionic group position in the monomer of this polysaccharide.

Carrageenan (Car) defines a family of sulfated galactans extracted from marine algae (Prechoux, Genicot, Rogniaux & Helbert, 2013; Souza, Hilliou, Bastos & Gonçalves, 2011; Usov, 2011). The disaccharide repetition moieties (i.e. carrabiose) of the polysaccharide is made with two galactose units identified as G and DA for respectively D-galactose and 3,6-anhydro-D-galactose, each of which can carry different number of sulfate functional group (Ueda, Saiki & Brady, 2001; Usov, 2011) (Fig.1). The number and position of the sulfate group on the carrabiose identifies the type of carrageenan (Campo, Kawano, da Silva Jr & Carvalho, 2009; Millane, Chandrasekaran & Arnott, 1988; Perez & Claudio, 2020; Souza, Hilliou, Bastos & Gonçalves, 2011; Viebke, Borgström & Piculell, 1995). Kappa-carrageenan (κ-Car) has one sulfate group at the position 4 of the G units and is coded as G4S-DA. Alpha-Carrageenan (α-Car) has one sulfate group at the position 2 of the DA units and is coded as G-DA2S accordingly (Bourgoin, Zablackis & Poli, 2008). Iota-carrageenan (ι-Car) has two sulfates on the carrabiose units on the same carbon position as for κ- and α-Car, and thus, is coded as G4S-DA2S. The number, the position and the distribution of ester sulfate along the carrageenans chain define the physicochemical properties of the polysaccharides (Millane, Chandrasekaran & Arnott, 1988; Souza, Hilliou, Bastos & Gonçalves, 2011). As an example, with the same concentration of positive charge counterions, the divalent counterions like calcium (Ca^{2+}) influence strongly the flow behavior of ι-Car solution than the monovalent counterions like potassium (K^+) (Bui, Nguyen, Renou & Nicolai, 2019; Elfaruk, Wen, Chi & Li, 2021). Conversely, K^+ ions change drastically the flow behavior of κ-Car solution compared with ι-Car (Lai, Wong & Lii, 2000; Norton & Goodall, 1983b). The selectivity of ι-Car and κ-Car to respectively divalent and

monovalent counterions and the fact that trivalent counterion induced gelation in λ-Car, which carries three sulfate groups on the carrabiose, lead to claim that the number of sulfate on the carrabiose is what determines the importance of counterion valency (Running, Falshaw & Janaswamy, 2012).

The exact role of the sulfate position on the counterions binding and importance of the counterion valency in carrageenan systems are unclear (Klevens, 1950; Lindman, Karlstrom & Stigsson, 2010; Running, Falshaw & Janaswamy, 2012). The κ-Car hydrogels, for example, exhibit severe syneresis behavior in presence of K^+ than ι-Car and other types of salts which are commonly used in food and biological domains (Thrimawithana, Young, Dunstan & Alany, 2010). Therefore, in order to understand the influence of the sulfate position on the rheological behavior of the carrageenans, we took advantage of the recent discovery of the endo-4O-ι-carrageenan sulfatase secreted by the marine bacteria *Pseudoalteromonas atlantica* T6c. This enzyme removes specifically the sulfate ester group located at the position 4 of the ι-carrabiose moiety and allows completely converting the ι-Car into α-Car (Prechoux, Genicot, Rogniaux & Helbert, 2013). We have investigated the rheological behavior of κ-Car and α-Car solution in presence of different types of salts to emphasize the role that the positions of $-SO_3^-$ may have in the flow properties of the polysaccharide.

2 Material and methods

2.1 Samples characteristics

Molecular weight. The samples were solubilized in 0.1 M $NaNO_3$ and filtered on 0.2 µm membrane. The samples were injected on two OHpak SB 806 M HQ Shodex columns mounted in series and eluted at 30°C in 0.1 M $NaNO_3$. Detection was monitored by a Optilab rEX Wyatt refractometer and a mini DAWN TREOS Wyatt light scattering working at three angles. The dn/dC was 0.142 mL/g. Polydispersity indices was calculated Ip = Mw/Mn. All measurements were done in triplicate.

Enzymatic preparation of alpha-carrageenan (α–Car). The α-carrageenan (Fig1) was prepared according to the method reported by (Prechoux, Genicot, Rogniaux & Helbert, 2013) using recombinant 4O-iota-carrageenan sulfatase. Briefly, the genePatl_0889 (GenBank accession number ABG39415) encoding the sulfatase with a N-terminal poly-histidine tag was over expressed in BL21-DE3 *Escherichia coli* strain and purified on a Nickel affinity column. Iota-carrageenan provided by Danisco (Brabrand, Denmark) was incubated with the purified

sulfatase in 50 mM Tris-HCl pH 7.5. Incubation with additional fresh enzymes was repeated until the complete conversion to α-carrageenan was achieved. The yield of desulfation was measured by ^{1}H NMR (Prechoux, Genicot, Rogniaux & Helbert, 2013). The polysaccharide was ultra-filtered on 10 Da membrane in water and lyophilized. The average molecular weight of the polysaccharide was $M_w = 3.8\times10^5$ g/mol, with an average polydispersity index of $M_w/M_n = 1.78$.

Kappa-carrageenan (k-Car). The κ-Car polysaccharide (Fig1) is a gift from Rhodia Food Switzerland, product name and reference: MEYPRO-GEL 01/2001 WG95-37 K-Car. The dialyzed product may contain a weak amount of glucose and was found in the pure potassium κ-Car form of total potassium at no more than 4.2 % (w/w); the other salts were considered to be only trace amounts. The measurement of its molecular weight was done in triplicate. The average molecular weight of the polysaccharide was $M_w = 3.3\times10^5$ g/mol, with an average polydispersity index of $M_w/M_n = 2.02$.

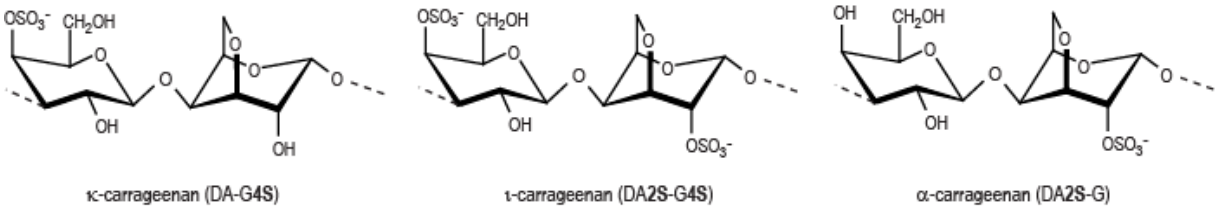

Figure 1: Structure of the carrabiose moieties composing kappa-, alpha- and iota-carrageenan.

2.2 Samples preparation

A 20 g/L solution was prepared by dissolving the κ-Car polysaccharides powder in demineralized water with 200 ppm sodium azide as the bacteriostatic agent under heat and stirring conditions. The resulting solution was dialyzed and filtered through 0.45 µm pore size. A 9 g/L of solution was prepared by dilution of the 20 g/L solution and was stocked in fridge at 5 °C, with which, all the samples were prepared by dilution with demineralized water containing 200 ppm sodium azide with salt at the appropriate concentration. The dilution gives the desired final concentration of polysaccharide and salt concentration at the appropriate temperature. The α-Car polysaccharide in the lyophilized form were dissolved in demineralized water with 200 ppm sodium azide under heat and stirring conditions to 9 g/l stock solution. The samples were prepared in the same way like the κ-Car using the appropriate salt.

2.3 samples characterization

Viscosity measurements. The viscosity measurements were performed in Couette geometry using a DHR3 Rheometer (TA Instrument). The Couette geometry consisted of a concentric cylinder geometry of an inner rotor cylinder (bob) and outer stator cylinder (cup) of respectively a radius R_1 of 14 mm and R_2 of 15 mm defining a horizontal gap (R_2 - R_1) of 1 mm and an average radius R of 14.5 mm as (R_1 + R_2)/2. The height of the bob was 42 mm and the vertical gap between the bob and cup was set at 2 mm. The minimum and maximum torque of the instrument were 5 μNm and 5×10^3 Nm respectively. Both the torque (M) and the angular velocity (Ω) of the bob, which were proportional with respectively the stress (σ) and shear rate ($\dot{\gamma}$), were measured by the rheometer, from which the viscosity (η) was displayed as $\sigma/\dot{\gamma}$. The viscosity was determined as a function of the shear rate from 0.3 s^{-1} to 30 s^{-1} to define the Newtonian flow domain at a constant temperature in the range between 5 °C and 60 °C. The viscosity was also measured at a constant shear rate of 15 s^{-1} while cooling or heating at 2 °C min^{-1} or a lower rate 0.5 °C.min^{-1}.

Viscoelastic modulus measurements. The rheological measurements were performed using a DHR3 Rheometer (TA Instrument) with etching conic geometry (Ø50 mm, 2.0°, TADC2°InR500) and etching plate. The conic geometry has a truncation gap of 110.0 µm. A portion of the prepared hot sample solution was loaded onto the Peltier of the rheometer and set at a temperature above the gelation temperature of the sample. After loading the sample, the surface was covered with a thin layer of mineral oil to avoid evaporation. Then, the temperature and the measurement program were run. The condition of each measurement will be specified in the text.

3 Results and discussion

3.1 Flow behavior of α-carrageenan solution

The viscosity of α-Car in presence of 80 mM KCl is displayed in Fig. 2a for cooling and heating ramps. The viscosity increases when the temperature is decreased, and sharply from ≈ 11.5 °C. The sharp increase of the viscosity was shown by Rochas and Rinaudo (1984) to be concomitant with the coil-helix transition. If the temperature is increased immediately from 5 °C, the viscosity decreases sharply and the helix-coil transition was found at ≈ 14.3 °C above the coil-helix transition (Rochas & Rinaudo, 1984). The thermal hysteresis was reported as a result of

inter-helical aggregation (Morris, Rees & Robinson, 1980; Piculell, Nilsson & Muhrbeck, 1992).

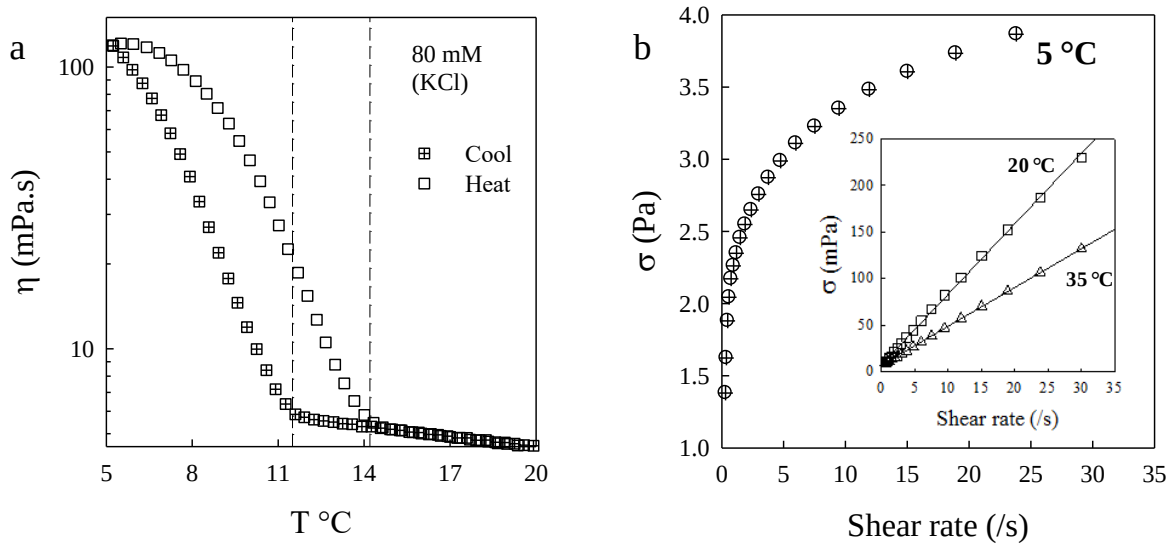

Figure 2: a) temperature dependence of α-Car solution viscosity for 3 g/L, 80 mM KCl, b) shear rate and stress relation displayed for the solution to show the viscosity behavior, at 5 °C in the helices domain the viscosity changes with the shear rate, in the coil domain the viscosity is constant (insert).

The thermal hysteresis defines three temperature domains which are identified in the Fig.2a as: (1) domain below the coil-helix transition temperature, < 11.5 °C, (2) domain between the coil-helix and helix-coil transition temperature, [11.5 °C, 14 °C] and (3) domain above the helix-coil transition temperature, > 14 °C. The conformational state of the carrageenan in temperature domain (2) depends on the temperature ramp (cooling or heating) but in the domain (1) or (3) the conformations of the polysaccharide chains were respectively either helices or coils. The shear rate dependence of the applied stress plots is shown in the Fig.2b. A non-linear relationship is observed, at 5 °C, in the domain below the coil-helix transition temperature and a linear relationship is observed at temperatures in the domain above the helix-coil transition temperature (insert of Fig.2b). We have observed that the flow behavior of κ-Car turns from Newtonian to non-Newtonian flow when the conformations of the polysaccharides turn from coils to helices (Elmarhoum & Ako, 2021). We think that similar conformational change could explain the temperature dependence of the flow behavior of α-Car. The impact of salt on the flow behavior of carrageenan solutions depends mainly on the kinetics of the helices aggregation and the kinetics increases with decreasing temperature below the coil-helix

transition temperature (Meunier, Nicolai, Durand & Parker, 1999). We didn't observe the gelation for α-Car solutions in the interval of temperature explored in Fig.2a, when in the same KCl and polysaccharide concentration the κ-Car solutions gelled at temperature below 50 °C with syneresis (Ako, 2015, 2017). A lower helices aggregation kinetics is expected in relation with the weak coil-helix transition temperature in comparison with κ-Car. We didn't exclude the fact that the α-Car solutions at temperature below 12 °C behave like a suspension of aggregates (Garrec, Guthrie & Norton, 2013).

3.2 Coil-helix and helix-coil transition temperature: effect of salt

The transition from random coils to helices conformation, which is measured using optical rotation technique, have been observed to be concomitance with the steep rising of the viscosity (Rochas & Rinaudo, 1984). Therefore, the onset of helix formation during cooling ramp is characterized by the temperature at which the viscosity starts to increase and is denoted as the coil-helix temperature (T_{ch}). Salt concentration dependence of the T_{ch} is shown in the Fig.3. The results for $CaCl_2$ salt are displayed for α-Car and the result for KCl salt is displayed in the insert of the Fig.3 for α-Car and κ-Car. The polysaccharides sensitivity to salt as a polyelectrolyte is expected (Ako, 2015; Ciancia, Milas & Rinaudo, 1997), but the fact that the coil-helix transition of α-Car is more sensitive to $CaCl_2$ than KCl was not obvious regarding the literature on κ-Car (Elmarhoum & Ako, 2021). Moreover, the sensitivity of κ-Car to KCl result in a greater coil-helix transition temperature than the sensitivity of α-Car to both KCl and $CaCl_2$. This finding emphasis the importance of the $-SO_3^-$ position in the monomer as a physicochemical factor, which determines the polysaccharide reaction to salt.

For α-Car, if $CaCl_2$ concentration is increased from 5 mM to 40 mM, the T_{ch} increases from ≈ 14 °C to ≈ 26 °C. The T_{ch} increases from ≈ 10 °C to 20 °C, if the KCl concentration is increased from 45 mM to ≈ 150 mM and the coil-helix transition was not observed for 20 mM KCl concentration, which is two time greater than 5 mM $CaCl_2$ in term of the concentration of positive charge counterions. Therefore, α-Car is more sensitive to divalent than the monovalent counterions. Based on this result, the behavior of α-Car with one sulfate anionic functional group on its monomer is rather similar to that of ι-Car with two sulfates anionic functional groups than κ-Car (Morris, Rees & Robinson, 1980).

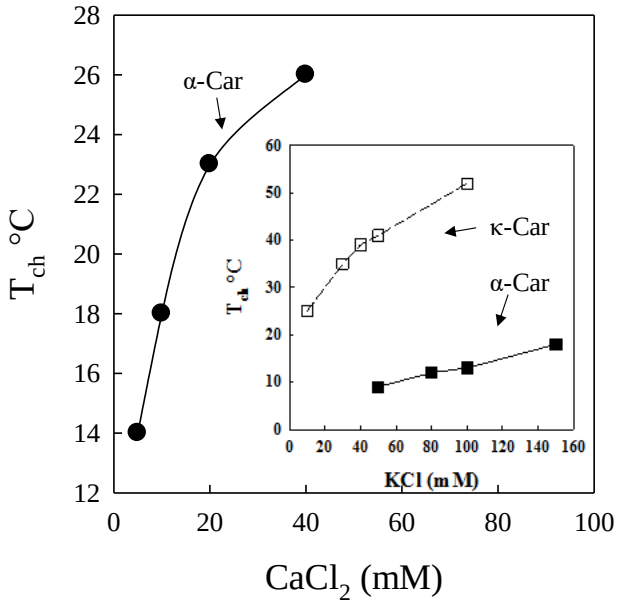

Figure 3: $CaCl_2$ dependence of the coil-helix transition temperature of α-Car and in the insert the KCl concentration dependence of the coil-helix transition of α-Car and κ-Car.

The κ-Car systems with one sulfate anionic functional group on its monomer react strongly in presence of KCl salt than the α-Car systems. The T_{ch} increases from ≈ 25 °C to ≈ 50 °C, if the KCl concentration is increased from 10 mM to 100 mM, with the hysteresis loop effect.

3.3 Monovalent salt sensitivity of α-Car

The fact that the conformational change of α-Car happens at a greater temperature in presence of calcium than potassium counterions, characterizes its greater sensitivity for the divalent salt than the monovalent salt (Morris, Rees & Robinson, 1980). At any rate, in the conditions where the coils conformations prevail, the viscosity of the solution doesn't depend on the cooling or heating ramps and the solution flow is Newtonian. In this section we have tried to bring some more results on the sensitivity of the polysaccharide for monovalent salts like; NaCl, KCl and KI.

In the Fig.4a, are shown the temperature dependence of the viscosity for the solution of 3 g/L as the reference (ref.) to show the effect of 10 mM of the selected monovalent salt. The results show a decrease of the viscosity in presence of the salts with no particular effect due to the type of salt for the concentration of 10 mM. Moreover, the KCl salt concentration is not enough to induce the coil-helix transition in the temperature range of the measurements as it was observed for κ-Car. Based on the fact that, the temperature dependence of κ-Car solutions viscosity for

10 mM of NaCl, KI or KCl are different (Ciancia, Milas & Rinaudo, 1997), we didn't expect that the temperature dependence of α-Car solutions viscosity being similar. We cannot explain the difference between the behavior of α-Car and κ-Car, without considering the sulfate group position. If the NaCl concentration is increased to 100 mM, the solutions exhibited a coil-helix transition around 15 °C and a helix-coil transition around 17 °C. This may appear to be a small hysteresis but when scan rate dependence is accounted for these would be superimposable (Fig.4b). In presence of 100 mM of KCl, the coil-helix transition is observed around 12 °C and two transitional temperatures were observed for the heating ramp; the first one around 17 °C and the second one correspond to the helix-coil transition around 42 °C.

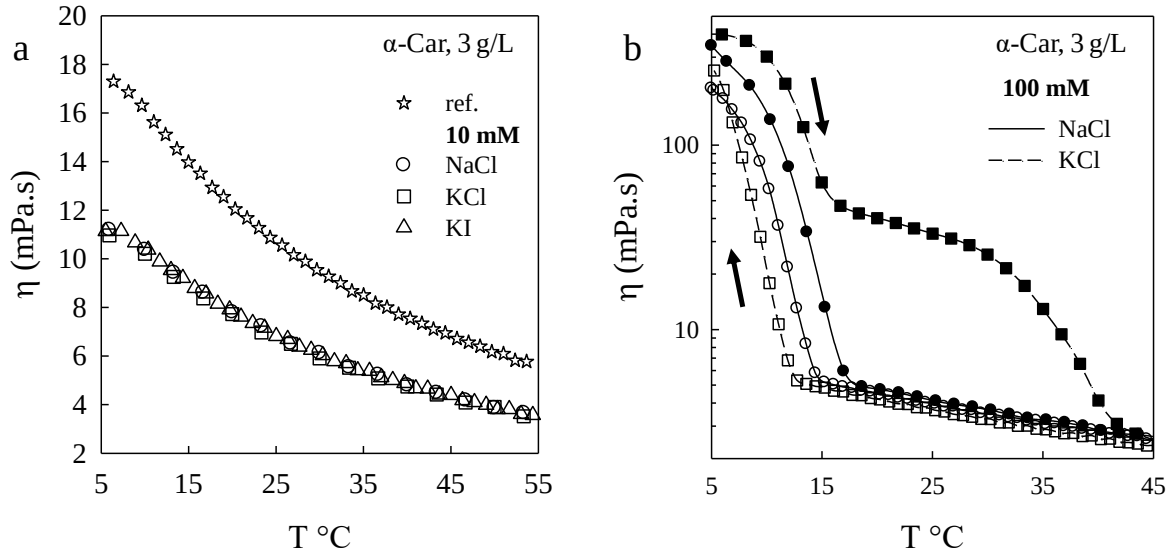

Figure 4: temperature dependence of the viscosity of α-Car solution,3 g/L in presence of a) 0 mM (ref.) and 10 mM of NaCl, KCl or KI, the cooling and heating ramps give similar results and b)100 mM of NaCl or KCl, the cooling (open symbols) and heating (full symbols) results are displayed.

The thermal hysteresis of the solution of α-Car with 100 mM KCl indicates an extensive aggregation of the helices which led the conserved solution to gel at 5 °C. The solution with 100 mM NaCl didn't gel after several days at 5 °C. The shift of the coil-helix transition temperature T_{ch} from 12 °C to 15 °C, when KCl is replaced by NaCl, leads to say that the conformational change of α-Car would be rather sensitive to NaCl than KCl. The role of monovalent salt to promote helix formation and then gelation for κ-Car systems was reported to follow the sequence RbCl > CsCl, KCl > NaCl > LiCl, HCl (Ciancia, Milas & Rinaudo, 1997; Rochas & Rinaudo, 1984). The superiority of the potassium on sodium to induce coil-

helix conformational change of κ-Car is inversed in the case of α-Car. This inversion may indicate that the anhydro-ring promotes the accessibility to the sulfate group on the 3,6-anhydro-D-Galactose unit by small size counterions. However, extensive aggregation of the helices and gelation in presence of 100 mM KCl, indicate that the ion-pair formation of K^+ with the $-SO_3^-$ is a time dependent process (Grasdalen & Smidsrod, 1981; Norton & Goodall, 1983a). The reduction of the sulfate charge by counterions would be fast for κ-Car, and thus, promotes immediate coil-helix transition and aggregation of the helices to gelation.

3.4 Influence of the degree of carrageenan sulfation

The gelation of different types of mono-composite (MC) of carrageenan polysaccharides made of α-carrabiose and ι-carrabiose on the same backbone are proposed in this section to show how the degree of conversion of ι-Car to α-Car can influence the coil-helix transition temperature. The gelation of a bi-composite (BC) solution, which is a blending of α-Car and ι-Car solution to the proportion of 67 wt.% and 33 wt.% respectively, is also shown. Given that the α-Car is obtained by conversion of ι-Car, the result of the bi-composite will indicate the influence that could have a few content of ι-Car in the α-Car solution on the coil-helix transition temperature (Piculell, Nilsson & Muhrbeck, 1992). The concentration of all the solutions is 6 g/L and were prepared with 20 mM of $CaCl_2$ then cooled to give the results in Fig.5. The temperature dependence of the G' of the solutions were measured during the cooling ramp. The result of the BC solution is marked with a star in the legend of Fig5.b. The gelation of carrageenan systems is a time dependent process which is connected to the helices aggregation kinetic, thus the gelling point as the point where G' = G" depends on the scan rate. The onset of elastic behavior of aqueous iota-carrageenan has been observed by Piculell et al., (1992) to closely follow the onset of helix formation, and the modulus of elasticity increases monotonically with an increasing helical content (Piculell, Nilsson & Muhrbeck, 1992). Therefore, if G' > G" is observed, the temperature at which the helices are formed, is considered here as the gelation temperature. In this section, we have worked in the conditions where for all the samples, G' > G" was observed during the cooling ramps.

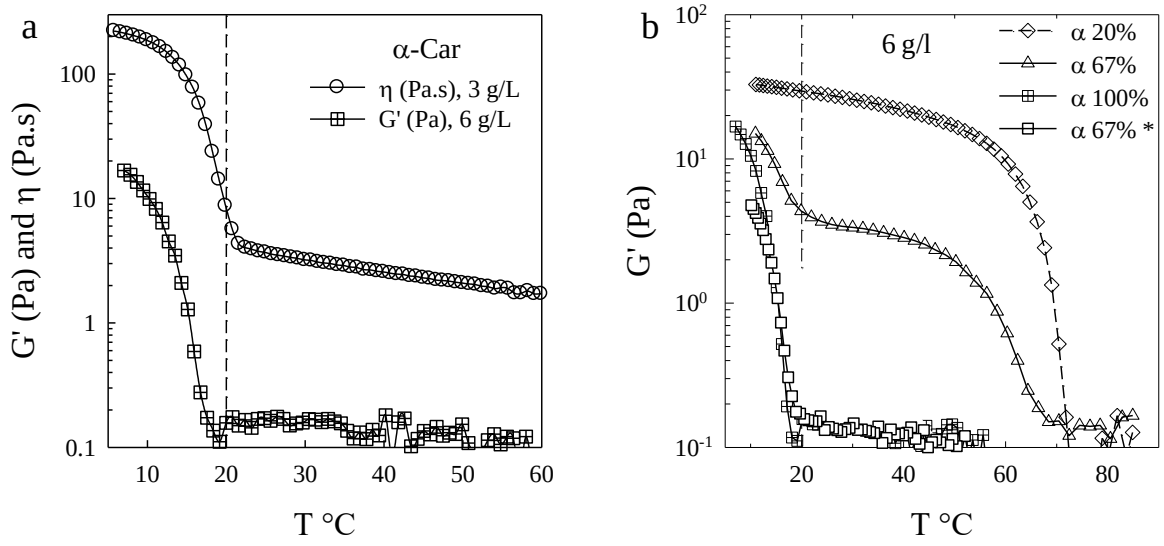

Figure 5: Temperature dependence of the G' and the viscosity of a) α-Car in presence of 20 mM $CaCl_2$ and b) different composition of α-Car and ι-Car carrabiose in the polysaccharide backbone. The composition α 67 % is a solution made with 67 wt% of α-Car and 33 wt% of ι-Car. The solutions were prepared with 20 mM $CaCl_2$.*

In Fig.5a, the gelation temperature is observed to be almost equal to the temperature at which the G' of the system increases sharply while cooling the solution. We can see that the domain of temperature where the viscosity increases coincides with that of G', which we said is concomitant with the formation of helices (Belton, Chilvers, Morris & Tanner, 1984; Ciancia, Milas & Rinaudo, 1997; Elmarhoum & Ako, 2021; Meunier, Nicolai, Durand & Parker, 1999; Norton & Goodall, 1983b; Rochas & Rinaudo, 1984). The α-Car solution and the solution of 67 wt.% α-Car with 33 wt.% ι-Car, indicated in the Fig.5b respectively as α 100 % and α 67 %*, show the same gelation temperature. Therefore, presumably a few content of ι-Car in the α-Car solution would not affect the coil-helix transition temperature of α-Car and its sensitivity to salt. The thermal behavior of α-Car solution seems to be very stable regarding a small variation of ι-Car concentration in wt.%. Considering the molecular weight of each composite of the blending solution, the 67 wt.% of α-Car may correspond to 90 mol%, which means that one molecules of ι-Car is surrounded by nine molecules of α-Car and this could explain the similarity between the thermal properties of the 100 mol% and 90 mol% α-Car solution. In the MC polysaccharide, the proportion of α-carrabiose and ι-carrabiose are in mol% and 67 % of α-Car in the MC shows the gelation temperature of the part related to both α-Car and ι-Car. This result, may indicate that the coil-helix transition would be rather an intramolecular mechanism. In the condition where the α-carrabioses are randomly distributed along the hybrid

carrageenan chain (Prechoux, Genicot, Rogniaux & Helbert, 2013), we should expect one gelation temperature. However, the probability to have a bloc of α-carrabioses along the hybrid chain which behave like a free chain of α-Car is increased by increasing the degree of ι-Car conversion to α-Car and this fact seems to correspond to the results in Fig.5b. Below 50 % of α-Car in the MC, the gelation temperature of α-Car was not clearly detectable. Supposed that the 20 mol% / 80 mol% of α-/ι-Car were distributed like a bloc copolymer, then the temperature dependence of G' would have shown distinctly the gelation temperature of α-Car and ι-Car. Bui et al., (2019) have mixed 50 wt.% of κ-Car and 50 wt.% of ι-Car in 50 mM $CaCl_2$ aqueous solution and they have observed two distinct gelation temperatures of the BC solution indicating independent coil-helix transition (Bui, Nguyen, Renou & Nicolai, 2019). However the authors observe that κ-Car network is more homogeneous in the mixed gels than in the corresponding individual gels and the mixed gels were stiffer than the individual gels. The independent coil-helix transition of the polysaccharide which occurs in both BC and MC systems may indicate that the reduction of the polymers net charge is preferentially intramolecular by which the helices and aggregates are formed.

The claim of intramolecular mechanism to explain the reduction of the polysaccharide charge or ion-pair formation could also refer to the finding of Rochas and Rinaudo (1984). The authors found that the ionic selectivity for potassium counterions work also even if the κ-Car is in the coil conformation. If so, then the coil-helix conformational change may take place in concentration well below the critical concentration, where the polysaccharide are supposed to be individual. Hence, the polysaccharide conformation would be single helix. However, the authors have rejected the single-helix formation presumably because they didn't observe a specific role of the potassium ion in the crosslinking mechanism of the polysaccharide. It is not clear the way the intramolecular charge neutralization mechanism conciliates the hypothesis of double helices and the aggregation of the helices in BC and MC model, except if the double helices are considered as aggregate of two single-helices.

We can note the absence of peak or maximum point for the G’ plots in Fig.5, which several authors reported for κ-Car gel systems as characteristic of slipping effect due to sever syneresis (release of liquid phenomena by the gels). The gelation of κ-Car solutions with K^+, Cs^+, Ca^{2+} gives gels with syneresis was reported by several authors (Ako, 2015; Lai, Wong & Lii, 2000; Piculell, Borgström, Chronakis, Quist & Viebke, 1997; Richardson & Goycoolea, 1994). The salt concentrations at which the syneresis was observed are relatively very weak compared with ι-Car (Piculell, Nilsson & Muhrbeck, 1992; Thrimawithana, Young, Dunstan & Alany, 2010)

and if the syneresis mechanism may exist for α-Car, then it should be caused by salt concentrations larger than those used for κ-Car and presumably over the experimental time conditions of this study. The gels coarsening and contraction cause syneresis in general, but in condition which is determined by the polysaccharide net charge reduction or neutralization, extensive helices aggregation induced syneresis reflects the salt ability to neutralize or reduce the intra and/or intermolecular repulsion forces. Therefore, sulfate group position on D-galactose unit is more favorable to neutralization by salt than the sulfate group position on 3,6-anhydro-D-galactose unit.

3.5 Discussion

Alpha-carrageenan and kappa-carrageenan are characterized respectively, by a mono sulfate group on the 3,6-anhydro-D-galactose unit and a mono sulfate group on the D-galactose unit. Zablackis et al., have studied the carrageenan extracted from *Catenella nipae Zanardini* , which according to the work of Falshaw et al., (1996) may correspond to hybrid α-/ι-Car of variable proportion (Bourgoin, Zablackis & Poli, 2008; Falshaw, Furneaux, Wong, Liao, Bacic & Chandrkrachang, 1996), and the content of α-carrabiose in the native hybrid polysaccharide would not exceed 40 mol% (Prechoux, Genicot, Rogniaux & Helbert, 2013). The sodium form of this polysaccharide (in 100 mM NaCl) did not gel but exhibit a greater viscosity than κ-Car (Zablackis & Santos, 1986), while the sodium form of ι-Car (in 100 mM NaCl) has been observed to form a gel (Piculell, Nilsson & Muhrbeck, 1992). In presence of salt the viscosity of the solutions of α-Car and κ-Car depends on the degree of their helices formation and aggregation. However, the decrease of the gelling capacity when the proportion of α-carrabiose increases in the hybrid polysaccharide indicates that the sulfate on the anhydro-D-galactose unit is less favorable for the inter-helical aggregation compared with the sulfate on the D-galactose unit. Therefore, lower inter-helical aggregation activity and higher inter-helical aggregation activity, respectively, characterize the function of the sulfate on the anhydro-D-galactose unit and the function of the sulfate on the D-galactose unit, which explain, respectively, the weak gelling capacity of α-Car and the strong gelling capacity of κ-Car.

The viscosity of the solution of 3 g/L of α-Car and κ-Car at 20 °C were respectively 12.2 mPa.s and 7.8 mPa.s. The viscosity of the free salt solution of α-Car is observed to be greater than the viscosity of the free salt solution of κ-Car at a similar molecular weight, polysaccharide concentration and temperature conditions. Intrachain repulsive forces and water molecules binding capacity would be greater for α-Car than κ-Car (Ako, Elmarhoum & Munialo, 2022),

and accordingly, the sulfate on the anhydro-D-galactose unit promotes more expansion of the polysaccharide than the sulfate on the D-galactose unit.

It is appropriate to emphasis that the α-Car system ionic selectivity for $CaCl_2$ rather than KCl was not expected, because the κ-Car system, which could derive from ι-Car too, is known to be more sensitive to KCl than $CaCl_2$. Therefore, the sensitivity of carrageenan systems to counterions is not only a matter of number of sulfate groups on the carrabiose (Running, Falshaw & Janaswamy, 2012) but a result of many physicochemical factors. The size of hydrated counterions is quoted to play a role in the distance between the cation and the sulfate group (Piculell, Nilsson & Muhrbeck, 1992). The cation mobility can also affect the ion-pair formation stability or equilibrium constant, i.e., the small size cations could have a greater mobility, and thus, lead to a less stable or strong ion-pair formation (Ciancia, Milas & Rinaudo, 1997; Grasdalen & Smidsrod, 1981). Although α-Car and ι-Car system are rather sensitive to $CaCl_2$, the conformational transition temperature of α-Car systems is found well below that of ι-Car systems, which reflect the intramolecular characteristic of the charge reduction mechanism in carrageenan systems. The ability of salt to reduce the charge carried by carrageenan polysaccharides could be pictured as an in-to-out process. The in-to-out neutralization process means that the system tries to neutralize first the charge carried by the carrabiose (intramolecular process), and if this fails like in the case of α-Car with calcium, the system tries to neutralize the charge carried by the carrageenan chain (intrachain process). In the intrachain process or interaction between carrabiose of same chain, if a block of carrabiose behave the same, like a block of α-Car in α-/ι-Car hybrid polysaccharide, then the conformation transition characterizing the block could be detectable. The neutralization process could continue or stop by interchain/intermolecular process (aggregation), in this process the two sulfates or carrabiose which bind the multi valence counterions do not belong to the same chain.

4 Conclusion

The importance of counterions in the helical formation of carrageenan depends on many physicochemical factors. We show in this treatise that the influence of the counterion valency depends on the position and number of the sulfate group carried by the carrabiose. The sulfate on the 3,6-anhydro-D-galactose unit, which characterizes α-carrageenan (G-DA2S), is rather sensitive to divalent counterions and the sulfate group on the D-galactose unit, which characterizes κ-carrageenan (G4S-DA), is rather sensitive to monovalent counterions. The two types of sulfate, which characterize ι-carrageenan (G4S-DA2S), is more sensitive to divalent

counterions than the one type of sulfate carried by α-carrageenan (G-DA2S). The temperature dependence of the G' of α-/ι-carrageenan, as a carrageenan block copolymer system in $CaCl_2$ solution, has shown distinctly the helical formation temperature of α-carrageenan and ι-carrageenan. Based on the results of this study, the counterion influence, which we qualify as in-to-out process, would be preferentially and gradually intramolecular, then intrachain and finally interchain process.

5 Acknowledgements

We thank Vincent VERDOOT for his technical assistance with the rheometer instruments. We thank Laurine Buon and Eric Bayma from Cermav for their kind assistance with the products composition. This work was financially supported by I-MEP2 PhD graduate school and the PolyNatCarnotInstitut. The LaboratoireRhéologie et Procédés (LRP) is part of the LabEx Tec 21 (Investissementsd'Avenir - grant agreement n°ANR-11-LABX-0030) and of the PolyNat Carnot InstitutInvestissementsd'Avenir - grant agreement n°ANR-11-CARN-030-01).

6 References

Ako, K. (2015). Influence of elasticity on the syneresis properties of kappa-carrageenan gels. *Carbohydrate Polymers, 115*, 408-414.

Ako, K. (2017). Influence of osmotic and weight pressure on water release from polysaccharide ionic gels. *Carbohydrate Polymers, 169*, 376-384.

Ako, K., Elmarhoum, S., & Munialo, C. D. (2022). The determination of the lower critical concentration temperature and intrinsic viscosity: The syneresis reaction of polymeric gels. *Food Hydrocolloids, 124*, 107346.

Belton, P. S., Chilvers, G. R., Morris, V. J., & Tanner, S. F. (1984). Effects of group I cations on the gelation of iota carrageenan. *International Journal of Biological Macromolecules, 6*, 303-308.

Bourgoin, A., Zablackis, E., & Poli, J. B. (2008). Characterization of a-carrageenan solution behavior by field-flow fractionation and multiangle light scattering. *Food Hydrocolloids, 22*, 1607-1611.

Bui, V. T. N. T., Nguyen, B. T., Renou, F., & Nicolai, T. (2019). Rheology and microstructure of mixtures of iota and kappa-carrageenan. *Food Hydrocolloids, 89*, 180-187.

Campo, V. L., Kawano, D. F., da Silva Jr, D. B., & Carvalho, I. (2009). Carrageenans: Biological properties, chemical modifications and structural analysis - A review. *Carbohydrate Polymers, 77*, 167-180.

Chen, H.-H., Xu, S.-Y., & Wang, Z. (2007). Interaction between flaxseed gum and meat protein. *Journal of Food Engineering, 80*, 1051-1059.

Ciancia, M., Milas, M., & Rinaudo, M. (1997). On the specific role of coions and counterions on kappa-carrageenan conformation. *International Journal of Biological Macromolecules, 20*, 35-41.

Divoux, T., Mao, B., & Snabre, P. (2015). Syneresis and delayed detachment in agar plates. *Soft Matter, 11,* 3677-3685.

Elfaruk, M. S., Wen, C., Chi, C., & Li, X. (2021). Effect of salt addition on iota-carrageenan solution properties. *Food Hydrocolloids, 113,* 106491.

Elmarhoum, S., & Ako, K. (2021). Lower critical concentration temperature as thermodynamic origin of syneresis: Case of kappa-carrageenan solution. *Carbohydrate Polymers, 267,* 118191.

Falshaw, R., Furneaux, R. H., Wong, H., Liao, M.-L., Bacic, A., & Chandrkrachang, S. (1996). Structural analysis of carrageenans from Burmese and Thai samples of Catenella nipae Zanardini. *Carbohydrate Research, 285,* 81-98.

Garrec, D. A., Guthrie, B., & Norton, I. T. (2013). Kappa carrageenan fluid gel material properties. Part 1: Rheology. *Food Hydrocolloids, 33,* 151-159.

Gonzalez, L. C., Loubes, M. A., Bertotto, M. M., Baeza, R. I., & Tolaba, M. (2021). Flow behavior and syneresis of ball milled rice starch and their correlations with starch structure. *Carbohydrate Polymer Technologies and Applications, 2,* 100168.

Grasdalen, H., & Smidsrod, O. (1981). (133)Cs NMR in the Sol-Gel States of Aqueous Carrageenan. Selective Site Binding of Cesium and Potassium Ions in k-Carrageenan Gels. *Macromolecules, 14,* 229-231.

Hoffman, A. S. (2012). Hydrogels for biomedical applications. *Advanced Drug Delivery Reviews, 64,* 18-23.

Jafari, A., Farahani, M., Sedighi, M., Rabiee, N., & Savoji, H. (2022). Carrageenans for tissue engineering and regenerative medicine applications: A review. *Carbohydrate Polymers, 281,* 119045.

Klevens, H. B. (1950). Solubilization. *Chemical Reviews, 47,* 1-74.

Lai, V. M. F., Wong, P. A.-L., & Lii, C.-Y. (2000). Effects of Cation Properties on Sol-gel Transition and Gel Properties of k-carrageenan. *Journal of Food Science, 65*(8), 1332-1337.

Laplante, S., Turgeon, S. L., & Paquin, P. (2006). Emulsion-stabilizing properties of chitosan in the presence of whey protein isolate: Effect of the mixture ratio, ionic strength and pH. *Carbohydrate Polymers, 65*, 479-487.

Lindman, B., Karlstrom, G., & Stigsson, L. (2010). On the mechanism of dissolution of cellulose. *Journal of Molecular Liquids, 156*, 76-81.

Meunier, V., Nicolai, T., Durand, D., & Parker, A. (1999). Light Scattering and Viscoelasticity of Aggregating and Gelling kappa-Carrageenan. *Macromolecules, 32*, 2610-2616.

Millane, R. P., Chandrasekaran, R., & Arnott, S. (1988). The molecular structure of kappa-carrageenan and comparison with iota-carrageenan. *Carbohydrate Research, 182*, 1-17.

Morris, E. R., Rees, D. A., & Robinson, G. (1980). Cation-specific Aggregation of Carrageenan Helices : Domain Model of Polymer Gel Structure. *Journal of Molecular Biology, 138*, 349-362.

Norton, I. T., & Goodall, D. M. (1983a). Equilibrium and Dynamic Studies of the Disorder-Order Transition of Kappa Carrageenan. *J. Chem. Soc., Faraday Trans. 1, 79*, 2489-2500.

Norton, I. T., & Goodall, D. M. (1983b). Role of Cations in the Conformation of Iota and Kappa Carrageenan. *Journal of the Chemical Society, Faraday Transactions 1, 79*, 2475-2488.

Peppas, N. A., Bures, P., Leobandung, W., & Ichikawa, H. (2000). Hydrogels in pharmaceutical formulations. *European Journal of Pharmaceutics and Biopharmaceutics, 50*, 27-46.

Perez, S. J. L. P., & Claudio, G. C. (2020). Molecular dynamics simulations of two double-helical hexamer fragments of iota-carrageenan in aqueous solution. *Journal of Molecular Graphics and Modelling, 98*, 107588.

Piculell, L., Borgström, J., Chronakis, I. S., Quist, P.-O., & Viebke, C. (1997). Organisation and association of k-carrageenan helices under different salt conditions. *International Journal of Biological Macromolecules, 21*, 141-153.

Piculell, L., Nilsson, S., & Muhrbeck, P. (1992). Effects of small amounts of kappa-carrageenan on the rheology of aqueous iota-carrageenan. *Carbohydrate Polymers, 18*, 199-208.

Prechoux, A., Genicot, S., Rogniaux, H., & Helbert, W. (2013). Controlling Carrageenan Structure Using a Novel Formylglycine-Dependent Sulfatase, an Endo-4S-iota-Carrageenan Sulfatase. *Marine Biotechnology, 15*, 265-274.

Richardson, R. K., & Goycoolea, F. M. (1994). Rheological measurement of kappa-carrageenan during gelation. *Carbohydrate Polymers, 24*, 223-225.

Rochas, C., & Rinaudo, M. (1984). Mechanism of gel formation in κ-Carrageenan. *Biopolymers, 23*(4), 735-745.

Running, C. A., Falshaw, R., & Janaswamy, S. (2012). Trivalent iron induced gelation in lambda-carrageenan. *Carbohydrate Polymers, 87*, 2735– 2739.

Souza, H. K. S., Hilliou, L., Bastos, M., & Gonçalves, M. P. (2011). Effect of molecular weight and chemical structure on thermal and rheological properties of gelling k/i-hybrid carrageenan solutions. *Carbohydrate Polymers, 85*, 429-438.

Thrimawithana, T. R., Young, S., Dunstan, D. E., & Alany, R. G. (2010). Texture and rheological characterization of kappa and iota carrageenan in the presence of counter ions. *Carbohydrate Polymers, 82*, 69-77.

Ueda, K., Saiki, M., & Brady, J. W. (2001). Molecular Dynamics Simulation and NMR Study of Aqueous Neocarrabiose 4(1)-Sulfate, a Building Block of K-Carrageenan. *Journal of Physical Chemistry B, 105*, 8629-8638.

Usov, A. I. (2011). Polysaccharides of the red algae. *Advances in Carbohydrate Chemistry and Biochemistry, 65*, 115-217.

Viebke, C., Borgström, J., & Piculell, L. (1995). Characterisation of kappa- and iota-carrageenan coils and helices by MALLS/GPC. *Carbohydrate Polymers, 27*, 145-154.

Zablackis, E., & Santos, G. A. (1986). The Carrageenan of Catenella nipae Zanard, a Marine Red Alga. *Botanica Marina, 29,* 319-322.

Zhang, Y., Yang, N., Zhang, Y., Hou, J., Han, H., Jin, Z., Shen, Y., & Guo, S. (2020). Effects of κ-carrageenan on pullulan's rheological and texture properties as well as pullulan hard capsule performances. *Carbohydrate Polymers, 238*, 116190.

Chapitre 6

Origine chimique de la synérèse : Partie B

Chapitre 6

Origine chimique de la synérèse : Partie B

Sommaire

Chapitre 6

Origine chimique de la synérèse : Partie B,

Influence de la position du groupement sulfate sur l'expansion des carraghénanes en solution

Résumé de l'article

La capacité de gonflement et de contraction des chaines de polysaccharide en solution ou dans le gel est un facteur important pour comprendre la synérèse. Cette partie met en évidence le rôle essentiel de la position du sulfate dans les interactions attractives ou répulsives au sein du volume des sphères que les chaines de kappa-carraghénane (κ-Car) et alpha-carraghénane (α-Car) forment en solution, en présence ou non de sel. L'étude est une analyse des viscosités des solutions des deux polysaccharides en fonction de la température, en utilisant le modèle que nous avons formulé pour déterminer la température de la plus faible viscosité notée T_c et le coefficient thermique de décroissance de la viscosité noté B_2. Le produit $B_2 \times T_c$ est défini comme le coefficient d'expansion thermique du système qui s'applique à l'expansion du volume des sphères et donc des polysaccharides. Le T_c et $B_2 \times T_c$ de l'eau sont respectivement (100 ± 5) °C et $(1.57 \pm 0.05) \times 10^{-2}$ /°C. On trouve 153 °C et 1.5×10^{-2} /°C pour κ-Car et pour α-Car on trouve 141 °C et 1.5×10^{-2} /°C en absence de sel. Le T_c des solutions de κ-Car croît de (150 ± 10) °C à (435 ± 45) °C si la concentration de KCl est élevée à 15 mM. Le T_c des solutions de α-Car croît de (140 ± 10) °C à (210 ± 5) °C si la concentration de $CaCl_2$ est élevée à 40 mM. Le coefficient d'expansion thermique de l'α-Car croît de 1.5×10^{-2} /°C à 1.55×10^{-2} /°C en présence de KCl alors qu'il décroit de 1.5×10^{-2} /°C à 1.2×10^{-2} /°C pour le κ-Car. L'énergie thermique pour provoquer l'expansion de l'α-Car jusqu'à la rupture des interactions intramoléculaires croît suivant T_c qui augmente de 140 °C à 165 °C si 5 mM de $CaCl_2$ est utilisé au lieu de 10 mM KCl avec une légère baisse du coefficient d'expansion. L'énergie pour rompre les interactions est très forte pour le κ-Car, de plus son coefficient d'expansion décroît significativement en présence de sel, ce qui démontre une forte tendance à la contraction liée à la structure moléculaire de κ-Car.

Mots clés : Volume exclu; Température de viscosité minimale; Liaison physique; Coefficient d'expansion thermique

https://doi.org/10.1016/j.ijbiomac.2022.11.128 ; International Journal of Biological Macromolecules. 223 (2022) 1138-1144

Highlights

* The sulfate groups position is tuned to change carrageenan sensitivity to salt.

* The sulfate group of 3,6-anhydro-D-galactose is rather sensitive to divalent salt.

* The sulfate groups of D-galactose is rather sensitive to monovalent salt.

* The α-carrageenan gels are more stable than κ-carrageenan gels against syneresis.

Graphical abstract

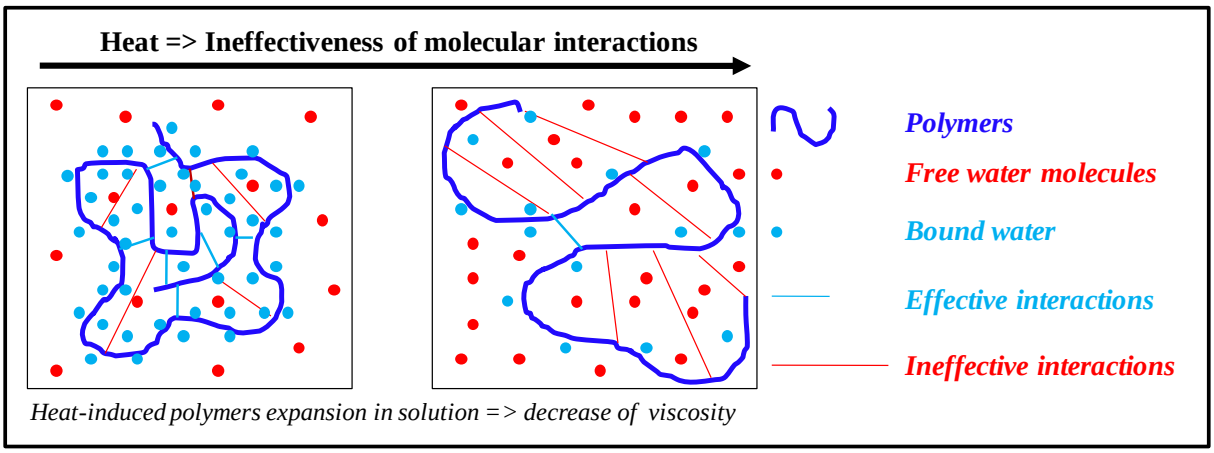

Rheological study of α- and κ-carrageenan expansion in solution as effects of the position of the sulfate group

Authors and affiliations:

Said ELMARHOUM, Komla AKO *

Univ. Grenoble Alpes, CNRS, Grenoble INP, LRP, 38000 Grenoble, France

*__Corresponding author__: *komla.ako@univ-grenoble-alpes.fr*; *akokomla@hotmail.com*

Abstract:

The viscosity of carrageenan solutions in the coil state was greater for α-carrageenan (α-Car) compared with that for κ-carrageenan (κ-Car); thus, the impact of one sulfate group on 3,6-anhydro-D-galactose was compared with the impact of one sulfate group on D-galactose units of the carrabiose residues. The thermal expansion coefficient of the solutions, $B_2 \times T_c$, characterizes the way the viscosity decreases because of extension of the physical bonds of the systems to their rupture point (T_c) under increasing temperature. The T_c and $B_2 \times T_c$ of water were equal to (100 ± 5) °C and $(1.57 \pm 0.05) \times 10^{-2}$/°C, respectively. The T_c of the α-Car and κ-Car systems increased after the addition of $CaCl_2$ and KCl, respectively, and with increasing polysaccharide concentration. However, the $B_2 \times T_c$ of the α-Car and κ-Car systems were rather sensitive to $CaCl_2$ and KCl, respectively. In the overall solutions examined, the expansion of α-Car systems was found to be between 1.5×10^{-2}/°C and 1.61×10^{-2}/°C, greater than the expansion of κ-Car systems, which was between 1.5×10^{-2}/°C and 1.2×10^{-2}/°C. Thus, α-Car is a good alternative to κ-Car for reducing syneresis phenomena, and its sensitivity as ι-Car to divalent cations would be due to the anhydro cycle.

Keywords: Carrageenan excluded volume; lower-viscosity temperature; physical bonds; thermal expansion coefficient.

1. Introduction

Carrageenan (Car) defines a family of sulfated galactans extracted from marine algae and features a disaccharide repetition (i.e., carrabiose, Fig.1), which is made with two galactose units, D-galactose (G) and 3,6-anhydro-D-galactose (DA), each of which can carry a variable number of sulfate functional groups [1, 2]. Kappa-carrageenan (κ-Car) has one sulfate group at position 4 of the G units, and alpha-carrageenan (α-Car) has one sulfate group at position 2 of the DA units [3]. To date, and to the best of our knowledge, α-Car has been much less studied, while numerous works have been reported on κ-Car in the literature; thus, we have partial knowledge of the role of the sulfate functional group position in the properties of Car solutions, namely, the polysaccharide expansion and ability to stop syneresis when the solution becomes a gel. The two types of polysaccharides provide good illustrations for the discussion of the position of the sulfate functional group and how this influences the intermolecular interactions and determines the expansion of the polysaccharide in solution [4].

Some applications, such as those based on hydrogel formation and suspension of particles in food, which involve dissolution of natural polymers, are very sensitive to the roles of the functional groups carried by the polymers [5, 6]. The influence of the number of sulfate groups carried by carrageenan carrabiose has been well shown in the literature. κ-Car, ι-Car and λ-Car, with one, two and three sulfate groups, respectively, are rather sensitive to mono-, di- and trivalent cations such as K^+, Ca^{2+} and Fe^{3+} [7, 8]. The functional molecules' ability to be charged or create hydrogen bonding play a major role in the conditions of dissolution and expansion of the polymers. The reactions of materials to stress are commonly discussed in terms of intra- and intermolecular interactions or physical bonds [9, 10], which are usually classified into two main classes: attractive and repulsive [11]. The temperature dependence of intramolecular and intermolecular interactions leads to the existence of two groups of compounds: those with dissolution in low thermal conditions (< 50 °C) and those that dissolve in high thermal conditions (> 60 °C) [4, 12, 13].

Based on the Newtonian approach and the definition of viscosity as molecular momentum, Ako et al. (2022) developed the temperature dependence of the viscosity model. The model shows the interaction in the systems as a dynamic mass that decreases when the systems evolve towards vapour and gas conditions or increases when they evolve towards gel or solid conditions. The dynamic mass is null when intermolecular attractive interactions vanish, and the viscosity is a result of solely the molecular mass momentum. The molecular mass was

termed the static mass by the authors, who demonstrated that the viscosity of a pure liquid is minimal at temperatures where the dynamic mass or attractive interactions vanish. The temperature dependence of the viscosities of α-Car and κ-Car systems in variable salt concentration conditions has been investigated in the Newtonian flow regime. The results are directly comparable in terms of interaction (dynamic mass) evolution because both systems have similar molecular (static) masses. Ako et al.[14] demonstrated that this dependence exists for all liquids at a temperature where the viscosity of the liquid is lower, and they determined the temperature (T_c), where the viscosity is lower for κ-Car solution controlling KCl salt and the polysaccharide concentration [14, 15]. In this treatise, we attempted to answer the question of how the position of the sulfate group on the polysaccharide backbone could affect polysaccharide expansion and solution viscosity accordingly. To this end, a comparative study between the viscosities of α-Car and κ-Car solutions was undertaken using the lower-viscosity concept [14].

2. Materials and methods

2.1. Product characteristics and sample preparation

Kappa-carrageenan (κ-Car). The κ-Car polysaccharide (Fig.1) is the same powder that Elmarhoum et al. used in a previous work [15]. It was a gift from Rhodia Food Switzerland (product name and reference: MEYPRO-GEL 01/2001 WG95-37 K-Car). The average molecular weight of the polysaccharide was $M_w = 3.3\times10^5$ g/mol, with an average polydispersity index of $M_w/M_n = 2.0$. The solutions of κ-Car and the salt addition were performed following the same method described in [15].

Alpha-Carrageenan (α-Car). The α-Car polysaccharide (Fig.1) was a gift from Cermav (Centre de recherche sur les macromolecules végétales), a leading laboratory in the natural polymer field, where the polysaccharide was prepared by an enzymatic technique according to the method reported by [16] using recombinant endo-4O-iota-carrageenan sulfatase.

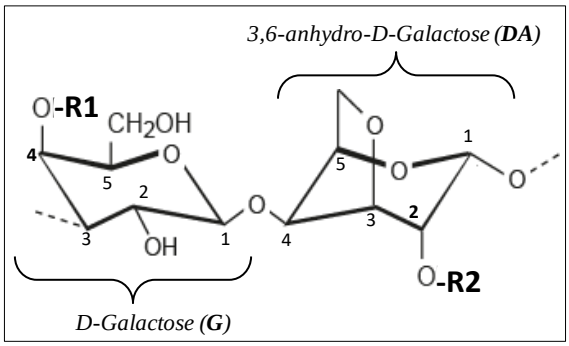

*Figure 1: Illustration of carrageenan carrabiose with different possibilities of creating kappa- (**R1** = -SO_3^- and **R2** = H), iota- (**R1** = -SO_3^- and **R2** = -SO_3^-) and alpha-carrageenan (**R2** = -SO_3^- and **R1** = H).*

The yield of desulfatation was controlled by ^{1}H NMR. The average molecular weight of the polysaccharide was $M_w = 3.8\times10^5$ g/mol, with an average polydispersity index of $M_w/M_n = 1.8$. The α-Car product was in lyophilized form and dissolved to prepare a stock solution (10 g/L) with which the samples were prepared following the same procedure as the κ-Car solutions.

2.2. Sample characterization

Viscosity measurements. The viscosity measurements were performed in Couette geometry using a DHR3 Rheometer (TA Instrument) under the same conditions as reported by [15]. The Couette geometry consisted of a concentric cylinder geometry of an inner rotor cylinder (bob) and an outer stator cylinder (cup) with radii R_1 of 14 mm and R_2 of 15 mm, respectively, defining a horizontal gap (R_2 - R_1) of 1 mm and an average radius R of 14.5 mm as (R_1 + R_2)/2. The height of the bob was 42 mm, and the vertical gap between the bob and cup was set at 2 mm. The minimum and maximum torques of the instrument were 5 μNm and 5×10^3 Nm, respectively. The temperature range corresponds to the temperature of the Newtonian flow domain, which will be indicated in the study because it depends on the types and concentration of salt for both systems. All the measurements of the viscosity were performed in the Newtonian flow domain at 15 s^{-1}, where the polysaccharide chains were in random coil conformation. According to the literature on carrageenan systems, the random coil conformation prevails when the temperature of the solution ranges above the helix-coil transition [17]. Therefore, coil-helix and sol-gel transitions were not considered in the current study but were extensively discussed by Elmarhoum et al. [15, 18].

Viscosity–temperature function and fit parameters. The temperature dependence of the viscosity data was determined by increasing temperature by 2 °C/min. The viscosity data, η^T, were divided by the viscosity at a reference temperature T_{ref}, for example $\eta^{20°C}$ or $\eta^{45°C}$, in the temperature range where the measurement precision was better. Then, the normalized viscosity data were computed as $\eta^T/\eta^{T_{ref}}$, and the logarithm of the results were plotted in line-line scale representation. The plots were fitted with a second-order polynomial function in agreement with the lower-viscosity concept [14], $B_0 + B_1T + B_2T^2$ as $B_2(T-T_{ref})(T-T_2)$, to the best of the mean square regression R^2 values between 0.99 and 1. The coefficient B_2 of the polynomial function and T_2 are the solution characteristic parameters by which the thermal expansion coefficient and the point where physical bonds between molecules become ineffective and are determined as $B_2 \times T_c$ and T_c, respectively, as $(T_{ref} + T_2)/2$ [14]. The lower-viscosity concept supposes that the T_c and boiling temperature (T_b) for a pure liquid are similar. The real meaning of T_c in relation to T_b was validated using water of T_b = 100 °C at 1013 hPa and mineral oil-330779 (*from Sigma–Aldrich, reference 330779 and CAS number 8042-47-5*), of T_b in the range 218 °C - 800 °C at 1013 hPa, indicated in the product data sheet version 6.4 of 02-09-2020.

3. Results and discussion

In solvent, the interactions between the polysaccharides involve hydrogen bonding and van der Waals, hydrophobic and electrostatic interactions [4], the balance of which determines the macroscopic flow behaviour of the solution. Polysaccharide expansion with solvent bonding ability is characterized by the excluded volume and intrinsic viscosity of the system, which are factors of the viscosity and concentration relationship [19, 20]. In dilute and semidilute concentration regimes, the polysaccharide-polysaccharide interactions are limited and are considerable in the entangled concentration regime [9, 19]. Therefore, the viscosity behaviours in the diluted concentration regimes of κ-Car and α-Car are mainly controlled by their expansion and solvent-bonding ability rather than polymer-polymer interactions [20]. These interactions are affected by the temperature and concentration of positive charges because of screening or neutralization of the negative charges on the polysaccharide [9, 14, 15]. Given that the two types of carrageenan differ by their sulfate group position in the carrabiose, we have discussed the role of sulfate in the interactions between the polysaccharide and solvent as a consequence of its position on the polysaccharide backbone. We previously demonstrated the relationships of these interactions in terms of mass with viscosity–temperature functions [14].

3.1. Viscosity–temperature function of two models of liquids

In this section, the temperature dependence of the viscosity of water and mineral oil-330779 is shown. Fig.2 shows the temperature dependence of the viscosity and the fit function for water with two adjustment parameters and one adjustment parameter considering $T_c = T_b$.

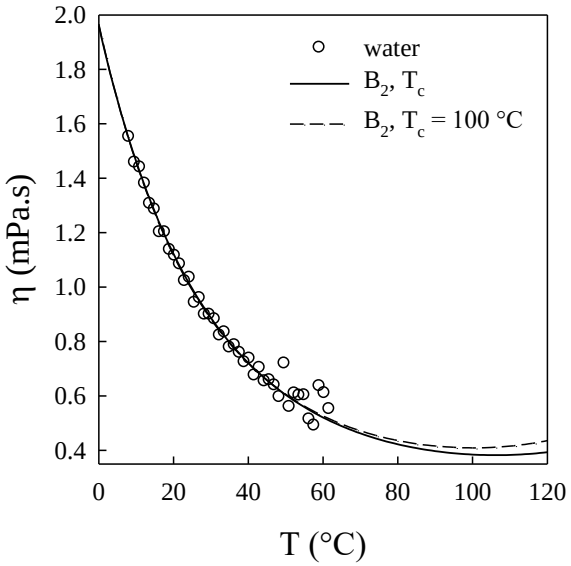

Figure 2: Temperature dependence of the viscosity of water and the viscosity–temperature fit function (Eq.1) using the viscosity at T_{ref} = 45 °C as a reference with two adjustment parameters B_2 and T_c (full line) and with one adjustment parameter B_2 (dashed line) considering the characteristic temperature T_c equal to the boiling point of water ≈ 100 °C at 1013 hPa.

The viscosity–temperature function is shown in Eq.1, where B_2 and T_2 are the two adjustment parameters of the fit, but the choice of T_{ref} in the temperature range where the viscosity value fluctuation is considerable could affect the fit quality. The parameter T_2 in Eq.2 is tuned by a characteristic temperature (T_c) value, in which T_c is defined to predict the physical bonding rupture point of the systems as where the liquid–gas transition could take place, in agreement with the lower-viscosity concept [14]. The T_c according to the model is the point where the viscosity of chemically pure components in a liquid state is minimal. The two examples of fluid provide good illustrations for the discussion of the T_c. For pure components, T_c matches quite well with T_b; if T_b is known, then only one parameter remains for fitting.

$$\eta^{T} = \eta^{T_{ref}} \cdot \exp\left[B_2 \cdot \left(T - T_{ref}\right)\left(T - T_2\right)\right] \qquad 1$$

where

$$T_2 = 2T_c - T_{ref} \quad 2$$

The B_2 and T_c from the polynomial regression fit were $1.45\times10^{-4}/°C^2$ and 106.2 °C, respectively, with an R^2 value of 0.988. The fit with only the B_2 parameter gives $1.57\times10^{-4}/°C^2$ with T_c = 100 °C. For water, the two fits through the viscosity data did not show a considerable difference. The shift between the fit only is revealed in the temperature range near T_c.

We observed that the quantity $B_2\times T_c$ works as a constant of the fit. The thermal expansion expression of the viscosity (Eq.3) is derived from Eq.1 as the fractional variation of the viscosity per degree change in temperature, in which we show the quantity $B_2\times T_c$,

$$\frac{1}{\eta}\left(\frac{\partial\eta}{\partial T}\right) = 2B_2 \cdot T - 2B_2 \cdot T_c \quad 3$$

and the B_2 parameter is a constant of the second derivation or as the coefficient of Eq.3, which we think is the parameter reflecting the thermal force that increases or decreases the viscosity with the contraction or dilatation of intermolecular physical bonds. The heat activity on the viscosity characterized by B_2 is applied at the molecular level to address the temperature dependence of intermolecular interactions. A weak B_2 means that a high temperature or heat energy is necessary to stretch the intermolecular physical bonds. Stretching the physical bonds by heat leads to volumetric expansion and thus changes the flow of pure liquid. Therefore, Eq.3 can be defined as the thermal expansion dependence of the viscosity, and when Eq.3 is expressed as

$$\frac{1}{\eta}\left(\frac{\partial\eta}{\partial T}\right) = 2B_2 \cdot T_c \cdot \left(\frac{T}{T_c} - 1\right) \quad 4$$

the quantity $B_2\times T_c$ is an interesting factor to scrutinize the thermal behaviour of the system viscosity. If $T << T_c$, then thermal expansion of the viscosity function is rather constant and equal to $2B_2\times T_c$. Its values are to some extent a result of the physical factors, which determine the liquid boiling point. For water, $B_2\times T_c = (1.57 \pm 0.05)\times10^{-2}/°C$ gives the results of Fig.2.

The determination of the characteristic temperature of a complex liquid as a mixture or liquid of undefined boiling temperature, such as mineral oil, was undertaken as an illustration for the discussion of parameter T_c in the sections on the polysaccharide solutions. Fig.3 shows the temperature dependence of the viscosity of the mineral oil, which has an initial boiling point and boiling range of 218 °C -800 °C. The viscosity–temperature fit is displayed in Fig.3 using

two adjustment parameters, B_2 and T_c. The fit with a combination of both B_2 and T_c is systematically applied to obtain the best fit with an R^2 close to 1. The result is shown in the full line in Fig.3, which corresponds to $B_2 \approx 1.36\times10^{-4}/°C^2$, and $T_c \approx 170$ °C implies $B_2\times T_c \approx 2.31\times10^{-2}/°C$. The T_c, which predicts the temperature of the minimum point of the viscosity as the liquid–gas transition point, is found at 48 °C below the initial boiling point of the oil at 218 °C. If the boiling temperatures of the mineral oil are used as T_c = 218 °C and T_c = 800 °C, then parameter B_2 remains to fit the viscosity–temperature data. The results are shown in Fig.3 as dashed and dotted lines corresponding to $B_2 \approx 1.06\times10^{-4}/°C^2$ and $B_2 \approx 2.6\times10^{-5}/°C^2$, respectively. The thermal expansion coefficients $B_2\times T_c$ from the fit for T_c = 218 °C and T_c = 800 °C are $\approx 2.31\times10^{-2}/°C$ and $\approx 2.08\times10^{-2}/°C$, respectively.

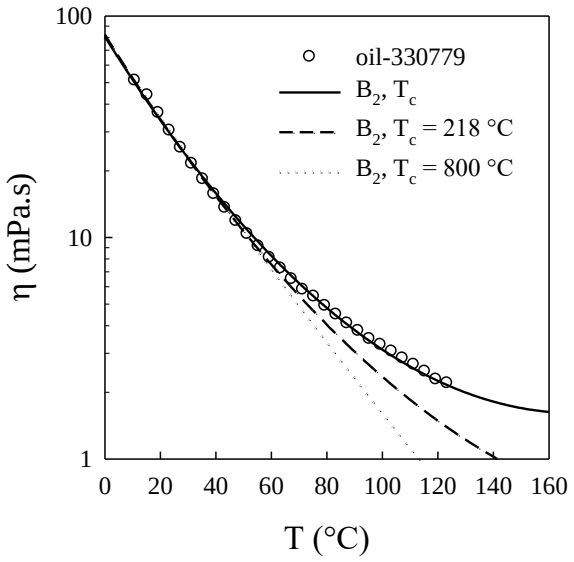

Figure 3: Temperature dependence of the viscosity and the viscosity–temperature fit (Eq.1) using the viscosity at T_{ref} = 45 °C as a reference with two adjustment parameters B_2 and T_c (full line) and with one adjustment parameter B_2 as dashed and dotted lines considering the characteristic temperature T_c equal to the initial boiling temperature of T_b = 218 °C and the highest boiling temperature of T_b = 800 °C, respectively.

Each liquid system has a characteristic thermal expansion function of viscosity and coefficient as well as a characteristic boiling temperature if the system is a molecularly pure liquid. The fact that variable boiling temperatures were reported for the mineral oil demonstrates that the oil is made of different types of molecular components. However, the mixture macroscopically behaves like one molecular component liquid (homogeneous system). Therefore, one characteristic temperature T_c is practical for the mixture in the viscosity experimental

measuring range. In case T_c is not known, both B_2 and T_c are tuned to have the best viscosity–temperature fit, and thus, a $T_c = T_b$ coincidence could be fortuitous. The fact that T_c is found at 170 °C below 218 °C means that the interactions between the substances composing the mineral oil are broken before the true liquid–gas transition takes place.

Unlike water, the fact that T_c falls below the temperature range of boiling means the boiling of mineral oil at atmospheric pressure (1013 hPa) consumes heat energy in addition to the physical bond rupture energy. This additional energy is likely due to the molecular mass effect, i.e., all things being equal, and evaporation of high-molecular-weight liquid costs more heat energy than that of small-molecular-weight liquid. The viscosity of a liquid in conditions where the associative bonds between molecules become negligible or ineffective depends on the liquid molecular weight, similar to the viscosity of a gas system. Therefore, the decrease in the viscosity of the liquid under heat is due to the decreasing intermolecular interaction strength. In the case of water, the coincidence between T_c and T_b could result from the weak effect of the molecular mass of water on the boiling temperature. In water, the contributions of intermolecular interactions to the viscosity are much more important than the contribution of molecular weight to the viscosity of the liquid phase. However, the molecular weight is considerable in the boiling temperature of the mineral oil. Therefore, the temperature of the lower viscosity of a solution or homogeneous liquid system characterizes the temperature T_c at which intermolecular interactions become ineffective rather than the boiling temperature, and $B_2 \times T_c$ could be taken as the physical bond expansion coefficient of the systems.

3.2. Viscosities of α-Car and κ-Car solutions

The temperature dependence of the viscosity of the two polysaccharides, α-Car and κ-Car, at 3 g/L is shown with their fit functions in Fig.4. The viscosities of the solutions at 20 ℃ were used as a reference, and the viscosity–temperature function parameters were adjusted to obtain the best fits. The solutions of both polysaccharides exhibit Newtonian flow, and their viscosity decreases with increasing temperature following the lower-viscosity concept of liquid. Their thermal expansion coefficient $B_2 \times T_c$ and lower-viscosity temperature T_c were $\approx 1.5 \times 10^{-2}$/°C and 141 °C, respectively, for α-Car and $\approx 1.5 \times 10^{-2}$/°C and 153 °C, respectively, for κ-Car, where values of $\approx 1.57 \times 10^{-2}$/°C and 100 °C were measured for water. In the literature, when the temperature dependence of the viscosity of a solution and its solvent are different, there is currently an interaction between the solid matter structures of the fluids, which characterizes its non-Newtonian flow behaviour [9]. The interactions in the system can lead to aggregation, cold-

or heat-induced gelation mechanisms, etc. [21-25]. Therefore, the fact that Newtonian flow and viscosity–temperature functions characterize the α-Car and κ-Car systems means that the solvent properties macroscopically dominate the solution behaviour. Under this condition, we may assume that polysaccharide-polysaccharide interactions are ineffective [9].

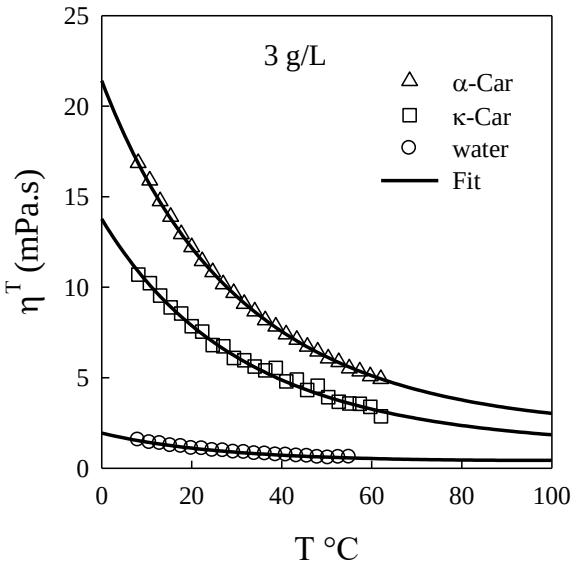

Figure 4: Temperature dependence of the viscosities of water, α-Car and κ-Car (3 g/L). The fit to Eq.1 parameters, i.e., *$B_2 \times T_c$ and T_c for the three systems, are 1.57×10^{-2}/°C and 100 °C (water), 1.5×10^{-2}/°C and 141 °C (α-Car), and 1.5×10^{-2}/°C and 153 °C (κ-Car), respectively, using the viscosity at T_{ref} = 20 °C as a reference. The R^2 values of the fit are 0.995, 0.999 and 0.992, respectively.*

It is interesting to observe that the temperature dependence of the viscosity of α-Car solutions evolves well above that of κ-Car solution, despite the similarity of their molecular structure and weight. With an identical expansion coefficient, $B_2 \times T_c \approx 1.5 \times 10^{-2}$/°C, the normalized viscosity, $\eta^T/\eta^{20°C}$, of both systems is equal in the range of temperatures well below their T_c, i.e., between 0 °C and 60 °C. This result shows two main differences caused by the position of the sulfate group, which are the viscosity and the thermal resistance of the physical bonds. The latter characterizes the energy of physical interactions at work in the systems. Compared with water, the viscosity and T_c of both systems increase, but $B_2 \times T_c$ decreases. In the range of temperatures above, for example, 60 °C, where the thermal behaviour of the viscosity between α-Car and κ-Car systems is considerably different, water–water molecules such as hydrogen bonding interactions are weakened by heat, and their contributions to the viscosity thermal behaviour are no longer important. Therefore, the main contribution of the type of polysaccharide to the

thermal behaviour of the systems is due to the polysaccharide intramolecular interactions. These interactions are monomer-monomer interactions with monomer-water molecule interactions inside the excluded volume [19]. These interactions are stronger in the case of κ-Car systems, as the T_c is greater than the T_c of α-Car systems. The intramolecular forces in the polysaccharide excluded volume are very much in focus in the thermal compliance of the solutions and the thermoelasticity of the polysaccharide chains in solution [9, 20]. Considering that the systems have similar heat capacity, it costs more energy to break the intramolecular physical bonds of κ-Car systems compared with α-Car systems. This could explain the fact that the viscosity of α-Car solutions is greater than the viscosity of κ-Car solutions, and weak attractive intramolecular interactions lead to greater expansion of the polymer in solution. Moreover, in the temperature domain where hydrogen bonding is favourable, a greater expansion capacity of the polysaccharide contributes to carrying more solvent molecules by the polysaccharide and thus increasing the viscosity [14, 20].

3.3. Effect of salts

κ-Car is characterized by the thermoreversibility of its conformation in solution from random coils to helices in the presence of salt [26]. The conformational transition has been characterized by optical rotation measurements and was shown to be concomitant with a sharp increase or decrease in viscosity if the temperature was decreased or increased, respectively [27]. The coils to helices conformational transitions were observed to characterize the Newtonian to non-Newtonian flow transition of the solution, and our study is restricted to the Newtonian regime [15]. Therefore, in case the solution viscosity dependence on temperature exhibits conformational transition as for κ-Car solution with 10 mM (KCl) below 30 °C (Fig.5), only the temperature range in which the coil conformation prevails is fitted with the viscosity–temperature function.

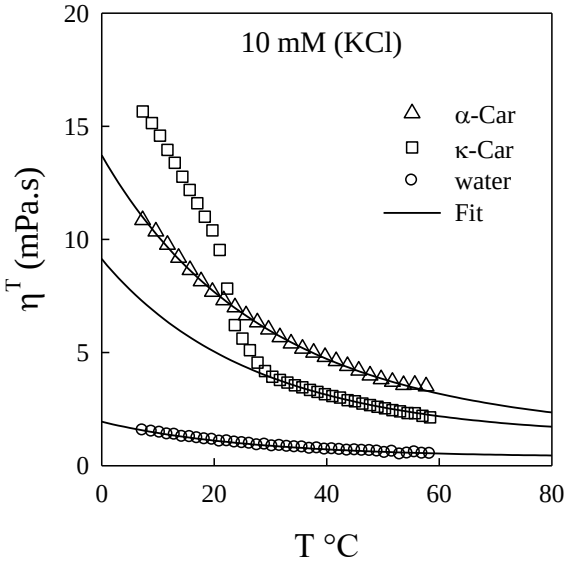

Figure 5: Temperature dependence of the viscosities of α-Car, κ-Car and water with their fit functions using the viscosity at T_{ref} = 45 °C. The $B_2 \times T_c$ and T_c for the three systems are, respectively, 1.55×10^{-2}/°C and 139 °C (α-Car); 1.40×10^{-2}/°C and 183 °C (κ-Car); and 1.57×10^{-2}/°C and 100 °C (water).

The viscosities of α-Car solutions remain greater in the coil conformation regime than the viscosities of the κ-Car solutions. For example, at 40 °C, Fig.4 to 5, the viscosities of the α-Car solutions remain greater than the viscosities of κ-Car solutions, despite the addition of salt. The viscosities of the solutions of the two polysaccharides decrease because of the addition of 10 mM KCl to the solutions, from ≈ 8 mPa.s to ≈ 5 mPa.s for α-Car solutions and from ≈ 5 mPa.s to ≈ 3 mPa.s for κ-Car solutions. The decrease is caused by the reduction of long-range repulsive intramolecular interactions such as electrostatic forces, which is due to $-SO_3^-$ screened or neutralized by K^+ and thus results in contraction of the excluded volume [19].

The cooling of the κ-Car solution in the presence of 10 mM KCl leads to the coil-helix transition of the polysaccharide below ≈ 25 °C, and the transition with aggregation of the helices leads to a sharp increase in the viscosity [17, 27]. The gelation occurrence of the solution and kinetics depend on the polysaccharide concentration and temperature. It took several hours for the κ-Car solutions to become gels at rest at 5 °C. However, for the α-Car solutions, gel formation was not expected because of the absence of a coil-helix conformation transition in the measuring range. Therefore, the viscosities of κ-Car solutions are greater than those of α-Car solutions in the temperature range < 30 °C, where κ-Car solutions behave like fluid gels or suspensions of aggregates [28, 29].

Unlike κ-Car, the α-Car polysaccharide surprisingly did not show a conformational change. Despite the similarity between κ-Car and α-Car, α-Car is not as sensitive as κ-Car to K^+ counterions. According to the current knowledge, the particular sensitivity to monovalent counterions of carrageenan is due to the monosulfate charge of its carrabiose moiety [8]. The ionic selectivity of α-/κ-Car on the coil-helix conformation transition of the polysaccharide and thus on the sol-gel transition has also been investigated [18]. The viscosity–temperature function predicts similar thermal resistance of the intermolecular interaction prevailing in the α-Car solutions before and after the addition of 10 mM KCl. The T_c remains similar, 141 °C for the solutions without added salt and 139 °C for the solutions with added salt. However, the thermal expansion coefficient $B_2 \times T_c$ seems to sensibly increase from 1.50×10^{-2}/°C for the solutions without added salt to 1.55×10^{-2}/°C for the solutions with added salt. The increase in $B_2 \times T_c$ implies an increase in the temperature dependence of the viscosity slope in the range of temperatures where hydrogen bonding is favourable. The weak increase in $B_2 \times T_c$ implies that the addition of KCl could have decreased the intramolecular hydrogen bonding interactions, which may result in a lower intrinsic viscosity and explain the decrease in viscosity [30]. However, if the decrease in the viscosity results from a decrease of the hydrodynamic volume of α-Car chains, with the screening effect of the K^+ counter ions, the short-range interactions, such as the van der Waals attractive forces, should increase the intramolecular hydrogen bonding [11]. Therefore, we may assume that the hydrodynamic volume of α-Car shrinks, but not enough to overcome long-range interactions, such as electrostatic repulsion forces to promote intramolecular hydrogen bonding.

For κ-Car systems, the viscosity–temperature function predicts a significant increase in T_c from 153 °C to 183 °C, with a decrease in the thermal expansion coefficient $B_2 \times T_c$ from 1.5×10^{-2}/°C to 1.4×10^{-2}/°C. The K^+ counterions would increase the hydrogen bonding interactions and decrease the intrinsic viscosity and/or hydrodynamic volume of the κ-Car chains. The K^+ counter ions are clearly efficient to form pair ions with the sulfate group and promote the short-range attractive forces in the κ-Car systems compared with the α-Car systems [31]. We can see that 10 mM KCl of monovalent counter ions did not affect the thermal properties of the α-Car systems as it did for κ-Car. Therefore, we explored the influence of $CaCl_2$ on the viscosity of α-Car because this salt influences the flow behaviour of the iota-Carrageenan (*i*-Car) [8, 32], which has one sulfate anion group on the 2 position of the 3,6-anhydro-D-galactose unit, as in α-Car, but also one additional sulfate group on the 4 position of the D-galactose unit, as in κ-Car [3].

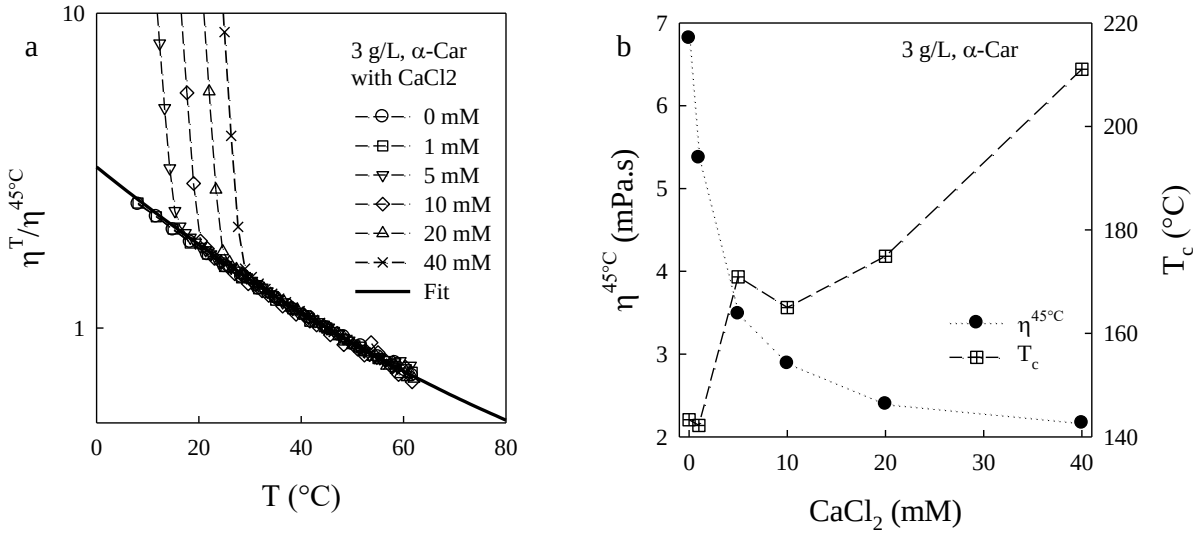

Figure 6: a) Temperature dependence of the normalized viscosity ($\eta/\eta^{45°C}$) in a log-line plot for different concentrations of $CaCl_2$ in a solution of 3 g/L α-Car with the fit function using $\eta^{45°C}$ as a reference. The fit plots are the average values of T_c = 168 ± 25 °C and $B_2 \times T_c$ = (1.51 ±0.03)×10^{-2} °C. b). The $CaCl_2$ dependence of $\eta^{45°C}$ and T_c for a 3 g/l solution of α-Car.

The temperature dependence of the viscosity for concentrations from 0 to 40 mM $CaCl_2$ in a 3 g/L solution of α-Car is shown in Fig.6a. The viscosity data have been divided by $\eta^{45°C}$ for the fit function and are plotted in log-line with the fit. The viscosity–temperature function fits only the viscosity of the solutions in the coil conformation of the polysaccharide. Fig.6b shows the $CaCl_2$ concentration dependence of T_c and $\eta^{45°C}$. The α-Car experienced the conformational transition in solution with $CaCl_2$ concentrations above 1 mM in the temperature range of the measurements.

The viscosity decreases with increasing $CaCl_2$ for α-Car solutions in the coil conformation regime, and the calcium increases T_c, as predicted by the fit function (Fig.6b). The viscosity–temperature function fits the grouped viscosity data with the average T_c and $B_2 \times T_c$ values of (168 ± 25) °C and (1.51 ± 0.03)×10^{-2}/°C, respectively. The large variation in T_c inversely implies a large variation in B_2, as the factor $B_2 \times T_c$ is almost constant. The way T_c and B_2 are balanced in the fit has been discussed previously (Section 3.1). Given that the T_c of α-Car solutions shifts well above the temperature range of the measurements, it is better that the coefficient $B_2 \times T_c$ is used to appreciate how much the intermolecular interactions are affected. If we assumed that the average value of T_c ± 25 °C characterizes the lower-viscosity point of the α-Car solutions in the presence of calcium, where intermolecular interactions are

ineffective, then the calcium increases the heat resistance of the physical bonds at work in the α-Car solutions from 140 °C to 168 °C. Conversely, the KCl salt increases the heat resistance of the physical bonds of κ-Car as T_c increases from (150 ± 10) °C to (435 ± 45) °C if the KCl concentration is increased to 15 mM. Therefore, the physical bonds in the solutions are energetically strengthened by salt for both systems; however, the K^+ counterions strengthen the physical bonds in the κ-Car solution more than the Ca^{2+} counterions in the α-Car solution. Moreover, the K^+ ions decrease the thermal expansion coefficient of κ-Car solutions as $B_2 \times T_c$ decreases from $(1.50 \pm 0.04) \times 10^{-2}$/°C to $(1.2 \pm 0.2) \times 10^{-2}$/°C, while calcium does not change the thermal expansion coefficient of α-Car solutions as $B_2 \times T_c$ remains constant at $(1.51 \pm 0.03) \times 10^{-2}$/°C. The ineffectiveness of calcium counterions on the thermal expansion coefficient of the α-Car solution could be explained by the fact that intermolecular electrostatic repulsion interactions are still at work, despite the addition of calcium salt to the solution. The screening of the carrabiose (monomer) monoanion by a divalent cation could turn the negative electrostatic repulsion to positive electrostatic repulsion with more or less strength, which was claimed by Elmarhoum et al. [18] to explain the effect of calcium counter ions on α-Car solutions compared with the effects of calcium on ι-Car solution and the effects of potassium on κ-Car solution. Actually, the temperature dependence of the electrostatic forces at work in the polysaccharide solutions could fundamentally allow a better understanding of the solution flow behaviour. The understanding may partly come from the temperature dependence of the static permittivity of water. Catenaccio et al. [33] reported a decrease in the static permittivity of water similar to the trend of the viscosity of water if the temperature is increased. Actually, the decrease of the static permittivity of water should lead to an increase in the electrostatic repulsive forces, and thus, contribution to expansion of the excluded volume is expected, in agreement with Coulomb's law of electrostatics, with all other factors being kept constant. The heat energy to render the intermolecular interactions inside the α-Car exclude volume ineffective is increased as T_c shifts from ≈ 140 °C to 165 °C if 5 mM Ca^{2+} is used instead of 10 mM K^+ because calcium counter ions decrease the electrostatic repulsive forces more than potassium counter ions. Thus, a lower expansion of the α-Car volume in solution is expected in the presence of calcium counter ions in comparison with potassium counter ions, which is in agreement with the slight decrease in the thermal expansion coefficient from 1.55×10^{-2}/°C to 1.51×10^{-2}/°C when 5 mM Ca^{2+} is used instead of 10 mM K^+. This finding leads to questions about the role of the anhydro cycle on the salt selectivity behaviour of these types of polysaccharides.

3.4. Effect of polysaccharide concentrations

The temperature dependence of the viscosities of various concentrations of α-Car and κ-Car in 10 mM KCl solution was examined. Fig.7a shows the results with the fits of the temperature dependence of the viscosity for α-Car. In Fig.7b, the concentration dependence of the viscosity at T_{ref} = 45 °C for both polysaccharides is displayed. The viscosity–temperature functions provide the best correlation factors ($R^2 \approx 0.999$) of T_c with $B_2 \times T_c$ of 131 °C with 1.52×10^{-2}/°C for 1 g/L, 132 °C with 1.58×10^{-2}/°C for 3 g/L and 144 °C with 1.61×10^{-2}/°C for 5 g/L. The T_c tends to increase from the T_c of water to 144 °C if the α-Car concentration is increased to 5 g/L. Under the same conditions, the T_c of κ-Car systems increases to 226 °C more than the increase in T_c of α-Car systems. A slight augmentation of $B_2 \times T_c$ with increasing α-Car concentration seems to appear from the expansion coefficient of 1 g/L, i.e., $(1.52 \pm 0.08) \times 10^{-2}$/°C to $(1.61 \pm 0.08) \times 10^{-2}$/°C.

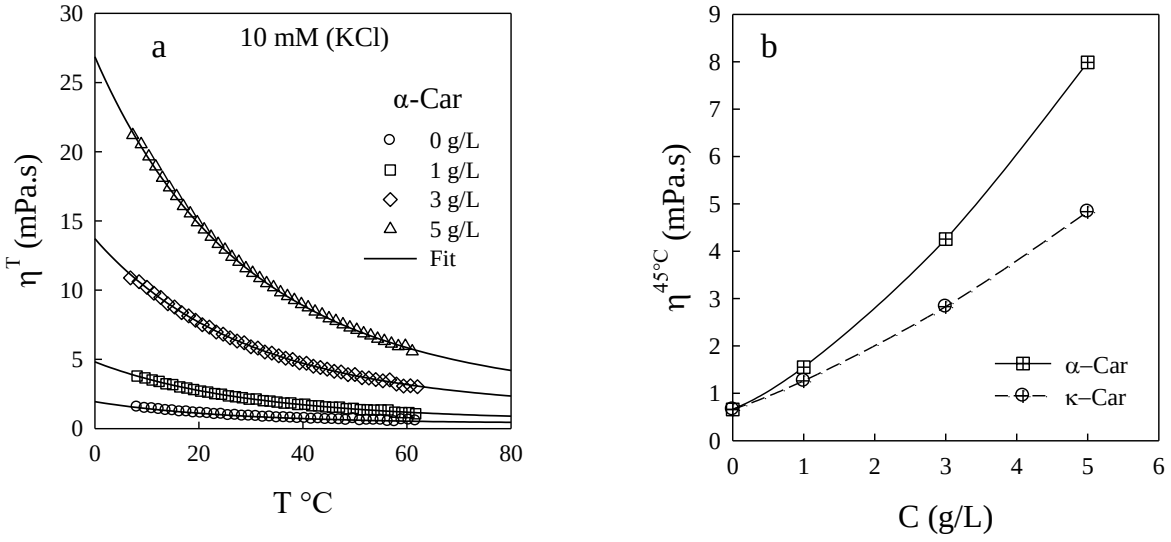

Figure 7: a) Temperature dependence of the viscosity with the fit for variable concentrations of α-Car in 10 mM (KCl) solution and b) the concentration dependence of the viscosity at T_{ref} = 45 °C of α-Car and κ-Car.

Unlike α-Car systems, the κ-Car concentration induces a weak decreasing tendency of the expansion coefficient to $(1.30 \pm 0.07) \times 10^{-2}$/°C. However, the effect of 10 mM KCl must be accounted for because in conditions with no salt, the influence of the κ-Car concentration was negligible [14]. The error bars of the thermal expansion coefficient did not allow us to clearly claim its increasing and decreasing tendencies. The comparison of the viscosity between α-Car and κ-Car in Fig.7b shows an expansion ability of α-Car greater than that of κ-Car with

increasing polysaccharide concentration. To confirm this, the viscosity data in Fig.7b were converted to the specific viscosity $\eta_{sp}= (\eta_C - \eta_0)/\eta_0$, where η_C and η_0 are the viscosity of the solution at concentration C and the viscosity of water, respectively. The specific viscosity per unit of concentration, η_u, of the systems as η_{sp}/C, of which extrapolation to concentration zero gives the intrinsic viscosity [14, 20], was determined, and if we calculated the η_u of α-Car systems by η_u of the κ-Car system as *f* in Eq.5 for the three concentrations 1 g/L, 3 g/L and 5 g/L,

$$f = \frac{\eta_u^{\alpha-Car}}{\eta_u^{k-Car}} \qquad 5$$

the results corresponding to the solution with 10 mM KCl at 45 °C are *f* = 1.5, 1.7 and 1.8, which show that the expansion ability of α-Car is higher than that of κ-Car polysaccharide in solution. The ability of α-Car to expand in solution more than κ-Car could contribute to an increasing tendency of the expansion coefficient $B_2 \times T_c$ if the α-Car concentration is increased. Alternatively, the expansion ability of κ-Car could decrease despite the increase in viscosity with increasing concentration because of increasing counterion concentration, and this fact may lead to a slight decrease in the expansion coefficient $B_2 \times T_c$. These features of the polysaccharides will explain their gelation and solvent exudation behaviours (syneresis) [15]. Although the two polysaccharides have similar molecular weights and carry one sulfate anion per carrabiose, α-Car systems have a greater expansion ability than κ-Car systems. Based on these results, α-Car gelation should show much less syneresis than κ-Car gelation.

4. Conclusion

Kappa-carrageenan (κ-Car) and alpha-carrageenan (α-Car) expansions in solution have been investigated by applying the lower-viscosity concept to the viscosity–temperature function. If the salt and polysaccharide concentrations are varied, the thermal expansion coefficient $B_2 \times T_c$ of α-Car systems ranges between 1.50×10^{-2}/°C and 1.62×10^{-2}/°C, while for κ-Car systems, $B_2 \times T_c$ ranges between 1.50×10^{-2}/°C and 1.2×10^{-2}/°C. In the coil conformation regime, the viscosity of α-Car systems was found to be greater than the viscosity of κ-Car. The salts increase the temperature (T_c), where the physical bonds of both systems are considered ineffective, but the T_c of the systems' sensitivity to salt depends on the type of salt. α-Car and κ-Car are sensitive to $CaCl_2$ and KCl, respectively. If the concentration of the polysaccharides is increased in 10 mM KCl at 45 °C, the specific viscosity per unit of concentration of α-Car and κ-Car increases with the concentration following a slope of ≈ 0.22 $L^2.g^{-2}$ and ≈ 0.09 $L^2.g^{-2}$. These results show

the greater ability of α-Car to expand in solution compared with κ-Car. The difference between α-Car and κ-Car regarding the salt effect is a result of the position of the sulfate group on the carrabiose moiety of the carrageenan polysaccharide. Thus, the position of the sulfate group on the carrabioses with the anhydro cycle makes the α-Car polysaccharide a good alternative to k-Car for reducing syneresis (gelation with solvent exudation) phenomena. The anhydro cycle has a considerable role in the reactivity of sulfate groups with counter ions.

5. Acknowledgements

We thank Professor William Helbert from the Centre de Recherche sur les Macromolecules Végétales (CERMAV) for the α-Carrageenan and Vincent VERDOOT for his technical assistance with the rheometer instruments. This work was financially supported by I-MEP2 PhD graduate school and the PolyNat Carnot Institut. The Laboratoire Rhéologie et Procédés (LRP) is part of LabEx Tec 21 (Investissements d'Avenir - grant agreement n°ANR-11-LABX-0030) and PolyNat Carnot Institut (Investissements d'Avenir - grant agreement n°ANR-11-CARN-030-01).

6. References

[1] A.I. Usov, Polysaccharides of the red algae, Advances in Carbohydrate Chemistry and Biochemistry 65 (2011) 115-217.

[2] K. Ueda, M. Saiki, J.W. Brady, Molecular Dynamics Simulation and NMR Study of Aqueous Neocarrabiose 4(1)-Sulfate, a Building Block of K-Carrageenan, Journal of Physical Chemistry B 105 (2001) 8629-8638.

[3] V.L. Campo, D.F. Kawano, D.B. da Silva Jr, I. Carvalho, Carrageenans: Biological properties, chemical modifications and structural analysis - A review, Carbohydrate Polymers 77 (2009) 167-180.

[4] B. Lindman, G. Karlstrom, L. Stigsson, On the mechanism of dissolution of cellulose, Journal of Molecular Liquids 156 (2010) 76-81.

[5] R.P. Millane, R. Chandrasekaran, S. Arnott, The molecular structure of kappa-carrageenan and comparison with iota-carrageenan, Carbohydrate Research 182 (1988) 1-17.

[6] H.K.S. Souza, L. Hilliou, M. Bastos, M.P. Gonçalves, Effect of molecular weight and chemical structure on thermal and rheological properties of gelling k/i-hybrid carrageenan solutions, Carbohydrate Polymers 85 (2011) 429-438.

[7] T.R. Thrimawithana, S. Young, D.E. Dunstan, R.G. Alany, Texture and rheological characterization of kappa and iota carrageenan in the presence of counter ions, Carbohydrate Polymers 82 (2010) 69-77.

[8] C.A. Running, R. Falshaw, S. Janaswamy, Trivalent iron induced gelation in lambda-carrageenan, Carbohydrate Polymers 87 (2012) 2735– 2739.

[9] V. Tirtaatmadja, D.E. Dunstan, D.V. Boger, Rheology of dextran solutions, Journal of Non-Newtonian Fluid Mechanics 97 (2001) 295-301.

[10] T.v. Vliet, H.J.M.v. Dijk, P. Zoon, P. Walstra, Relation between syneresis and rheological properties of particle gels, Colloid Polymer Science 269 (1991) 620-627.

[11] W. Kunz, P.L. Nostro, B.W. Ninham, The present state of affairs with Hofmeister effects, Current Opinion in Colloid and Interface Science 9 (2004) 1-18.

[12] K. Ako, D. Durand, T. Nicolai, Phase separation driven by aggregation can be reversed by elasticity in gelling mixtures of polysaccharides and proteins, Soft Matter 7 (2011) 2507-2516.

[13] S.K. Sathe, V.D. Zaffran, S. Gupta, T. Li, Protein Solubilization, Journal of the American Oil Chemists Society 95 (2018) 883-901.

[14] K. Ako, S. Elmarhoum, C.D. Munialo, The determination of the lower critical concentration temperature and intrinsic viscosity: The syneresis reaction of polymeric gels, Food Hydrocolloids 124 (2022) 107346.

[15] S. Elmarhoum, K. Ako, Lower critical concentration temperature as thermodynamic origin of syneresis: Case of kappa-carrageenan solution, Carbohydrate Polymers 267 (2021) 118191.

[16] A. Prechoux, S. Genicot, H. Rogniaux, W. Helbert, Controlling Carrageenan Structure Using a Novel Formylglycine-Dependent Sulfatase, an Endo-4S-iota-Carrageenan Sulfatase, Marine Biotechnology 15 (2013) 265-274.

[17] M. Ciancia, M. Milas, M. Rinaudo, On the specific role of coions and counterions on kappa-carrageenan conformation, International Journal of Biological Macromolecules 20 (1997) 35-41.

[18] S. Elmarhoum, S. Mathieu, K. Ako, W. Helbert, Sulfate groups position determines the ionic selectivity and syneresis properties of carrageenan systems, carbohydrate Polymers 299 (2023) 120166.

[19] R.H. Colby, Structure and linear viscoelasticity of flexible polymer solutions: comparison of polyelectrolyte and neutral polymer solutions, Rheologica Acta 49 (2010) 425-442.

[20] M.A. Masuelli, Dextrans in Aqueous Solution. Experimental Review on Intrinsic Viscosity Measurements and Temperature Effect, Journal of Polymer and Biopolymer Physics Chemistry 1 (2013) 13-21.

[21] M. Wu, Z. Shi, Y. Ming, C. Wang, X. Qiu, G. Li, T. Ma, Thermostable and rheological properties of natural and genetically engineered xanthan gums in different solutions at high temperature, International Journal of Biological Macromolecules 182 (2021) 1208-1217.

[22] N.B. Wyatt, C.M. Gunther, M.W. Liberatore, Increasing viscosity in entangled polyelectrolyte solutions by the addition of salt, Polymer 52 (2011) 2437-2444.

[23] W. Inthavong, C. Chassenieux, T. Nicolai, Viscosity of mixtures of protein aggregates with different sizes and morphologies, Soft Matter 15 (2019) 4682-4688.

[24] K. Ako, T. Nicolai, D. Durand, Salt-Induced Gelation of Globular Protein Aggregates: Structure and Kinetics, Biomacromolecules 11 (2010) 864-871.

[25] M. Matsuo, T. Tanaka, L. Ma, Gelation mechanism of agarose and k-carrageenan solutions estimated in terms of concentration fluctuation, Polymer 43 (2002) 5299-5309.

[26] S. Liu, W.L. Chan, L. Li, Rheological Properties and Scaling Laws of κ-Carrageenan in Aqueous Solution 48 (2015) 7649-7657.

[27] C. Rochas, M. Rinaudo, Mechanism of gel formation in κ-Carrageenan, Biopolymers 23 (1984) 735-745.

[28] V. Meunier, T. Nicolai, D. Durand, Structure of aggregating kappa-carrageenan fractions studied by light scattering, International Journal of Biological Macromolecules 28 (2001) 157-165.

[29] D.A. Garrec, B. Guthrie, I.T. Norton, Kappa carrageenan fluid gel material properties. Part 1: Rheology, Food Hydrocolloids 33 (2013) 151-159.

[30] D. Slootmaekers, C. De Jonghe, H. Reynaers, F.A. Varkevisser, C.J. van Treslong, Static light scattering from κ-carrageenan solutions, International Journal of Biological Macromolecules 10 (1988) 160-168.

[31] B. Hu, L. Du, S. Matsukawa, NMR study on the network structure of a mixed gel of kappa and iota carrageenans, Carbohydrate Polymers 150 (2016) 57-64.

[32] V.T.N.T. Bui, B.T. Nguyen, F. Renou, T. Nicolai, Rheology and microstructure of mixtures of iota and kappa-carrageenan, Food Hydrocolloids 89 (2019) 180-187.

[33] A. Catenaccio, Y. Daruich, C. Magallanes, Temperature dependence of the permittivity of water, Chemical Physics Letters 367 (2003) 669-671.

Conclusion générale et perspectives

Conclusion générale et perspectives

1 Conclusion générale

La synérèse est équivalent à une perte de la masse de liquide que transporte un gel. Cette perte de liquide entraine la contraction du gel. Dans de nombreuses applications, la perte d'eau des hydrogels pose des problèmes de qualités, d'esthétique, de sécurité dans le domaine de la santé où l'hydrogel est utilisé pour cultiver des cellules pour des analyses médicales et plus globalement des problèmes de coût important pour les fabricants de ces produits du domaine agroalimentaire et pharmaceutique. La synérèse est une démonstration de la dynamique des gels, immédiatement ou longtemps après la gélification. Elle se présente comme un phénomène continu dont l'évolution suit différentes phases du début jusqu'à la fin. Il est difficile de mesurer le début et la fin de la synérèse, des difficultés relatives à la précision des méthodes expérimentales couramment utilisées. Au début, la masse de liquide perdue est faible pour être mesurer avec une bonne précision, il faut attendre que la masse de liquide soit significative pour réaliser la mesure et commencer à suivre l'évolution de la synérèse. Cette phase initiale dite t_0 est inaccessible avec nos méthodes actuelles qui se concentre sur l'observation macroscopique de la dynamique du gel. Dans la phase finale supposément, les variations de perte du liquide sont très faibles lorsque ces variations sont rapportées par rapport à la masse du gel. Les quantités de liquide expulsées du gel sont si faibles qu'elles restent sur le gel par capillarité et ne sont donc pas mesurables par les méthodes de prélèvement du liquide expulsé.

Nous avons donc étudié dans cette thèse la possibilité de mesurer la synérèse en utilisant la microscopie à fluorescence et un rhéomètre capable de suivre : pour la première technique les variations de dimension du gel d'épaisseur de quelques µm disposé dans une cellule entre lame et lamelle, pour la deuxième technique des variations de hauteur du gel de quelques µm en procédant par macro-indentation. La première technique exige un marquage du gel ou l'incorporation dans le gel de particules fluorescentes et une analyse quantitative des images qui traduit l'évolution de la synérèse. Les résultats sont encourageant en ce sens que si les conditions expérimentales sont bien optimisées on peut voir le début de la synérèse qui se manifeste par le détachement horizontal des gels du bord de la cellule, mais l'influence des particules fluorescentes qu'on a utilisées sur la synérèse du gel n'a pas été étudiée. La méthode par macro-indentation se sert du capteur de force du rhéomètre pour détecter la hauteur du gel à chaque

détachement de sa surface de la sonde. L'évolution de la hauteur du gel se traduit en évolution de la synérèse. La fréquence à laquelle la sonde va chercher la surface du gel dans son déplacement vertical se trouve avoir une influence significative sur la synérèse du gel au repos. Plus la fréquence est grande, plus la synérèse du gel est importante. A très faible fréquence, l'eau dans le gel s'évapore par l'espace qui s'épare la surface de la sonde et celle du gel. Ces résultats qu'on retrouve dans le chapitre 2 de cette thèse montrent une fois de plus, les difficultés techniques dans la mesure et l'étude de la synérèse.

Nous avons développé une approche originale de l'étude de la synérèse en s'intéressant à la dynamique des unités microscopiques ou mésoscopiques qui forment le gel. Nous présentons dans ce rapport uniquement que les résultats de la dynamique des unités microscopiques. Les gels que nous avons étudiés sont des hydrogels à base de kappa-carraghénane principalement. Le kappa-carraghénane de cette étude est un polysaccharide de poids moléculaire $\approx 3.3\times10^5$ g/mol constitué par un enchainement linéaire de disaccharide appelé aussi carrabiose. Le carrabiose du kappa-carraghénane est représenté par le code G4S-DA, il est formé de deux monosaccharides : le D-galactose (G) avec un groupement sulfate à la position 4 soit (G4S) et le 3,6-anhydro-D-galactose (DA). Le kappa-carraghénane se présente comme une unité microscopique du gel sous la forme d'une chaine d'environ 800 perles. Nous avons montré par des mesures rhéologiques que le volume microscopique que la chaine occupe dans le gel peut croître ou décroître en fonction de la température, du type de sel et de la concentration de sel. Ces études sont réalisées en solution car les mesures de viscosité de la solution sont exemptes des artéfacts qui affectent directement les mesures de la synérèse lorsqu'elles sont effectuées sur le gel. En procédant de la sorte, nous avons mis en évidence une partie fondamentale des causes de la synérèse dans les gels. Dans un premier temps, un modèle a été établi entre la température et la viscosité des liquides que nous avons formulé en énonçant le concept de "température de viscosité minimale des liquides" selon lequel tout liquide à un seul constituant possède une viscosité minimale à une température donnée. Au-dessus de cette température, le liquide aura tendance à changer d'état liquide à l'état gazeux, c'est l'évaporation. La dynamique ou agitation moléculaire n'étant plus entravée par les interactions moléculaires, la viscosité du système transitoire mais de plus en plus dominé par la vapeur ne peut qu'augmenter suivant l'augmentation de la pression ou de la quantité de mouvement des molécules du liquide. Le modèle situe la température de la viscosité minimale de l'eau entre 96 et 106 °C avec une moyenne de 100 °C sur le nombre d'ajustement du modèle aux mesures de la viscosité de l'eau que nous avons réalisées entre 5 et 60 °C avec un taux de fidélité entre 99 % et 100 %. La

température de changement d'état de l'eau à pression atmosphérique étant de 100 °C, nous avons généré des valeurs de viscosité des solutions de kappa-carraghénane dans la gamme de température entre 60 et 100 °C en utilisant le modèle. Ce sont ces données de viscosité qui nous ont permis de déterminer des valeurs de viscosité intrinsèques des solutions de kappa-carraghénane sur une large intervalle de température de 5 à 100 °C et de voir aussi l'évolution de la concentration critique (C*) des solutions en fonction de la température. La viscosité intrinsèque caractérise l'évolution de l'affinité du polysaccharide pour l'eau. En effet, l'évolution de la concentration critique des solutions de polymère est un indicateur robuste de l'évolution du volume qu'occupe le polymère dans la solution. Lorsque la température de conservation du gel contraint la chaine de polysaccharide à réduire son volume, on notera que l'état gel de la solution est un frein à l'évolution du volume du polysaccharide. C'est cette tension dans le gel qui produit la contraction progressive lente ou rapide du gel. Les résultats de ces études sont présentés dans les chapitres 3 et 4 de ce rapport.

Après l'étude du comportement de la chaine de polysaccharide, nous nous sommes intéressés à la position du groupement fonctionnel sulfate sur le D-galactose en comparant les résultats du kappa-carraghénan avec les résultats de l'alpha-carraghénane et de l'iota-carraghénane. Les carrabioses alpha- et iota-carraghénane sont représentés respectivement par le code G-DA2S et G4S-DA2S. Cette étude a révélé que le groupement sulfate du G4S est plus sensible au potassium et le groupement sulfate du DA2S est plus sensible au sel divalent. Cependant, la sensibilité au sel divalent est plus prononcée pour le G4S-DA2S que le G-DA2S. La position du groupement sulfate tout près du cycle anhydro semble constituer un frein à la neutralisation des ions sulfates par des sels monovalents. Les sels divalents sont plus efficaces à réduire les répulsions électrostatiques dans le système plus que les monovalents, mais les divalents semble transformer les répulsions électrostatiques entre charge négative en répulsions électrostatiques entre charge positive de faible intensité. En absence de sel, la viscosité des solutions d'alpha-carraghénane (G-DA2S) est plus grande que celle du kappa-carraghénane. En présence de sel (KCl) et dans les mêmes conditions que le kappa-carraghénane, les gels d'alpha-carraghénane n'ont pas montré de sensibilité remarquable à la synérèse. Les résultats de cette étude se trouvent dans les chapitres 5 et 6.

2 Perspectives

L'étude de la synérèse est un sujet complexe qui nécessite des recherches approfondies pour mieux comprendre le phénomène et trouver des solutions pour contrôler la perte d'eau des gels. Les perspectives de recherche futures pourraient inclure :

Tout d'abord, les études peuvent se concentrer sur la recherche de solutions pour éviter ou minimiser la synérèse dans les applications où cela pose des problèmes. Par exemple, dans le domaine de la santé, où les hydrogels sont utilisés pour cultiver des cellules pour des analyses médicales, il serait important de trouver des moyens de minimiser la synérèse pour éviter toute altération des échantillons. De même, dans les industries agroalimentaires et pharmaceutiques, des recherches peuvent être menées pour développer des produits qui minimisent la synérèse et pour améliorer les processus de fabrication.

En ce qui concerne la recherche fondamentale, des études supplémentaires peuvent être menées pour mieux comprendre la dynamique des gels et la synérèse. Les techniques de mesure doivent être améliorées pour permettre une meilleure compréhension de la synérèse, en particulier pour la phase initiale, t0, qui est actuellement difficile à mesurer avec précision. Au vu des résultats obtenus dans le deuxième chapitre, nous pouvons dégager deux pistes de réflexion, la première consiste à améliorer le système anti-évaporation et de travailler à une température plus basse (5 °C) grâce au système Peltier du rhéomètre ARES-G2. L'objectif est de minimiser l'effet d'évaporation par rapport à la cinétique de la synérèse. Sinon, il serait possible de couvrir la surface latérale du gel par une couche d'huile minérale. Cette amélioration du protocole expérimental permettra d'étudier la synérèse des gels en appliquant différentes forces et de corréler les propriétés rhéologiques du gel avec la synérèse.

Les recherches peuvent également se concentrer sur l'étude des unités mésoscopiques qui sont des agrégats de polysaccharide (sous forme d'hélices) et qui forment le gel, pour mieux comprendre comment la synérèse se produit à ce niveau.

Explorer l'utilisation de techniques de caractérisation avancées pour mieux comprendre la dynamique des gels de polysaccharides, telles que la diffusion de la lumière, la microscopie confocale, la microscopie électronique à balayage, et d'autres techniques.

Aussi, approfondir l'étude de la structure moléculaire des polysaccharides, en particulier les carraghénanes, afin de mieux comprendre leur comportement dans des environnements différents et d'optimiser leur utilisation.

Enfin, nous poursuivrons également les études sur le séchage des gels en fonctions de la composition des solutions.

En résumé, la compréhension de la dynamique des gels de polysaccharides et de leur comportement dans différents environnements pourrait conduire à de nouvelles applications dans divers domaines, tels que la biomédecine, la cosmétique, et les technologies avancées.

Liste de publications

Liste de publications

1 Publications Scientifiques

Said Elmarhoum, Komla Ako, Lower critical concentration temperature as thermodynamic origin of syneresis: Case of kappa-carrageenan solution. Carbohydrate Polymers (2021), Volume 267 (118191).

Komla Ako, **Said Elmarhoum**, Claire D. Munialo, The determination of the lower critical concentration temperature and intrinsic viscosity: The syneresis reaction of polymeric gels. Food Hydrocolloids (2022), Volume 124 (107346).

Said Elmarhoum, Sophie Mathieu, Komla Ako, William Helbert, Sulfate groups position determines the ionic sensitivity and syneresis properties of carrageenan systems. Carbohydrate Polymers (2023), Volume 299 (120166).

Said Elmarhoum, Komla Ako. Rheological study of α- and κ-carrageenan expansion in solution as effects of the position of the sulfate group. International Journal of Biological Macromolecules (2022), Volume 223, 1138-1144.

Alireza Yousefi, **Said Elmarhoum**, Shahla Khodabakhshaghdam, Komla Ako, Ghader Hosseinzadeh, Study on the impact of temperature, salts, sugars and pH on dilute solution properties of Lepidium perfoliatum seed gum. Food Science & Nutrition (2022).

Said Elmarhoum, Komla Ako, Claire D. Munialo, Yahya Rharbi, Helicity degree of carrageenan conformation determines the polysaccharide and water interactions. Submitted to Carbohydrate Polymers **(Annexe)**.

2 Présentations orales

- Journées des Jeunes Rhéologues : 22 et 23 Juin 2022, Brest, France

  Effet de sel et de température sur l'agrégation et la synérèse des systèmes de polysaccharide : Cas de kappa-Carraghénane.

- Séminaire interne (Laboratoire Rhéologie et Procédés), Grenoble le 20/01/2022

  Etude de la dynamique des gels physique en relation avec la synérèse.

3 Présentation par affiche

- Journées des Jeunes Rhéologues : 22 et 23 Juin 2022, Brest, France

  Étude de mesure de la synérèse des gels de Kappa-Carraghénane par macro-indentation.

- First Scientific Day PEM department - Doctoral schools EEATS, I-MEP2, Physics: October 21, 2021, Grenoble

  Lower critical concentration temperature as thermodynamic origin of syneresis reaction of polymeric gels: Case of Kappa-Carrageenan.

- 7th International Polysaccharide Conference: 11-15 October 2021, Nantes. France

  The determination of the lower critical concentration temperature and intrinsic viscosity: The syneresis reaction of polymeric gels.

Annexe

Contents lists available at ScienceDirect

Carbohydrate Polymers

journal homepage: www.elsevier.com/locate/carbpol

Helicity degree of carrageenan conformation determines the polysaccharide and water interactions

Authors and affiliations:

Said ELMARHOUM [a], Komla AKO [a, *], Claire D. MUNIALO [b] & Yahya RHARBI [a]

a) Univ. Grenoble Alpes, CNRS, Grenoble INP, LRP, 38000 Grenoble, France
b) School of Life Sciences, Coventry University, Priory Street, Coventry, CV1 5FB, UK

***Corresponding author**: *komla.ako@univ-grenoble-alpes.fr*; *akokomla@hotmail.com*

Abstract:

The polysaccharide in solution at critical concentration, Cc (g/L), is assimilated to a nano hydrogel (nHG) made of a single polysaccharide chain. Taking as reference the characteristic temperature of 20 ± 2 °C at which kappa-carrageenan nHG swelling is greater with a Cc = 0.55 ± 0.05 g/L, the temperature of the minimum deswelling in presence of KCl were found at 30 ± 2 °C for 5 mM with a Cc = 1.15 ± 0.05 g/L but not measurable above 100 °C for 10 mM of which Cc = 1.3 ± 0.05 g/L. Lowering the temperature to 5 °C, contraction of the nHG and further coil-helix transition with self-assembly induce a prompt increase of the sample's viscosity which steadily evolves with time in logarithmic scale. Accordingly, the relative increment of the viscosity per unit of concentration, Rv (L/g), should increase in agreement with increasing polysaccharide concentration. But the Rv decreases for kappa-carrageenan (κ-Car) samples above 3.5 ± 0.5 g/L in presence of 10 mM KCl under steady shear 15 s-1. This reflects a decrease of k-Car helicity degree, knowing that the polysaccharide is rather hydrophilic when its helicity degree is the lowest.

Keywords: Polysaccharide; Nanohydrogel; Kinetics; Coil-helix; Reduced viscosity

1. Introduction

As dissolution of the polysaccharides in aqueous phase precede most of the polysaccharide applications in food and nonfood areas, understanding their solubility, therefore, becomes critically important (Elfaruk, Wen, Chi & Li, 2021; Gerentes, Vachoud, Doury & Domard, 2002). Pectin powder has to be dissolved in aqueous media prior to any application (Einhorn-Stoll, 2018). Solubilization of polysaccharide in water is currently performed at high temperature (> 60 °C). For ionic polysaccharide like kappa-carrageenan, the upper critical solution temperature (UCST) or the temperature above which a clear solution is observed depend strongly on the ionic strength and type of counter ions (Heyda, Soll, Yuan & Dzubiella, 2014). Below the UCST, the polysaccharide solutions can turn to aggregate suspensions, fluid gels and gels, likewise, the viscosity of the solution increases to infinity at the gel point (Garrec, Guthrie & Norton, 2013; Rochas & Rinaudo, 1984). However, aggregation and gelation processes may not be achieved on time-scale of observation, if the interactions between polysaccharide and water are still favorable even below the UCST (Elfaruk, Wen, Chi & Li, 2021; Meunier, Nicolai & Durand, 2000). Therefore, the viscosity kinetics of the polysaccharide solutions undergoing these processes, is to some extent determined by the polysaccharide and water interactions.

The disaccharide repetition unit, called carrabiose units, that form the neutral backbone of alpha- and kappa-carrageenans are composed of 3-linked β-D-Galactose (G) and 4-linked 3,6-anhydro-D-galactose (DA). For the two selected carrageenans, only the position of the unique sulfate (S) group on the carrabiose is different between them (Elmarhoum, Mathieu, Ako & Helbert, 2023). Therefore, the kappa-Carrageenan (κ-Car) and alpha-Carrageenan (α-Car) are represented as G4S-DA and G-DA2S respectively. It is worth to note that the α-Car as native polysaccharide doesn't exist naturally, but is made by a desulfation enzymatic reaction from iota-carrageenan (i-Car), which polysaccharide is coded as G4S-DA2S. The production of α-Car is a breakthrough in the study of carrageenan functional properties. Comparative studies between monosulfated carrabiose polysaccharide are new, thus, they provide chemical or molecular origin information on the physical properties of the widely studied kappa-carrageenan systems, namely the interaction between this polysaccharide and water.

At temperature below and equal the UCST, the helices start to aggregate as soon as they are formed (Meunier, Nicolai & Durand, 2000; Norton & Goodall, 1983). Therefore, the interaction between the polysaccahride and water are unfavorable with the polysaccharides in helix conformation. Moreover, If salt concentration is increased or the temperature is decreased, the optical rotation of the polysaccharide in solution increases significantly characterizing the coil-helix transition amplitude, which correlate with an immediate aggregation and gelation mechanisms (Meunier, Nicolai & Durand, 2000). Conversely, these

mechanisms are very slow near the coil-helix temperature whatever the salt concentration in agreement with weak optical rotation amplitude. Based on these observations, a decrease of the polysaccharide and water attractive interactions is expected to correlate with an increase of the helicity degree (Tanaka & Wada, 1973). In the other hand, lower aggregation/gelation rate may reflect a lower helicity degree. The correlation could be resolved by analyzing the viscosity properties of the polysaccharide solutions considering the influence of temperature, salt, polysaccharide concentration and time parameters. Therefore this work aims to investigate the polysaccharide and water interactions based on the systems viscosity properties.

2. Materials and methods

2.1 Polysaccharides and samples preparation

The kappa-Carrageenan (κ-Car) was a gift from Rhodia Food Switzerland (product name and reference: MEYPRO-GEL 01/2001 WG95-37 κ-Car) of average molecular weight of 3.3×105 g/mol and polydispersity index of Mw/Mn = 2.0. The alpha-Carrageenan (α-Car) was a gift from Cermav (Centre de recherche sur les macromolecules végétales) of average molecular weight of 3.8×105 g/mol and polydispersity index of Mw/Mn = 1.8. The solutions of the two polysaccharides were prepared following the same preparation as reported in our previous works (Elmarhoum, Mathieu, Ako & Helbert, 2023). The stock solutions of the polysaccharide are dialyzed and free of added salts. The samples were prepared by dilution to different concentrations of polysaccharide and salt (KCl) where it is applicable. The samples with 0 mM salt indicates dilution of the stock solution with deminerilized water or as the polysaccharide solution in dialyzed form. The solutions with salt were heated between 70 °C and 90 °C until they become completely transparent, ≈ 15 min, then they were cooled prior to any use. These samples are considered as fresh samples only during cooling and are no longer fresh if the cooling process was stopped or broken. The cooling ramp was 2 °C/min. The conservation of the sample before the measurements could last from 10 s to 10 weeks. The aged samples were reset by heating before new measurements were performed.

2.2 Rheological measurements

The viscosity of hydrocolloidal suspensions changes with the hydrocolloid's structural properties. Therefore, the viscosity quantity is consistent for characterizing the aggregation of hydrogel-forming polysaccharide in aqueous phase. Kinetics of the viscosity at different shear rate, shear rate sweep of fresh and aged samples were performed in Couette geometry using a DHR3 Rheometer (TA Instrument) with a thermo regulator. The Couette geometry consisted of a concentric cylinder geometry of an inner rotor cylinder (bob) and an outer stator cylinder (cup) with radii R1 of 14 mm and R2 of 15 mm, respectively, defining a horizontal gap (R2 - R1) of 1 mm and an average radius R of 14.5 mm as (R1 + R2)/2. The height of the bob was 42 mm, and the vertical gap between the bob and cup was set at 2 mm. The measurements were done in the same experimental conditions as reported previously (Elmarhoum & Ako, 2021).

2.3 Viscosity kinetics measurements

For all the samples exhibiting a coil-helix transition, kinetics of the sample's viscosity was done at constant temperature below the coil-helix temperature (Tch). The time delay to cool the solution from Tch to the kinetics measurement temperatures depend on the cooling rate. For an example, the solutions in presence of 10 mM KCl show a Tch = 25 °C, hence it takes 10 min to cool the solutions from 25 °C to 5 °C with a cooling rate of 2 °C/min during which the nucleation and nuclei characteristics of the solutions change following the temperature variation.

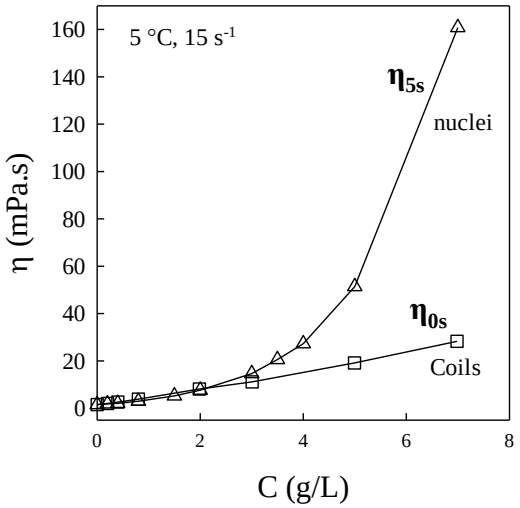

Figure 1: Concentration dependence of viscosity of Kappa-carrageenan (κ-Car) solution in presence of 0 and 10 mM KCl salt at 5 °C under shear rate of 15 s-1. The η5s is the viscosity at 5s after the temperature is set at 5 °C and η0s is the viscosity without added salt.

The kinetics started immediately, which means 5 s for the first viscosity value at the measurement temperature. Because instantaneously connected helices occur in the sample as soon as the temperature has reached Tch, the viscosity dependently may result from the presence of nuclei in the sample between 0 and 5 s (Fig.1). In term of the sample viscosities, 0 and 5 s correspond to the viscosity of the samples without salt and the first viscosity value at the measurement temperature respectively. The cooling rate was 2 °C/min and shear rate by default was 15 s-1 for all samples tested, if not it will be specified.

3. Results and discussion

3.1 The κ-Car and α-Car polysaccharide solutions

Viscous flow is a kinetic phenomenon, whereas conformational characteristic is a result of thermodynamic properties of the polymers in solution (Colby, 2010). Therefore, the correlation between viscosity and conformational characteristic of the polysaccharide herein is derived from Newtonian's flow of the polysaccharide solutions. The relationship between the temperature and viscosity of κ-Car and α-Car solution characterizes the inter/intra molecular interactions at work in the solution. Polysaccharide concentration dependence of the relationship between the temperature and viscosity shed light on the thermodynamic properties of κ-Car solution in the random coil state domain. Taking the dialyzed solution as reference (0 mM), we have shown that if the KCl salt concentration (5 and 10 mM) is increased, the temperature of characteristic critical concentration Cc (g/L) increases (Fig.2). Common consideration of Cc (g/L) in polymer physical chemistry supposes that bulk and excluded volume concentration should be the same at Cc (g/L). Therefore, considering that excluded volume (Vp) is spherical, i.e, Vp = 4πRp3/3, at Cc (g/L) the concentration equal mp/Vp with mp the average mass of a single polymer in the Vp. With the polysaccharide molecular mass Mp known, the expression of Cc (g/L) is given as:

$$Cc = \frac{3M_p}{4\pi R_P^3 N_A} \quad (1)$$

where the inverse of Avogadro's number, 1/NA, is the mol quantity of a single polymer. Given that, the polysaccharide average mass is constant, the variation of Cc (g/L) as shown in Fig.2 stand for the polysaccharide volume in aqueous phase. The arrows in Fig.2 indicate the position of the minimum Cc (g/L) as well as the corresponding temperature as the lower critical concentration temperature (LCCT).

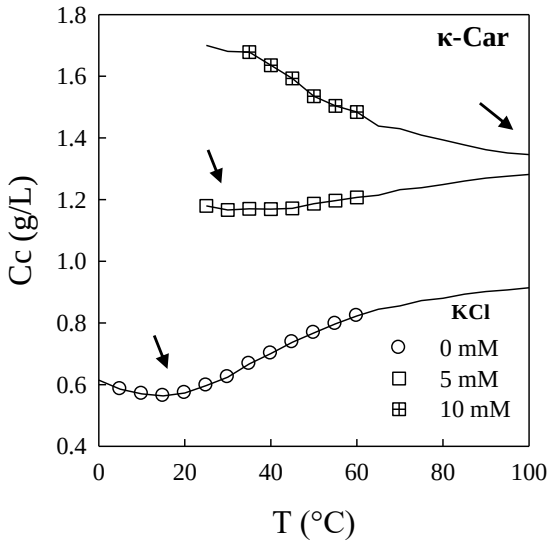

Figure 2: Temperature dependence of critical concentration of the kappa-carrageenan solution for different KCl salt concentration. The arrows indicate the lower critical concentration with its temperature.

The minimum Cc (g/L) increases with the LCCT when the KCl salt concentration is increased. KCl salt concentration above 5 mM seems not applicable for determining the LCCT of κ-Car, therefore the results of 10 mM and above are simply indicative of the LCCT tendency. The particular weak value of the KCl concentration stems from the ionic selectivity property of κ-Car, which is characterized by a strong reaction in presence of KCl salt more than NaCl salt. The consequence of this selectivity is that gels of κ-Car exhibit severe syneresis phenomenon in presence of KCl rather than other food grade monovalent salt. The thermodynamic origin of this phenomenon could be explained by the contraction of the polysaccharide excluded volume, and accordingly, an increase of the solution Cc (g/L). The polysaccharide excluded volume is the pervaded volume of chemically linear links and physically cross links between the monosaccharide's molecules, and thus, is similar to a physical and chemical nanohydrogel (nHG) particles. Considering the bulk as a compact collection of such particles, viscosity, therefore, becomes a bulk flow issue of condensed suspension of nHGs near the Cc (g/L). Correlation of the rheological properties of this independently estimated volume is not illusory. Small and big nHG will lead to respectively high and weak Cc (g/L). Therefore, shrinking and swelling properties of the nHG derive from bulk flow in the polysaccharide concentration ranging below the entangled concentration regime (Colby, 2010). In dilute solution regime, these properties derive from the polysaccharide intrachain interactions namely, hydrodynamic, excluded volume effect, water-monosaccharide and carrabiose-carrabiose interactions. These intrachain interactions determine the polysaccharide expansion and its conformational characteristics, which is strongly dependent on the polysaccharide affinity for the liquid media in term of poor-, theta- and good-solvent. For the dialyzed solution, the κ-Car concentration dependence of the viscosity was shown to increase following a scaling law, with a scaling power equal to 1.15. According to the scaling law theory of viscosity, a full repulsion between the carrabiose should lead to a scaling power of 0.5 were neutral polymer in a good solvent yields 1.3. This result supposes that intrachain interactions between the carrabioses are not fully repulsive and the aqueous media is not good enough to promote full stretching of the polysaccharide. The length scale of the polysaccharide chain that resists to stretching or swelling is considered as the unperturbe size (R0) of the polysaccharide (Colby, 2010). Thus, we think that water molecules should be out of this size domain due to excluded volume effect, because the free energy or elastic energy cost to swell the nanohydrogel on length scale smaller than R0 is huge compared with Boltzmann energy (kT) and greater than the entropic energy. Conversely, monosaccharide-monosaccharide attractive interactions should sharply decrease on length scale larger than R0 giving way to water-monosaccharide interactions to take place.

When k-Car is converted to a-Car by transfer of the sulfate group from the C4 of D-galactose to the C2 of 3,6-anhydro-D-galactose, we can see a significant increase of the viscosity of the dialyzed solution (Elmarhoum & Ako, 2022). The specific viscosity per unit of concentration, noted ηu (in L/g), properties of polymers derived from conformational characteristic as a result of excluded volume and water-polymer interactions. These interactions respectively determine the Cc (g/L) and intrinsic viscosity of the system as the limit of ηu when the polymer concentration decreased to 0 g/L (Ako, Elmarhoum & Munialo, 2022). Therefore, the ratio between ηu of a-Car and k-Car represent better the conformational contribution to the viscosity difference between the two polysaccharides. The temperature dependence of ηu of a-Car and k-Car are displayed in the insert of Fig.3 as ηuα and ηuκ respectively for the concentration of 3 g/L in dialyzed solution (0 mM). The Fig.3 shows the temperature dependence of ηuα / ηuκ. These experimental measurement data are shown in open circle and are fitted using the temperature-viscosity function reported in our previous works (Eq.1). The model is based on lower-viscosity-temperature (LVT) concept used to characterize the thermal property of the polysaccharide solutions.

$$\eta^{T} = \eta^{Tref} \cdot \exp\left[B_2 \cdot \left(T - T_{ref}\right)\left(T - T_2\right)\right] \qquad 2$$

where

$$T_2 = 2T_c - T_{ref} \qquad 3$$

and B2 with Tc are adjusting parameters in respect of Ako et al., (2022) definition of these parameters (Ako, Elmarhoum & Munialo, 2022; Elmarhoum & Ako, 2022). The quantity B2×Tc (/°C) is less dependent on the adjustment, it was defined as the thermal expansion coefficient of the polymer chains, which stand also for the thermal expansion properties of the nanohydrogels (nHGs). The Tc gives information on the free energy cost to break the interactions between nHGs, therefore Tc is a bulk depending phenomenon. However, to some extent we can hypothesized that, monomer-monomer interchain interaction could work for monomer-monomer intrachain interaction.

For pure liquid, Tc characterizes the temperature where molecular interactions become ineffective. But for small molecular weight liquid like water, Tc could characterize the boiling point. Though the specific viscosity per concentration shows a decreases tendency with increasing temperature for both α-Car and κ-Car polysaccharides, we can see from the fit function in Fig.3 that both the swelling and the water molecules binding properties of κ-Car are more impaired by heat. Considering f = ηuα / ηuκ, the fluctuation of the experimental measurement data between 5 °C and 60 °C leads to take the quotient f as an average value with a standard deviation of 1.65 ± 0.05. In presence of 10 mM KCl and in the T-range [5 °C, 60 °C], the average quotient f was 1.70 ± 0.05, which supposes that 10 mM KCl salt impairs the swelling and binding water molecules properties of κ-Car compared with α-Car. Conversely, κ-Car polysaccharides in solution exhibits a prompt tendency to gelation trough formation of helices and aggregates.

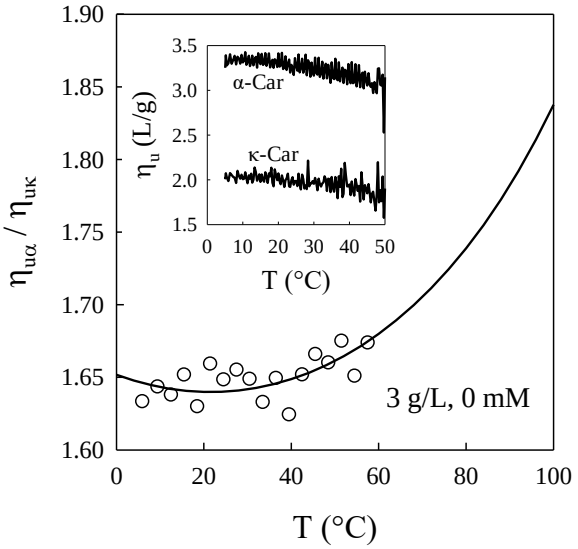

Figure 3: Temperature dependence of the ratio between α-Car reduced viscosity and κ-Car reduced viscosity. The insert shows the reduced viscosity of the two polysaccharides.

The thermal expansion of κ-Car and α-Car nHGs fit together with the coefficient B2×Tc = 1.5×10-2 /°C. But the Tc are different as its value depends on the bulk concentration. We found for the concentration of 3 g/L, 141 °C for α-Car and 153 °C for κ-Car. Actually, the interaction potential between the nHG partially overlaps and this increases in intensity and density with the increase of the concentration above the Cc (g/L) (Elmarhoum & Ako, 2021). The regime of the concentration 3 g/L is semidilute for both systems and the difference between their Tc may explain a difference in term of intensity and density of monomer-monomer interchain interactions including the interaction between water and the polysaccharides. With Tc of α-Car below the Tc of κ-Car, it results that monomer-monomer attractive interactions are greater for κ-Car than for α-Car in dialyzed solution. When 10 mM KCl was added to the dialyzed solution and the solutions was heated above 30 °C to melt κ-Car aggregates and helices, the temperature dependence of the viscosity fit well with the expansion coefficient B2×Tc and Tc of respectively 1.4×10-2 /°C and 183 °C. The α-Car solution with 10 mM KCl fit well with respectively 1.55×10-2 /°C and 139 °C and didn't exhibit any feature similar to the helix-coil conformational transition above 5 °C. The addition of salt to the solutions shed light on the polyelectrolyte effect on the thermal expansion properties of the polysaccharide including the repulsion interaction between the monomers in both inter and intrachain interactions. Water and polysaccharide interaction are influenced by salt accordingly. The 10 mM KCl salt has decreased the thermal expansion coefficient of κ-Car nHGs and increased the monomer-monomer attractive interaction due to screening electrostatic repulsion effect. The α-Car nHGs seems to be not sensitive as much as κ-Car nHGs to 10 mM KCl, but a weak increase of the thermal expansion coefficient was observed for α-Car. In addition to these results, we report a quotient f of 1.7 at 45 °C between the ηu of α-Car and κ-Car at 3 g/L, the quotient f was found to increase from 1.5 to 1.8, if the polysaccharide concentration is increased from 1 g/L to 5 g/L. We confirm by these results the relative lower ability of κ-Car to expand and swell in monovalent aqueous phase, which we have attributed to the sulfate group position effect in the carrabiose. The ionic selectivity feature of these results was reported previously (Elmarhoum & Ako, 2022; Elmarhoum, Mathieu, Ako & Helbert, 2023).

3.2 The solution viscosity and self-assembly dynamic

The formation of helices is reported for the conformational properties of hydrogel-forming carrageenan (Bui, Nguyen, Renou & Nicolai, 2019; Ciancia, Milas & Rinaudo, 1997; Morris, Rees & Robinson, 1980). The κ-Car polysaccharide has shown in solution a prompt aggregation and gelation properties particularly in presence of KCl salt. The kinetics of both mechanisms in competition influence the viscoelasticity of the samples. Therefore, when a fresh solution of κ-Car in presence of KCl is cooled to temperature range (T-range) below the coil-helix temperature (Tch), the viscosity of the fresh sample sharply increases, likewise, the slope increases with the polysaccharide and salt concentrations. Though aggregation promotes gelation with increasing salt concentration at constant polysaccharide concentration, it could be fatal for the samples gelation in presence of relatively high concentration of KCl salt (100 mM) for weak polysaccharide concentrations (< 3 g/L). Immediately, after cooling the fresh sample, if the sample was heated, the elasticity or alternatively viscosity of the samples decreases to reach the viscosity of the solution above the helix-coil temperature (Thc). The temperature hysteresis or gap between Tch and Thc is reported as a result of the self-assembly property of the hydrocolloids. Therefore, the viscosity stability of such hydrocolloid samples at a given temperature (T) depends not only on their sel assembling kinetics (long-time viscosity property) but also on the real-time property of the interactions between the hydrocolloids.

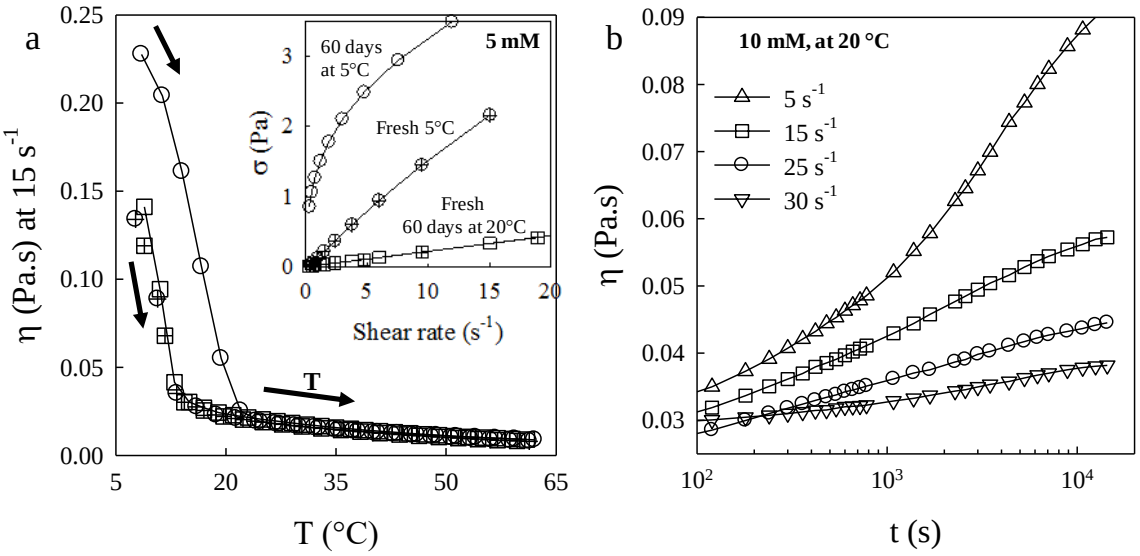

Figure 4: a) Temperature dependence of the viscosity of κ-Car samples. The samples were loaded at 5 °C then heated. The open symbol are samples aged-at-rest 60 days at 5 °C (circle) and at temperature above the helix-coil, 20 °C (square). The crossed symbol are freshly prepared samples (circle) and reset to fresh from the aging sample (square). Shear rate dependence of the shear stress for the different tested samples. **b)** Kinetics of the viscosity of 3 g/L, κ-Car in presence of 10 mM KCl at 20 °C for different shear rate.

Fresh and aged samples at T > Thc, i.e, in random coil state, yield the same viscosity properties (insert of Fig. 4a). For an example; the sample with 5 mM are fresh at storage temperature of 20 °C even after 60 days (square symbols in the insert of Fig. 4a), because their Thc = 15 ± 2 °C (square symbols in the Fig. 4a). Hence, no distinction was made between the samples conserved at temperature above Thc and the fresh or reset samples. However, the aged samples in T-range below Tch have shown distinctly two exciting viscosity properties: the real-time viscosity decreases with increasing the steady shear rate (open circle in the insert of Fig.4a) and the long-time viscosity increases with time at variable steady shear rate (Fig.4b). The mechanisms underlying these observations stems from the polysaccharide-water and polysaccharide-polysaccharide interactions dynamic. The interaction dynamics and links between the helices part of the polysaccharide chains are determined by temperature and salt concentrations. Some of them are broken and/or their formation impeded by the shear rate. We have surprisingly observed that unlike κ-Car the viscosity of α-Car solution decreases with time under shear. We show the results in the Fig.5 for 3 g/L in presence of 100 mM KCl and 20 mM CaCl2 at 5 °C. Alpha-carrageenan shows less sensitivity to KCl salt as its solution in presence of 100 mM KCl didn't gel upon time scale over 12 h, conversely the CaCl2 salt induces gelation of the polysaccharide and this was observed for 6 g/L but not for the duplicated 3 g/L samples at rest during the rheological tests. The coil-helix transitions of the polysaccharide were observed for 100 mM KCl and 20 mM CaCl2 at respectively ≈ 12 °C and 23 °C. Comparatively, the gelation of α-Car is very less faster than the gelation of κ-Car and need considerable addition of monovalent salt like the gelation of the samples in presence of 400 mM KCl. The decrease of a-Car samples viscosities under 15 s-1 demonstrates that cross-links and interhelical interaction dynamics respectively yield at applied steady shear stress and rate. Furthermore, the initial viscosity of the tested α-Car samples are 10 times greater than the viscosity of tested κ-Car samples with same polysaccharide concentration. Therefore, we think that the α-Car helices self-assembly into open aggregates, very less dens than those formed in the κ-Car systems. As soon as the helices are nucleated, they form a bigger size of swollen aggregate domains, thus they become more unstable under shear.

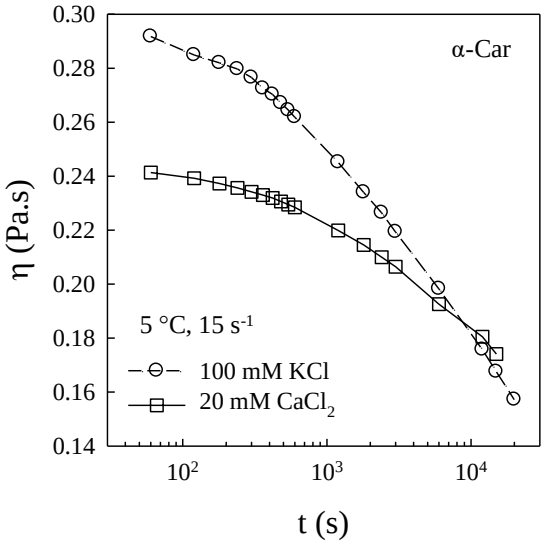

Figure 5: Kinetics of the viscosity under shear rate 15 s-1 of 3 g/L, α-Car in presence of salt at 5 °C.

The shear rate (s-1) defines the gradient of velocity between the inner rotor (bob) and outer stator (cup) cylinder on gap of ΔR = 1 mm. It interferes with the physical links properties in the sample to determine the length scale δr, below which the sample remains thick and unperturbed like a solid by the shearing. Under shear, the sample is arranged in layers number N as (ΔR/ δr). The thickness δr increases to bulk with decreasing shear rate toward 0 s-1, which correspond to the sample at rest. It is worth to note that, there is no real information on viscosity below δr and that the samples viscosity should result from the interfaces (shear band) between the stratum (δr). The cross-linking dynamics within the unperturbed layer should lead to sizes of clusters

no larger than δr. In this case, the time dependence of the sample's viscosity at constant shear rate characterizes the dynamic and strength of polysaccharide-polysaccahride interactions in balance with the interaction between polysaccharide and water in the shear bands. If the links strength and frequencies of the cross-linking, helices stacking mechanisms are greater enough to overcome the shear stress and rate, the viscosity of the sample should increase with time to stability when one of both linking dynamic and strength failed against the shear rate or stress respectively. Actually, three distinctly points result from the viscosity properties of κ-Car show in Fig.4b.

In point (1) the viscosity increases with time because of connection kinetics between the helices, indicating that the connections frequencies and strength are greater than the applied shear rate and stress respectively.

In point (2) the viscosity stability is threshold by the shear rate and the decrease of the viscosity with shear rate threshold indicates that the connections are characterized by multi-frequencies cross-linking dynamic. Hence, all polysaccharide-polysaccharide linking dynamics lower than the applied shear frequency no more contribute to the gelation mechanisms driven by the coil-helix conformational transition.

In point (3) the viscosity amplitude decreases if the shear rate, alternatively shear stress, is increased. But, given that the samples were loaded in solution state prior to the links formation, no information would result on the links strength in relation with the shear rate or stress.

A strong liaison could be formed between the helices after several weeks and months in both under shear and 0 shear condition. We observed that the viscosities of aged-at-rest samples decrease under increasing shear rate toward stability above the viscosity of fresh samples. This observation is shown in the insert of Fig.4a for the 60 days aged sample at 5 °C as shear rate dependence of the shear stress. Likewise, the links between helices are characterized by multilevel of strength, therefore the shear stress acts like a shear stress threshold applicable on mesoscopic scale (few number of stacking helices) (Meunier, Nicolai & Durand, 2000). For the purpose we define the stress threshold viscosity (ηS) and frequency threshold viscosity (ηF) as the viscosity of aged-at-rest and fresh samples respectively when a steady shear stress σ or rate $\dot{\gamma}$ is applied on the samples. The links in the aged-at-rest samples that may resist to the applied shear stress will remain in the unperturbed layer of thickness δr and the links that not sustained the applied shear stress will be progressively broken or disentangled in the shear band to the yielded viscosity ηS. The stress threshold viscosity ηS and frequency threshold viscosity ηF from respectively aged-at-rest and fresh samples are used to characterize the gelation mechanisms driven by the helix-helix interactions. The thermodynamic properties of these interchain connections strength determine the melting temperature, viscoelasticity of the unperturbed layer's δr and viscosity properties of the aggregate suspensions and fluid gel.

3.3 Time dependence of viscosity of aggregating / gelling samples

Interchain interactions and further formation of connection between the polysaccharides may lead to diverse sample characteristics. The solutions, aggregates suspensions, partially cross-linked aggregate suspensions (fluid gel), fine stranded or coarsen gels are most of the sample's characteristics reported in the literature (Bui, Nguyen, Renou & Nicolai, 2019; Garrec, Guthrie & Norton, 2013; Hermansson, Eriksson & Jordansson, 1991; Rochas, Rinaudo & Vincendon, 1980). However, these characteristics are determined by the kinetics and thermodynamics properties of the polysaccharide conformational transition (coil-helix) and interchain connections (Brunchi, Morariu & Bercea, 2014; Croguennoc, Meunier, Durand & Nicolai, 2000). In presence of KCl the kinetics of the coil-helix transition is very fast and nuclei are formed immediately at Tch such that their contribution individually in the sample's viscosity and kinetics are a complex issue. The viscosity kinetics are analyzed through consideration of helices aggregation and/or percolation. Meunier et al., (2000) have assumed two distinctly populations of the polysaccharides in solution for determining the aggregation / gelation kinetics using light scattering measurements; one in fully helical conformation and the other in coil conformation, though for the authors one may consider that real polysaccharide would be partially in helical or coil state (Meunier, Nicolai & Durand, 2000; Tanaka & Wada, 1973). But the later coil state leads to non-aggregating samples and thus are stable regarding the samples viscosity properties. We have compared the ηF and ηS at shear rate 5, 15 and 30 s-1 of different polysaccharide concentration in presence of 5, 10 and 15 mM KCl for 5 °C and 20 °C corresponding to the storage temperature of the samples. The behaviors of the viscosity data are the same between the two storage temperature. Moreover, not only 5 °C work for the three KCl salt concentration, but also allows a better contrast between ηF and ηS. The results are shown in table 1 for the storage samples at 5 °C. For these measurements, we remind that fresh samples are reset from the aged ones and the ηF measurements were done in the same run after the ηS measurements by introducing in the measurement programs a heating and cooling temperature sweep of the initially aged samples. By doing this, we maintain the same concentrations and also the instrument setting.

Table 1: Viscosity at 5 °C of kappa-carrageenan samples in various measurements conditions aged and fresh (reset) samples at 5, 15 and 30 s-1 for 0.2 g/L to 9 g/L in presence of 5, 10, 15 mM KCl.

		0.2 g/L	1g/L	5 g/L	9 g/L	0.2 g/L	1g/L	5 g/L	9 g/L	0.2 g/L	1g/L	5 g/L	9 g/L
		in 5 mM, KCl at 5 °C				in 10 mM, KCl at 5 °C				in 15 mM, KCl at 5 °C			
		viscosity in **mPa.s**				viscosity in **mPa.s**				viscosity in **mPa.s**			
ηF, reset	5 s-1	1.9	4.0	40.5	165.0	1.9	4.1			1.9	8.7		
ηS, 60 days after		2.0	4.5	127.7	522.4	2.7	22.7	gel	gel	3.6	59.2	gel	gel
ηF, reset	15 s-1	1.9	3.9	38.7	145.6	1.9	4.1			2.0	7.7		
ηS, 60 days after		1.9	4.4	84.7	253.3	2.5	14.7	gel	gel	3.1	28.8	gel	gel
ηF, reset	30 s-1	1.9	3.8	36.3	125.2	1.9	4.0			2.0	6.8		
ηS, 60 days after		1.9	4.3	63.6	166.6	2.4	11.2	gel	gel	2.8	19.4	gel	gel

The samples of 0.2 g/L in presence of 5 mM at 5 °C were already stable above the shear rate of 5 s-1 and interactions strength between the aggregates in suspension likely yield below a steady shear stress of 10 mPa. If the KCl concentration was increased to 10 mM, then to 15 mM, the increment of viscosity between the fresh samples and aged-at-rest samples characterizes the interaction relaxation frequencies (shear rate in Hz) and the upper yield stress or link strength between aggregates in the suspension. In presence of 10 mM and 15 mM KCl, the interaction relaxation frequencies likely are threshold below 5 Hz for both salt concentration. However, when they are formed at rest (0 /s shear rate) in presence of 10 mM and 15 mM KCl, some of the resulting links sustain to respectively applied steady shear stress of 73 mPa and 85 mPa. If now the concentration is increased to 1 g/L in presence of 5 mM KCl, interaction frequencies above 30 Hz appear. Some of the links which are formed at rest could resist to shear stress above 129 mPa, however these links may not emerge under the shear rate below 30 /s. The more the polysaccharide concentration and KCl salt, the faster the formation of links. However, increasing KCl concentration to 15 mM didn't accelerate the links formation between nuclei for 0.2 g/L. We think that diffusion coefficient likely limited the nuclei aggregation. Therefore, it may exist a critical concentration between 0.2 g/L and 1 g/L at which, the nuclei cross linking dependence on diffusion phenomenon is negligible. This concentration could be close to the critical concentration Cc (g/L) of the polysaccharide in coil state and may characterize the concentration of true gel formation (Meunier, Nicolai & Durand, 2000). For instance, the samples of 0.5 g/L, κ-Car didn't form a true gel (simply tilting the container) after 60 days at 5 °C in presence of KCl concentration ranging below 50 mM, while the samples of 1 g/L have gelled in presence of 25 mM, KCl but collapse to liquid samples in presence of 100 mM, KCl. The polysaccharide need to overlap their potential of interactions in solutions at least partially prior to find the salt conditions for the sample gelation. In this case, the polysaccharide conformational states are rather relevant than their random motions (Lin, Lindsay, Weitz, Ball, Klein & Meakin, 1989; Savel'ev, Marchesoni, Taloni & Nori, 2006; Tanaka & Wada, 1973). Hence, the viscosity kinetics would therefore result from conformational transition evolution from fine stranded filaments to stiff segments. But, interconnections speed and strength between the filaments and stacking domains of the stiff segments could be weaken by decreasing either the salt, polysaccharide concentration or both. For these types of systems, the concentration of solid matters is not sufficient to determine the thermodynamic chemical potential. Because of its critical role, we may consider or define the conformational transition of the polysaccharide as a potential of activity of the polysaccharide in solution, which activity influence the viscosity. But, what is the optimum degree of the helix conformation in a given aqueous phase which characterizes the thermodynamic stability of the polysaccharide system? How the polysaccharide concentration regimes (dilute, semi dilute, entangled) influence the helix optimum degree? The optical rotation of κ-Car reaches with time different degrees in function of combined ionic strength and temperature effects. Its rate is also influenced and equilibrium was not clearly demonstrated by the system after over 12 h in log time scale (Meunier, Nicolai & Durand, 2000). It is well known from earlier reports on salt effects that particularly KCl promotes stiffness and stacking domains for κ-Car polysaccharides in solution (Ako, 2015; Hermansson, 1989; Hermansson, Eriksson & Jordansson, 1991). But these local phase separation processes could be fatal to the sample water holding capacity and macroscopic stability. Understanding the kinetics, will contribute to resolve the origin of the resulting instabilities. The helices start to aggregate as soon as they are nucleated and because of time imprecision on the nucleation kinetic we may consider the measurements beginning time step (δt = 5s), hence η5s is took as a threshold, and anything that may happens further in the sample is therefore due to only interactions and physical bounds formation between the nuclei prevailing in the samples within δt. Hence, the viscosity at any time t, ηt, minus η5s is divided by η5s to give the reduced relative increment viscosity, Rv (L/g). The reduced viscosities Rv (L/g) are determined for all tested samples (Eq.3) in function of time and concentration. Taking variable time window from the viscosity kinetics in Fig.6a, for examples 30 s, 5 min, 1 h, 3 h and 6h, the concentration dependence of Rv were determined (Fig.6b) to analyze the effects of interactions through the polysaccharide concentrations influence on the viscosity kinetics. Indirectly, the analysis may conclude on the conformational dynamics dependence on polysaccharide concentration for a given condition of temperature, salt concentration and shear rate.

$$R_v = \frac{\eta_t - \eta_{5s}}{\eta_{5s} \cdot C} \qquad 4$$

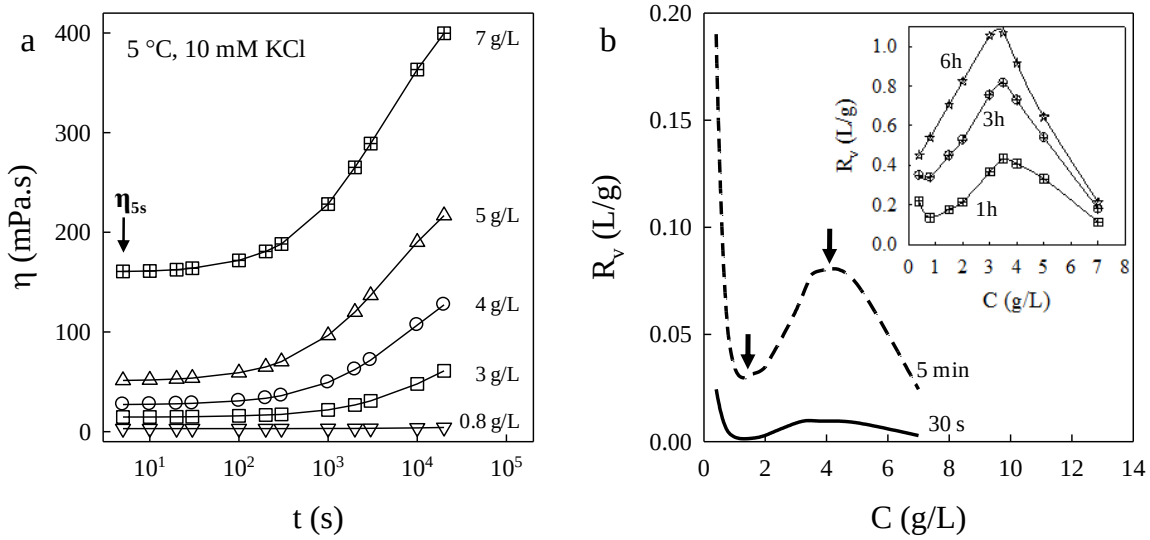

Figure 6: a) Kinetics of the viscosity under 15 s-1 for differente κ-Car concentration in presence of 10 mM KCl. **b)** Concentration dependence of the relative increment viscosity per unit of concentration (Rv) for different selected time steps, 30 s, 5 min and 1h, 3h, 6h (insert).

The time dependence of viscosity of higher polysaccharide concentration evolves above lower polysaccharide concentration samples, because the viscosity of the samples at the beginning η5s increases with increasing polysaccharide concentration. The logarithmic scale of time shows that the viscosity of the samples still increases and is not about to reach equilibrium. However, the reduced viscosities in Fig.6b show an interesting behavior with concentration, which is characterized by two characteristic concentrations in C-range between 0.2 g/L and 7 g/L. If we take the viscosity values of the samples in time step of 30 s, we observe that the relative increment of the viscosity starts to increase and to decrease from roughly the concentration of 1 ± 0.5 g/L and 3.5 ± 0.5 g/L respectively. Time steps above 30 s show the same extrema of concentration, but the increase and decrease of the reduced viscosity after 3 h are stiff within the C-range from 1 g/L to 3.5 g/L and from 3.5 g/L to 7 g/L with respectively a slop of 0.23 and -0.24 (insert of Fig.6b). Given that the viscosity increase with time is observed for all of the samples, the decrease of reduced viscosity in C-range from 3.5 g/L to 7 g/L is not in agreement with both concentration and viscosity increase. Therefore, although helix degree and number of interchain connections increase with time, this likely not happen in agreement with the increase of polysaccahride concentration above 3.5 ± 0.5 g/L. In a given aqueous phase and above the critical concentration from which the conformational transitions control the aggregation/gelation mechanisms rather than the polysaccharide diffusion coefficient, the increase of polysaccharide concentration beyond a maximum concentration value will hinder or frozen the conformational kinetic to a certain degree. The effect may delay the interactions and connection degrees in time, strength or both. The delay in strength means same kinetics, but with weak reduced viscosity. The delay in time means same reduced viscosity will be found for higher concentration, but later. Vertical and horizontal shift of the reduced viscosities dependence on time, could help to at least conclude on whether lower and higher concentration follow the same kinetics and connection strength development or not. To shift the reduced threshold viscosity, we simply divided the time dependence of the reduced threshold viscosities by their values at time step of 6h. The time axis is displayed in logarithmic sacle of t/δt with δt = 5 s. As we can see in Fig.7, all the samples of concentration above the characteristic minimum concentration of 1 ± 0.5 g/L, fall on same master curve acceptably (see the guide line for eye in Fig.7). The result, we think is an indication that the samples of concentration above ≈ 1 g/L follow roughly same kinetics but with different links strength between the polysaccharide in either filaments, helices or aggregate forms.

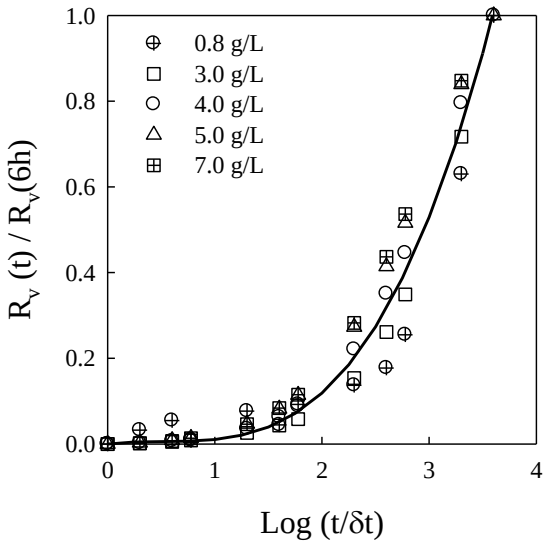

Figure 7: Master curve of the reduced viscosity kinetics for all the samples concentration displayed in Fig.6a. The δt = 5 s is the time for the measurement beginning and 6 h is the total time of the kinetics measurement.

The samples below 1 g/L, for instance 0.4 g/L and 0.2 g/L tested, are not on the master kinetics curve because their concentrations fall in dilute concentration regime, accordingly interchain liaisons likely are not dominant. Alternatively, the viscosity kinetic properties of these samples likely result from intrachain rather than interchain interactions and aggregations are controlled by diffusion. However, coil-helix transition without aggregation (lower concentration) seems to have lower impact on viscosity kinetics. Two months later, the samples of concentration above 4 g/L in presence of 10 mM have gelled at rest. Considering this result with the fact that viscosity of the samples in C-range between ≈ 1 g/L and 7 g/L (tested) follow roughly the same kinetics, we may think that after months and years under 15 s-1 shear rate at 5 °C, the concentration dependence of reduced threshold viscosity of the samples between ≈ 1 g/L and 3.5 g/L with ≈ 3.5 g/L and 7 g/L may finally fall on the same negative slope. Hence, may be the samples ranging below 1 g/L could show an increase of reduced threshold viscosity in function of concentration. Accordingly, the characteristic maximum concentration initially found at ≈ 3.5 g/L could after several hours, days or months shift to ≈ 1 g/L and the characteristic minimum concentration initially at ≈ 1 g/L will be shifted to let's say the Cc (g/L) or may be lower after years. The study of the polysaccharide in solution demonstrates that affinity between polysaccharide and water are better when the polysaccharide is in coil than helix conformational state. Therefore, according to our analysis, it results that the affinity of polysaccharide to water property is not colligative but conformational issue. The affinity would increase because helix degree decreases with increasing polysaccharide concentration in even potassium aqueous phase.

4. Conclusion

The viscosity properties of κ-Car and α-Car polysaccharide solutions were investigated in different measurement conditions to characterizes the interactions between water and the polysaccharides. The mono sulfate group position on the D-galactose unit of κ-Car polysaccharide carrabioses, promotes less expansion of the polysaccharide and react strongly with KCl than the mono sulfate group position on the 3,6-anhydro-D-galactose unit of α-Car. Accordingly, κ-Car exhibits sever aggregation and gelation properties in KCl aqueous phase extremely faster than α-Car when the temperature is set below the coil-helix transition temperature (Tch). The rheological properties of the polysaccharide are reversible and because of this thermosensitivity, the polysaccharides critical concentration Cc (g/L) changes with temperature. A variation of Cc (g/L) that we have assimilated to swelling and deswelling properties of a nanohydrogel (nHG) made of a single polysaccharide chaine. The concentration dependence of viscosity is shown to be characterized by a power law relationship (η α C1.15) which tell that water is not good enough for the polysaccharide maximum expansion. Therefore, water molecules likely are excluded from unperturbed length scale of the polysaccharide (nHG), within which intrachain carrabiose-carrabiose interaction are very strong. The short time scale (6h) and long time scale (2 months) analysis of the viscosity properties of thermally reset fresh sample and aged samples have shown two interesting characteristic behaviors. For the first one, interchain cross-links happening with different cross-linking frequencies can be cut off by applying a shear rate threshold is demonstrated on the fresh sample undergoing gelation processes. But for the aged samples in liquid state, the cross-links strength were shown to be characterized by different level of strength, which can be broken by applying a shear stress threshold. For the second one, because coil-helix transition induced aggregation and increase of the viscosity, the

reduced threshold viscosities of the samples are supposed to increase with aggregation time and polysaccharide concentration. However, we have observed that the reduced threshold viscosity decreases, if the polysaccharide concentration is increased above 3.5 ± 0.5 g/L, meaning that the degrees of helicity and the viscosity activity of the helices accordingly decrease with increasing concentration. Therefore, increasing the polysaccharide concentration impede the helix transition achievement, and control by this way the hydrophilic property of the polysaccahride.

Declaration of competing interest

The authors declare no conflicts of interest.

5. Acknowledgements

We thank Professor William Helbert from the Centre de Recherche sur les Macromolecules Végétales (CERMAV) for the α-Carrageenan and Vincent VERDOOT for his technical assistance with the rheometer instruments. This work was financially supported by I-MEP2 PhD graduate school and the PolyNat Carnot Institut. The Laboratoire Rhéologie et Procédés (LRP) is part of LabEx Tec 21 (Investissements d'Avenir - grant agreement n°ANR-11-LABX-0030) and PolyNat Carnot Institut (Investissements d'Avenir - grant agreement n°ANR-11-CARN-030-01).

6. References

Ako, K. (2015). Influence of elasticity on the syneresis properties of kappa-carrageenan gels. Carbohydrate Polymers, 115, 408-414.

Ako, K., Elmarhoum, S., & Munialo, C. D. (2022). The determination of the lower critical concentration temperature and intrinsic viscosity: The syneresis reaction of polymeric gels. Food Hydrocolloids, 124, 107346.

Brunchi, C.-E., Morariu, S., & Bercea, M. (2014). Intrinsic viscosity and conformational parameters of xanthan inaqueous solutions: Salt addition effect. Colloids and Surfaces B, 122, 512-519.

Bui, V. T. N. T., Nguyen, B. T., Renou, F., & Nicolai, T. (2019). Rheology and microstructure of mixtures of iota and kappa-carrageenan. Food Hydrocolloids, 89, 180-187.

Ciancia, M., Milas, M., & Rinaudo, M. (1997). On the specific role of coions and counterions on kappa-carrageenan conformation. International Journal of Biological Macromolecules, 20, 35-41.

Colby, R. H. (2010). Structure and linear viscoelasticity of flexible polymer solutions: comparison of polyelectrolyte and neutral polymer solutions. Rheologica Acta, 49, 425-442.

Croguennoc, P., Meunier, V., Durand, D., & Nicolai, T. (2000). Characterization of Semidilute k-Carrageenan Solutions. Macromolecules, 33, 7471-7474.

Einhorn-Stoll, U. (2018). Pectin-water interactions in foods - From powder to gel. Food Hydrocolloids, 78, 109-119.

Elfaruk, M. S., Wen, C., Chi, C., & Li, X. (2021). Effect of salt addition on iota-carrageenan solution properties. Food Hydrocolloids, 113, 106491.

Elmarhoum, S., & Ako, K. (2021). Lower critical concentration temperature as thermodynamic origin of syneresis: Case of kappa-carrageenan solution. Carbohydrate Polymers, 267, 118191.

Elmarhoum, S., & Ako, K. (2022). Rheological study of α- and κ-carrageenan expansion in solution as effects of the position of the sulfate group. International Journal of Biological Macromolecules, 223, 1138-1144.

Elmarhoum, S., Mathieu, S., Ako, K., & Helbert, W. (2023). Sulfate groups position determines the ionic selectivity and syneresis properties of carrageenan systems. Carbohydrate Polymers, 299, 120166.

Garrec, D. A., Guthrie, B., & Norton, I. T. (2013). Kappa carrageenan fluid gel material properties. Part 1: Rheology. Food Hydrocolloids, 33, 151-159.

Gerentes, P., Vachoud, L., Doury, J., & Domard, A. (2002). Study of a chitin-based gel as injectable material in periodontal surgery. Biomaterials, 23, 1295-1302.

Hermansson, A.-M. (1989). Rheological and Microstructural Evidence for Transient States During Gelation of Kappa-Carrageenan in the Presence of Potassium. Carbohydrate Polymers, 10, 163-181.

Hermansson, A.-M., Eriksson, E., & Jordansson, E. (1991). Effects of Potassium, Sodium and Calcium on the Microstructure and Rheologicai Behaviour of Kappa-Carrageenan Gels. Carbohydrate Polymers, 16, 297-320.

Heyda, J., Soll, S., Yuan, J., & Dzubiella, J. (2014). Thermodynamic Description of the LCST of Charged Thermoresponsive Copolymers. Macromolecules, 47, 2096-2102.

Lin, M. Y., Lindsay, H. M., Weitz, D. A., Ball, R. C., Klein, R., & Meakin, P. (1989). Universality in colloid aggregation. Nature, 339, 360-362.

Meunier, V., Nicolai, T., & Durand, D. (2000). Structure and Kinetics of Aggregating kappa-Carrageenan Studied by Light Scattering. Macromolecules, 33, 2497-2504.

Morris, E. R., Rees, D. A., & Robinson, G. (1980). Cation-specific Aggregation of Carrageenan Helices : Domain Model of Polymer Gel Structure. Journal of Molecular Biology, 138, 349-362.

Norton, I. T., & Goodall, D. M. (1983). Equilibrium and Dynamic Studies of the Disorder-Order Transition of Kappa Carrageenan. J. Chem. Soc., Faraday Trans. 1, 79, 2489-2500.

Rochas, C., & Rinaudo, M. (1984). Mechanism of gel formation in κ-Carrageenan. Biopolymers, 23(4), 735-745.

Rochas, C., Rinaudo, M., & Vincendon, M. (1980). Structural and conformational investigation of carrageenans. Biopolymers, 19(12), 2165-2175.

Savel'ev, S., Marchesoni, F., Taloni, A., & Nori, F. (2006). Diffusion of interacting Brownian particles: Jamming and anomalous diffusion. Physical Review E, 74, 1-9 (021119).

Tanaka, T., & Wada, A. (1973). Dynamical aspects of helix-coil transitions in biopolymers. II. J. Chem. Phys., 59, 3799-3810.

Résumé

L'application des polysaccharides n'est pas que très utile dans le domaine agroalimentaire, elle prend de plus en plus d'importance dans le domaine des technologies avancées et biomédicales. L'abondance de cette ressource, sa biocompatibilité et biodégrabilité étant un atout majeur pour l'exploitation de son potentiel en science et technologie. Dans cette thèse, nous nous sommes intéressés aux gels de polysaccharides qui sont parfois des états intermédiaires entre la solution et le produit fini, par exemple, sous forme de film pour l'encapsulation des médicaments, ou des applications en cosmétiques. Cependant, la synérèse, contraction des gels au repos avec expulsion d'eau, limite leurs usages. Nous avons surtout étudié la dynamique des gels en relation avec la synérèse comme une conséquence directe de celle des unités microscopiques et mésoscopiques dont ils sont formés. Nous avons émis l'hypothèse de l'existence d'une viscosité minimale thermique des liquides, c'est-à-dire, qu'il existe une température à laquelle la viscosité de tout liquide est la plus basse et qu'à ce point thermique les interactions ou liaison physique dans le liquide ne contribuent plus à la viscosité de l'état liquide. L'effacement progressif de ces interactions se traduit aussi par l'extension progressive des interactions au sein du volume occupé par les polymères : monomère-monomère, polymère-solvant et solvant-solvant. L'expansion du volume qu'occupent les polymères se manifeste dans l'évolution de la viscosité des solutions en fonction de la température. Laquelle évolution nous a permis de déterminer la température de l'expansion maximale des chaines de polysaccharide qu'on note LCCT. En comparant, les conditions thermiques des solutions (au point LCCT) et les conditions thermiques de gélification des solutions, nous avons pu mettre en évidence l'origine thermodynamique de la synérèse applicable à tous les systèmes. Nous nous sommes intéressés à la famille des carraghénanes dont les carrabioses sont des disaccharides qui s'identifient par les liaisons entre le D-galactose et 3,6-anhydro-D-galactose représentés respectivement par les lettres (G) et (DA) avec ou sans groupements sulfatés. L'étude du kappa-carraghénane (G4S-DA), de l'alpha-carraghénane (G-DA2S) et de l'iota-carraghénane (G4S-DA2S) met en évidence le rôle de la structure moléculaire (chimie) à l'origine de la synérèse de ce type de polysaccharide.

Mots clés: Polysaccharide; carraghénane; gel; synérèse; viscosité; expansion thermique; viscosité minimale thermique; LCCT; concentration critique; volume exclu.